UNIVERSIDAD DE ALMERÍA

Dpto. de Biología y Geología

Área de Genética

Doctorado en Agricultura Protegida

Role of Ethylene and Jasmonate on traits of agronomic interest in *Cucurbita pepo*: a genomic approach

Tesis Doctoral

Gustavo Cebrián Castillo

Almería, Julio 2022

Ph.D. DISSERTATION

Funciones del Etileno y Jasmonato en caracteres de interés agronómico en *Cucurbita pepo*: un enfoque genómico

Role of Ethylene and Jasmonate on traits of agronomic interest in *Cucurbita pepo*: a genomic approach

Área de Genética

Departamento de Biología y Geología

Escuela Superior de Ingeniería y Facultad de Ciencias Experimentales

Universidad de Almería

Gustavo Cebrián Castillo

Almería, Julio 2022

Dpto. de Biología y Geología

Área de Genética

Universidad de Almería

Dr. Manuel Jamilena Quesada, Catedrático del Área de Genética de la Universidad de Almería y Dr. J. Miguel Guzmán Palomino, Doctor del Área de Producción Vegetal de la Universidad de Almería.

HACEN CONSTAR:

Que el presente trabajo se ha realizado bajo nuestra dirección y recoge la labor realizada por el licenciado Gustavo Cebrián Castillo para optar al Grado de Doctor.

Fdo. Dr. Manuel Jamilena Quesada Fdo. Dr. J. Miguel Guzmán Palomino

“Aprende del esfuerzo, honesto y certero. La mente que se abre a una nueva idea, jamás volverá a su tamaño original”

Scientific contributions

Scientific contributions related to the doctoral thesis

Peer-Reviewed Articles

Cebrián G, Segura M, Martínez J, Iglesias-Moya J, Martínez C, Garrido D, Jamilena M. 2022. Jasmonate-deficient mutant *lox3a* reveals crosstalk between JA and ET in the differential regulation of male and female flower opening and early fruit development in *Cucurbita pepo.*
Submitted to *New Phytologist*. (IF: 10.15)

Cebrián G, Iglesias-Moya J, Romero J, Martínez C, Garrido D, Jamilena M. 2022. The ethylene biosynthesis gene *CpACO1A*: a new player in the regulation of sex determination and female flower development in *Cucurbita pepo.*
Frontiers in Plant Science **12**, 817922. (IF: 5.75)
https://doi.org/10.3389/fpls.2021.817922

Cebrián G, Iglesias-Moya J, García A, Martínez J, Romero J, Regalado JJ, Martínez C, Valenzuela JL, Jamilena M. 2021. Involvement of ethylene receptors in the salt tolerance response of *Cucurbita pepo*.
Horticulture Research **8**, 73. (IF: 6.79)
https://doi.org/10.1038/s41438-021-00508-z

Cebrián G, García A, Aguado E, Romero J, Chana-Muñoz A, Martínez C, Valenzuela JL, Guzmán M, Jamilena M. 2019. Use of germination and early radicle growth parameters for assessing oxidative stress tolerance in Zucchini squash.
Acta Horticulturae **1294**, 163-168
https://doi.org/10.17660/ActaHortic.2020.1294.21

Proceedings and congress communications

Cebrián G, García A, Iglesias-Moya J, Romero J, Martínez C, Garrido D, Jamilena M. 2021. Two induced EMS mutations conferring parthenocarpy in *Cucurbita pepo*. XII Eucarpia Meeting on Cucurbit Genetics and Breeding. Almería (Spain) May 24-28, pp 85. ISBN 978-84-1351-090-3.

Cebrián G, García A, Aguado E, Romero J, Iglesias-Moya J, Valenzuela, JL, Guzmán M, Martínez C, Jamilena M. 2019. Evaluación de la tolerancia a la salinidad en el mutante de insensibilidad a etileno *ein1* de *C. pepo.* II Congreso de Jóvenes Investigadores en Ciencias Agroalimentarias. Almería (Spain), Oct 17, pp 247. ISBN 978-84-09-17547-5.

Cebrián G, García A, Aguado E, Romero J, Chana-Muñoz A, Martínez C, Valenzuela JL, Guzmán M, Jamilena M. 2019. Use of germination and early radicle growth parameters for assessing oxidative stress tolerance in Zucchini squash. VI International Symposium on Cucurbits. Ghent (Belgium) Jun 30- Jul 04, pp 9.

Cebrián G, García A, Aguado E, Romero J, Manzano S, Martínez C, Guzmán M, Jamilena M. 2018. Effect of salinity on the germination and seedling growth of *Cucurbita pepo* ethylene mutants. I Congreso de Jóvenes Investigadores en Ciencias Agroalimentarias. Almería (Spain), Dec 20, pp 304-305.

Cebrián G, García A, Manzano S, Aguado E, Romero J, Garrido D, Guzmán M, Jamilena M. 2017. Phenotyping for oxidative stress tolerance in zucchini squash *Cucurbita pepo.* The XIV Solanaceae and III Cucurbitaceae genomics joint conference. Valencia (Spain), Sep 03-06, pp 180.

Other contributions

Other associated peer-reviewed articles

García A, Aguado E, **Cebrián G,** Iglesias-Moya J, Romero J, Martínez C, Garrido D, Rebolloso MM, Valenzuela JL, Jamilena M. 2020. Effect of ethylene-insensitive mutation *etr2b* on postharvest chilling injury in zucchini fruit. *Agriculture* **10**, 532.
https://doi.org/10.3390/agriculture10110532.

Romero-Masegosa J, Martínez C, Aguado E, García A, **Cebrián G,** Iglesias-Moya J, Paris HS, Jamilena M. 2020. Response of *Cucurbita* spp. to tomato leaf curl New Delhi virus inoculation and identification of a dominant source of resistance in *Cucurbita moschata.*
Plant Pathology **70**, 206-218.
https://doi.org/10.1111/ppa.13268.

Romero J, Aguado E, Martínez C, García A, **Cebrián C,** Paris HS, Jamilena M. 2019. A novel dominant resistance gene for ToLCNDV in *Cucurbita spp*.
Acta Horticulturae **1294**, 233-238.
https://doi.org/10.17660/ActaHortic.2020.1294.29.

Chana-Muñoz A, García A, Aguado E, Romero J, **Cebrián G,** Iglesias-Moya J, Garrido D, Cañizares J, Valenzuela JL, Jamilena M. 2019. RNA-seq reveals molecular mechanisms behind chilling injury tolerance in ISW-treated zucchini fruit during cold storage.
Acta Horticulturae **1294**,149-154.
https://doi.org/10.17660/ ActaHortic.2020.1294.19.

García A, Aguado E, Parra G, Manzano S, Martínez C, Megías Z, **Cebrián G,** Romero J, Beltrán S, Garrido D, Jamilena M. 2018. Phenomic and genomic characterization of a mutant platform in *Cucurbita pepo*.
Frontiers in Plant Science **9**, 1049.
https://doi.org/10.3389/fpls.2018.01049.

García A, Valenzuela JL, Manzano S, **Cebrián G,** Romero J, Aguado E, Garrido D, Jamilena M. 2017. Postharvest fruit quality in ethylene insensitive mutants of zucchini squash.
Acta Horticulturae **1256**, 217-222.
https://doi.org/10.17660/ActaHortic.2019.1256.30.

Jamilena M, Manzano S, Valenzuela JL, García A, Aguado E, Romero J, **Cebrián G.** 2017. Mutaciones útiles para la mejora genética de hortícolas.
Horticultura **328**, 52-58.

Other proceedings and congress communications

Romero J, Martínez C, Aguado E, García A, Iglesias-Moya J, **Cebrián G,** Jamilena M. 2021. BSA-seq reveals QTLs associated to ToLCNDV resistance in *Cucurbita moschata.* XII Eucarpia Meeting on Cucurbit Genetics and Breeding. Almería (Spain), May 24-28, pp 76. ISBN 978-84-1351-090-3.

Alonso S, **Cebrián G,** Iglesias-Moya J, Gautam KK, García A, Martínez C, Jamilena M. 2021. Screening of a Zucchini mutant collection for abiotic stress tolerance. XII Eucarpia Meeting on Cucurbit Genetics and Breeding. Almería (Spain), May 24-28, pp 34. ISBN 978-84-1351-090-3.

Iglesias-Moya J, Alonso S, **Cebrián G,** Romero J, García A, Martínez C, Jamilena M. 2021. The enhanced salt tolerance of the squash *etr2b* mutant is mediated by ABA. XII Eucarpia Meeting on Cucurbit Genetics and Breeding. Almería (Spain) May 24-28, pp 38. ISBN 978-84-1351-090-3.

García A, Aguado E, Romero J, **Cebrián G,** Martínez C, Garrido D, Jamilena M. 2019. Characterization of two novel androecious mutants in *Cucurbita pepo* L. VI International Symposium on Cucurbits. Ghent (Belgium), Jun 30-Jul 04, pp 96.

Aguado E, García A, Martínez C, Iglesias-Moya J, Romero J, **Cebrián G,** Jamilena M. 2019. Generation, selection and characterisation of ethylene insensitive mutants in watermelon. VI International Symposium on Cucurbits. Ghent (Belgium), Jun 30-July 04, pp 95.

Romero J, Aguado E, Martínez C, García A, Manzano S, **Cebrián G,** Paris HS, Jamilena M. 2018. Evaluación de distintas variedades de *Cucurbita* para resistencia al virus ToLCNDV. I Congreso de Jóvenes Investigadores en Ciencias Agroalimentarias. Almería (Spain), Dec 20, pp 352-353.

García A, Aguado E, Martínez C, Manzano S, Romero J, **Cebrián G,** Garrido D, Jamilena M. 2018. Genetic interactions between three ethylene insensitive mutants in the regulation of sex expression and sex determination in squash. I Congreso de Jóvenes Investigadores en Ciencias Agroalimentarias. Almería (Spain), Dec 20, pp 314-315.

Aguado E, García A, Manzano S, Martínez C, Romero J, **Cebrián G,** Jamilena M. 2018. Herencia de la trimonoecia en *Citrullus lanatus.* I Congreso de Jóvenes Investigadores en Ciencias Agroalimentarias. Almería (Spain), Dec 20, pp 278-279.

García A, Aguado E, Manzano S, Romero J, **Cebrián G,** Garrido D, Jamilena M. 2018. Genetic interactions between *EIN1*, *EIN2* and *EIN3* in the regulation of sex expression and sex determination in squash. Cucurbitaceae. Daves, California (USA), Nov 12-15, pp 73.

Aguado E, García A, Manzano S, Romero J, **Cebrián G,** Jamilena M. 2018. Genetic analysis of trimonoecy in watermelon. Cucurbitaceae. Daves, California (USA), Nov 12-15, pp 70.

Aguado E, Manzano S, García A, **Cebrián G,** Romero J, Valenzuela JL, Jamilena M. 2018. Análisis genético del papel de gen *CitACS4* en la maduración y calidad de la fruta de sandía. XII Simposio Nacional y X Ibérico de Maduración y Postcosecha 2018. Badajoz (Spain), Jun 04-07, pp 61-64. ISBN: 978-84-09-02799-6.

Villegas M, Manzano S, García A, Aguado E, Romero J, **Cebrián G,** Sances A, Valenzuela JL, Jamilena M. 2018. Papel del etileno en el comportamiento diferencial de la maduración del fruto en cuatro variedades de pimiento. XII Simposio Nacional y X Ibérico de Maduración y Postcosecha 2018. Badajoz (Spain), Jun 04-07, pp 69-71. ISBN: 978-84-09-02799-6.

García A, Romero J, **Cebrián G,** Aguado E, Manzano S, Guzmán M, Garrido D, Jamilena M. 2017. Rapid high-throughput phenotyping of an EMS mutant platform of *Cucurbita pepo* for tolerance to abiotic and biotic stresses. The COST/EPPN2020 workshop "Current and future applications of phenotyping for plant breeding". Novi Sad (Serbian),Sep 29-30, pp 93. ISBN 978-86-80417-77-6.

García A, Manzano S, Martínez C, Megías Z, Aguado E, **Cebrián G,** Romero J, Loska D, Beltran S, Cañizares J, Garrido D, Jamilena M. 2017. Evaluation of an EMS-induced squash library using phenomic and genomic approaches. The XIV Solanaceae and III Cucurbitaceae genomics joint conference. Valencia (Spain), Sep 03-06, pp 60.

Resumen

Cucurbita pepo es un cultivo hortícola económicamente importante a nivel mundial. El control genético de los rasgos morfológicos y fisiológicos que afectan la producción y la calidad de los cultivos es esencial para desarrollar programas de fitomejoramiento que mejoren, no sólo la producción de los cultivos o su tolerancia a los estreses bióticos y abióticos, sino también, los rasgos relacionados con la calidad, como la partenocarpia.

En zonas semiáridas, los estreses abióticos, como la salinidad, se están convirtiendo en factores cada vez más importantes afectando, el desarrollo vegetativo y reproductivo y la producción de los cultivos. El etileno (ET) tiene un papel relevante y contrastante en las respuestas de las plantas a los estreses ambientales. En esta tesis, hemos analizado los efectos sobre la tolerancia a la sal, de tres mutaciones de ganancia de función, *etr1a*, *etr1b* y *etr2b*, que afectan a los receptores de ET, CpETR1A, CpETR1B y CpETR2B de *Cucurbita pepo*. Se ha demostrado que los receptores de ET juegan un papel positivo en la tolerancia a la sal, mejorando la germinación, el establecimiento de plántulas y el posterior crecimiento vegetativo de las plantas. Los mutantes *etr1b*, *etr1a* y *etr2b* germinaron antes que WT bajo estrés salino y sus tasas de crecimiento en raíces y brotes, tanto en plántulas como en plantas, se vieron menos afectadas por la sal. Se encontró, que la respuesta de tolerancia a la sal en *etr2b* estaba asociada con una acumulación reducida de Na^+ en brotes y hojas, así como una mayor acumulación de solutos compatibles, que incluyen; prolina, carbohidratos totales y compuestos antioxidantes. Además, varios genes que codifican transportadores de cationes monovalentes de membrana, como; intercambiadores de Na^+/H^+ y K^+/H^+ (*NHX*), antiportadores de salida de K^+ (*KEA*), transportadores de alta afinidad de K^+ (*HKT*) y transportadores de captación de K^+ (*KUP*), también estaban altamente regulados por la salinidad en *etr2b* frente a WT. De acuerdo con ello, nuestros datos indican que la mayor tolerancia a la sal de *etr2b* está dirigida por la inducción de genes que excluyen el Na^+ de los órganos fotosintéticos, al tiempo que mantienen la homeostasis de K^+/Na^+ y el ajuste osmótico. La mayor regulación positiva de los genes involucrados en la señalización de Ca^{2+} (*CRCK*) y la biosíntesis de ABA (*NCED*) en hojas de *etr2b* bajo estrés salino, nos indica que la función de los receptores de ET en la respuesta al estrés salino puede estar mediada por las vías de señalización de Ca^{2+} y ABA, siendo el ET un regulador negativo de la tolerancia a la sal en *C. pepo*.

El ET es también el regulador clave de la expresión (ES) y el determinismo sexual (DS) en las especies monoicas de la familia Cucurbitaceae. Esta hormona, no sólo controla la proporción de flores masculinas y femeninas en la planta, sino también el mecanismo que hace que cada meristemo floral se determine como una flor femenina o masculina. Esto último se logra deteniendo el desarrollo del estambre o el carpelo en las primeras etapas del desarrollo de la flor. Hasta la fecha, se han descrito que muchos de los diferentes genes de biosíntesis y señalización de ET regulan los rasgos ES y DS en cucurbitáceas. Sin embargo, la interacción entre ET y otras hormonas en la regulación del desarrollo floral es poco conocida. En esta tesis hemos analizado un nuevo mutante de EMS en *C. pepo* que se ve afectado en DS. La mutación convierte las flores femeninas en hermafroditas e interrumpe la tasa de crecimiento y la maduración de los pétalos y carpelos, lo que retrasa la apertura de las flores femeninas, promoviendo el crecimiento de los ovarios y con ello, el desarrollo partenocárpico de los frutos. La re-secuenciación del genoma

completo permitió la identificación de la mutación causal del fenotipo, como una mutación sin sentido (G > A) en la región codificante de *CpACO1A*, un gen que codifica, una enzima ACO tipo I, la cual, comparte una alta identidad con *C. sativus* CsACO3 y *C. melo* CmACO1. El llamado *aco1a* redujo la actividad de ACO y la producción de ET en diferentes órganos donde se expresa el gen y redujo la sensibilidad a ET en las flores. *CpACO1A* y otros genes DS, incluidos, *CpACO2B*, *CpACS11A* y *CpACS27A*, mostraron una regulación de retroalimentación por ET de manera específica y temporal en los tejidos. Se descubrió que el ET y la regulación de retroalimentación positiva de *CpACO1A*, *CpACO2B*, *CpACS11A* y *CpACS27A* son responsables de determinar el destino del meristemo floral hacia una flor femenina, al promover el desarrollo de los carpelos y detener el desarrollo de los estambres. Además de su papel como hormona DS, el contenido de hormonas en *aco1a* sugirieron, que el papel positivo de ET en la maduración de los pétalos y la apertura de las flores, puede estar mediado por la inducción de la biosíntesis de ácido jasmónico (JA), mientras que su papel negativo en el crecimiento de los ovarios y el cuajado de los frutos podría estar mediado por su efecto represivo sobre la biosíntesis de auxinas (IAA).

En los últimos años, se ha descubierto que el JA es una hormona relevante en el desarrollo floral en numerosas especies, aunque, su función en el desarrollo floral de las cucurbitáceas y DS es desconocida. En esta tesis, se abordó la diafonía entre ET y JA en la regulación diferencial de la apertura de flores masculinas y femeninas y el desarrollo temprano de los frutos en *Cucurbita pepo* utilizando un nuevo mutante, *lox3a*, deficiente en JA, así como, los mutantes insensibles y deficientes en ET, *aco1a* y *etr2b*. La mutación EMS en *lox3a* suprimió la apertura de flores, tanto masculinas como femeninas, e indujo un desarrollo partenocárpico de los frutos. El análisis por BSA-seq y posterior mapeo fino, permitió la identificación de *lox3a* en el sitio de corte y empalme 5' del intrón 6 de *CpLOX3A*, un gen *LIPOXIGENASA* involucrado en la biosíntesis de JA. El contenido reducido de JA y la expresión disminuida de genes de biosíntesis (*CpLOX3A*, *CpAOS1A* y *CpJAR1B*) y señalización (*CpJAZ1B*, *CpCOI1B* y *CpMYB21B*) en flores masculinas y femeninas de *lox3a*, así como, el rescate del fenotipo *lox3a* mediante la aplicación externa de MeJA, demostraron que JA controla la elongación de pétalos y la apertura de las flores, así como, el aborto de los frutos en ausencia de fertilización. JA también rescató el fenotipo de los mutantes de ET, *aco1a* y *etr2b*, que son específicamente defectuosos en la apertura de las flores femeninas y el aborto de los frutos. Estos datos indican que el ET es inducido en las flores femeninas hacia la antesis, activando la producción de JA y promoviendo la apertura de la flor femenina y el aborto del ovario no fecundado. Dado que los ovarios de *aco1a* y *etr2b* retrasan su aborto hasta que las flores no alcanzan la apertura y el ovario de *lox3a* también aborta inmediatamente después de la apertura de la flor en respuesta a MeJA, proponemos, que la apertura de la flor puede actuar como un interruptor que desencadene el cuajado del fruto y desarrollo de los ovarios fertilizados, pero alternativamente, pueda inducir el aborto del ovario no fertilizado. Tanto el ET como el JA en los pétalos maduros y senescentes pueden servir como señales remotas que deciden el desarrollo alternativo del ovario y el fruto.

Palabras clave: tolerancia a la sal; germinación; etileno; ABA; ácido jasmónico; determinación del sexo; desarrollo floral; apertura de flores; diafonía JA-ET; partenocarpia.

Summary

Cucurbita pepo is an economically important horticultural crop worldwide. The genetic control of the morphological and physiological traits that affect crop production and quality is essential to develop breeding programs that improve not only crop production or tolerance to biotic and abiotic stresses, but also quality-related traits such as parthenocarpy.

In semiarid zones, abiotic stresses such as salinity are becoming increasingly important factors affecting both vegetative and reproductive development and crop production. Ethylene (ET) has a relevant and contrasting role in plant response to environmental stresses. In the present thesis, we have analysed the effects of three gain-of-function mutations, *etr1a*, *etr1b* and *etr2b*, affecting the ET receptors CpETR1A, CpETR1B and CpETR2B of *Cucurbita pepo*, on salt tolerance. It has been demonstrated that ET receptors play a positive role on salt tolerance, enhancing germination, seedling establishment, and subsequent vegetative plant growth. The mutants *etr1b*, *etr1a,* and *etr2b* germinated earlier than WT under salt stress, and root and shoot growth rates in both seedlings and plants were less affected by salt. The enhanced salt tolerance response of *etr2b* was found to be associated with a reduced accumulation of Na^+ in shoots and leaves, as well as a higher accumulation of compatible solutes, including proline, total carbohydrates, and antioxidant compounds. Several genes coding for membrane monovalent cation transporters, Na^+/H^+ and K^+/H^+ exchangers (*NHXs*), K^+ efflux antiporters (*KEAs*), high-affinity K^+ transporters (*HKTs*), and K^+ uptake transporters (*KUPs*) were also highly upregulated by salinity in *etr2b* versus WT. In addition, our data indicate that the enhanced salt tolerance of *etr2b* is led by the induction of genes that exclude Na^+ from photosynthetic organs, while maintaining K^+/Na^+ homeostasis and osmotic adjustment. The higher up-regulation of genes involved in Ca^{2+} signalling (*CRCKs*) and ABA biosynthesis (*NCED*) in *etr2b* leaves under salt stress indicates that the function of ET receptors in salt stress response can be mediated by Ca^{2+} and ABA signalling pathways, being ET a negative regulator of salt tolerance in *C. pepo.*

ET is also the key regulator of sex expression (SE) and sex determinations (SD) in the monoecious species of the Cucurbitaceae family. This hormone not only controls the ratio of male to female flowers on the plant, but also the mechanism that makes each floral meristem to be determined as a female or a male flower. The latter is achieved by arresting the development of stamen or carpel primordia in early stages of flower development. Different ET biosynthesis and signalling genes has been reported to regulate SD and SE traits in cucurbits. However, the interaction between ET and other hormones in the regulation of flower development is poorly understood. In this thesis, we analysed a new *C. pepo* EMS mutant that is affected in SD. The mutation converts female into hermaphrodite flowers and disrupts the growth rate and maturation of petals and carpels, delaying female flower opening, and promoting the growth rate of ovaries and the parthenocarpic development of the fruit. Whole-genome resequencing allowed the identification of the casual mutation

of the phenotype as a missense (G > A) mutation in the coding region of *CpACO1A*, a gene coding for a type I ACO enzyme that shares a high identity with *C. sativus* CsACO3 and *C. melo* CmACO1.The so-called *aco1a* reduced ACO activity and ET production in different organs where the gene is expressed, and reduced ET sensitivity in flowers. *CpACO1A* and other sex-determining genes, including *CpACO2B*, *CpACS11A* and *CpACS27A*, showed a feedback regulation by ET in a tissue- and temporal-specific manner. ET and the positive feedback regulation of *CpACO1A*, *CpACO2B*, *CpACS11A*, and *CpACS27A* was found to be responsible for determining the fate of the floral meristem towards a female flower by promoting the development of carpels and arresting the development of stamens. In addition to its role as a sex-determining hormone, other hormone contents in *aco1a* suggested that the positive role of ET on petal maturation and flower opening can be mediated by inducing the biosynthesis of JA, while its negative role on ovary growth and fruit set could be mediated by its repressive effect on IAA biosynthesis.

JA has been found to be a relevant hormone on flower development in numerous species, but its function in cucurbit floral development and SD is unknown. Crosstalk between ET and JA in the differential regulation of male and female flower opening and in early fruit development in *Cucurbita pepo* was addressed by using the novel JA-deficient mutant *lox3a* and the ET-deficient and -insensitive mutants *aco1a* and *etr2b*. The EMS *lox3a* mutation suppressed both male and female flower opening, and induced the development of parthenocarpic fruit. A BSA-seq and fine mapping approach allowed the identification of *lox3a* in the 5'-splicing site of intron 6 in *CpLOX3A*, a *LYPOXYGENASE* gene involved in JA biosynthesis. The reduced JA content and diminished expression of JA biosynthesis (*CpLOX3A*, *CpAOS1A* and *CpJAR1B*) and signalling (*CpJAZ1B*, *CpCOI1B* and *CpMYB21B*) genes in male and female flowers of *lox3a*, and the rescue of *lox3a* phenotype by external application of MeJA, demonstrated that JA controls petal elongation and flower opening, as well as fruit abortion in the absence of fertilization. JA also rescued the phenotype of ET mutants *aco1a* and *etr2b*, which are specifically defective in female flower opening and fruit abortion. These data indicate that ET is induced in female flowers towards anthesis, activating JA production and promoting the aperture of the female flower and the abortion of the unfertilized ovary. Given that *aco1a* and *etr2b* ovaries delayed their abortion until the flower reached opening, and the *lox3a* ovary also aborted immediately after flower opening in response to MeJA, we proposed that flower opening can act as a switch that triggers fruit set and development in fertilized ovaries but may alternatively induce the abortion of the unfertilized ovary. Both ET and JA from mature and senescent petals can serve as remote signals that determine the alternative development of the ovary and fruit.

Keywords: salt tolerance; germination; ethylene; ABA; Jasmonic acid; sex determination; flower development; flower opening; JA-ET crosstalk; parthenocarpy.

Abbreviation list

A

A: Anthesis
A-2: 2 days before anthesis
ABA: Abscisic acid
ABAs: *ABA DEFICIENTS*
ACO: ACC OXIDASE
aco1a: *1-aminocyclopropane-1-carboxylic acid oxidase 1a*
ACS: ACC SYNTHASE
AF: Allele frequency
AI: Andromonoecy index
ANOVA: Analysis of variance
AM: Arbuscular mycorrhizal
A95V: Amino acid substitution of Alanine by Valine at position 95

B

BA: 6-Benzyladenine
BC_1S_1: Backcross-1 selfed-1
BC_2: Backcross-2
BC_2S_1: Backcross-2 selfed-1
BHQ-1: Black hole quencher-1
BLAST: Blast alignment search tool
bp: base pair
BRs: Brassinosteroids
BWA: Burrows-wheeler aligner

C

°C: Degrees Celsius
Ca: Calcium element
Ca^{2+}: Calcium ion
CaM: Calmodulins
CBL: Calcineurin B-like
cDNA: complementary DNA
CKs: Cytokines
Cl^-: Chlorides
cm: centimeters
CML: CaM-like
CRCKs: Calmodulin binding receptor-like cytoplasmic kinases
Ct: Control
cTP: Chloroplast transit peptide
CTAB: Cetyltrimethylammonium bromide
CuGenDB: Cucurbit Genomics Database
CUPSAT: Cologne university protein stability analysis tool
CWR: Crop wild relatives

D

d: days
DAS: Days after sowing
ΔΔG: Delta Delta Gibbs
DIOX_N: non-haem dioxygenase in morphine synthesis N-terminal
DNA: Deoxyribonucleic acid
DP: Read Depth
dS/m: deciSiemens per meter
DW: Distilled water
DW: Dry weight

E

E340K: Amino acid substitution of Glutamic acid by Lysine at position 340
EF1α: Elongation factor 1-alpha
ein2: *ethylene insensitive 2*
EIN4: ETHYLENE INSENSITIVE 4
EMS: Ethyl methanesulfonate
ER: Endoplasmic reticulum
ERS1/2: ETHYLENE RESPONSE 1/2
ET: Ethylene
ETR1/2: ETHYLENE RECEPTOR 1/2
etr1a: *ethylene receptor 1a*
etr1a-1: *ethylene receptor 1a-1*
etr1b: *ethylene receptor 1b*
etr2b: *ethylene receptor 2b*

F

FB: Floral bub
FFB: Female floral bud
FID: Flame ionization detector
Fig.: Figure
FW: Fresh weight

G

g: grams
GA3: Gibberellic acid

GAs: Gibberellins
GBS: Genotyping by sequencing
GC: Gas chromatograph
GOF: Gain-of-function
GQ: Genotype quality
GSDS: Gene Structure Display Server
GWAS: Genome-wide association studies

H

h: hours
HAK/KT/KUP: High-affinity K^+ transporters
HCl: Hydrochloric acid
HKT1: High-affinity K^+ transporter 1

I

IAA: Indole-3-acetid acid
IBA: Indole-3-butyric acid
ICP-OES: Inductively coupled plasma optical emission spectroscopy
i.e.: *id est*
IGV: Integrative Genomics Viewer
ISO: International Organisation for Standardisation

J

JA: Jasmonic acid
JAs: Jasmonates
JA-Ile: Jasmonic acid-isoleucine

K

K: Potassium element
K^+: Potassium ion
KASP: Kompetitive allele specific PCR
Kb: Kilobyte
KEAs: K^+/H^+ efflux antiporters
Kg: Kilogram
KUPs: K^+ uptake permeases

L

L: Liter
LOF: Loss-of-function
LOQ: Limit of Quantification
LOX: Lipoxygenase
lox3a: *lipoxygenase 3a*
LRs: Lateral roots
LSD: Least significant difference

M

MAPP: Multivariate analysis of protein polymorphism
µL: microliter
µmol micromole
µg: microgram
1MCP: 1-Methylcyclopropene
Mb: Megabyte
MEGA X: Molecular Evolutionary Genetics Analysis X
MeJA: Methyl jasmonate
MFB: Male floral bud
MHZ7/OsEIN2: Ethylene-insensitive protein 2
min: minute
mg: milligram
mL: milliliter
mm: millimeter
mM: millimolar
MOCA1: MONOCATION-INDUCED $[Ca^{2+}]I$ INCREASES 1
MOPS: 3-(N-morpholino) propanesulfonic acid
MUpro: Predictions of Protein Stability Changes Upon Mutations

N

N: Nitrogen
n.d: no data
Na: Sodium element
Na^+: Sodium ion
NaCl: Sodium chloride
NCBI: National Center for Biotechnology Information
NCEDs: Nine-cisepoxycarotenoid dioxygenases
ng: nanogram
NHXs: Na^+/H^+ exchanger
nL: nanoliter
nm: manometer
nmol: nanomole
No.: Number
NO_3^-: Nitrate

NSCCs: Non-selective cation channels

P

%: Percentage
P5L: Amino acid substitution of Proline by Leucine at position 5
P36L: Amino acid substitution of Proline by Leucine at position 36
PCD: Programmed cell death
PCR: Polymerase chain reaction
PE150 bp: Paired-end 150 bp
ppb: parts per billion
ppm: parts per million
PVPP: Polyvinylpolypyrrolidone
PYR: PYRABACTIN RESISTANCE
PYL: PYRABACTIN RESISTANCE LIKE

Q

qPCR: quantitative PCR
qRT-PCR: quantitative real time PCR

R

RCSB PDB: Research Collaboratory for Structural Bioinformatics Protein Data Bank
RH: Relative humidity
RNA: Ribonucleic acid
ROS: Reactive oxygen species

S

s: second
SA: Salicylic acid
SAM: S-adenosyl-L-methionine
SE: Sex expression
SD: Sex determination
SNAP^2: Predicting Functional Effects of Sequence Variants
SNP: Single Nucleotide Polymorphism
SnRKs: SUCROSE NON-FERMENTING RELATED PROTEIN KINASES
SOS1: SALT OVERLY SENSITIVE 1
SLs: Strigolactones

T

T94I: Amino acid substitution of Threonine by Isoleucine at position 94
TF: Transcription factor
TSS: Total soluble sugars

U

Ub: Ubiquitination
UPLCQ-TOF/MS/MS: Ultra-high performance liquid chromatography quadrupole time-of-flight mass spectrometry

W

WEI2: Weak ET insensitive 2
WGS: Whole genome sequencing
WT: Wild type

X

x *g*: Relative Centrifugal Force

Table of contents

Resumen **16**

Summary **20**

Abbreviation list **24**

1. Introduction **34**

1.1. *Cucurbita pepo* **36**

1.1.1. Origin, domestication, and taxonomy 36
1.1.2. Genomic resources 38

1.2. Ethylene: biosynthesis, perception and signaling **40**

1.2.1. Ethylene biosynthesis 40
1.2.2. Ethylene perception 43
1.2.3. Ethylene signaling pathway 45

1.3. Jasmonates: biosynthesis, perception and signaling **47**

1.3.1. Jasmonates biosynthesis 48
1.3.2. Jasmonates perception and signaling 51

1.4. Hormonal regulation of abiotic stress tolerance: salinity stress **53**

1.4.1. Hormonal role on salinity stress response 53
1.4.1.1. **ABA** - "The stress response hormone" 55
1.4.1.2. **SA** and **JA** - "Homeostasis and spatiotemporal specificity" 55
1.4.1.3. **IAA** - "Mediated root growth plasticity" 56
1.4.1.4. **GAs** and **CKs** - "Self-sacrifice to help plants to survive" 56
1.4.1.5. **BRs** and **SLs** - "Positive interaction with other signal molecules" 57

1.4.2. Ethylene (ET) signaling under salinity stress 58
1.4.2.1. **ET** - "Contrasting signaling roles for salt tolerance" 58

1.5. Flower development in cucurbits **60**

1.5.1. Sex expression (SE) and sex determination (SD) 60
1.5.2. Environmental factors controlling SE and SD 61
1.5.3. Hormonal factors regulating SE and SD 62
1.5.4. Molecular and genetic control in SE and SD 64

1.6. Hormonal regulation of cucurbits flower development **66**

1.6.1. Involvement of ET in flower development and fruit set 66
1.6.2. Involvement of JA in flower development and fruit set 68

2. Objectives **72**

3. Involvement of ethylene receptors in the salt tolerance response of *Cucurbita pepo* **78**

3.1. Abstract **80**

3.2. Introduction **81**

Table of contents

3.3. Materials and methods…….. 85

3.3.1. Plant material…… 85
3.3.2. Seed germination under salinity stress…….. 85
3.3.3. Seedling and plantlets growth under salinity stress…… 86
3.3.4. Vegetative growth of WT and *etr2b* under salinity stress…… 87
3.3.5. Evaluation of stress-associated metabolites in WT and *etr2b* plants. 87
3.3.6. Comparison of micro- and macro-elements in WT and *etr2b* plants.. 88
3.3.7. Assessment of gene expression by qRT-PCR in WT and *etr2b* plant 88
3.3.8. Phylogenetic analysis…… 89
3.3.9. Statistical analysis…… 89

3.4. Results…… 89

3.4.1. Tolerance of *etr1b*, *etr1a*, and *etr2b* to salt stress during germination and early stages of seedling development…….. 89
3.4.2. Growth and ionic balance of WT and *etr2b* plant in response to salt stress…….... 94
3.4.3. Comparison of stress metabolites and gene expression in WT and *etr2b* in response to salt stress…..…….. 96

3.5. Discussion…… 99

3.5.1. ETR receptors modulate salt tolerance response at germination and during seedling and plant vegetative growth…… 99
3.5.2. Mechanisms of salt tolerance in *C. pepo etr* mutants…… 102

4. The ethylene biosynthesis gene *CpACO1A*: a new player in the regulation of sex determination and female flower development in *Cucurbita pepo* 106

4.1. Abstract…….. 108

4.2. Introduction……... 109

4.3. Materials and methods……... 111

4.3.1. Plant material and isolation of mutants……... 111
4.3.2. Phenotyping for monoecy stability, sex expression, and floral traits.. 111
4.3.3. Identification of *aco1a* mutation by whole-genome sequencing analysis……... 112
4.3.4. Validation of the identified mutations by high-throughput genotyping of individual segregating plants……... 113
4.3.5. 1-aminocyclopropane-1-carboxylic acid oxidase enzyme activity….. 113
4.3.6. Ethylene production measurements……... 114
4.3.7. Assessing ethylene sensitivity…… 114
4.3.8. Hormone concentration measurements…… 115
4.3.9. Bioinformatics and phylogenetic analysis…….. 115
4.3.10. Assessment of relative gene expression by quantitative RT-PCR... 116
4.3.11. Statistical analyses…… 116

4.4. Results…… 117

4.4.1. *aco1a* impairs sex determination and petals and ovary development 117
4.4.2. *aco1a* is a missense mutation causing P5L substitution in the ethylene biosynthesis enzyme CpACO1A…… 120

Table of contents

4.4.3. Gene structure and phylogenetic relationships of *CpACO1A*……. 123
4.4.4. The *aco1a* mutation impairs *CpACO1A* expression, ACO activity, and ethylene production and sensitivity……. 125
4.4.5. Expression of different sex-determining genes in WT and *aco1a* flowers……. 129
4.4.6. Hormone imbalance in early female development of *aco1a* flowers... 131

4.5. Discussion……. 132

4.5.1. *aco1a* disrupts ethylene biosynthesis and hormonal balance during female flower development…….. 132
4.5.2. *CpACO1A* prevents stamen development in squash female flowers. 134
4.5.3. *CpACO1A* controls flower opening and ovary development in the absence of pollination……... 135

5. Jasmonate-deficient mutant *lox3a* reveals crosstalk between JA and ET in the differential regulation of male and female flower opening and early fruit development in *Cucurbita pepo* 138

5.1. Abstract…….. 140

5.2. Introduction……... 141

5.3. Materials and methods……... 142

5.3.1. Plant material and isolation of mutants……... 144
5.3.2. Phenotyping for sex expression and floral traits…… 144
5.3.3. Identification of *lox3a* mutation by WGS……. 145
5.3.4. High-throughput SNP genotyping for validating the *lox3a* mutation.. 146
5.3.5. Analysis of 5´splicing site mutation by Sanger sequencing……. 146
5.3.6. Assessing ET production and sensitivity…… 147
5.3.7. MeJA external treatments……. 147
5.3.8. JA concentration measurement……... 148
5.3.9. Bioinformatics and phylogenetic analysis…….. 148
5.3.10. Assessment of gene expression by RT-qPCR…… 149
5.3.11. Statistical analyses……. 149

5.4. Results…… 150

5.4.1. *lox3a*, *a new mutant* impaired the maturation of petals and flower opening……... 150
5.4.2. *lox3a* is a 5´-splicing site mutation in the JA biosynthesis gene *CpLOX3A*……... 153
5.4.3. *CpLOX3A* structure and phylogeny……. 155
5.4.4. JA rescues the phenotype of the JA deficient *lox3a*……. 157
5.4.5. Crosstalk between JA and ET in flower maturation and opening…… 162

5.5. Discussion……. 165

5.5.1. *lox3a* is a JA-deficient mutant affected in flower opening and ovary development……..... 165
5.5.2. Crosstalk between ET and JA in the differential regulation of female- and male-flower development and opening……. 168
5.5.3. Crosstalk between ET and JA in parthenocarpic fruit development… 170

Table of contents

6. General conclusions **174**

7. References **180**

8. Supplementary material **204**

8.1. Supplementary tables…… 206

Table S3.1. Primers and TaqMan probes used for genotyping *etr1a*, *etr1b* and *etr2b* mutations…….. 206
Table S3.2. List of primer sequences used for qRT-PCR analysis…… 206
Table S4.1. List of the *ACO* genes and proteins used in phylogenetic analysis……... 207
Table S4.2. Primers used for gene expression analysis by qPCR…… 208
Table S4.3. Inheritance of *aco1a* mutant in the backcrossing and selfing generations……. 208
Table S4.4. Validation of the identified mutations by high-throughput genotyping of individual segregating plants……... 209
Table S4.5. EMS mutations in chromosome 4 of *aco1a* mutant line…….. 214
Table S5.1. Inheritance of lox3a mutant in the backcrossing and selfing generations……. 214
Table S5.2. List of the *LOX* genes and proteins used in phylogenetic analysis……... 215
Table S5.3. Primers used for gene expression analysis by qPCR…….. 216

8.2. Supplementary figures……... 217

Figure S3.1. Device designed to study *C. pepo* seed germination between two sandwich glasses…… 217
Figure S3.2. Phylogenetic relationships for different gene families in *Cucurbita pepo* and Arabidopsis……. 217
Figure S5.1. Sex expression and sex determination of WT and *lox3a* plants 218
Figure S5.2. Schematic representation of the effects of G > A transition on the 5´-splicing site of intron 6 in the JA biosynthesis gene *CpLOX3A*……. 219
Figure S5.3. Relative gene expression of *LOX* genes in vegetative and reproductive organs of WT and *lox3a* plants…….. 220

8.3. Supplementary dataset…….. 221

Dataset S5.1. Fine mapping of the three identified mutations in *lox3a* plants……... 221

9. Annexes **226**

1. Introduction

1.1. *Cucurbita pepo*

1.1.1. Origin, domestication, and taxonomy

Cucurbitaceae family includes several economically important vegetables crops cultivated and distributed worldwide. These are cucumber (*Cucumis sativus* L.), melon (*Cucumis melo* L.), watermelon (*Citrullus lanatus* (Thunb. Matsum. and Nakai.) and species of pumpkins, gourds, and squash (*Cucurbita* L. *spp*.) (Paris, 2016*a*; Kates *et al.*, 2017; Xanthopoulou *et al.*, 2019; Chomicki *et al.*, 2020). *Cucurbita* L. *spp.* are native to the Americas and have the highest diversity within the Cucurbitaceae family. Wild plants are tendril-bearing, branched vines, procumbent or climbing, with slender stems (Decker, 1988; Sanjur *et al.*, 2002; Paris, 2010; Paris *et al.*, 2012). The peculiarity of the cultivated species lies in the highly diversity of fruits, varying widely in size, shape, surface topography, color, and color pattern.

The genus *Cucurbita* consists of 13 species, of which at least five have been domesticated: *Cucurbita pepo* L, *Cucurbita moschata* Duchesne, *Cucurbita maxima* Duchesne, *Cucurbita argyrosperma* Huber and *Cucurbita ficifolia* Bouché (Bisognin, 2002; Paris, 2016*b*). All species of *Cucurbita* are diploids with 20 pairs of chromosomes (2n = 2x = 40) (Whitaker and Davis, 1962). *Cucurbita pepo* is the most economically important species within the genus and phenotypically the most polymorphic. It comprises five taxa, three crop wild relatives (CWRs)*, Cucurbita pepo* ssp. *fraterna*, *Cucurbita pepo* ssp. *ovifera* var. *texana*, and *Cucurbita pepo* ssp. *ovifera* var. *ozarkana*; as well as the two cultivated*, Cucurbita pepo* ssp. *pepo* and *Cucurbita pepo* ssp. *ovifera* var. *ovifera* (Paris, 2016*a*; Xanthopoulou *et al.*, 2019; Martínez-González *et al.*, 2021). It has been documented two independent domestication events for *Cucurbita pepo* (Decker, 1988; Paris, 2010; Kates *et al.*, 2017). One is presumed to have occurred 10,000 years ago in Mexico and corresponds to *Cucurbita pepo* ssp. *pepo* possibly from *Cucurbita pepo* ssp. f*raterna*. However, there is genetic evidence indicating that *C. pepo* ssp. *fraterna* is more closely related to *C. pepo* ssp. *ovifera* than to *C. pepo* ssp. *pepo* (Decker, 1988; Smith, 1997; Martínez-González *et al.*, 2021). The second domestication event tookplace 5,000 years ago in Southeast United States for *C. pepo* ssp. *ovifera* var. *ovifera*, likely from *C. pepo* ssp. *ovifera* var. *ozarkana* (Sanjur *et al.*, 2002; Smith, 2006). In additions, *Cucurbita pepo* ssp. *fraterna*, is not cultivated and grows wild in northeastern

Mexico, this ssp. is considered by some to be the wild progenitor of ssp. *pepo* (Xanthopoulou *et al.*, 2019; Martínez-González *et al.*, 2021). Whole-genome sequencing (WGS) has provided an improved understanding of the underlying genomic regions involved in the independent evolution and domestication of two cultivated ssp. *Cucurbita pepo* ssp. *pepo* and *Cucurbita pepo* ssp. *ovifera* var. *ovifera.* The *Cucurbita pepo* ssp. *pepo* encompasses most of the cultivated germplasm, but no wild relatives have been discovered. The *Cucurbita pepo* ssp. *ovifera* var. *ovifera* encompasses the remaining cultivated germplasm (Xanthopoulou *et al.*, 2019).

The two cultivated subspecie of *C. pepo* are composed of four edible-fruit types, also known as fruit-shape morphotypes. Fruit-shape is a polygenically inherited trait that changed little during fruit growth and is of utmost consumer importance (**Fig. 1**). Based on molecular genetic polymorphisms, the *Cucurbita pepo* ssp. *pepo* is the most widely cultivated of the two ssp. includes Vegetable Marrow, Cocozelle, Pumpkin and Zucchini groups. Its immature fruits are very popular vegetable around the world especially those of the Vegetable Marrow, Cocozelle and Zucchini Group. On the other hand, *Cucurbita pepo* ssp. *ovifera* var. *ovifera* includes the morphotypes Acorn, Scallop, Crookneck and Straightneck (Xanthopoulou *et al.*, 2019) (**Fig. 1**).

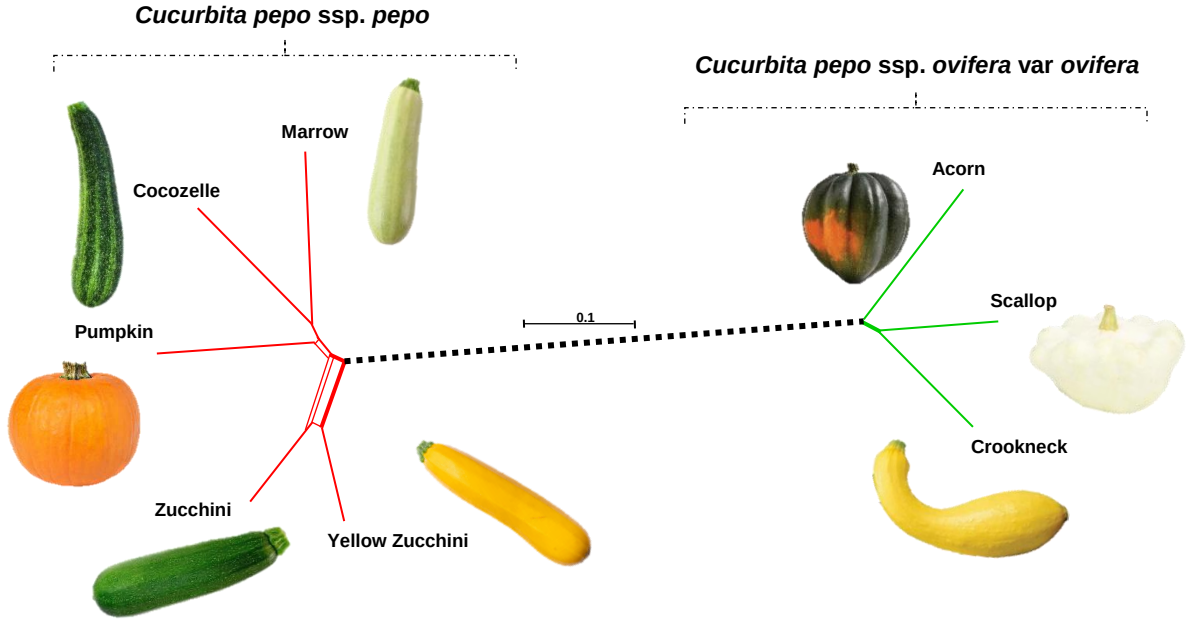

Figure 1. Phylogenetic network showing the relationship of the different morphotypes of *Cucurbita pepo.* Adapted from Xanthopoulou *et al*., 2019.

1.1.2. Genomic resources

The growing demand of consumers for obtaining fresh, high-quality, healthy, and sustainable products, as well as the concern to know and try new varieties, has led in recent years to a strong development of new genomic tools. Despite the importance of *Cucurbita* genus, not many genetic and genomic tools were available until recently. Fortunately, the rise of new sequencing technologies in the last years has helped to increase genetic knowledge, a clearer understanding of the biology of the species of this genus (Montero-Pau *et al.*, 2016; Paris, 2016*b*, 2018). As a result, we have extensive phytogenic resources, including molecular markers, sequenced genomes, and genotyping by sequencing (GBS) combined with genome-wide association studies (GWAS) that has led to the discovery of SNPs controlling horticulturally important traits enabling the improve of skills in breeding programs of the *Cucurbita* crops. The main goals of this breeding program are related to yield, along with fruit quality and resistance to disease or environmental stresses (Esteras *et al.*, 2012; Sun *et al.*, 2017; Montero-Pau *et al.*, 2018; García *et al.*, 2018; Xanthopoulou *et al.*, 2019).

In additions, the new sequencing technologies have confirmed another piece of evidence, the genus *Cucurbita* presents complete genome duplication, a fact not observed in other species of the Cucurbitaceae family (cucumber, melon and watermelon) (Esteras *et al.*, 2012, Weeden, 1984). Recently, the novo-assembly of three *Cucurbita* genomes (*C. pepo*, *C. maxima* and *C. moschata*) have confirmed an allotetraploid origin of *Cucurbita* genus from two progenitors that diverged approximately 30 million years ago (Sun *et al.*, 2017; Montero-Pau *et al.*, 2018). Further, after the allotetraploidization event, a low level of interchromosomal exchanges took place, suggesting high karyotype stability (Sun *et al.*, 2017). However, differences in the expression patterns have been detected between the two subgenomes. The annotation of *Cucurbita pepo* genome shows that it consists of 263 Mb and 27,868 gene models organized into 20 chromosomes (Sun *et al*., 2017; Montero-Pau *et al.*, 2018; Zheng *et al.*, 2019; Xanthopoulou *et al.*, 2019).

Due to rapid advances in sequencing technologies, high-quality reference genomic sequences of various cucurbit crops accessions have been generated and are available for query in various genomics and functional genomics databases Cucurbit Genomic Database (CuGenDB) (http://cucurbitgenomics

.org/) brings together a set of genomes and transcriptomes of the species of the Cucurbitaceae family, an important tool for evolutionary, genetic and breeding studies, including the discovery of new gene function (Zheng *et al.*, 2019).

In addition to existing natural variability, there are sources of induced variability, consisting of populations and platforms of mutants generated through the use of mutagenic agents. Currently, the populations of these mutant plants have become an important source of variability for both functional genomic analyses and plant breeding programs (Tai, 2013; C.Li *et al.*, 2018; García *et al.*, 2018). One of the most common mutant agents used for inducing mutations in plants is ethyl methanesulfonate (EMS), a chemical mutagen that induces single randomly distributed nucleotide changes (G > A / C > T) in DNA (Sega, 1984; Amini, 2014). The aleatory effect of this chemical mutagen is an advantage due to the variety of mutations that can be generated (synonymous, non-synonymous, splice acceptor or donor mutations, among others). However, it should be considered that this could also be an inconvenient, since large mutant populations have to be screened for finding the desired gene mutation.

The proliferation of mutant platforms has occurred mainly in cultivated species of high agronomic interest, such as legumes, cereals, greens and vegetables species of the Solanaceae, Brassicaceae and Cucurbitaceae families (Harloff *et al.*, 2012; Okabe *et al.*, 2013; Boualem *et al.*, 2014; Vicente-Dólera *et al.*, 2014; García *et al.*, 2018). Once established, the mutant platforms can be used for direct phenotyping screenings (forward genetics), but also for high throughput screening of DNA, allowing the detection of single point mutations (SNPs) in a number of specific genes (reverse genetics). TILLING (*Targeted Induced local Lesions IN Genomes*) is a high performance and low cost reverse genetic tool allowing the identification of gene mutations in large mutant platforms (Sikora *et al.*, 2011; Kurowska *et al.*, 2011; Chen *et al.*, 2014; Tadele, 2016; Till *et al.*, 2018). TILLING has not only increased sequence-function association processes, this technology goes beyond functional genomics and can be useful in crop breeding programs.

In *Cucurbita pepo*, the first mutant platform was developed for assessing different target genes by using TILLING (Vicente-Dólera *et al.*, 2014), but a larger mutant and TILLING platform was recently developed in *Cucurbita pepo* for forward and reverse genetic analyses (García *et al*., 2018).

Currently, new useful agronomically interesting mutants are being available thanks to massive high-throughput screenings of mutant collections based on plant phenotyping. Although a large number of plants have to be evaluated for each of the traits under study, the development of new sequencing tools is also making forward genetics a powerful tool for revealing the genes that control agronomically important traits (Long *et al.*, 2008; Li *et al.*, 2015; Van den Broeck *et al.*, 2020).

1.2. Ethylene: biosynthesis, perception, and signaling

Ethylene (IUPAC name ethene) is the simplest olefin gas and was the first gaseous molecule shown to function as phytohormone. It is well-known in different plants species, to affect and regulates multiple aspects of plant developmental processes (practically all), such as dormancy rupture, germination, plant growth, root nodulation, cell respiration, sex expression, flowers developments, fruit ripening, fruit postharvest quality, senescence, and abscission as well as responses to various stresses, such as flooding, drought, high salt, and soil compaction among many others (Byers *et al.*, 1972; Bleecker and Kende, 2000; Achard *et al.*, 2006; Binder *et al.*, 2012; Khan *et al.*, 2017; Binder, 2020; Riyazuddin *et al.*, 2020; Martínez and Jamilena, 2021). Ethylene exerts its action at very low concentrations in almost all tissues of the plant, which requires a modulation of its production at different plant developmental stages. Due to its importance in plants, the molecular control of the biosynthesis, perception and signaling pathways has been subject to intensive study, being cucurbits one of the most studied mode (Binder *et al.*, 2012; Ju and Chang, 2015; Binder, 2020; Pattyn *et al.*, 2021).

1.2.1. Ethylene biosynthesis

The ethylene biosynthesis pathway is relatively simple, taking place via only two committed enzymatic reactions. The first step is the formation of the general substrate *S*-adenosyl-L-methionine (SAM) by the enzyme SAdoMet synthetase (SAMS) from Yang cycle methionine (**Fig. 2**) (Adams *et al.*, 1979; Houben and Van de Poel, 2019; Pattyn *et al.*, 2021). SAM is also used as substrate for many other biochemical biosynthesis pathways, including polyamines (spermidine and spermine), molecules involved in many aspects of plant growth, development and

stress responses, and as a donor in transmethylations reactions catalysed by methyltransferases, enzymes which catalyse methylation of a wide range of substrates, such as histones, DNA and RNA to modify transcription and translation (Loenen, 2018). The most critical step in ethylene biosynthesis is the conversion of SAM into 1-aminocyclopropane-1-carboxylate (ACC) or 5′-methylthioadenosine (MTA), catalysed by ACC Synthase (ACS). In the final step, ACC is oxidized by ACC oxidase (ACO) to form ethylene, producing CO_2 and cyanide (the toxicity of the cyanide by-product is rapidly dealt with by conversion into β-cyanoalanine) (**Fig. 2**) (Houben and Van de Poel, 2019; Pattyn *et al*., 2021).

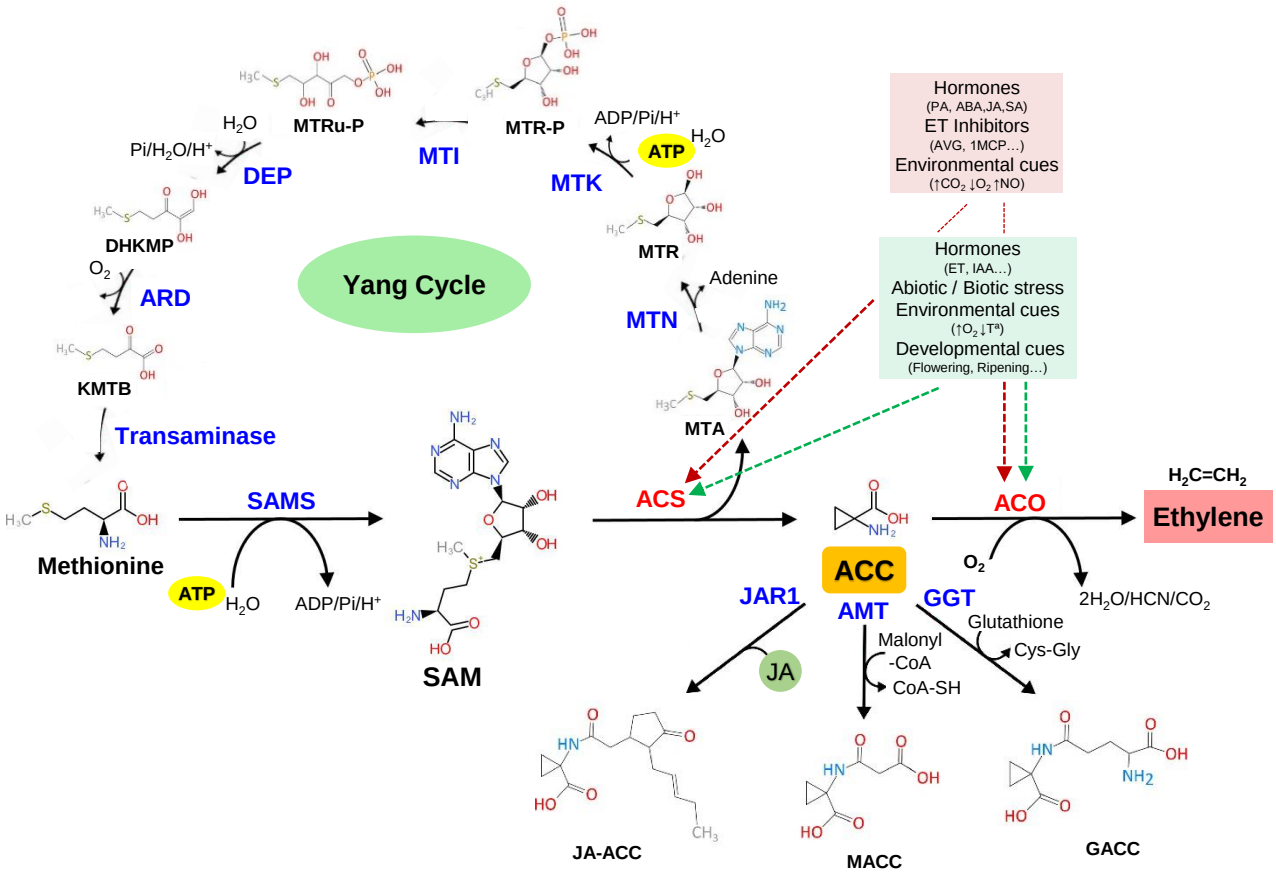

Figure 2. Structural representation of ethylene biosynthesis pathway from Methionine (Yang Cycle by-product) and regulation of the enzymes ACC synthase (ACS) and ACC oxidase (ACO). Green and red boxes indicate different promoting and blocking agents for the two-biosynthesis enzymes, respectively. Adapted from, García, 2019, Houben and Van de Poel, 2019 and Pattyn *et al*., 2020.

ACS enzymes are encoded by a multigene family and belongs to the family of pyridoxal-5′-phosphate (PLP) dependent aminotransferases, which require vitamin B6 as a co-factor for activity (Boller *et al.*, 1979; Pattyn *et al.*, 2021). In the Cucurbitaceae species, several different genes have been cloned which are highly homologous with the isoforms described in Arabidopsis and tomato, being *Cucumis sativus* in which more isoforms have been described (*CsACS1*, *CsACS1G*, *CsACS2*, *CsACS3*, *CsACS4*, and *CsACS11*) (Kamachi *et al*., 1997; Trebitsh *et al*., 1997; Shiomi *et al*., 1998; Boualem *et al*., 2015, 2016). Other orthologous genes described have been, *CmACS7* and *CmACS11* in *Cucumis melo* (Boualem *et al.*, 2009, 2015) or *CitACS4* in *Citrullus lanatus* (Manzano *et al.*, 2016; Ji *et al.*, 2016; J.Zhang *et al.*, 2017; Aguado *et al.*, 2020). The discovery of a complete duplication in the genus *Cucurbita* has allowed the identification of at least two paralogous for most of *ACS* genes, although that only one of the copies has maintained its function (Martínez *et al.*, 2014; García *et al.*, 2020*a*,*b*).

ACO enzymes also belong to multigene families. They are member of the 2-oxoglutarate-dependent dioxygenase (2OGD) superfamily, which require ferrous iron (Fe^{2+}) as the active-site co-factor, and 2OG and molecular oxygen as co-substrates for activity (Kawai *et al.*, 2014). ACO is unique within this family because it uses ascorbate, not 2OG, as a co-substrate (Houben and Van de Poel, 2019; Pattyn *et al.*, 2021). In the same way as the ACS, several different genes and isoforms have been described in Cucurbitaceae species. In *Cucumis sativus* four *ACO* genes have been isolated, *CsACO1*, *CsACO2*, *CsACO3* and *CsACO4* (Kahana *et al.*, 1999; Chen, 2012; Chen *et al.*, 2016). Other orthologous genes, including *CmACO1* and *CmACO3,* have been discovered in *Cucumis melo* (Dahmani-Mardas *et al.*, 2010; Chen *et al.*, 2016). Two *CpACO2* paralogs have been found in the duplicated genome of *Cucurbita pepo*, but only one of each maintains its expression and function (García, 2019; García *et al.*, 2020*a,b*).

Because ACS and ACO are the only two enzymes involved in ethylene biosynthesis, much of the regulation of overall ethylene production occurs by manipulating transcription, translation and protein stability of these two enzymes (Pattyn *et al.*, 2021). Furthermore, ACS and ACO show tissue specific expression and localisation patterns indicating that both ACS and ACO are under tight regulatory control, which takes place at the transcriptional, posttranscriptional and posttranslational level (Riyazuddin *et al.*, 2020; Pattyn *et al.*, 2021).

Thus, a diverse group of factors can enhance ethylene production by modulating the transcription or the activity of ACS and ACO, including abiotic and biotic stresses, as well as hormonal, genetic and environmental stimuli (**Fig. 2**) (Pattyn *et al.*, 2021). Additionally, the ethylene production is also regulated by ACC homeostasis, which encompasses ACC biosynthesis, transport, and conjugation for its derivates, malonyl-ACC (MACC), glutamyl-ACC (GACC) and jasmonyl-ACC (JA-ACC) (**Fig. 2**) (Houben and Van de Poel, 2019; Riyazuddin *et al.*, 2020; Pattyn *et al.*, 2021).

1.2.2. Ethylene perception

The first step in ethylene perception is the binding of ethylene to receptors. Ethylene receptors, as well as other component-like receptors (phytochromes and cytokinin), have been acquired by plants from the cyanobacterium that gave rise to chloroplasts. Recent phylogenetic analysis suggest that common origin (Shakeel *et al.*, 2013; Ju and Chang, 2015). Early studies and subsequent research on specific receptor isoforms from various plants have confirmed that ethylene receptors are localized to the endoplasmic reticulum (ER) (Chen *et al.*, 2002; Ju and Chang, 2012). The ethylene perception and signaling genes have been identified by the analysis of mutants with altered ethylene response in Arabidopsis (Binder *et al.*, 2012). Five ethylene receptors have been identified and are referred to as ethylene response 1 and 2 (AtETR1, AtETR2), ethylene response sensor 1 and 2 (AtERS1, AtERS2), and ethylene insensitive 4 (AtEIN4). Mutations in any one of these receptors prevents ethylene binding and leads to an ethylene-insensitive phenotype (Binder *et al.*, 2012; Schott-Verdugo *et al.*, 2019; Binder, 2020). However, there are also some mutations in these receptors that have no effect on ethylene binding but affect the signaling function of the receptor.

Mutations in ethylene receptor genes fall into two main categories: (**I**) dominant gain-of-function (GOF) mutations conferring ethylene insensitivity, and (**II**) recessive loss-of-function (LOF) mutations that have little effect as single mutations, but show a constitutive ethylene response in combination with other mutations (Bleecker *et al.*, 1988; Guzmán and Ecker, 1990; Chang *et al.*, 1993). The different receptor isoforms have similar domain architecture with three transmembrane α-helices at the N-terminus, stabilized by two disulfide bonds,

which comprises (with Cu^+ cofactor) the ethylene-binding domain and, followed by a GAF (cGMP-specific phosphodiesterases, adenylyl cyclases, and FhlA), and a kinase domain.

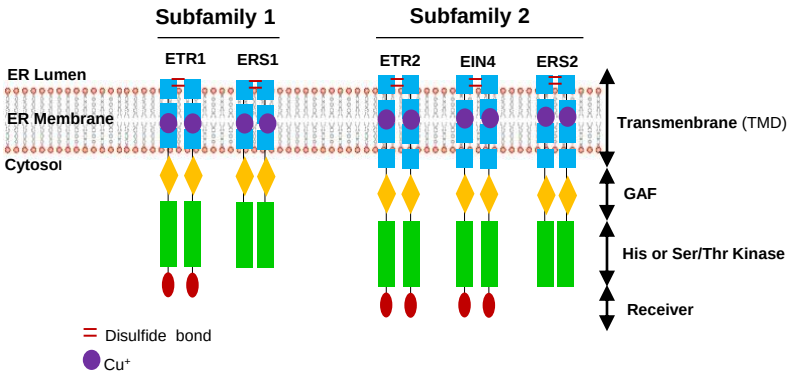

Figure 3. Diagram of ethylene receptors domains in Arabidopsis. The receptors are dimers stabilized by two disulphide Cu^+ bonds located in the endoplasmic reticulum (ER) membrane. All the receptors family contain similar overall modular structure: an N-terminal transmembrane sensor domain (TMD) followed by a GAF and kinase domain. ETR1 is a histidine kinase, ETR2, ERS1, ERS2 and EIN4 are serine/threonine Kinases. In ETR1, ETR2 and EIN4 this structure is complemented by a C-terminal receiver domain. Adapted from Binder, 2020.

Three of the five receptors also contain a receiver domain (**Fig. 3**), (Schott-Verdugo *et al*., 2019; Binder, 2020). Based on their protein structure, two subfamilies of ethylene receptors have been described. ETR1 and ERS1 in subfamily 1 and ETR2, EIN4 and ERS2 in subfamily 2 (containing additional amino acids at the N terminus of unknown function) (Wang *et al.*, 2006). The receptors can be further distinguished by their kinase activity. ETR1 has histidine kinase activity, whereas ETR2, ERS2, and EIN4 have serine/threonine kinase activity, and ERS1 has been documented to have both, depending on assay conditions (**Fig. 3**) (Gamble *et al.*, 1998; Moussatche and Klee, 2004; Binder, 2020). In recent years, it has been possible to better understand what is the role of the ethylene receptors in cucurbits. In *Cucurbita pepo* has been possible isolated four GOF mutants, *etr1a*, *etr1a-1*, *etr1b* and *etr2b,* all exhibiting a reduced response to ethylene, as well as concomitant changes in developmental traits regulated by ethylene (García *et al.*, 2018, García, 2019). The duplicated genome of *C. pepo* contains six ethylene receptor genes, two paralogs for either *ETR1* (*CpETR1A* and *CpETR1B*), *ERS1* (*CpERS1A* and *CpERS1B*) and *ETR2*

(*CpETR2A* and *CpETR2B*), and the identified mutations affect three of the ethylene receptor genes (García, 2019; García *et al.*, 2018; 2020*a*,*b*).

1.2.3. Ethylene signaling pathway

Ethylene transduction pathway is initiated when the hormone is perceived by the receptors, whose function is negatively regulated by ethylene. Two proteins, CTR1 and EIN2, are the central components of ethylene signaling, that physically interact with the receptors and each other (**Fig. 4**). CTR1, a serine/threonine protein kinase, acts like a negative regulator of ethylene signaling, while EIN2 is required to activate ethylene response (Alonso *et al.*, 1999; Ju *et al.*, 2012). Current models predict that in the absence of ethylene (**Fig. 4A**), the activity of ethylene receptors keep CTR1 active. CTR1 directly phosphorylates EIN2, which may result in EIN2 ubiquitination (Ub) via a Skp1 Cullen F-box (SCF)-E3 ubiquitin ligase complex containing the EIN2-targeting protein 1 and 2 (ETP1/2) and subsequent proteolysis by the 26S proteasome (Qiao *et al.*, 2009). A downstream consequence of this, is that the EIN3/EIL1/EIL2 transcription factors are targeted for ubiquitination by an SCF-E3 complex that contains the EBF1 and EBF2 F-box proteins (Potuschak *et al.*, 2003; Binder *et al.*, 2007). The breakdown of these transcription factors prevents ethylene responses. Thus, in the absence of ethylene, ethylene signal transduction pathway is blocked because EIN2 level is low (**Fig. 4A**) (Binder *et al.*, 2012; Binder, 2020).

In the presence of ethylene (canonical signaling, **Fig. 4B**), the receptors and CTR1 are inhibited, reducing phosphorylation of EIN2 (Ju *et al.*, 2012). The interaction between ethylene and the binding sites of the receptors is mediated by Cu^{2+}, which is transferred to the receptors by the protein RESPONSIVE TO ANTAGONIST 1 (RAN1) (Hoppen *et al.*, 2019). The conformational change in the receptors complexes reduces CTR1 kinase activity being sequestered by the receptors so that CTR1 (inactive) can no longer phosphorylate EIN2, there is less EIN2 ubiquitination, resulting in an increase in EIN2 levels and subsequent cleavage of EIN2 by an unknown protease to release the C-terminal portion of EIN2 (EIN2-C) from the membrane-bound N-terminal (EIN2-N) portion (**Fig. 4B**) (Bisson and Groth, 2010; Shakeel *et al.*, 2013, 2015).

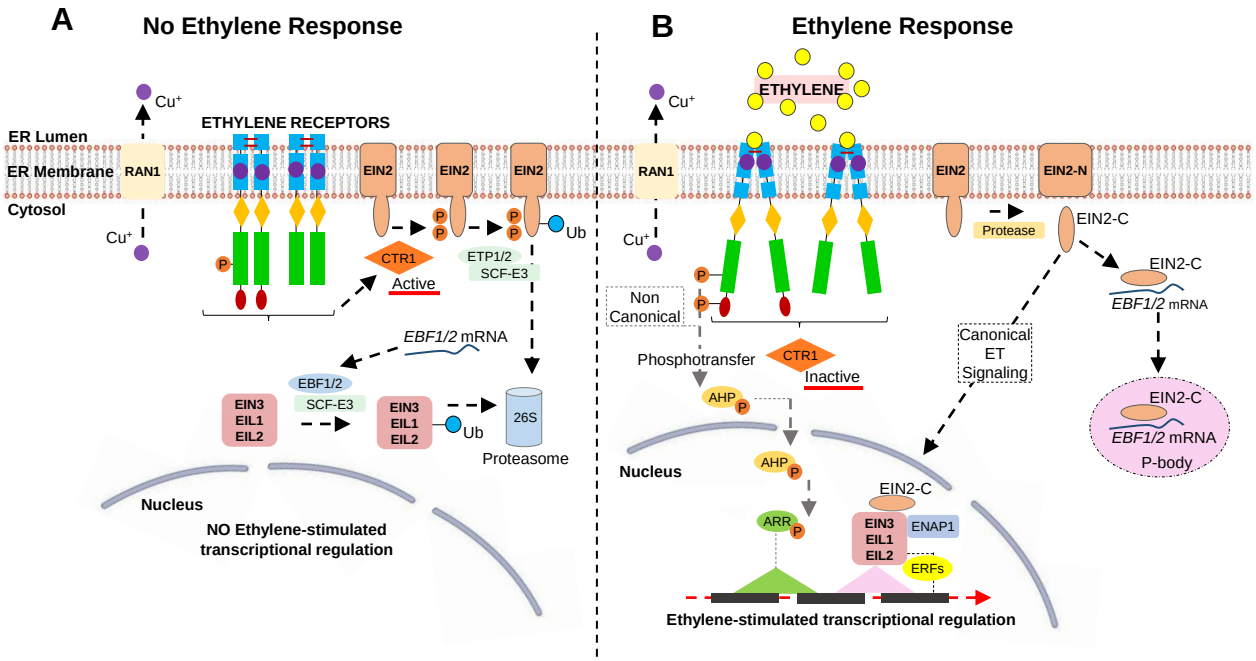

Figure 4. Model for ethylene signal transduction in Arabidopsis. Ethylene (ET) is perceived by ETR1, ETR2, ERS1, ERS2 and EIN4 receptors located in endoplasmic reticulum (ER) membrane. RAN1 is a copper transporter that delivers copper ions to the lumen of ER, where it is required for the biogenesis of receptors and cofactor to facilitate ethylene binding. (**A**), in the absence of ET, receptors bind to the Raf-like kinase CTR1 regulates negatively the downstream ethylene response pathway, by phosphorylates the C-terminal domain of EIN2. This results in the ubiquitination (Ub) of EIN2 by an SCF E3 containing the ETP1/2 F-box proteins, leading to EIN2 degradation by the 26S proteasome. Given the EIN2 levels are low, SCF-E3 containing the EBF1/2 F-box proteins ubiquitinates (Ub) EIN3 and EIL1, leading to their degradation by the proteasome and preventing them from affecting transcription in the nucleus. (**B**), in the presence of ET, the receptors bind ET via a Cu^{+} cofactor. The conformational change in the receptors complexes reduces CTR1 kinase activity being sequestered by the receptors so that CTR1 can no longer phosphorylate EIN2. With high EIN2 levels, an unknown protease cleaves EIN2, releasing the C-terminal end (EIN2-C) from the N-terminal end (EIN2-N). One fate of EIN2-C is to bind the RNAs for EBF1 and EBF2 and become sequestered in processing bodies (P-bodies) and causing higher EIN3/EIL1 levels. The other fate of EIN2-C is to translocate to the nucleus, increasing the transcription of EIN3/EIL1 via ENAP1 and promoting of ERFs responses (canonical pathway). In parallel with this pathway, phosphoryl transfer from a conserved histidine in the ETR1 DHp domain to an aspartate in the receiver domain occurs. This is followed by phosphoryl transfer from this residue to AHPs and finally to ARRs, resulting in transcriptional changes of ERF genes (non-canonical pathway). Adapted from Binder, 2020.

The role of EIN2-N is unknown, but EIN2-C has two known roles. One is to bind the mRNAs that encode for EBF1 and EBF2, whereupon this protein/RNA complex associates with processing bodies and subsequently, degraded by exoribonuclease 4 (XRN4/EIN5). This favours high level of EIN3/EIL1/EIL2, leading to more ethylene signaling (Potuschak *et al.*, 2003; Binder *et al.*, 2007). The other role of EIN2-C is to diffuse into the nucleus, where it associates with EIN2 nuclear associated protein 1 (ENAP1). Both regulates transcriptional and translational to EIN3/EIL1/EIL2 transcription factor causing and promoting of ERFs responses (**Fig. 4B**) (Chao *et al.*, 1997; Binder *et al.*, 2012; Binder, 2020).

In addition, in recent years, it is getting to know the existence of nonlinear components to what has been considered the canonical pathway raises the possibility that other ethylene-signaling pathways exist outside of or as branch points from this core pathway (non-canonical) (**Fig. 4B**) (Qiu *et al.*, 2012; Bakshi *et al.*, 2018; Binder *et al.*, 2012; Binder, 2020). These alternative pathways are not necessary for ethylene responses but appear to have roles in modulating responses to ethylene or in altering responses to other hormones (ABA), germination or environmental factors (abiotic stress) (Wang *et al.*, 2003; Bakshi *et al.*, 2018). In this pathway, the phosphoryl (P) is transferred from the histidine kinase ETR1 DHp domain to histidine-containing phosphotransfer proteins (AHP) and finally to response regulator proteins (ARR) that function as transcription factors promoting ET responses (**Fig. 4B**) (Urao *et al.*, 2000; Scharein *et al.*, 2008; Scharein and Groth, 2011). The exact pathways for this have yet to be delineated, but the affinity between ETR1 and AHP1 is altered by their phosphorylation state, where it is highest if one protein is phosphorylated, and the other is not, and appears that at least some of these roles are independent of CTR1 and EIN2 pathway (Binder *et al.*, 2012; Binder, 2020).

1.3. Jasmonates: biosynthesis, perception, and signaling

The history of JA research ever since the first isolation of MeJA in 1962. Jasmonic acid (JA) and its metabolic derivatives, such as jasmonic acid isoleucine (JA-Ile) and methyl jasmonate (MeJA), collectively known as jasmonates (JAs), are a class of lipid-derived, natural, and widely distributed phytohormones in higher plants. JAs have been studied for decades as key signaling compounds involved in many aspects of plant development and

especially in the activation of defense responses under stress responses (plant immunity), such as wounding, herbivory, or necrotrophic pathogen infection. However, studies in recent decades have remarkably expanded our knowledge on the importance of JA in many other developmental processes, including seedling development, lateral root formation, senescence, flower development, sex determination, and the circadian clock. All this has allowed to elucidate the molecular basis underlying JA biosynthesis, transportation, signal transduction and the crosstalk with other signaling pathways (Kombrink, 2012; Wasternack and Song, 2017; Huang *et al.*, 2017; Delgado *et al.*, 2021; Li *et al.*, 2021). In cucurbits, the role of jasmonates is poorly understood, which makes it even more interesting to investigate the functional role of this phytohormone in plant development.

1.3.1. Jasmonate biosynthesis

In Arabidopsis, three JA biosynthetic pathways have been identified: (**I**) the octadecane pathway starting from α-linolenic acid (α-LeA, 18:3), (**II**) the hexadecane pathway starting from hexadecatrienoic acid (16:3), and (**III**) the 12-oxo-phytodienoic acid (OPDA) reductase 3 (OPR3)-independent pathway (**Fig. 5**). All three pathways require multiple enzymatic reactions that take place sequentially in the chloroplast, peroxisome and finally in the cytosol (Wasternack and Song, 2017; Huang *et al.*, 2017; Li *et al.*, 2021).

The (**I**) and (**II**) pathways start with the release of the polyunsaturated fatty acids α-LeA (18:3) and hexadecatrienoic acid (16:3) hydrolysed from the membrane of chloroplast or other plastid (depending on the cell type). This takes place by one of the seven different branches of the so-called lipoxygenase (LOX) pathway (Wasternack, 2007). LOXs (a nonheme iron containing dioxygenases that form fatty acid hydroperoxides from polyunsaturated substrates) are subdivided into 9-LOXs and 13-LOXs according to the carbon atom at which molecular oxygen is introduced (Bannenberg *et al.*, 2009). In addition, 13-LOXs can be further classified into type I and type II based on the absence or the presence of a putative chloroplast transit peptide in the enzyme (cTP) (Maynard *et al.*, 2021). In Arabidopsis, the 13-LOX members AtLOX2, AtLOX3, AtLOX4 and AtLOX6 are localized in the chloroplast, whereas the 9-LOX members AtLOX1 and AtLOX5 are probably localized in the cytosol (Caldelari *et al.*, 2011;

Chauvin *et al.*, 2013; Maynard *et al.*, 2021). The distribution of α-LeA between the chloroplast and cytosol can thus modulate the metabolic flux between 13-LOX- and 9-LOX-derived oxylipins (**Fig. 5**) (Wasternack and Song, 2017; Li *et al.*, 2021).

Allene Oxide Synthase (AOS) and Allene Oxide Cyclase (AOC) are the next enzymes that acts in the octadecanoid pathway for JA biosynthesis in chloroplast. OPDA or dn-OPDA products generated by the 13-LOX/AOS/AOC pathway must leave the chloroplast and enter the peroxisome and then reduced by the flavin-dependent 12-Oxophytodienoate Reductase 3 (OPR3), the preferred route (red arrows in **Fig. 5**) (Schaller *et al.*, 2008; Stenzel *et al.*, 2012; Farmer and Goossens, 2019). OPDA is released from the chloroplast into the cytosol through JASSY, a Bet v1-like protein localized at the outer membrane of the chloroplast envelope, was shown to bind with OPDA and function as a membrane channel. Subsequently, OPDA is import into the peroxisome by ATP-binding cassette D group (ABCD) transporter CTS for a rapid and efficient JA production (Theodoulou *et al*., 2005; Ohkama-Ohtsu *et al*., 2011).

Recently, an alternative pathway (III) for JA synthesis has been revealed in which OPR3 activity is completely depleted (**Fig. 5**). OPDA and hexadecatrienoic acid-derived dn-OPDA are metabolized to tetranor-OPDA (tn-OPDA) and 4,5-didehydro-JA (4,5-ddh-JA), which is thought to be reduced to JA by OPR2 after release into the cytosol (Chini *et al*., 2018; Wasternack and Hause, 2018). This cytosol OPR2-dependent and OPR3-independent JA biosynthesis pathway may be ancient, and processes or activate under certain environmental conditions. Nevertheless, the majority of JA biosynthesis still occurs through OPR3 (Wasternack and Song, 2017;Wasternack and Hause, 2018; Li *et al*., 2021).

Peroxisomal JA is then translocated to the cytosol and can be metabolized into active, partially active, and inactive compounds. JA-Ile is the most biologically active of the JAs, and its perception activates core JA signaling (Li *et al*., 2021). The conjugation of JA with isoleucine has been shown to be catalysed in the cytosol by jasmonoyl-isoleucine synthetase (JAR1) (Staswick and Tiryaki, 2004). In addition, JA-Ala, JA-Val, JA-Leu, and JA-Met have also been identified as endogenous bioactive JA conjugates, all of them, participates of the Coronatine Insensitive 1 (COI1) dependent signaling (Yan *et al*., 2016). In addition, JA/JA-Ile can also undergo glycosylation (12-O-Glucosyl-JA), hydroxylation (by JOXs

and JAOs), methyl esterification (MeJA), and sulfonation (12-HSO4-JA) in cytosol, vacuole (OPDA-GSH) and ER (12-OH-JA-Ile), constituting what is known as JA homeostasis catabolism and providing a further layer of regulation for JA-Ile homeostasis and thereby it's signaling (**Fig. 5**) (Wasternack and Song, 2017; Wasternack and Hause, 2018; Wasternack and Feussner, 2018; Li *et al.*, 2021)

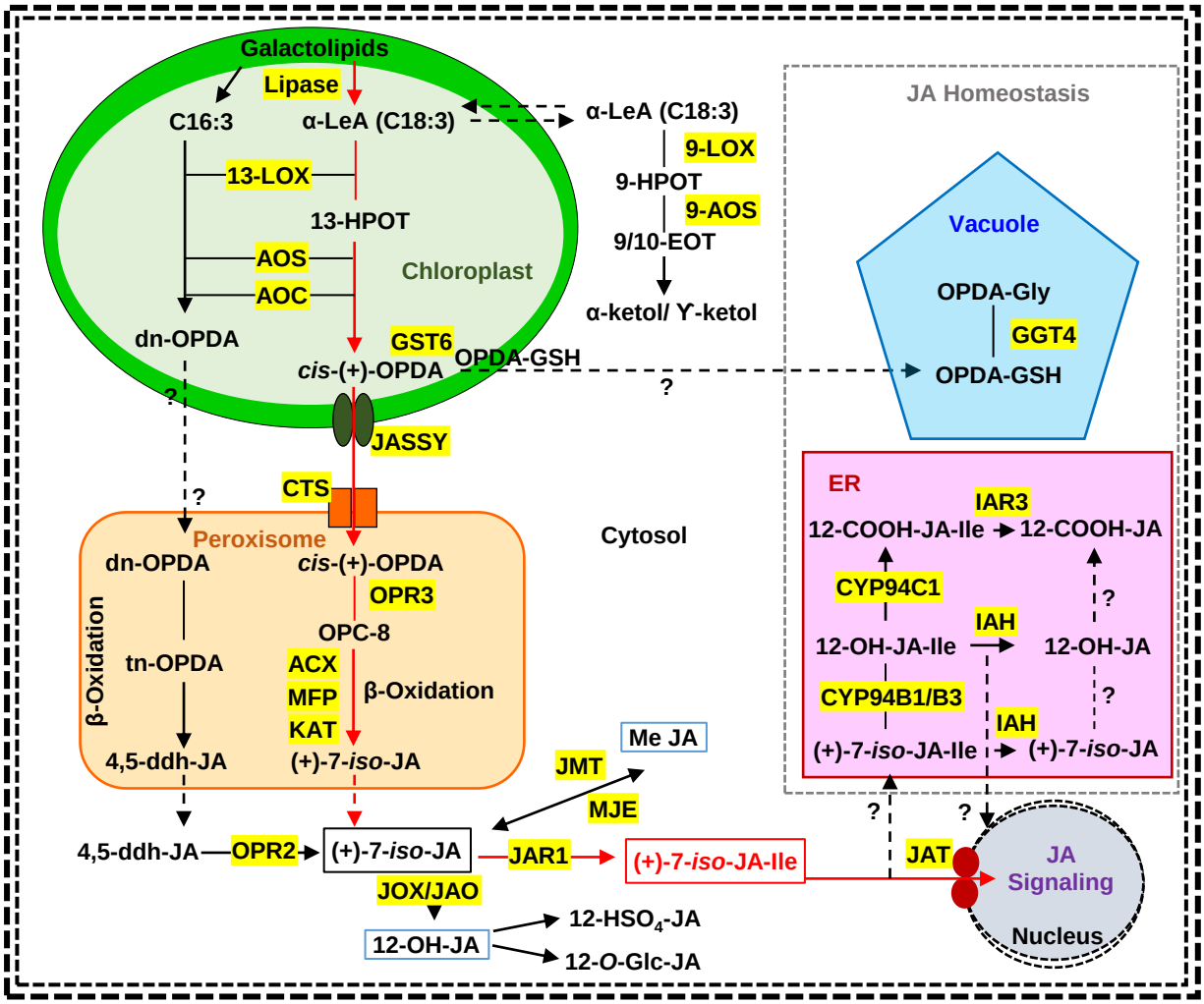

Figure 5. Intracellular compartmentation of the biosynthesis and metabolism of JAs in Arabidopsis. The biosynthesis occurs sequentially in the plastid/chloroplast and peroxisome /cytosol from α-LeA (the main route indicated by red arrows) or from hexadecatrienoic acid (16:3). Also, the recently an alternative pathway OPR3-independent, from 4,5-ddh-JA and OPR2 in cytosol. In cytosol, JA derivatives are produced, including the bioactive JA-Ile ((+)-7-*iso*-JA-Ile), which then enter the nucleus to activate core JA signaling and other compounds (Me JA; 12-OH-JA; 12-HSO4-JA; 12-*O*-Glc-JA), involved in the JA homeostasis catabolism (preferably in vacuole and ER). Also shown are JASSY, CTS and JAT transports involved in the efflux of the different components for JA signaling. Adapted from Wasternack and Song, 2017 and Li *et al.,* 2021.

1.3.2. Jasmonate perception and signaling

The receptor for JA is localized in the nucleus as well as, their bind ligands (**Fig. 6**). The perception and signaling of JA mediates sensing levels of the dynamic bioactive JAs, predominantly the most active naturally occurring isomer (+)-7-iso-JA-Ile (Kombrink, 2012; Yan *et al.*, 2016). The prompt transition of transcriptional states between repression and activation (**Fig. 6**) is mediated by the interplay between the transcriptional activators MYCs/MYBs (MYC2/3/4 and MYB21/24/57) and repressor JAZ/TIFY (JASMONATE-ZIM DOMAIN) proteins (Chini *et al.*, 2007; Fernández-Calvo *et al.*, 2011; Li *et al.*, 2021). Jasmonate transporters (JATs), a half-molecule G group of ABC transporters (ABCGs) members, mediates the nuclear entry of JA-Ile, and SCF^{COI1}-JAZ acts as coreceptor in the perception and signaling. JATs also cooperate with JAR1 (**Fig. 5**), maintaining a critical nuclear JA-Ile level to activate JA signaling (Kombrink, 2012; Stitz *et al.*, 2014; Wasternack and Song, 2017; Li *et al.*, 2021).

So that, at low JA-Ile levels (**Fig. 6A**), JAZ proteins bind directly with MYCs/MYBs and, via JAZ-bound NOVEL INTERACTOR OF JAZ (NINJA) adaptor protein and potentially other corepressors, indirectly recruit the TOPLESS (TPL) scaffolding protein, which silences gene expression through interactions with histones, histone deacetylase (HDA), and the Mediator complex. This repressor complex inhibits the transcriptional activity of MYC/MYB transcription factors (Chini *et al.*, 2007; Thines *et al.*, 2007; Sheard *et al.*, 2010).

Elevated JA-Ile accumulation promotes the binding of its bioactive form (+)-7-iso-JA-Ile and JAZ to the COI1 component of the SCF E3 ubiquitin ligase complex (SCF^{COI1}), the polyubiquitylation of JAZs, and the subsequent degradation of JAZs by the 26S proteasome (**Fig. 6B**) (Chini *et al.*, 2007; Thines *et al.*, 2007). JAZ degradation unmasks the MED25 (Mediator subunit 25) binding site on MYC/MYB to engage the Mediator complex and recruit additional coactivators HAC1 (histone acetyltransferase 1) and LUH (Leunig homolog), allowing the formation of the transcription preinitiation complex with RNA polymerase II (Poll II) and thereby activating G-box motifs of promoters of JA-responsive genes (such as *TAT1*) for JA signaling (**Fig. 6B**) (Chen *et al.*, 2012; Kombrink, 2012; Wasternack and Song, 2017; Wang *et al.*, 2019; Li *et al.*, 2021)

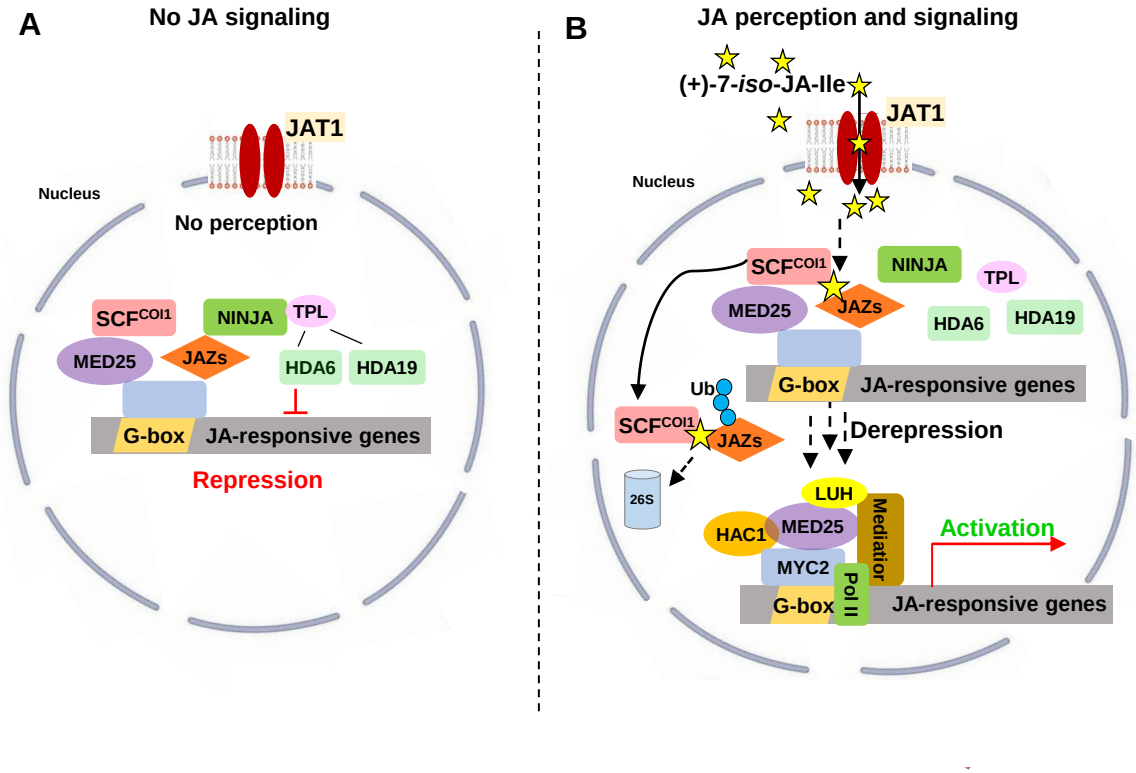

Figure 6. Sensing of JA-Ile levels and signaling dynamics in the nucleus of Arabidopsis. (**A**) Transcriptional states repression of JA-responsive genes. At low JA-Ile levels accumulated JAZ proteins that bind and repress MYCs, involving indirect recruitment of TPL via JAZ-bound NINJA. (**B**) Elevated JA-Ile level promotes the binding JA-Ile/JAZ/SCF^{COI1} coreceptor, and subsequent the polyubiquitylation of JAZ by the 26S proteasome. The degradation of JAZ unmasks the MED25 binding site on MYCs to engage the Mediator complex (plus coactivators: HAC1/ LUH), resulting in the formation of the transcription preinitiation complex with RNA polymerase II (Pol II) and the activation of JA-responsive genes. Adapted from Li *et al*., 2021.

1.4. Hormonal regulation of abiotic stress tolerance: salinity stress

One of the great challenges facing agriculture today is the development of production systems that mitigate the harmful effects of climate change, including drought and salinity. Abiotic stresses are responsible for an almost 50% reduction in the yield of major cereal crops. In arid and semi-arid areas, both soil and water salinity represent two of the most important abiotic stresses that limit crop production. Soil salinization has rendered ~20% of the world's cultivated land unproductive and is expanding at an annual rate of 10%, resulting in the salinization of nearly 50% of agricultural land by 2050. The reduction in cultivated land poses a severe warning to food security and sustainable development (Muchate *et al.*, 2016; Rahneshan *et al.*, 2018) .Plants are able to respond quickly to abiotic stresses. A rapid stress signal perception, followed by the amplification of the signal through a series of secondary messengers and transcriptional regulators are able to mediate specific responses to stress. Regarding salt stress, the uptake of inorganic ions to maintain the turgor pressure, membrane monovalent cation transporters (KUPs/KEAs/NHXs/HKTs), Ca^{2+}/CaM/CML signaling, ROS detoxification, salt overly sensitive (SOS) signaling, downstream transcription factors (including MYBs, WRKYs, ABFs, bZIP, NACs, CAMTA, MADS-box, bHLH, DREB1/CBF, AREB/ABF, Salt-responsive ERF1 (SERF1), and AP2/ERFs) and finally, the action of different phytohormones (ABA, JA, SA, GAs, IAA, CKs, BRs, SLs and ET) integrate the extend and complex salt-responsive mechanisms to combat salt stress (**Fig. 7**) (Munns and Tester, 2008; Ghanem *et al.*, 2008; Isayenkov and Maathuis, 2019; Van Zelm *et al.*, 2020; Yu *et al.*, 2020; Choudhary *et al.*, 2021).

1.4.1. Hormonal role on salinity stress responses

In response to salinity stress, plants display generally retarded growth responses. Stress hormones such as ABA, SA, JA, and ET and growth hormones including IAA, CKs, GAs, and BR have been found to play an important role in mediating salinity stress signals and controlling the balance between growth and stress responses (**Fig. 7**) (Muchate *et al.*, 2016; Van Zelm *et al.*, 2020).

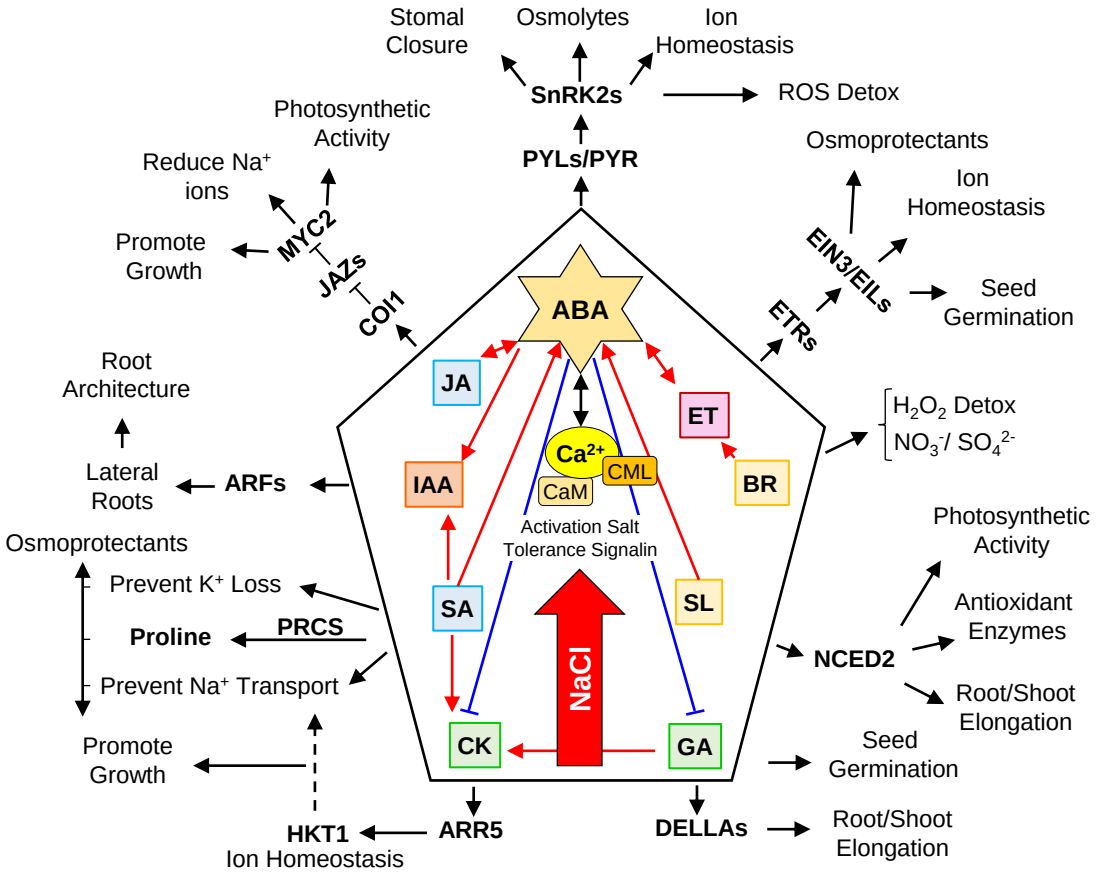

Figure 7. Hormone-mediated salt tolerance and its physiological effects during salinity stress. In response to salt stress, plants exhibit a sophisticated crosstalk among hormones (red and blue arrow) and hormones signaling pathways response (black arrow). The 'pointer' in the middle indicates how plant growth adaptation is mediated through the coordination of growth hormones and stress hormones depending on the concentration of NaCl inside the cell, emphasizing Ca^{2+}, as a messenger and activator of salt tolerance signaling. Abbreviations: ABA, abscisic acid; ARRs, cytokinin response regulator; BR, brassinosteroids; COI1, coronatine-Insensitive 1; CK, cytokinin; DELLA, aspartate-glutamate-leucine-leucine-alanine; ET, ethylene; ETR1, ethylene receptors; EIN3, ethylene insensitive 3; GA, gibberellin; HKT1, high-affinity K^+ transporter 1; JA, jasmonic acid; JAZ, jasmonate zim domain protein; MYC, myelocytomatosis oncogene; NCEDs, 9-cis-epoxycarotenoid dioxygenases; P5CS, polycomb group protein PSC; PYR/ PYL, pyrabactin resistance 1-like; SA, salicylic acid; SnRK, sucrose nonfermenting 1-related protein kinase; SL, strigolactone. Adapted from Yu *et al*., 2020 and Choudhary *et al*., 2021.

1.4.1.1. **ABA** - "*The stress response hormone"*

ABA plays an irreplaceable role in salt stress defence. ABA functions as a central integrator that links and reprograms the complex developmental process (Chen *et al.*, 2020; Van Zelm *et al.*, 2020). ABA regulates stomatal opening and closure by activating sucrose nonfermenting 1-related protein kinases (SnRK2s), which functions as the major switch in ABA signaling to respond to salt stress. AREB/ABF (ABA-responsive transcription factors) are phosphorylated by SnRK2s and subsequently mediating of ion homeostasis and ROS removal under salt stress (Cai *et al.*, 2017). Other important ABA-induced transcription factor is ASR (Abscisic acid-Stress-Ripening) also implicated in ROS homeostasis. It has been found that the overexpression of these transcription factors enhances salt tolerance and maintains yield in rice, wheat or maize (Li *et al.*, 2017; Qiu *et al.*, 2021). ABA also plays a crucial role in increasing free calcium (Ca) (and vice versa) by releasing Ca^{2+} from intracellular storage compartments and activating plasma-membrane-bound channels, such as MOCA1, NHXs and HKTs to cope with Na^{+} toxicity (Seifikalhor *et al.*, 2019). Other components of ABA mediating salt tolerance include Ca^{2+} sensor Calmodulin (CaM), CaM-like (CML) and calcineurin B-like proteins (CBL), involved in ABA signaling pathway, and 9-cis-epoxycarotenoid dioxygenases (NCEDs), which are involved in ABA biosynthesis (Lefebvre *et al.*, 2006; DeFalco *et al.*, 2010; Virdi *et al.*, 2015; Jiang *et al.*, 2019; Van Zelm *et al.*, 2020; Yu *et al.*, 2020).

1.4.1.2. **SA** and **JA** - "*Homeostasis and spatiotemporal specificity"*

SA and JA not only help plants build strong defence systems but also promotes their growth under salt stress. SA induced salt tolerance by enhancing the antioxidant system and the biosynthesis of osmolytes, maintains osmotic homeostasis, ion uptake and ROS scavenging, among other functions (Sharma *et al.*, 2019*b*; Yang *et al.*, 2019; Elhakem, 2020). In additions, SA triggers the accumulation of Total Soluble Sugars (TSS) and activate the expression of *P5CS,* responsible for proline accumulation, an essential osmolytes in response to salt stress (Lee *et al.*, 2010). SA also intervenes in maintaining a favourable balance of auxin and CK, which promote growth, and high level of ABA (Yu *et al.*, 2020; Choudhary *et al.*, 2021). On the other hand, JA is involved in salt tolerance by maintaining and promoting the plant growth. JAs delay leaf senescence, positively regulating Na^{+} translocation, increasing K^{+} accumulation, and maintaining ROS

and ion homeostasis (Qiu *et al.*, 2014). This regulation occurs in a temporally specific and tissue/organ-dependent manner, this is, JAs confers spatiotemporal specificity and flexibility (Wasternack and Song, 2017; Yu *et al.*, 2020; Delgado *et al.*, 2021). For example, rice *cpm2* and *hebiba* mutants are less sensitive to salt due to lower Na^+ accumulation in shoots, but no difference was detected in roots (Hazman *et al.*, 2015). Similarly, the maize *opr7 opr8* double mutant exhibited a reduced salt response in shoots but displayed an exaggerated response in roots (Ahmad *et al.*, 2019). Moreover, *coi1* mutant is more sensitive to salt stress at the initial stage of seed germination but shows no difference at the late growth stage after seed germination (Ding *et al.*, 2016).

1.4.1.3. **IAA** - "*Mediated root growth plasticity"*

Root system plasticity is crucial for surviving under variable soil conditions in which auxin plays an important role, regulating the root architecture during salinity stress (Iglesias *et al.*, 2010; Liu *et al.*, 2015). IAA signaling is triggered through the TRANSPORT INHIBITOR RESPONSE 1 (TIR1) and the closely related AUXIN SIGNALING F-BOX (AFB) F-box proteins, which recruit Aux/IAA repressors to the SCFTIR1/AFB complex for ubiquitination and proteasome-mediated degradation, releasing the inhibition of AUXIN RESPONSE FACTORS (ARFs), and eventually activate auxin-induced gene expression (Ryu and Cho, 2015; Leyser, 2018). The IAA responsive gene expression is modulated by redistribution of IAA in response to salt stress, redistribution mediated by the IAA polar transport and favoured by the auxin transporters AUX1 and PIN1/2 (Jiang *et al.*, 2016). Likewise, *RCc3* (rice root-specific gene) or *TaSAUR75* overexpression induced the auxin accumulation in roots, which improved the root architecture, fomenting the formation of lateral roots (LRs) and significantly increased the salt tolerance and yield (X.Li *et al.*, 2018; Lu *et al.*, 2019). However, recently studies suggesting, that this IAA responses are mediated by ABA-IAA crosstalk, dependent of NaCl concentrations, i.e., high NaCl concentrations, cause excessive accumulation of ABA, disrupting the distribution of IAA and LRs development (Lu *et al.*, 2019; Yu *et al.*, 2020).

1.4.1.4. **GAs** and **CKs** - "*Self-sacrifice to help plants to survive"*

While GA accumulation and signaling are crucial for seed germination under salinity, GA level reduction and signaling are necessary to mitigate salt stress and

enhance plant tolerance. The same is true for CKs, in which a reduction in endogenous CKs levels are necessary to enhanced tolerance to salt stress (Yu *et al.*, 2020; Choudhary *et al.*, 2021). In rice, GA signaling initiates with the hormone perception receptor GIBBERELLIN INSENSITIVE DWARF1 (GID1). Later, the ubiquitin-binding protein DOMINANT SUPPRESSOR of KAR2 (OsDSKA2a) mediates degradation of GA-deactivating enzyme, ELONGATED UPPERMOST INTERNODE (EUI), activating de GAs response. However, salt stress decreases the level of OsDSK2a, thereby enhancing the accumulation of EUI and reduction of bioactive GA levels, and consequently, inducing an inhibition and slows plant growth (J.Wang *et al.*, 2020; Yu *et al.*, 2020). Similarly, the overexpression of the Cytochrome P450 monooxygenases (*OsCYP71D8L*), a GA catabolic gene, enhances salt tolerance by reducing GA content, what keeps high chlorophyll and soluble sugar contents (Zhou *et al.*, 2020).

Likewise, maize mutant lines, encodes to the *ent*-copalyl diphosphate synthase, a GA biosynthetic enzyme, showed dwarf growth, delayed senescence of leaf accompanied by reduced GA content under salt stress, as well as high antioxidant enzymes activity, higher content in total soluble sugars and elevated Na^+ retention (Y.Zhang *et al.*, 2020). In addition, accumulating evidence indicates that CKs play negative roles in plant salt adaption. Reduction in endogenous CK levels resulted from either knockout of the CK biosynthesis enzyme isopentenyl transferase (IPT), or the overexpression of CK oxidases/dehydrogenases (CKXs), a key enzyme in CK catabolism, led to enhanced tolerance to salt stress, confirming that CK negatively regulates plant salt tolerance in Arabidopsis (Nishiyama *et al.*, 2011; Joshi *et al.*, 2018; Yu *et al.*, 2020).

1.4.1.5. **BRs** and **SLs** - *"Positive interaction with other signal molecules"*

Accumulating evidence uncovers the role of BRs in plant adaptation to salinity. Exogenous BR application alleviated salt-induced growth inhibition in multiple plant species (Arabidopsis, tomato, cucumber, maize…) (Tanveer *et al.*, 2018). Some key enzymes associated with BR biosynthesis are found necessary for plant salt adaption. In tomato and cucumber, exogenous BR treatment induced H_2O_2 generation and ET accumulation, the two molecules mutually positively regulating each other to facilitate antioxidant enzyme activities under salt stress (Wei *et al.*, 2015; Zhu *et al.*, 2016). In maize, BRs induce the accumulation of Ca^{2+} and H_2O_2 to promote ZmCCaMK-mediated antioxidant defense (Yan *et al.*,

2015). These studies indicate that BR-induced ROS scavenging regulates plant salt adaption. On the other hand, the involvement of SLs in salt tolerance has been proposed recently. Application of GR24, a synthetic SL, enhanced plant growth under salt stress conditions improving the root and shoot length, accompanied by increased photosynthetic and antioxidant activities (Ma *et al.*, 2017). Further, arbuscular mycorrhizal (AM) fungi are known to produce SLs, which helps plants to survive stress conditions like salinity. These SLs mediate plant salt tolerance through the interaction with ABA signaling (Aroca *et al.*, 2013; Yu *et al.*, 2020).

1.4.2. Ethylene (ET) signaling under salinity stress

1.4.2.1. **ET** - "*Contrasting signaling roles for salt tolerance"*

This gaseous plant hormone regulates many vital cellular processes starting from seed germination to photosynthesis for maintaining the plants' growth and yield under salinity stress, although its role is controversial. Generally, reports collectively suggest a positive regulatory role of ET in salt stress tolerance in plants.

In Arabidopsis, grapevine, maize or tomato, ET have been found as an essential positive mediator of salinity stress tolerance. Consistent with other stress hormones, ET accumulates under salt stress, suggesting necessary roles for ET in the salt response (Cao *et al.*, 2007*a,b*; Sharma *et al.*, 2019*a*; Riyazuddin *et al.*, 2020; Yu *et al.*, 2020). ET modulates salinity stress responses largely via maintaining the homeostasis of Na^+/K^+, nutrients assimilation (NO_3^- or SO_4^{2-}), maintaining stomatal conductance, water use efficiency and reactive oxygen species (ROS) by inducing antioxidant defense (Cao *et al.*, 2007*a,b*; Romera *et al.*, 2016; Riyazuddin *et al.*, 2020). However, other authors have also been reported negative roles of ET in salinity stress response in plants like rice or tobacco. Exogenous treatment with ET in rice resulted in salinity hypersensitivity, showing reduced growth, grain filling, and development of spikelets (Müller and Munné-Bosch, 2015; Hussain *et al.*, 2018). By contrast, exogenous application of 1-MCP (an ET action inhibitor) to the rice spikelets resulted in improved physiological, agronomical, and biochemical characteristics under salinity stress (Hussain *et al.*, 2019). Similarly, transgenic plants with reduced ET biosynthesis showed elevated salinity tolerance in tobacco (Tavladoraki *et al.*, 2011).

Gene mutation and transgenic analyses have shown that almost all the components of ET biosynthesis respond to salinity stress either positively or negatively. However, the functions of ET signaling pathway in the response of plant to salt stress are unclear and contrasting between species (Tao *et al.*, 2015; Dubois *et al.*, 2018; Riyazuddin *et al.*, 2020). In Arabidopsis, the positive elements of the ethylene response are generally upregulated in response to salt and are positive regulators of salt tolerance; whereas, negative elements are downregulated by salt and are considered to be negative regulators of salt tolerance (Tao *et al.*, 2015). In Arabidopsis, several studies based on gene mutations showed that the ethylene signal from EIN2 to the nucleus is transduced by EIN3/EILs. Overexpression of *EIN2* or *EIN3* remarkably enhanced tolerance to salinity stress (Achard *et al.*, 2006; Lei *et al.*, 2011). Interestingly, LOF *ethylene insensitive* mutants *ein2*; *ein3-1* and *ein3eil1* showed severe sensitivity to salinity stress (Wilson *et al.*, 2014*a*,*b*; Binder, 2020). In contrast, orthologous ethylene positive signaling genes, including *MHZ7/OsEIN2* (encode to *AtEIN2*), *MHZ6/OSEIL1* and *OsEIL2* (encode to *AtEIN3/EILs*), have an opposite function in rice, since their suppression produces salinity tolerance, while their individual overexpression enhances salt sensitivity (Tao *et al.*, 2015; Yang *et al.*, 2015*a,b*; Jin *et al.*, 2020).

The five ethylene receptors of Arabidopsis, ETR1, ERS1, ETR2, ERS2 and EIN4, are negative regulators of the ethylene signal pathway, but play a contrasting role in salt tolerance (Binder *et al.*, 2012; Wilson *et al.*, 2014*a,b*; Bakshi *et al.*, 2018). Both gain-of-function (GOF) and loss-of-function (LOF) mutants have been described for the five Arabidopsis ethylene receptor genes. Dominant GOF mutations in a single receptor gene lead to ethylene insensitivity; whereas, recessive LOF mutations confer little or no phenotype, but the combination of two or three LOF ethylene receptor mutations confers constitutive ethylene responses (Riyazuddin *et al.*, 2020). The function of the five Arabidopsis ethylene receptor genes in salt tolerance has been investigated in LOF mutants during germination, finding that ETR1 and EIN4 inhibit, while ETR2 stimulates and ERS1 and ERS2 have no effect on seed germination under salt stress. In additions, these contrasting roles in germination do not appear to require an ethylene canonical signaling pathway, but occur by regulating ABA signal transduction (Binder *et al.*, 2012; Wilson *et al.*, 2014*a,b*; Bakshi *et al.*, 2015, 2018;

Binder, 2020). By contrast, silencing of alfalfa *MsETR2* abolishes ethylene-triggered tolerance to salt stress, indicating that this ethylene receptor is a positive regulator of salt tolerance in alfalfa (Y.Wang *et al.*, 2020).

1.5. Flower development in cucurbits

1.5.1. Sex expression (SE) and sex determination (SD)

While most plant flowers are hermaphrodite and develop bisexual flowers, only a few proportions of plant species have adopted monoecy or dioecy as reproductive strategy, producing female or male unisexual flowers spatiotemporally separated, respectively (Jabbour *et al.*, 2022). Within the Cucurbitaceae family, most of its species develop unisexual female and male flowers, showing monoecy or dioecy (Guo *et al.*, 2020). As in other plant families, these two sex morphotypes have evolved from hermaphrodite species; however, many evolutionary events have occurred in cucurbits allowing easy conversion from dioecy to monoecy and vice versa (Zhang *et al.*, 2006; Guo *et al.*, 2020). The variability in sex morphotypes is higher in the domesticated species of the family (Chomicki *et al.*, 2020), which together with recent advances in genomics, make cucurbits an ideal model to study the genetic and molecular mechanisms that control SE and SD in plants. In the monoecious *Cucurbita pepo*, different sexual flowering morphotypes have been identified and described (**Fig. 8**) (Li *et al.*, 2019; Martínez and Jamilena, 2021).

In monoecious cucurbits, unisexual flowers are not clustered together in male or female inflorescences, as occurs for example in maize, but are individually developed in each node throughout three consecutive sexual phases: **I**) First, the male phase, appear at the base nodes of the plant, and no female flower is generated at this stage. **II**) The mixed phase, female flowers alternate with male flowers; usually, one female flower appears after several male flowers, and **III**) the female phase, which occurs at the end of the blooming season, female flowers appear continuously, but these are not suitable for generating fruits (**Fig. 8**) (Galun, 1962; Kubicki, 1969*a,b,c*). In these plants the control of sex not only refers to SD, that is, the mechanisms that determine the fate of each specific floral meristem towards a male or a female flower, but also to what is called SE, that is, the general level of ‘femaleness’ or ‘maleness’ of a plant (Diggle *et al.*, 2011; Pannell, 2017).

Both of these depend upon the control of the duration of sexual phases, as well as to the ratio of female-to-male flowers. SD and SE of flowers are mainly influenced by sex determining genes, environmental factors, and several phytohormones such as ET, IAA, GAs, CK, ABA, BR, SA, or JA. Among these, ET is the main regulator of SE and SD in cucurbits (Cho *et al.*, 2017; Lai *et al.*, 2018*a,b*; Li *et al.*, 2019; Martínez and Jamilena, 2021). A change in any of these factors can alter the predicted floral development, allowing the appearance of the different sexual morphotypes (**Fig. 8**).

Andromonoecious: Plants with male and bisexual flowers.
Trimonoecious: Plants with male, female, and bisexual flowers.
Gynoecious: Plants with female flowers only.
Androecious: Plants with male flowers only.

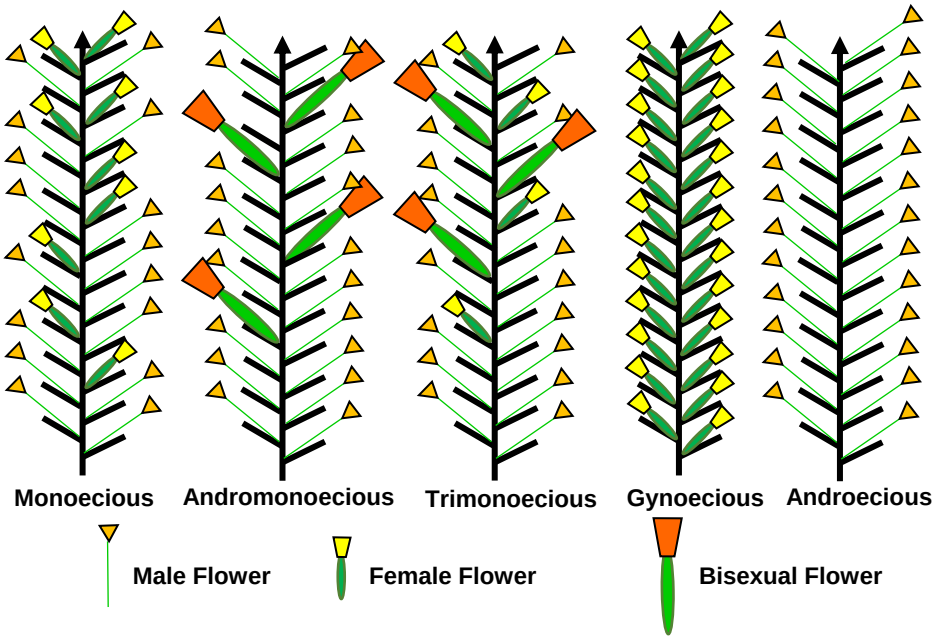

Figure 8. Sexual morphotypes observed in *Cucurbita pepo.* Schematic and phenotypic representation of the distribution of male and female flowers in the plant. Adapted from Martínez and Jamilena, 2021.

1.5.2. Environmental factors controlling SE and SD

The female/male flower ratio in cucurbits is largely unstable, which is affected by environment changes. Environmental factors, such as, light intensity and quality, nutrition and water dosage, and mechanical stress, modulate and influence on the SE and SD (Takahashi and Suge, 1980; Cantliffe, 1981; Bachman and McMahon, 1997; Lai *et al*., 2018*a*). However, these environmental

factors are relatively less decisive than temperature and photoperiod of which effects on cucurbits SE and SD have been characterized many years ago (Lai *et al.*, 2018*a*). So, it has been reported that winter conditions, with short days, low light intensity and low night temperatures, promote female flower production, while summer conditions, with longer days, and higher light intensity, are able to induce the production of male flowers in cucumber, melon, and squash (Miao *et al.*, 2011; Ikram *et al.*, 2017; Lai *et al.*, 2018a,*b*). In watermelon, the contrary seems to be the case; summer conditions promoting femaleness and winter conditions maleness (Ji *et al.*, 2015; Aguado *et al.*, 2020). On the other hand, high temperatures (in the same species) decrease the female flower node ratio or also, promote the conversion of female into bisexual flowers, implying that the sex determination mechanism which arrests stamen development in female flowers is under environmental control (Manzano *et al.*, 2014).

These phenomenon of environment-dependent SE and SD are not only restricted to cucurbits but seem a common feature in higher plants (Heslop-Harrison, 1957). In additions, the mechanisms underlying environmental SE and SD are poorly understood, though the control of temperature and photoperiod seems to be mediated by phytohormones production and signaling, especially ethylene (ET) (Martínez and Jamilena, 2021). The analysis of transcriptome and methylome of cucumber shoot apices growing under different temperature and photoperiod predicted potential epigenetic changes associated with sex environmental control (Lai *et al.*, 2018*b*). The differential methylation and expression of several MADs-box, and ET biosynthesis, perception and signaling genes (*CsACS2*, *CsACO3*, *CsETR1*, and *AP2/ERF*) may account for both temperature-dependent and photoperiod-dependent regulation of cucumber sex expression (Lai *et al.*, 2017, 2018*b*; Martínez and Jamilena, 2021).

1.5.3. Hormonal factors regulating SE and SD

Hormones mediate flower development in cucurbits, being ET the key hormone regulating SE and SD. However, a correct hormonal balance is necessary for a proper floral development, and ET is not the only hormone involved in sex determination (Martínez and Jamilena, 2021). Many works, which refer to external applications, internal hormone content and genetic cues, point out the importance of ET in the SE and SD of cucurbits.

Thus, applications of anti-ET biosynthesis agent (aminoethoxyvinylglycine, AVG) and the anti-ethylene perception agent (silver thiosulphate, STS) increase the number of male flowers per plant (Byers *et al.*, 1972; Owens *et al.*, 1980; J.Zhang *et al*., 2017). Contrary to this, ethephon, an ET-releasing agent, has a feminizing effect upon differing sex morphotypes of *C. melo*, C. *sativus*, and *C. pepo.* However, a totally opposite way is observed in other cucurbits like *C. lanatus* (ET enhances maleness and delaying female) (Manzano *et al.*, 2014; Pawełkowicz *et al*., 2019; Li *et al*., 2019; Martínez and Jamilena, 2021).

Other hormonal effects in cucurbits flower development have also been studied through external applications. The gibberellins (GAs) effect on SE and SD depends on the species and the sex morphotype (Peterson and Anhder, 1960; J.Zhang *et al.*, 2017). In monoecious and gynoecious lines of *C. sativus* and monoecious and andromonoecious lines of *C. melo* and *C. lanatus*, GAs induces plant masculinization, increasing the number of male flowers and delaying the occurrence of the first pistillate (female or bisexual) flower (Galun, 1959; Peterson and Anhder, 1960; Shifriss and George, 1964; Girek *et al*., 2013). However, the application of GAs does not promote masculinization in gynoecious and hermaphroditic *C. lanatus* plants while, the inhibitors of GAs promote feminization in *C. sativus* or *C. pepo* (Yin and Quinn, 1995; J.Zhang *et al*., 2017).

Effects also haves been reported in other different species (Pawełkowicz *et al.*, 2019). Other notable hormones are the auxins (IAA) and brassinosteroids (BRs). In both monoecious and gynoecious lines of *C. sativus,* as well as in monoecious lines of *C. melo, C. maxima* and *C. pepo*, IAA promote plants feminization, increasing the percentage of female flowers (Byers *et al*., 1972; Trebitsh *et al.*, 1987). This effect has also been seen in other species such as *M. annua, Z. mays,* or *C. sativa.* However, the inhibition of auxin biosynthesis had no effect on *C. sativus* SE, indicating that endogenous auxin has no major role in the sex expression of cucumber (Trebitsh *et al.*, 1987; An *et al.*, 2020). Similar happens with BRs, external application onto *C. sativus, C. melo* and *C. pepo,* reduces the number of male flowers, increasing the percentage of female. The effects of these three hormones appear to be mediated by endogenous ethylene, whose production and sensitivity levels are altered by the application of GAs, IAA, or BRs (Papadopoulou and Grumet, 2005; Manzano *et al.*, 2011; Martínez and Jamilena, 2021).

Different hormones are known to control SD and flower development in other plant system, including cytokinin (CK) and jasmonates (JAs). In *Z. mays tasselseed* mutants (*ts1*, *ts2, ts5* and *sk1*) exhibit failure in abortion of gynoecium in male flowers (tassel), causing the development of female flowers on the tassel (Browse, 2009; Yan *et al.*, 2014; Yuan and Zhang, 2015; Lunde *et al.*, 2019). These mutations affect biosynthesis and signaling genes of the JA pathway. Recent studies also have reported the relevant role of JAs in Arabidopsis, tomato and rice develop flowers (Upadhyay and Mattoo, 2018; Acosta and Przybyl, 2019; Pak *et al.*, 2021). The implication of CKs in SE and SD has been reporter in several genus such as *Vitis*, *Spinacia*, *Cannabis* and *Pinus*. In these genus, exogenous application of CKs converted male flowers to hermaphroditic flowers inducing a feminization of plants. In kiwifruit, a CK response regulator *Shy Girl* was found to be a potential sex determinant gene acting as the suppressor of carpel development (Akagi *et al.*, 2018; Caseys, 2018; Luo *et al.*, 2020). In cucurbits, the function of JAs and CKs in SE/SD and flowers development is much less known.

1.5.4. Molecular and genetic control of SE and SD

In bases of several genetic studies in cucumber and melon, is known that the different sex morphotypes observed in cucurbits (**Fig. 8**), are controlled by four main loci, *F*, *M*, *A*, and *Gy*. These loci have been identified and characterized, and most of them corresponds to genes that encode for ethylene biosynthesis enzymes ACS and ACO (Pan *et al.*, 2018; Pawełkowicz *et al.*, 2019; Li *et al.*, 2019; Martínez and Jamilena, 2021).

The *locus F/f* (Female), has been identified as an additional nearby copy of the *CsACS1* gene, being designated as *CsACS1G,* which induces a feminizing effect due to the higher endogenous production of ethylene. Homozygous plants containing the dominant *F* allele are gynoecious (Trebitsh *et al.*, 1997; Knopf and Trebitsh, 2006; Li *et al.*, 2020). The *locus M/m* (Monoecious) also encodes for a member of the ACS family, *CsACS2*. In melon, watermelon and squash the orthologous genes have been also identified corresponding to *CmACS7, CitACS4* or *CpACS27A*, respectively (Boualem *et al.*, 2009; Martínez *et al.*, 2014; Manzano *et al.*, 2016; Ji *et al.*, 2016). *CsACS2* and *CmACS7* are female specific genes that are expressed when the pistil begins to develop (Saito *et al*., 2007).

Its expression is consistent with the action of ethylene in the arrest of stamen development in female flowers. Therefore, the dominant *M* allele confers monoecy, while *m* allele, confers andromonoecy (Boualem *et al.*, 2008, 2016).

The *locus A/a* (androecious) is other ACS gene member-family named *CsACS11* in cucumber and *CmACS11* in melon (Boualem *et al.*, 2015). Homozygous plants for the *a* allele are androecious, although allele *a* is hypostatic to the *F* gene, being genotypes *mmffaa* and *M_ffaa* completely androecious. Mutations in *CsACO2* gene also lead to androecy in cucumber indicating that this gene is also involved in carpel development and probably collaborates with *ACS11* in this function (Chen *et al.*, 2016). Finally, the *locus Gy/gy* (gynoecious) encodes for *CsWIP1* in cucumber and *CmWIP1* in melon, a TF that regulates carpel abortion during the development of male flowers, and the mutations lead to gynoecy (Martin *et al.*, 2009; Boualem *et al.*, 2015; Chen *et al.*, 2016; Hu *et al.*, 2017). Recently, in watermelon, the orthologous gene has also been identified, corresponding to *ClWIP1*, with same function as in melon and cucumber (J.Zhang *et al.*, 2020). The evidence suggests that *WIP1* expression is repressed by *ACS11*, allowing the coexistence of male and female flowers in the plant (Boualem *et al.*, 2015; Chen *et al.*, 2016).

Recently, other components of the ethylene-signaling pathway have been identified, which modulate the sexual phenotype of cucurbits plants, as are the case of the ethylene receptors (*ETRs*) or the ethylene responsive factors (*ERFs*). The expression of *CsETR1*, *CsETR2* and *CsERS* in the apical shoots of cucumber is known to be higher in gynoecious than in monoecious lines, and their expressions are upregulated in the transition to female flowering (Yamasaki *et al.*, 2003). Downregulation of *CsETR1* appears to be required for the arrest of stamen development during female flower development (Wang *et al.*, 2010). Recently García *et al* (2018; 2020*a,b*) has reported that *etr1a*, *etr1a-1*, *etr1b*, and *etr2b* GOF mutations in squash ethylene receptors genes *CpETR1A/CpETR1B* and *CpETR2B*, lead to andromonoecy and androecy concomitantly with a reduced ethylene sensitivity (García, 2019).

In addition, the phenotypes of homozygous and heterozygous single- and double-mutant plants indicates that the two ethylene receptors cooperate in the control of the ethylene response in the control of SD and SE (García *et al.*, 2020*b*; Martínez and Jamilena, 2021). Ethylene responsive factors (*ERFs*) also modulate

the sexual phenotype. Overexpression of *ERF025* increases ethylene production, upregulating *ACS* and *ACO* genes and consequently influencing sex determination (Wang *et al.*, 2017). *ACS2* and *ACS11*, identified as sex determining genes, have been found to be directly regulated at a transcriptional level by *ERF110* (Tao *et al.*, 2018). In addition, biochemical experiments have demonstrated that *ERF31* could bind the *M* promoter thereby activating its expression. *CsERF31* responded to the ethylene signal derived from *CsACS2*, mediating the positive feedback regulation of ethylene by activating *M* expression (Pan *et al.*, 2018). Despite sex determination and sex expression in cucurbits species have been subjected to several studies, the complete molecular regulation of these processes is still unclear (Pan *et al.*, 2018; Pawełkowicz *et al.*, 2019; Li *et al.*, 2019; Martínez and Jamilena, 2021).

1.6. Hormonal regulation of cucurbits flower development

1.6.1. Involvement of ET in flower development and fruit set

In addition to its involvement on SE and SD, ET is known to regulate the growth and development of other floral organs in the pistillate flowers of squash, including the corolla and the ovary/fruit. García *et al.* (2020*a,b*) found that the occurrence of stamens in the pistillate flowers of *C. pepo* ethylene receptors mutants *etr1a*, *etr1a-1*, *etr1b* and *etr2b,* was associated with a delayed anthesis time, demonstrating that ethylene is a positive regulator of petal growth and maturation in female flowers of squash (García, 2019; Martínez and Jamilena, 2021). The female anthesis time coincided with the male flower, where ethylene production is very low. Consequently, female flower also showed an induced fruit set and early fruit development in the absence of pollination (parthenocarpic fruit). These studies suggest that ET, which is the hormone that activates the developmental program of a female flower, also mediates the growing rate and maturation of other female flower tissues in squash (Manzano *et al.*, 2014; García *et al.*, 2020*a*,*b*; Martínez and Jamilena, 2021).

Martínez *et al*. (2013) have also reported that external treatments with ET inhibitors were able induce fruit set and early fruit development in the absence of pollination (parthenocarpic fruit), and that fruit set is concomitant with a reduction in ET production, ET biosynthesis, and signaling gene expression in the days immediately after anthesis.

The negative role of ET in fruit set has been also found in tomato, where ET and signaling genes are down-regulated in early-developing fruit and the blocking of ET perception, using the ethylene-insensitive mutation *sletr1-1* or treatments with 1MCP, leads to parthenocarpic fruits through the induction of IAA and GAs (Shinozaki *et al.*, 2015, 2018*a,b*). Fruit set represents the very first step of fruit development. Current evidence supports that combined action of three hormones, IAA, GAs, and CK, plays a major role in the regulation of fruit set (Trebitsh *et al.*, 1987; Ding *et al.*, 2013; Martínez *et al.*, 2013; Shinozaki *et al.*, 2015, 2020; Zhang *et al.*, 2021). It has been shown that IAA interact with GAs and that both hormones stimulate cell division and expansion during fruit set. In tomato, *SlARF5* and *7* auxin response factor, has been reported to increase GA content, by upregulating GA biosynthesis signaling (De Jong *et al.*, 2011; Li *et al.*, 2016; Liu *et al.*, 2018).

Recent studies have showed that ABA also plays an important role in regulating tomato fruit set, further adding to the complexity of the network that regulates this process (Kai *et al.*, 2019*a*,*b*). In the Cucurbitaceae family, IAA is the key hormones regulating fruit set, establishing a close relationship with ET (Martínez *et al.*, 2013). ET and IAA can interact synergistically or antagonistically to control a variety of plant development processes, such as fruit development, fruit ripening, root formation and hypocotyl elongation as well as, the formation of plant male and female organs (Stepanova *et al.*, 2007; Martínez *et al.*, 2013; Böttcher *et al.*, 2013; An *et al.*, 2020; Zhang *et al.*, 2021).

In Arabidopsis male flower, both hormones regulate stamen formation and development. ET induces the programmed cell death (PCD) of the tapetum and middle layer, which leads to anther dehiscence and pollen release, while IAA induces anther dehiscence or pollen tube elongation (Hua *et al.*, 1998; Yau *et al.*, 2004). The same happens in female flowers (Ferrándiz *et al.*, 2010; Martínez-Fernández *et al.*, 2014). ET induces the early stage of ovule development and the arrest of stamen development and IAA synthesis in apical domain of gynoecium plays an important role in style and ovary formation (An *et al.*, 2020).

Taken together, these findings support the idea that ET and IAA play important roles in male and female reproductive organs and fruit set of higher plants (An *et al.*, 2020) . In cucurbits, these synergistically and antagonistically interactions were reported by Martínez *et al*. (2013) whereas is feasible that the

two hormones are specifically accumulated in different floral organs. i.e., ET in the upper flower organs for promoting the development of carpels and petals and arresting the development of stamens, and IAA in the inferior ovary for inducing fruit set and development (Martínez and Jamilena, 2021).

1.6.2. Involvement of JA in flower development and fruit set

The central role of JA in flower development has been recently reported. It has been discovered that JA participates in reproductive development, controlling important processes such as flowering time, flower opening, stamen development and pollen fertility in Arabidopsis, tomato, rice, and maize, but with contrasting roles between species (Huang *et al.*, 2017; Wasternack and Song, 2017; Browse and Wallis, 2019; Li *et al.*, 2021). In Arabidopsis, flower buds of the JA-deficient mutant *defective in anther dehiscence1* (*dad1*) are developed normally until two days before flower opening (anthesis) (Ishiguro *et al.*, 2001). Afterwards the development of *dad1* flowers are retarded and unopened buds are clustered in the inflorescence. In addition, *dad1* flowers also showed male-sterility, with delayed anther dehiscence and up to 97% of pollen grain infertility (Ishiguro *et al*., 2001; Browse and Wallis, 2019). Several JA biosynthesis mutants, including *fad3 fad7 fad8* (McConn and Browse, 1996), *lox3 lox4* (Caldelari *et al.*, 2011), *dde2-2* and *dde1* (Von Malek *et al.*, 2002; Sanders *et al*., 2000), *aos* (Park *et al.*, 2002), *opr3* and *opr3-3* (Stintzi and Browse, 2000; Chini *et al.*, 2018) and *acx1* and *acx5* (Schilmiller *et al.*, 2007), and mutants impairing in JA signal transduction such as *coi1* (Feys *et al.*, 1994), *myb21* and *myb21 myb24* (Mandaokar *et al.*, 2006) and *jai3-1* (Chini *et al.*, 2007), showed similar male sterile phenotypes, with reduced filament elongation and lack of anther dehiscence. In additions, external treatments of flower buds with JA can restore WT phenotype, demonstrating that JA is a positive regulator of flower opening, anther dehiscence, and pollen development in Arabidopsis (Von Malek *et al.*, 2002; Caldelari *et al.*, 2011; Reeves *et al.*, 2012; Niwa *et al.*, 2018; Pak *et al.*, 2021).

The function of JA in flower development of other plant systems is less known. In tomato *COI1* defective mutants are not male sterile, though pollen germination and viability is lower than in WT, with a premature dehydration and dehiscence of the anther (Niwa *et al.*, 2018; Upadhyay and Mattoo, 2018;

Schubert *et al.*, 2019*b*). *jai1* also show a delayed petal elongation and flower opening and promote female sterile, producing no seed upon pollination with WT or *jai1-1* pollen, although fruit set and fruit development appear similar to WT. Recently studies have also revealed that the transcription factor *SlMYB21* induces petal elongation and flower opening, pollen maturation, and gynoecium function in tomato (Niwa *et al.*, 2018; Upadhyay and Mattoo, 2018; Schubert *et al.*, 2019*a,b*).

Regarding monocots, rice mutants *eg1* (impaired in *DAD1* homologue), *eg2-1D* (impaired in *OsTIFY3/OsJAZ1*) and *ospex5* (impaired in *OsOPR7*) exhibit altered spikelet morphology with changes in floral organ identity and number, as well as defective floral meristem determinacy (Nguyen *et al.*, 2019; You *et al.*, 2019). In addition, *cpm2/hebiba* mutant plants (impaired in *OsAOC*) also exhibited complete male sterility. All these mutants accumulate almost no OPDA, JA, and other derivatives (Riemann *et al.*, 2013; Nguyen *et al.*, 2019; You *et al.*, 2019). Therefore, in rice has been suggested that JA signaling module, JAZ/JA-Ile/COI1/MYC2, is fundamental to control spikelet and floret development from the beginning of the floral meristem (Cai *et al.*, 2014; Browse and Wallis, 2019; Nguyen *et al.*, 2019). JA also controls flower development and sex determination in the monoecious maize. Mutations in *TASSEL SEED 1* (*TS1*), a gene encoding for JA biosynthesis enzyme ZmLOX8, results in a completely feminized tassel (Acosta *et al.*, 2009; Browse, 2009). The phenotype of *opr7 opr8* (orthologs of *OPR3*) and *ts5* (dispaired in the CYP94B enzyme that inactivates JA-Ile), are similar to *ts1*, suggesting that JA is necessary to control the development of male flowers and monoecy in maize (Yan *et al.*, 2012, 2014; Lunde *et al.*, 2019).

In the monoecious cucurbits, the implications of JA on the control of flower developments are unknown. However, recently it has been reported that the silencing of cucumber *CsGL2-LIKE* delays male flowering and reduces pollen vigor and seed viability (Cai *et al.*, 2020). In cucurbits, the key hormone involved in sex determination and flower development is ET, so it is very interesting to know the crosstalk between JA and ET. In tomato, the first crosstalk analysis between JA and ET supported an essential role of JAs in the temporal inhibition of ET production to prevent premature desiccation of stamens and to ensure proper timing in flower development (Schubert *et al.*, 2019*a*,*b*). Crosses between *jai1-1* (JA-Ile co-receptor COI1 mutant) and *Nr* (*Never ripe*, an *ETR3* ethylene

insensitive mutant), leading to JA- and ET-insensitive double mutant plants (*jai1-1/Nr*), showed a complementation of the *jai1-1* phenotype in terms of pollen release. However, this contrasts to Arabidopsis, where both hormones act in parallel to regulate timing of floral organ abscission (Schubert *et al.*, 2019*a*,*b*).

2. Objectives

Cucurbitaceae family includes of major economically important vegetables crops cultivated and distributed worldwide. *Cucurbita pepo*, and in particular the Zucchini morphotype, is the most valuable species of this genus regarding greenhouse production in the province of Almería, Spain. In terms of crop area, Zucchini is the fourth most important greenhouse crop in the province of Almería, after watermelon, pepper, and tomato; in terms of yield, it ranks fifth, after pepper, tomato, watermelon, and cucumber. In 2021, Almería produced 489,144 t of Zucchini, in a greenhouse-cultivated area of 8,061 ha. 348,372 t were destined for European export (Cajamar, 2021). Given the importance of the species, it would be necessary to study the physiological and genetic factors weakening the production of this crop, favouring so the development of breeding programs that provide solutions to increase not only crop production and tolerance to biotic and abiotic stresses, but also quality-related traits such as parthenocarpy.

Ethylene is the key regulator of sex expression and sex determinations in the monoecious species of the Cucurbitaceae family. In *Cucurbita pepo*, different ethylene biosynthesis and signaling genes has been reported to regulate sex determination and sex expression traits in recent years. Despite this, ethylene gene interactions are poorly understood. On the other hand, the involvement of this hormone in the vegetative development of *Cucurbita pepo* under stress conditions, as well as its interaction with other stress hormones, is also poorly known. Although ethylene is a critical hormone in cucurbit floral development, its interaction with other hormones has not been so far investigated. Jasmonic acid (JA) has been found to be a relevant hormone for flower development in numerous species, but its function in cucurbit flower development and sex determination is unknown.

The main objective of this thesis was to gain insight into the roles of ethylene (ET) and jasmonic acid (JA) in flower development and abiotic stress tolerance in *Cucurbita pepo*.

The specific objectives were as follows:

FIRST. To characterise at molecular and functional level the effect of three gain-of-functions (GOF) mutations affecting the ethylene receptors CpETR1B, CpETR1A and CpETR2B of *Cucurbita pepo* on salt stress response during germination, seedling establishment and vegetative growth of plants, revealing the role of ethylene in plant response to stress.

SECOND. To characterise at molecular and functional level the ethylene biosynthesis gene *CpACO1A* in the control of sex expression, sex determination, and fruit set in *Cucurbita pepo*, determining its transcriptional regulation and its interactions with other sex-determining genes.

THIRD. To characterise at a molecular and functional level the involvement of the jasmonate biosynthesis gene *CpLOX3A* on *Cucurbita pepo* flower development and parthenocarpy fruit set, investigating its interaction with other JA and ethylene biosynthesis and signaling genes.

3. Involvement of ethylene receptors in the salt tolerance response of *Cucurbita pepo*

3.1. Abstract

Abiotic stresses have a negative effect on crop production, affecting both vegetative and reproductive development. Ethylene plays a relevant role in plant response to environmental stresses, but the specific contribution of ethylene biosynthesis and signaling components in the salt stress response differs between Arabidopsis and rice, the two most studied model plants. In this paper, we study the effect of three gain-of-function mutations affecting the ethylene receptors *CpETR1B*, *CpETR1A*, and *CpETR2B* of *Cucurbita pepo* on salt stress response during germination, seedling establishment, and subsequent vegetative growth of plants. The mutations all reduced ethylene sensitivity, but enhanced salt tolerance, during both germination and vegetative growth, demonstrating that the three ethylene receptors play a positive role in salt tolerance. Under salt stress, *etr1b*, *etr1a*, and *etr2b* germinate earlier than WT, and the root and shoot growth rates of both seedlings and plants were less affected in mutant than in WT. The enhanced salt tolerance response of the *etr2b* plants was associated with a reduced accumulation of Na^+ in shoots and leaves, as well as with a higher accumulation of compatible solutes, including proline and total carbohydrates, and antioxidant compounds, such as anthocyanin. Many membrane monovalent cation transporters, including Na^+/H^+ and K^+/H^+ exchangers (NHXs), K^+ efflux antiporters (KEAs), high-affinity K^+ transporters (HKTs), and K^+ uptake transporters (KUPs) were also highly upregulated by salt in *etr2b* in comparison with WT. In aggregate, these data indicate that the enhanced salt tolerance of the mutant is led by the induction of genes that exclude Na^+ in photosynthetic organs, while maintaining K^+/Na^+ homeostasis and osmotic adjustment. If the salt response of *etr* mutants occurs via the ethylene signaling pathway, our data show that ethylene is a negative regulator of salt tolerance during germination and vegetative growth. Nevertheless, the higher upregulation of genes involved in Ca^{2+} signaling (*CpCRCK2A* and *CpCRCK2B*) and ABA biosynthesis (*CpNCED3A* and *CpNCED3B*) in *etr2b* leaves under salt stress likely indicates that the function of ethylene receptors in salt stress response in *C. pepo* can be mediated by Ca^{2+} and ABA signaling pathways.

Keywords: salt tolerance; germination; ethylene; ABA; membrane ion transporters, squash.

3.2. Introduction

One of the great challenges facing agriculture today is the development of production systems that mitigate the deleterious effects of climate change, including drought and salinity (P.Zhang *et al.*, 2017). In arid and semi-arid areas, soil and water salinity constitute two of the most important abiotic stresses that limit crop production. At present, more than 1 billion hectares worldwide are affected by soil salinity (Montanarella *et al.,* 2015).

Crop development and performance is severely affected by salinity. The primary effects of salinity are very similar to those caused by drought. A high concentration of salt in the soil reduces the plant's ability to absorb water, known as the osmotic effect due to salinity. This not only leads to reduced absorption of essential elements, such as K^+, Ca^{2+} and NO_3^-, but also a toxic accumulation of Na^+ and Cl^- in aerial parts of the plant (Isayenkov and Maathuis, 2019). The accumulation of salt in leaf cells inhibits cell expansion and photosynthetic activity, which ultimately leads to a reduction in crop yield (Gull *et al.*, 2019).

The entrance and the perception of Na^+ in roots are little known processes. Sodium can enter the root through non-selective cation channels (NSCCs) (Demidchik and Maathuis, 2007), although extracellular cation receptors, such as MONOCATION INDUCED [Ca^{2+}] and INCREASES 1 (MOCA1), have been detected, which are capable of sensing sodium and other cations, as well as promoting the influx of Ca^{2+} into the cell (Jiang *et al.*, 2019; Van Zelm *et al.*, 2020). The perception of the stress signal triggers a secondary signaling by reactive oxygen species (ROS) and abscisic acid (ABA), which also regulate the intracellular level of Ca^{2+}. The cytosolic calcium activates phosphorylation cascades of Ca^{2+}-dependent proteins or calcium sensors, including calmodulins (CaM), CaM-like (CML) and calcineurin B-like proteins (CBL), which leads to regulation of stress response genes (Choi *et al.*, 2014; Manishankar *et al.*, 2018).

To deal with salinity, plants have implemented three general mechanisms that improve plant tolerance to salt stress: **I**) restoration of ion homeostasis (Na^+/K^+ homeostasis); **II**) restoration of osmotic homeostasis; and **III**) prevention and repair of cell damage. Ionic homeostasis mediated by membrane ion transporters constitutes the main response mechanism against salt stress. Plasma membrane Na^+/H^+ antiporters, such SALT OVERLY SENSITIVE 1 (SOS1/AtNHX7) and AtNHX8, extrude Na^+ into the extracellular medium in

response to an increase in intracellular Ca^{2+}. HIGH-AFFINITY K^+ TRANSPORTER1-like (HTK1-like) also has a strong affinity for Na^+ (Manishankar *et al.*, 2018), which excludes the translocation of Na^+ (Sunarpi *et al.*, 2005; Pardo, 2010). Tonoplast Na^+/H^+ antiporters, such as Na^+/H^+ EXCHANGER 1-4 of Arabidopsis (NHX1-4), are also activated by Ca^{2+}, transporting Na^+ (and K^+) into the vacuole (Rodríguez-Rosales *et al.*, 2009; Bassil *et al.*, 2011; Reguera *et al.*, 2015), reducing toxic Na^+ in the cytoplasm, and decreasing the osmotic potential of the cell. The overexpression of both plasma membrane and tonoplast antiporters results in a greater tolerance to salinity in a wide range of plant species (Apse *et al.*, 1999; Zhang and Blumwald, 2001; Mian *et al.*, 2011). K^+ transporters, including the high-affinity transporter family HAK/KT/KUP, the HKT family of high-affinity K^+ transporters and the KEA family of K^+ efflux antiporters, are also involved in salt tolerance by maintaining K^+/Na^+ homeostasis (Sunarpi *et al.*, 2005; Mian *et al.*, 2011). To restore osmotic homeostasis and cell volume and turgor, salt also activates the production of compatible solutes or osmolytes, including proline, sugar alcohols, sorbitol and anthocyanins, among others (Slama *et al.*, 2015; Munns and Gilliham, 2015). These osmolytes also function as protectors of membranes and proteins by reducing oxidative damage (Keunen e*t al.*, 2013; Niu *et al.*, 2018).

The phytohormones ABA and ethylene play key roles in the defensive response of plants against abiotic stresses (Lockhart, 2013; Van Zelm *et al.*, 2020). ABA is a positive regulator of plant defensive response. Under both salinity and water deficit, plants induce the production of ABA biosynthesis genes, such as *NINE-CIS-EPOXYCAROTENOID DIOXYGENASES* (*NCEDs*) and A*BA DEFICIENTS* (*ABAs*). ABA is then perceived by the ABA receptors PYRABACTIN RESISTANCE/PYRABACTIN RESISTANCE LIKE (PYR/PYL), which induce phosphorylation activity of the ABA-dependent SUCROSE NON-FERMENTING RELATED PROTEIN KINASES (SnRKs) family, and the activation of the ABA-dependent transcriptional network involved in ionic and osmotic adjustments in response to salt stress (Verma *et al.*, 2019; Van Zelm *et al.*, 2020).

The function of ethylene in salt-stress response is, however, more controversial (Tao *et al.*, 2015). It is generally presumed that ethylene improves the response of plants to salt stress (Arraes *et al.*, 2015). However, other authors

supported a negative role of ethylene during salt stress, at least in certain growth stages in which its induction can activate oxidative stress and leaf senescence (Albacete *et al.*, 2009). In Arabidopsis, ethylene positively regulates salinity response, and both ethylene biosynthesis and signaling genes are required for salt tolerance (Peng *et al.*, 2014; Riyazuddin *et al.*, 2020). The biosynthesis *ACS* and *ACO* genes in Arabidopsis are induced under salinity conditions, but certain individual members can play a negative role in salt tolerance (Dong *et al.*, 2011; Chen *et al.*, 2014; Li *et al.*, 2014). The ethylene signaling elements also participate in the response of plant to salt stress, but their functions are also unclear (Tao *et al.*, 2015). In Arabidopsis, the positive elements of the ethylene response are generally upregulated in response to salt and are positive regulators of salt tolerance; whereas, negative elements are downregulated by salt and are considered to be negative regulators of salt tolerance (Tao *et al.*, 2015). In contrast, orthologous ethylene positive signaling genes, including *MHZ7/OsEIN2*, *MHZ6/OSEIL1* and *OsEIL2*, have an opposite function in rice, since their suppression produces salinity tolerance, while their individual overexpression enhances salt sensitivity (Yang *et al.*, 2015*b*).

The five ethylene receptors of Arabidopsis, ETR1, ERS1, ETR2, ERS2 and EIN4, are negative regulators of the ethylene signal pathway, but play a contrasting role in salt tolerance. They possess highly similar amino acid sequences and domain structures. The ethylene binding property of all of the receptors resides in three or four N-terminal transmembrane helices that are located within the membrane of the endoplasmic reticulum (Binder *et al.*, 2012; Ju and Chang, 2015). These N domains are connected by a GAF domain to a C-terminal His protein kinase domain that is positioned in the cytoplasm (Binder *et al.*, 2012; Ju and Chang, 2015). ETR1, ETR2, and EIN4 have an additional C-terminal receiver domain (Binder *et al.*, 2012). Both gain-of-function and loss-of-function mutants have been described for the five Arabidopsis ethylene receptor genes. Dominant gain-of-function mutations in a single receptor gene lead to ethylene insensitivity; whereas, recessive loss-of-function mutations confer little or no phenotype, but the combination of two or three loss-of-function ethylene receptor mutations confers constitutive ethylene responses (Hua and Meyerowitz, 1998). The function of the five Arabidopsis ethylene receptor genes in salt tolerance has been investigated in loss-of-function mutants during

germination, finding that ETR1 and EIN4 inhibit, while ETR2 stimulates and ERS1 and ERS2 have no effect on, seed germination under salt stress (Wilson *et al.*, 2014*a,b*). These contrasting roles do not appear to require an ethylene canonical signaling pathway, but occur by regulating ABA signal transduction (Wilson *et al.*, 2014*b*; Tao *et al.*, 2015; Arraes *et al.*, 2015; Bakshi *et al.*, 2018). Silencing of alfalfa *MsETR2* abolishes ethylene-triggered tolerance to salt stress, indicating that this ethylene receptor is a positive regulator of salt tolerance in alfalfa (Y.Wang *et al.*, 2020).

Recently, García et al (2018) isolated four *Cucurbita pepo* mutants*, etr1a, etr1a-1, etr1b* and *etr2b,* all exhibiting a reduced response to ethylene, as well as concomitant changes in developmental traits regulated by ethylene (García *et al.*, 2020*a,b*). The four mutations affected sex determination in this monoecious species, as well as female fertility. They convert female into male or female-sterile hermaphrodite flowers, which prevents self-fertilization of homozygous mutant plants, and forces the maintenance of mutations in segregating populations (García *et al.*, 2020*a,b*). The duplicated genome of *C. pepo* (Montero-Pau *et al.*, 2018) contains six ethylene receptor genes, two paralogs for either *ETR1* (*CpETR1A* and *CpETR1B*), *ERS1* (*CpERS1A* and *CpERS1B*) and *ETR2* (*CpETR2A* and *CpETR2B*), and the identified mutations affect three of the ethylene receptor genes. *etr1a-1* and *etr1a* are A95V and P36L amino acid exchanges in the first and third transmembrane helix of CpETR1A, respectively, *etr1b* is a T94I amino acid exchange in the third transmembrane helix of CpETR1B, and *etr2b* is an E340K amino acid exchange in the coiled-coil domain between the GAF and histidine-kinase domains of CpETR2B (García *et al.*, 2020*a,b*).

In this chapter, we investigated the response of *etr1b*, *etr1a*, and *etr2b* gain-of-function mutants to salt stress during germination, seedling establishment, and subsequent vegetative growth. Since the three mutants showed enhanced salt tolerance response during all studied developmental stages and reduced content of Na^+ in photosynthetic organs, we also analysed the molecular mechanisms involved in the enhanced salt tolerance of the *Cucurbita etr* mutants, including accumulation of osmoprotectants and activation of gene networks involved in the biosynthesis of ABA, Ca^{2+} signaling elements, and Na^+ and K^+ membrane transporters reducing the accumulation of toxic Na^+ in shoots and leaves.

3.3. Materials and methods

3.3.1. Plant material

The ethylene receptor mutants analysed in this study, *etr1b*, *etr1a* and *etr2b*, were selected from a high throughput screening of a *Cucurbita pepo* mutant collection by using the triple response of etiolated seedlings to ethylene (García *et al.*, 2018). In addition to their reduced triple response to ethylene, the three mutations convert female into hermaphrodite or male flowers, reducing or preventing self-fertilization (García *et al.*, 2020*a,b*). The mutants were therefore maintained in BC_2S_1 segregating generations, obtained by crossing each mutant twice or more times with the background genotype MUC16, and then selfed. The mutations affect *CpETR1B*, *CpETR1A*, and *CpETR2B* genes; thus, the WT and mutant plants in segregating populations were selected by detecting the WT and *etr1b, etr1a*, and *etr2b* alleles using real-time PCR with TaqMan probes (García *et al.*, 2020*a,b*). DNA was isolated from the cotyledon of seedlings after the development of the first true leaf (5 or 7 d after sowing, DAS) by using the CTAB protocol. The multiplex PCRs were done using the Bioline SensiFAST™ Probe No-ROX Kit, a set of forward and reverse primers amplifying the polymorphic sequence, and two allele-specific probes descriptive of the SNP of interest. The WT probe was labelled with FAM dye, while the mutant probe was labelled with HEX reporter dye. BHQ1 quencher molecule was used in both probes (**Table S3.1**).

3.3.2. Seed germination under salinity stress

Seed germination of WT and *etr1b*, *etr1a*, and *etr2b* was tested under salinity stress. Seeds were sterilized with a 5% sodium hypochlorite solution for 10 min and rinsed in distilled water three times, before being incubated in 50 ml Falcon tubes containing 25 ml of distilled water (control) or 100 mM NaCl for 12 h at 25 ºC in darkness under continuous shaking. After the imbibition, the seeds were transferred to a dispositive designed to study seed germination (**Fig. S3.1**). Seeds were placed in a foam strip between two pieces of filter paper and two panes of glass of 12 x 20 cm. This “sandwich glass” was secured with two clips and situated vertically in a recipient with water (control) or 100 mM NaCl solution for seeds to germinate and grow vertically.

The sandwich glass with seeds was then incubated in a growth chamber in darkness at 24 ºC and 80% RH for 55 h. 300 BC_2S_1 seeds, segregating for each *etr* mutant, were germinated, and grown using both water and salt in four independent experiments. The germinated seeds were recorded every 2 h for 55 h through digital images that were processed using ImageJ®. Seeds were considered germinated when the seed coat was broken and primary root protrusion was visible (> 1 mm). Germination initiation, time of germination at 50% of seeds, and average germination time were determined according to procedures described by Ranal and De Santana (2006). Root elongation from both WT and *etr* mutants was assessed from seedling images at 48 h of initiating germination.

3.3.3. Seedling and plantlets growth under salinity stress

After germination, seeds were transplanted into 54 seedling trays filled with a mixture of perlite and coconut fiber (20-80%), a substrate with low cation exchange capacity. 150 seeds of each genotype (WT/WT and *etr*/*etr*), 75 germinated under salt stress and 75 germinated in water, were distributed in three independent experiments. Trays were incubated in a growth chamber in darkness at 24 ºC and 80% RH for 72 h, and hypocotyl elongation was assessed in all plants. Control seedlings were irrigated with a nutritive Hoogland solution with a conductivity of 2 $dS*m^{-1}$; whereas, for those subjected to salt stress, the nutritive solution was supplemented with 35 mM of NaCl, which increased its conductivity to 5 $dS*m^{-1}$.

Seedlings of each segregating population were then genotyped with Taqman probes, and 72 WT/WT and 72 *etr*/*etr* plants from each mutant family were transplanted into 1 L pots containing the same substrate as previously and grown for 20 additional days at 24 ºC under long-day photoperiod (16 h light /8 h dark) and 70% RH in three independent experiments. Half of the plants (36) continued to be irrigated with the standard nutritive solution as previously, while the other half (36) were supplemented with 35 mM of NaCl. Leaf and root biomass were compared between each WT and *etr* mutant grown under both control and salinity conditions.

3.3.4. Vegetative growth of WT and *etr2b* under salinity stress

Although *etr* mutations affect female fertility and prevent selfing (García *et al.*, 2020*a,b*), we were able to pollinate the mutant flowers several days prior to anthesis, thus forcing self-fertilization of the mutant plants and obtaining 100% mutant offspring. This was only achieved in the *etr2b* mutant, which allowed the evaluation of a higher number of plants implementing the analysis of growth parameters in additional plant developmental stages, as well as biochemical and gene expression studies in this mutant. In this mutant family, separated WT and *ert2b* plants were cultivated for up to 45 d under either control or salt conditions following the protocol described in the previous section.

The development of different growth parameters, including root length, plant height, and root and leaf fresh and dry weight, were compared between WT and *ert2b* at 5, 10, 20, 30, and 45 DAS. Three independent replicates of 10 plants each were analysed for each genotype and irrigation conditions at each developmental stage. At 45 DAS, plants were also used to analyse the effect of *etr2b* mutation on the content in micro- and macro-elements, the accumulation of stress metabolites, and the relative expression of stress-related genes.

3.3.5. Evaluation of stress-associated metabolites in WT and *etr2b* plants

The concentration of different stress metabolites, including proline, total carbohydrates and anthocyanins, was assessed in dry leaves and dry roots of WT and *etr2b* plants at 45 DAS under control and salinity stress conditions. All determinations were carried out in triplicate, each containing plant material from four plants.

Proline was determined through the ninhydrin method (Abrahám *et al.*, 2010) with minor modifications. 100 mg of dry sample was incubated in a 2 ml of ethanol 60% at 4 ºC for 12 h. 0.5 ml of this solution was then mixed with 1 ml of ninhydrin 1%, dissolved in 60% acetic acid, and incubated at 95 ºC for 20 min at room temperature. Proline concentration was finally determined by spectrophotometry at 520 nm and expressed as $\mu mol*g^{-1}$ DW. Total carbohydrates concentration was assessed by the phenol-sulphuric method (Chow and Landhäusser, 2004) with minor modifications. 100 mg of dry sample was incubated in 5 ml of ethanol 80% at 80 ºC for 1 h, and 1 ml of this solution was then mixed with 1 ml of a solution of phenol 5% and 5 ml of sulphuric acid

95-97%. Total carbohydrates were determined at 490 nm and expressed as mg*g^{-1} DW. Anthocyanin content was measured according to Mancinelli (1990). 100 mg of dry sample was incubated at 4 ºC for 12 h in 3 ml of a solution of ethanol acidified with 1% of HCl 37%. The spectrophotometry measurements were done at 530 nm and 657 nm, and the concentrations expressed as µg*g^{-1} DW. All spectrophotometric readings were performed on 96-well microplates using the BioTek® UV-Visible Epoch™ spectrophotometer.

3.3.6. Comparison of micro- and macro-elements in WT and *etr2b* plants

Micro- and macro-elements were measured in 5 g of dry leaves and roots coming from the same three samples for each genotype and salinity condition used in the determination of stress metabolites. The elemental measurements were carried out according to the standard protocols dictated by the International Organization for Standardization (ISO) (https://www.iso.org/home.html). Total nitrogen was measured through elemental analysis (ISO-13878), chloride was determined by fragmented flow analysis (ISO-15682), and the rest of macro- and micro-nutrients studied (phosphorus, potassium, calcium, magnesium, sulphur, iron, manganese, copper, zinc, boron, molybdenum, and sodium) were assessed by ICP-OES Spectrophotometry (ISO-11885).

3.3.7. Assessment of gene expression by qRT–PCR in WT and *etr2b* plant

The relative expression of different salt-stress associated genes was assessed by quantitative reverse transcription (qRT)-PCR in WT and *etr2b* plants grown under control and salt conditions for 45 DAS. The analysis was performed in three biological replicates for each genotype and growing condition, each one derived from a pool of leaves from four plants. Total RNA was isolated from 1 g of leaves according to the protocol of the GeneJET Plant RNA Purification Kit (Thermo Fisher). RNA was reverted to cDNA with the ADNc RevertAid™ Kit (Thermo Fisher). The qRT-PCR was performed in 10 µl total volume with 1×Top Green qPCR Super Mix (BioRad) in the CFX96 Touch Real-Time PCR Detection System Thermocycler (BioRad). The gene expression values were calculated using the $2^{-\Delta\Delta CT}$ method (Livak and Schmittgen, 2001). EF1α was used as the internal reference gene. **Table S3.2** shows the primers used for qRT-PCR reactions in each analysed gene.

3.3.8. Phylogenetic analysis

MEGA X software (Kumar *et al.*, 2018) was used to establish the phylogenetic relationships between *C. pepo* and *Arabidopsis thaliana* genes encoding for Na^+ and K^+ membrane transporters (KUPs, KEAs, NHXs, and HKTs), abscisic acid biosynthesis enzymes (NCEDs), and Calmodulin-binding receptor-like cytoplasmic kinases (CRCKs). Phylogenetic trees were performed using the Maximum Likelihood method based on the Poisson correction model, with 2000 bootstrap replicates. The protein sequences and information were obtained from the Arabidopsis Information Resource (https://www.arabidopsis.org/) and the Cucurbit Genomic Database (http://cucurbitgenomics.org/).

3.3.9. Statistical analysis

Data were analysed for multiple comparisons by analysis of variance (ANOVA) using the statistical software Statgraphic Centurion XVIII. Differences between genotypes and treatments were separated by the least significant difference (LSD) at a significance level of $p \leq 0.05$.

3.4. Results

3.4.1 Tolerance of *etr1b*, *etr1a*, and *etr2b* to salt stress during germination and early stages of seedling development

To determine the ability of *etr* mutants to germinate in the presence of NaCl, WT and *etr1b*, *etr1a*, and *etr2b* mutant seeds were germinated in both water and 100 mM of NaCl up to 55 h, recording the initiation of seed germination every 2 h. The results are shown in **Fig. 1**. In water, both WT and the three *etr* mutants showed a similar germination rate, although the mutant seed was slightly delayed with respect to WT (**Fig. 1A**). Moreover, the NaCl treatment delayed germination of both WT and *etrs*, but the delayed time was much higher in the WT, meaning that the three *etr* mutants germinated faster than WT under salt stress. The salt treatment affected WT and mutant seed differently for different germination parameters, including germination initiation, average time for 50% germination, and average germination time (**Fig. 1B, C, D**).

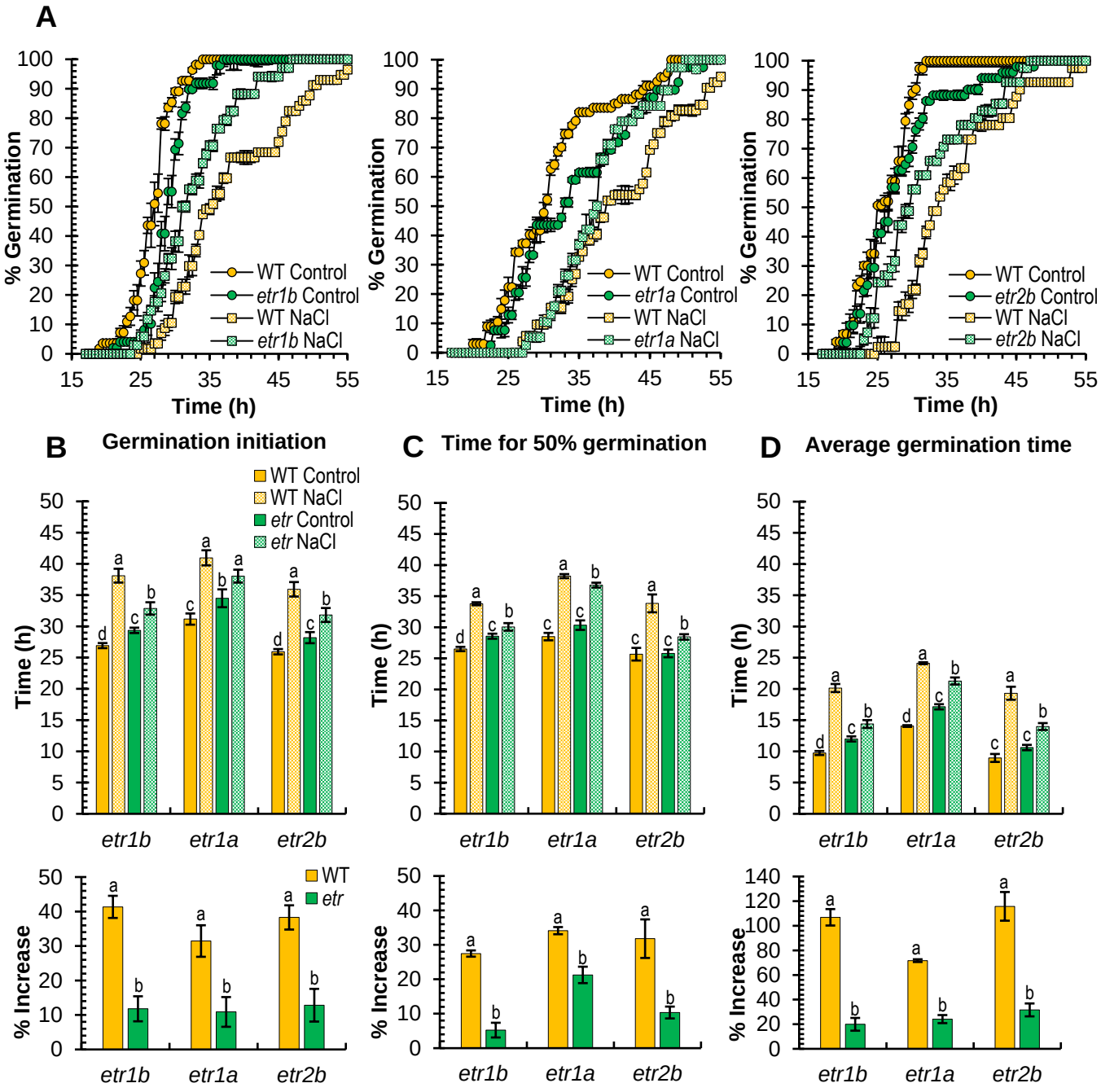

Figure 1. (**A**) Germination rates of WT and *etr1b, etr1a*, and *etr2b* ethylene receptor mutants under control and NaCl conditions. The percentage of germination was analysed every 2 h at the indicated time points. The data represent means of three independent replicates with at least 50 seeds counted per replicate. (**B**, **C**, and **D**). Effect of NaCl stress treatment on germination initiation, time at which 50% of seed is germinated, and average germination time. The bottom graphs show the percentage of increase of each parameter in response to salt stress in WT and mutant plants with respect to plants of the same genotype grown under control conditions. Means were obtained from four independent replicates with at least 50 seeds per replicate. Different letters indicate statistically significant differences ($p \leq 0.05$) between samples.

In water, the assessment of the three germination parameters in *etr* seeds was highly similar to that of WT. Under salt stress, however, there was a significant increase in germination initiation, 50% of germination and average germination time in WT and mutant seeds, but the percentage of increase of these three parameters in NaCl with respect to water was significantly lower in the three mutants compared with their corresponding WT genotypes (**Fig. 1B**). Taken together, the data revealed that the three *etr* mutants are all more tolerant to salt stress than their corresponding WT during germination.

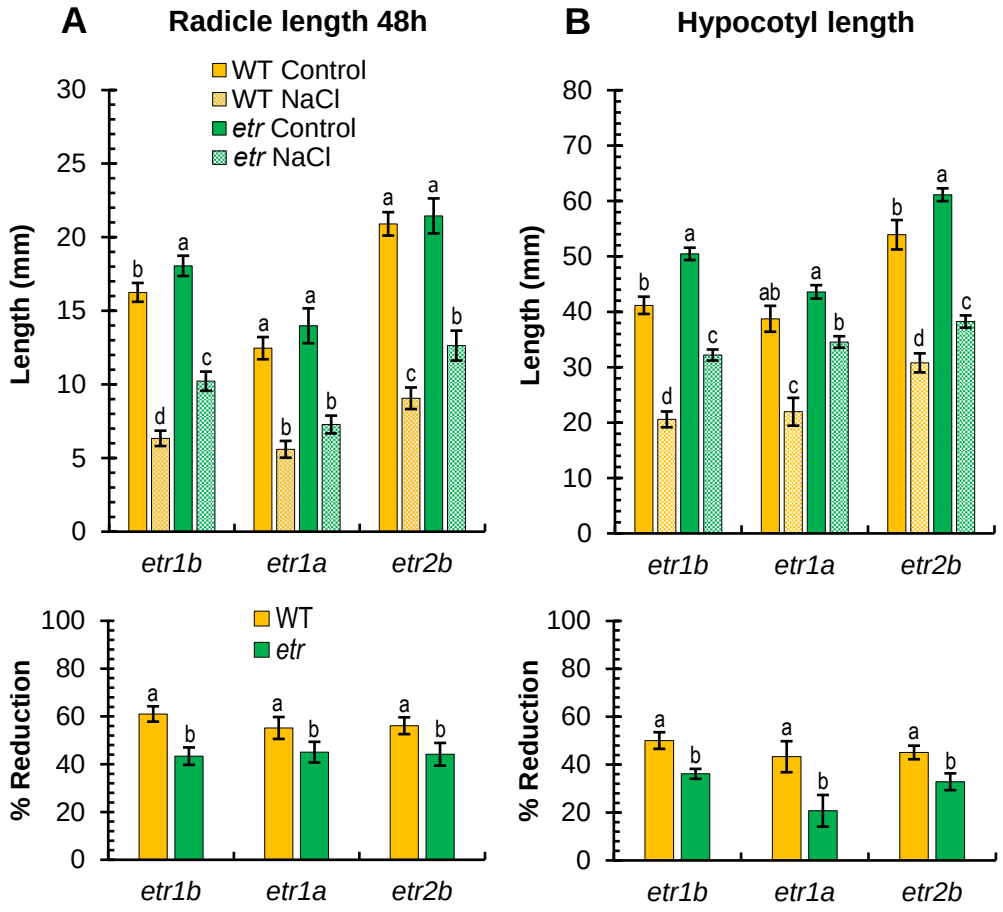

Figure 2. Effect of salt stress on growth parameters of WT and *etr1b*, *etr1a*, and *etr2b* seedlings. (**A**) Effect of salt stress on radicle length at 48 h. (**B**) Effect of salt stress on hypocotyl length in seedlings growing in darkness for 72 h. The bottom graphs of each figure show the percentage of reduction of each parameter in response to salt stress in WT and mutant plants with respect to plants of the same genotype growing under control conditions. Different letters indicate statistically significant differences ($p \leq 0.05$) between samples.

Seedling growth was also differentially reduced by salinity in WT and ethylene-insensitive mutants (**Fig. 2**). Radicle and hypocotyl growth rates were both reduced in response to NaCl treatments in WT and *etr* mutants, but the mutant seedlings were always less affected than WT ones (**Fig. 2**). When germinated and grown in water, the length of the radicle 48 h after germination was similar in WT and mutants, but the reduction of the radicle length under salt stress conditions was much more noticeable in the WT seedlings (**Fig. 2A**). The same was true for the length of the hypocotyl 3 d after germination, a parameter that was much more reduced in WT than in *etr* mutants (**Fig. 2B**). Under salt stress, in fact, WT seedlings reduced the length of their hypocotyls by approximately 50%, while *etr* mutants exhibited a reduction of only 20-35% (**Fig. 2A, B**).

Figures 3A and **3B** show the effect of salt stress on the root and shoot growth, and root balls of WT and *etr* mutants, 20 d post-germination. Under control conditions, the root and leaf biomass of mutant seedlings was much higher than that of WT, indicating a higher vigor in the three mutant plants (**Fig. 3C, D**). Although root biomass was decreased considerably under salt stress, that of mutant plants was similar to that of the WT control plants grown in water (**Fig. 3C**). The biomass of the aerial part of the plant was also significantly higher in the *etr* mutants, and although reduced by the NaCl treatment, the leaf biomass of the mutant plants under salt stress was also higher than that of the WT (**Fig. 3D**). The reduction in leaf and root biomass in response to salt stress was not significantly different between WT and mutant plants (**Fig. 3C, D**). These data demonstrate that *etr1b*, *etr1a* and *etr2b* seedlings were more vigorous than those of WT under control and salt conditions, but the responsiveness of WT and mutant plants to salt stress did not significantly differ, at least during the first 20 d of vegetative development.

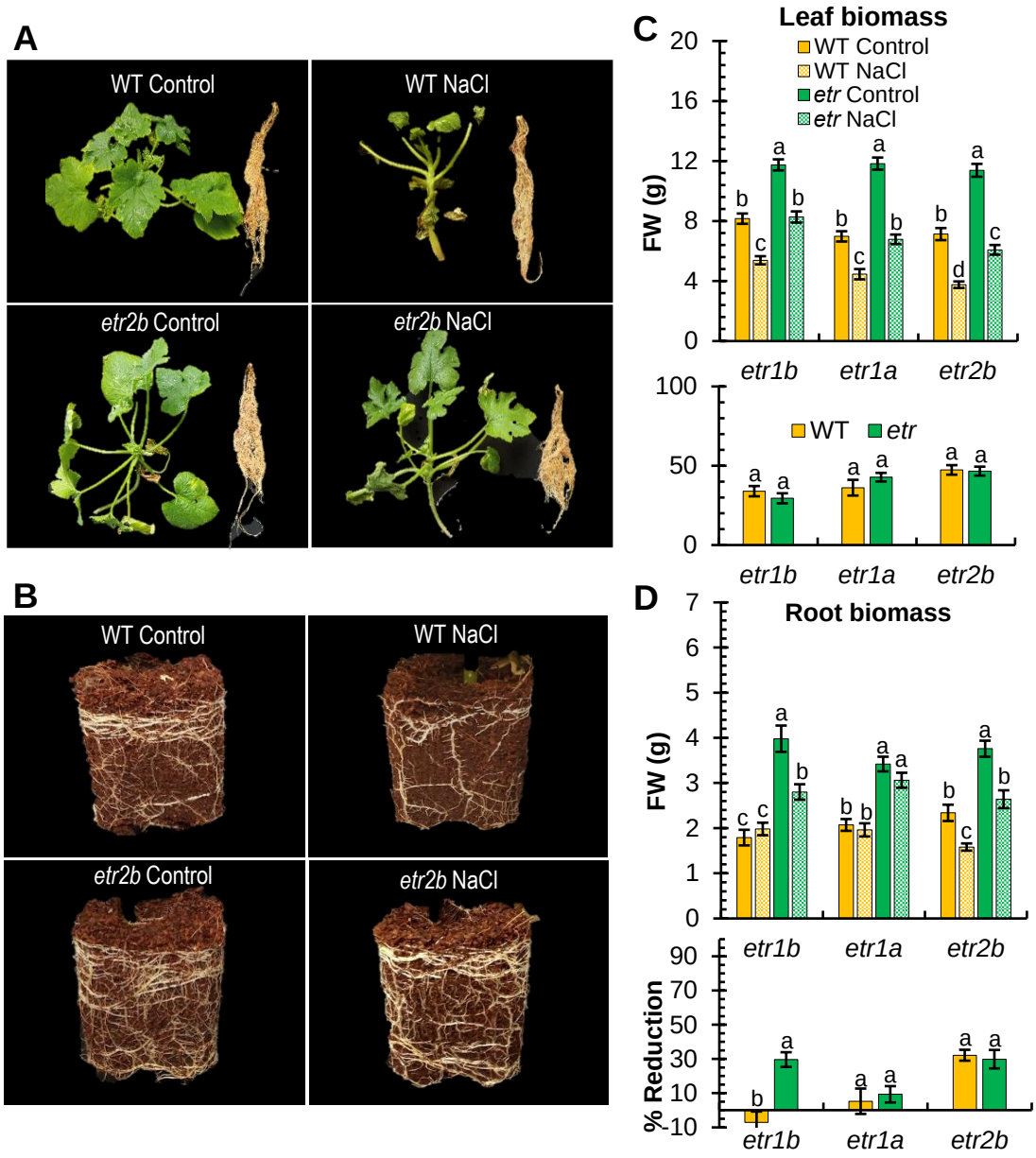

Figure 3. Effect of salt stress on the growth of WT and *etr1b*, *etr1a*, and *etr2b* plants grown for 20 d under control and NaCl conditions. (**A**) WT and *etr2b* shoots and roots. (**B**) Root balls of WT and *etr2b* plants. (**C-D**) Effect of salt stress on leaf and root biomass. The bottom graphs of each figure show the percentage of reduction of each parameter in response to salt stress in WT and mutant plants with respect to plants of the same genotype growing under control conditions. Different letters indicate statistically significant differences ($p \leq 0.05$) between samples.

3.4.2. Growth and ionic balance of WT and *etr2b* plant in response to salt stress

The separation of WT and *etr2b* offspring (see Materials and Methods) allowed further analyses of this ethylene receptor mutant. WT and *etr2b* plants were grown under control and saline conditions up to 45 d after sowing (DAS) (**Fig. 4**). The growth of roots, shoots and leaves was always higher in the mutant (**Fig. 4**) under both control and salt stress, which confirmed the higher vigor of the ethylene receptor mutants observed in previous experiments, and the higher salt tolerance of the mutant. However, the relative response of WT and mutant plants to salt stress differed throughout plant development. At early stages (5 and 10 DAS) *etr2b* and WT responded similarly to salt stress, reducing both plant height and root length (**Fig. 4A, B**). The reduction in leaf and root biomass between 5 and 30 DAS was also similar in WT and mutant plants (**Fig. 4C, D**).

At 45 DAS, however, the salt sensitivity of the mutant was significantly lower than that of the WT, with *etr2b* exhibiting a significantly lower percentage of reduction in leaf and root biomass than WT (**Fig. 4C, D**). These data indicate that *etr2b*, and probably the other two ethylene receptor mutants, have an enhanced tolerance to salt stress not only during germination, but also during plant vegetative development.

Figure 4. Effect of salt stress on root and leaf development of WT and ethylene receptor *etr2b* mutant of *C. pepo* at different days after sowing (DAS). The graphs at the top in **A**, **B**, **C**, and **D** show the growth rates of root length and plant height, as well as root and leaf biomass, in plants growing under control and NaCl conditions. The graphs at the bottom show the percentage of reduction of the same parameters in response to salt stress in WT and mutant plants with respect to plants growing under control conditions. Different letters indicate statistically significant differences ($p \leq 0.05$) between samples.

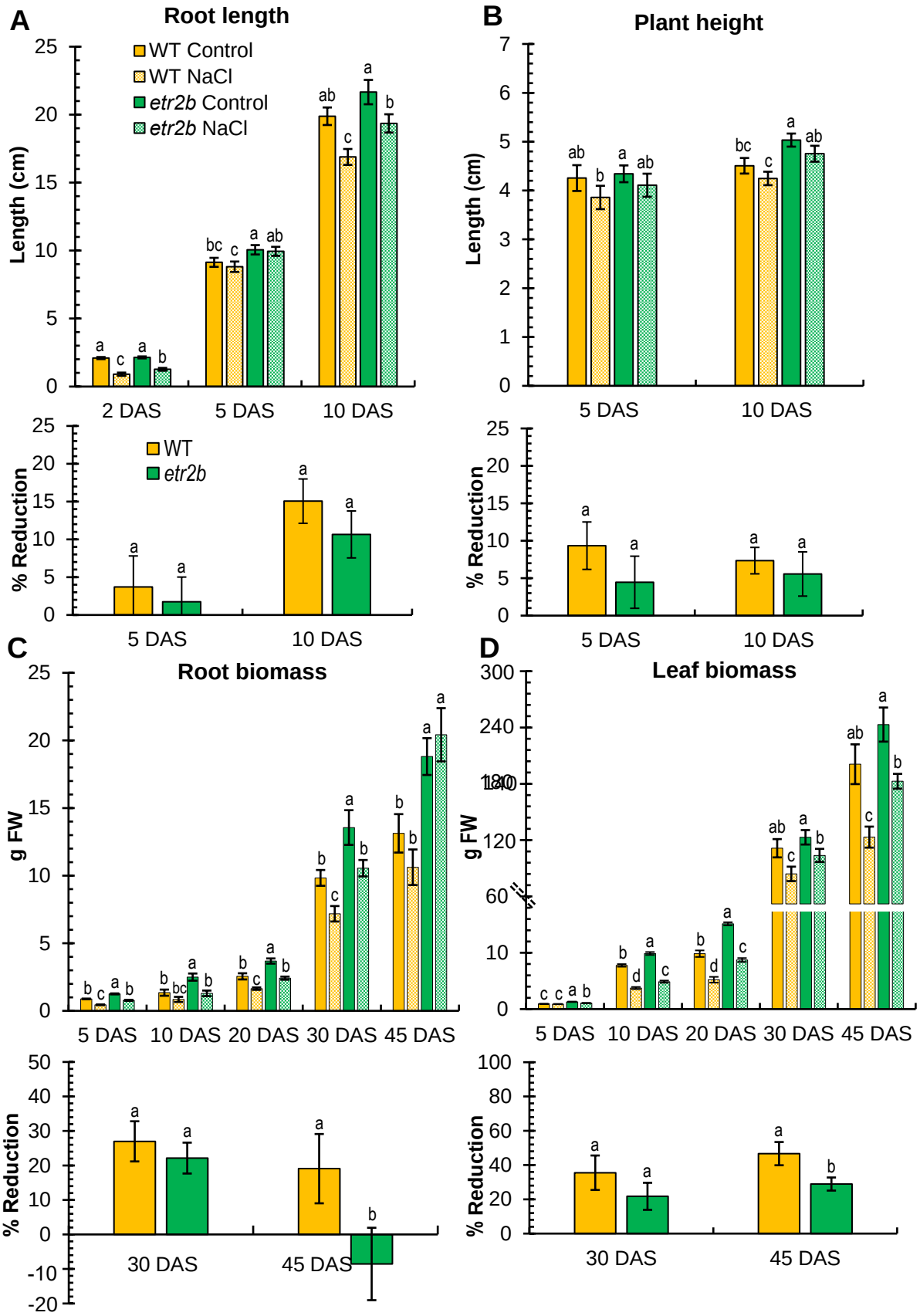
A
Root length
WT Control
WT NaCl
etr2b Control
etr2b NaCl
Length (cm)
2 DAS
5 DAS
10 DAS
B
Plant height
Length (cm)
5 DAS
10 DAS
% Reduction
WT
etr2b
5 DAS
10 DAS
C
Root biomass
g FW
5 DAS
10 DAS
20 DAS
30 DAS
45 DAS
% Reduction
30 DAS
45 DAS
D
Leaf biomass
g FW
5 DAS
10 DAS
20 DAS
30 DAS
45 DAS
% Reduction
30 DAS
45 DAS

Table 1 shows the effect of salinity on the nutrient content of WT and *etr2b* leaves and roots. For most of the nutrients, no significant differences were found between WT and *etr2b* plants in either roots or in leaves. For K and Ca, no differences were identified between WT and *etr2b*, except that the Ca content was slightly lower in the mutant under non-saline conditions. The total N content was reduced in response to salt stress in both WT and mutant leaves, but no difference was detected between the response of the two genotypes. As expected, salt-stressed plants increased their content of the phytotoxic elements Cl^- and Na. In leaves of salt-stressed plants, Na accumulated at least 4.5 mg/kg more in WT than in *etr2b*, but Cl^- content was found to be similar in the two genotypes. In roots, however, no significant difference was found between WT and *etr2b* for either Na or Cl^- (**Table 1**).

Table 1: Content of macronutrients, micronutrients, and phytotoxic elements in WT and *etr2b* mutant leaves and roots of plants grown under Control and NaCl conditions for a total of 45 days after sowing (DAS).

	Macronutrients (%)						Micronutrients (mg/kg)					Phytotoxic Elements (mg/kg)	
	N Total	P	K	Ca	Mg	S	Fe	Mn	Cu	Zn	B	Cl^-	Na
Leaves													
WT Control	5.23 a	1.40 a	7.19 a	4.16 ab	0.50 a	0.38 a	187.67 a	202.33 a	5.91 c	77.73 b	131.33 a	45.85 c	1.92 c
WT NaCl	4.54 c	1.20 a	6.85 a	4.06 ab	0.44 a	0.39 a	245.33 a	219.67 a	15.73 a	100.20 a	117.67 a	86.05 a	14.19 a
etr2b Control	5.08 b	1.54 a	8.24 a	3.72 b	0.43 a	0.40 a	235.00 a	220.33 a	6.69 c	85.23 ab	125.50 a	63.71 b	1.76 c
etr2b NaCl	4.56 c	1.18 a	7.23 a	4.50 a	0.46 a	0.38 a	199.67 a	240.33 a	10.10 b	86.80 ab	110.00 a	82.73 a	9.61 b
Root													
WT Control	3.23 b	1.66 a	2.00 a	1.47 a	0.17 a	0.28 a	319.00 a	165.67 b	8.29 b	69.23 ab	33.80 ab	7.37 b	7.32 b
WT NaCl	3.19 b	1.32 c	2.40 a	0.81 b	0.16 a	0.33 a	292.00 a	212.50 ab	8.57 ab	59.85 b	30.35 bc	20.78 a	13.92 a
etr2b Control	3.29 ab	1.58 ab	2.35 a	1.27 ab	0.16 a	0.33 a	312.33 a	178.00 b	9.28 ab	62.77 ab	35.47 a	10.76 b	8.32 b
etr2b NaCl	3.47 a	1.41 bc	2.33 a	1.12 ab	0.16 a	0.33 a	289.67 a	232.00 a	10.95 a	76.50 a	30.33 c	18.82 a	12.91 a

Different letters within the same column indicate significant differences between means ($P<0.05$).

3.4.3. Comparison of stress metabolites and gene expression in WT and *etr2b* in response to salt stress

To gain insight into the mechanisms that regulate the enhanced salt tolerance of *etr2b*, the content of some metabolites and the expression of genes related to salt stress in different plant systems were measured. **Figure 5** shows the contents of proline, total carbohydrate, and anthocyanin in leaves and roots of WT and mutant plants grown under either control or salinity conditions for 45 d. Under control conditions, most of the assessments were similar in WT and *etr2b* plants, although *etr2b* roots showed a decreased content of proline, and *etr2b* leaves reduced their content in total carbohydrates (**Fig. 5**). In salt-stressed plants, the response of WT and mutant plants was completely dissimilar. Salt induced the accumulation of proline, total carbohydrates and anthocyanins in both roots and leaves of the mutant plants, but hardly changed their contents in WT in either roots or in leaves (**Fig. 5A, B, C**).

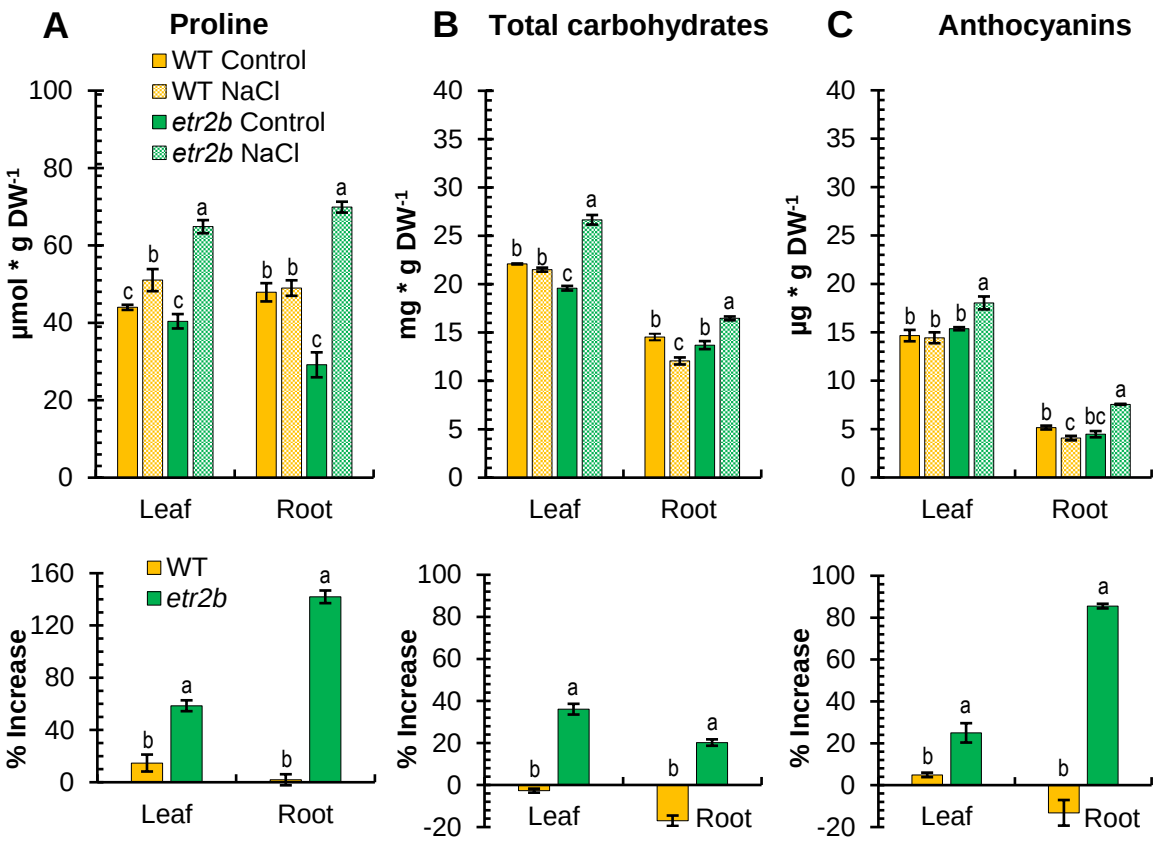

Figure 5. Content of stress metabolites in WT and *etr2b* mutant leaves of plants growing under control and NaCl conditions for a total of 45 d after sowing (DAS). The bottom graphs show the increment in metabolite content in response to salt stress in WT and mutant plants. DW, dry weight. Different letters indicate statistically significant differences ($p \leq 0.05$) between samples.

The expression of genes associated with abiotic stress tolerance was also compared in WT and *etr2b* plants grown over 45 d under standard and saline stress conditions. Since the *C. pepo* genome is duplicated, we investigated the expression of paralogs from both A and B subgenomes (indicated by the letter A or B at the end of the gene name, respectively). The phylogenetic relationship between *C. pepo* selected genes (**Table S3.2**) and Arabidopsis homologs with known functions was previously examined for each gene family (**Fig. S3.2**), thus providing a likely function of the analysed genes in *C. pepo*. In fact, the name that we assigned to each *C. pepo* gene corresponds to the Arabidopsis gene which had the most conserved protein identity (**Fig. S3.2**). The expression of most of the genes associated with salt tolerance was much more induced in the mutant than in the WT plants, indicating an enhanced response of *etr2b* plants to salt stress (**Fig. 6**).

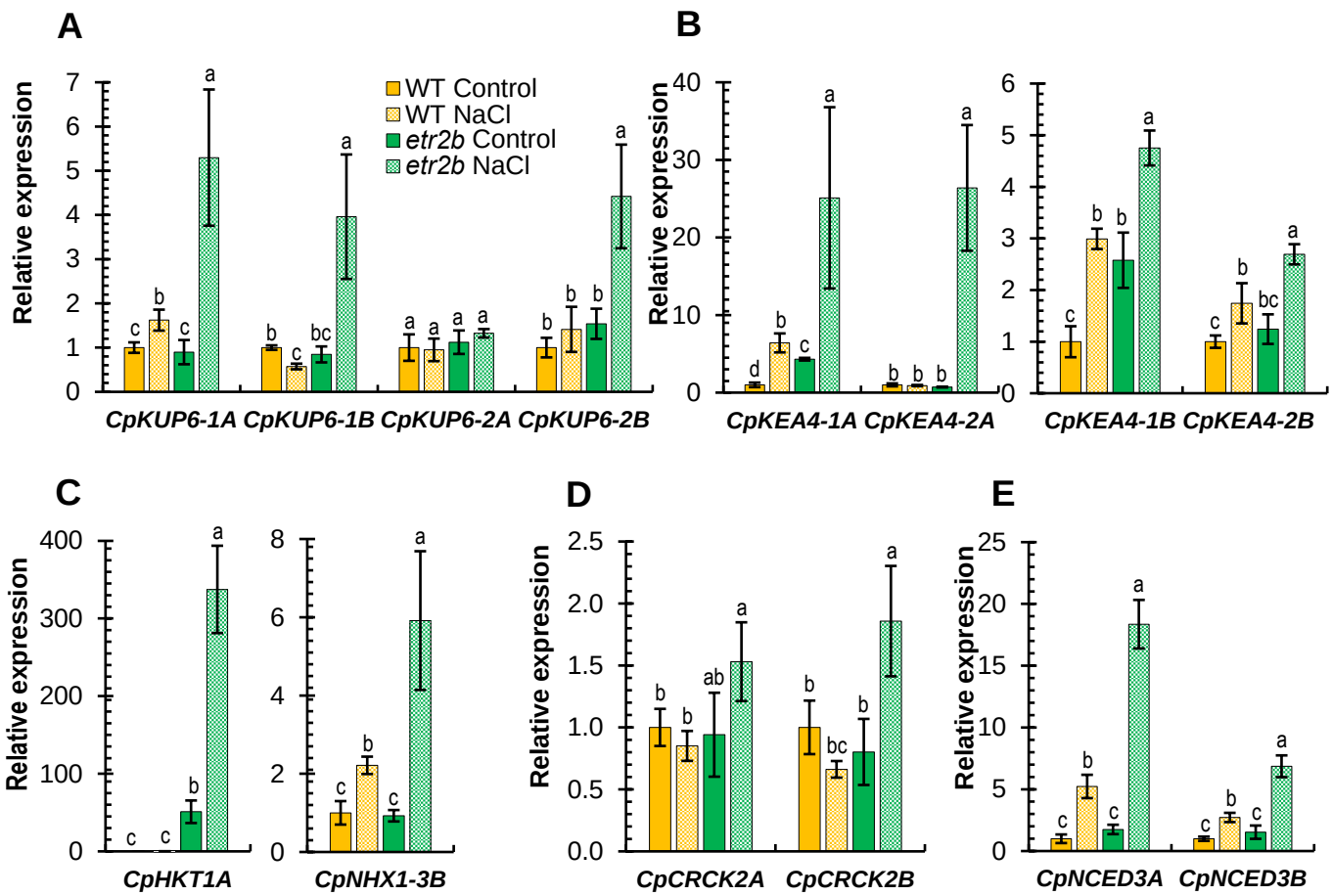

Figure 6. Relative expression of genes encoding for ion transporters (*CpKUPs*, *CpKEAs*, *CpHKT*, and *CpNHX*) and salt stress signaling elements Calmodulin-binding receptor-like cytoplasmic kinase, *CpCRCKs* and ABA biosynthesis, *CpNCEDs* in leaves of WT, and *etr2b* plants grown for 45 d under control and NaCl conditions. In each family, the number of each gene corresponds to that of Arabidopsis with the highest identity at the protein sequence level, and the A and B letters at the end of each gene corresponds to paralogs derived from the A and B subgenomes of *C. pepo*, respectively. The relative level of each transcript was assessed by qRT–PCR in three independent replicates and normalized by the ΔΔCT method. Different letters indicate statistically significant differences ($p \leq 0.05$) between samples.

K^+ transporter genes, including K^+ uptake permeases or KUPs (*CpKUP6-1A, CpKUP6-1B and CpKUP6-2A, CpKUP6-2B*), and K^+/H^+ efflux antiporters or KEAs (*CpKEA4-1A, CpKEA4-1B* and *CpKEA4-2A, CpKEA4-2B*), with the exception of *CpKUP6-2A*, were upregulated by NaCl in both WT and *etr2b*, but the upregulation in the mutant was between 2 and 25 times higher than in the WT (**Figs. 6A, B**). Under control conditions, some of them, including, *CpKEA4-1A*, *CpKEA4-1B*, were also more expressed in mutant than in WT plants.

The same is true for genes encoding Na^+/H^+ exchanger *CpNHX1-3B* and Na^+ transporter *CpHKT1A,* which were only upregulated in *etr2b* plants when grown under saline conditions (**Fig. 6C**). Of particular interest is the *CpHKT1A* gene, whose expression was already highest in non-stressed mutant plants, and was upregulated more than 300-fold in response to salinity in only the *etr2b* mutant (**Fig. 6C**). Genes involved in abiotic stress signaling pathways, including Ca^{2+} signaling gene Calmodulin-binding receptor-like kinases *CpCRCK2A* and *CpCRCK2B*, and ABA biosynthesis genes *CpNCED3A* and *CpNCED3B*, were also more highly induced in *etr2b* plants than in WT in response to salt stress (**Fig. 6D, E**).

3.5. Discussion

Ethylene is a key modulator of plant response to salt stress, but its specific role in different plant species and plant developmental stages is unclear (Tao *et al.*, 2015; Yang *et al.*, 2015*a*; Dubois *et al.*, 2018; Riyazuddin *et al.*, 2020). In Arabidopsis and other plants, including maize and tomato, ethylene positively regulates salt stress tolerance (Yang *et al.*, 2013; Arraes *et al.*, 2015; Gharbi *et al.*, 2017), however, in other plant species, such as rice and tobacco, ethylene plays a negative role in salinity stress response (Tao *et al.*, 2015; Yang *et al.*, 2015*b*). In this paper, we demonstrate that ethylene is also involved in the salt stress response of *C. pepo*. All of the physiological and molecular data presented in this paper indicate that gain-of-function mutations in three *C. pepo* ethylene receptor genes increase salt stress tolerance at germination and during seedling and plant vegetative development, suggesting that ethylene is a negative regulator of salt tolerance in *C. pepo*.

3.5.1. ETR receptors modulate salt tolerance response at germination and during seedling and plant vegetative growth

Seed germination is severely affected by salinity, being the first process involved in the stress tolerance response (Van Zelm *et al.*, 2020). The phenotypes of loss-of-function mutants in Arabidopsis have demonstrated that ETR1 and EIN4 inhibit, while ETR2 enhances, seed germination under salt stress, and ERS1 and ERS2 have no significant effect on seed germination (Wilson *et al.*, 2014*a,b*; Bakshi *et al.*, 2018).

Accordingly, Arabidopsis loss-of-function mutations for ETR1, including *etr1-6* and *etr1-7*, are more tolerant to salt stress and germinate before WT; whereas, gain-of-function mutants for ETR1, including *etr1-1*, *etr1-2* and *etr1-3*, are more sensitive to salt stress and germinate later than WT under salt stress (Chiwocha *et al.*, 2005; Wang *et al.*, 2008; Li *et al.*, 2013). The accelerated germination of the three analysed gain-of-function *etr1b, etr1a*, and *etr2b* of *C. pepo* under salt stress indicate that CpETR1B, CpETR1A, and CpETR2B are positive regulators of squash seed germination under salt stress. If this function is dependent on ethylene and the ethylene signal transduction pathway, ethylene would play a negative role in *C. pepo* salt tolerance, which is similar to what occurs in rice (Tao *et al.*, 2015).

However, given that in Arabidopsis the function of ETRs in seed germination can take place independently of the canonical ethylene signal transduction pathway, but appears to be mediated by ABA signaling (Wilson *et al.*, 2014*b*; Bakshi *et al.*, 2018), it is also likely that the mechanisms underlying the function of squash ETRs under salt stress may also occur through ABA rather than the ethylene signaling pathway. The fact that the three *etrs* exhibit similar salt stress tolerance, but differ in the magnitude of their ethylene response (*etr1b* showed the most residual responsiveness and *etr2b* the least (García *et al.*, 2020*b*), suggests that the function of *C. pepo* ETRs on germination under salt stress could take place independently of ethylene. The reduced germination rate of ethylene-insensitive *etr* mutants in water may also be the consequence of an increased biosynthesis or sensitivity to ABA, as found in Arabidopsis ethylene-insensitive mutants *etr1* and *ein2* (Beaudoin *et al.*, 2000). Furthermore, the higher induction of the ABA biosynthesis genes *CpNCED3A* and *CpNCED3B* in *etr2b* plants under salt stress also supports the involvement of ABA in the salt tolerance of this mutant. The assessment of ABA sensitivity and ABA biosynthesis of *C. pepo etr* mutants in the presence and the absence of NaCl will provide insight into the interactions between ABA and ethylene signaling cascades during seed germination.

We also observed that the three *C. pepo etr* mutations promote seedling and plant growth, resulting in higher plant height, and higher root and leaf biomass when grown under control standard conditions. This higher vegetative vigor of *etr* mutants was also identified in adult plants (García *et al.*, 2020*a,b*),

indicating that ethylene is a negative regulator throughout the vegetative development cycle of the plant. The stimulating effect of ethylene insensitivity on vegetative growth was also found in Arabidopsis ethylene-insensitive gain-of-function mutants (Bleecker *et al.*, 1988; Grbic and Bleecker, 1995; Wang *et al.*, 2008), although other studies found no differences in total leaf area between WT and the *etr1-1* mutant at earlier stages of vegetative development (Tholen *et al.*, 2004). The higher constitutive growth and vigor of squash ethylene-insensitive mutants was correlated with their higher salt tolerance during seedling and vegetative plant development.

These data contrast with those found in Arabidopsis, in which the higher vegetative growth of the ethylene insensitive gain-of-function *etr1-1* mutant and the transgenic Arabidopsis plants overexpressing the tobacco ethylene receptor NTHK1 were associated with a higher salt sensitivity, while the reduced seedling growth of the *etr1-7* loss-of-function mutant was associated with greater salt tolerance (Cao *et al.*, 2007*a,b*; Wang *et al.*, 2008). The reduced ABA sensitivity of *etr1-7* and the enhanced ABA sensitivity of *etr1-1* may account for differences in plant growth and salt-tolerance, as explained for germination (Beaudoin *et al.*, 2000; Wang *et al.*, 2008).

The enhanced salt tolerance of *C. pepo etrs* during seedling and plant vegetative growth could result from the inhibitory role of ethylene receptors in the ethylene signaling pathway (García *et al.*, 2020*a,b*). However, it is also likely that the vegetative growth regulation of ethylene receptors occurs through the abscisic acid signaling pathway, as has been observed for ETRs and EIN2 in Arabidopsis (Beaudoin *et al.*, 2000; Wang *et al.*, 2008; Kazan, 2015). Genes involved in both ABA biosynthesis and intracellular Ca^{2+} signaling pathway were more induced in the mutant than in WT, which indicates that these two signaling pathways can coordinate the tolerance response of *etr2b* to salt stress. ABA is known to control the expression of ion transport genes and the influx of Ca^{2+} in the guard cells that leads to stomata closure limiting water loss in leaves (De Falco *et al.*, 2010; Osakabe *et al.*, 2013), but also a number of ABA responsive genes that are involved in ion homeostasis and osmotic adjustment (Verslues and Bray, 2006).

3.5.2. Mechanisms of salt tolerance in *C. pepo etr* mutants

A number of physiological and molecular responses, including Na^+ detoxification, ion homeostasis, osmotic adjustment and ROS scavenging, have been developed in plants to combat salt stress (Van Zelm *et al.*, 2020). The exclusion of Na^+ in photosynthetic organs is a mechanism that is widely used by salt-tolerant genotypes to maintain vegetative growth while dealing with the high toxicity of these elements in leaves (Isayenkov and Maathuis, 2019). In our experiments, the leaves of the salt-stressed WT plant accumulated seven times more Na than non-stressed plants, but the leaves of the salt-tolerant *etr2b* only accumulated 5.3 more Na.

Given that WT and *etr2b* roots have similar Na content, these data demonstrate a high ability of the salt-tolerant mutant to restrict the transport of Na^+ from roots to leaves. The exclusion of Na^+ and the higher growth rates of *etr2b* plants are likely to be regulated by the induced Na^+ and K^+ transporter genes in the leaf. As occurs with Arabidopsis AtNHX1 and AtNHX2 Na^+/H^+ antiporters in the tonoplast, the induced *CpNHX1-3B* may be involved in sequestering Na^+ into the vacuole, thus reducing the content of Na^+ in the cytoplasm and alleviating osmotic stress (Leidi *et al.*, 2010; Fukuda *et al.*, 2011). They also function as K^+/H^+ antiporters to maintain K^+ homeostasis (Bassil *et al.*, 2011). The CpHTK1A transporter is particularly interesting because it was upregulated 300 times more in *etr2b* than in WT. HTKs are high affinity transporters for both Na^+ and K^+, mediating root Na^+ uptake, Na^+ unloading from xylem sap, and leaf Na^+ refluxing to the phloem, which are mechanisms that increase leaf Na^+ exclusion (Berthomieu *et al.*, 2003; Garciadeblás *et al.*, 2003; Horie *et al.*, 2009; Kobayashi *et al.*, 2017).

Gene expression data also suggest a positive role of the K^+ transporters KEAs and KUPs in combating salt stress. The Arabidopsis KEAs are K^+/H^+ antiporters that mediate pH and K^+ homeostasis in the inner and thylakoid membranes of chloroplast (KEA1, KEA2, and KEA3) or in endomembrane compartments (KEA4, KEA5, and KEA6) (Zhu *et al.*, 2018). The *C. pepo KEAs* genes that were highly induced in *etr2b* under salt stress are highly homologous to the second clade. KUP/HAK/KT, on the other hand, is a large family of high affinity K^+ transporters that function in potassium acquisition and translocation from roots to shoots (Yang *et al.*, 2014; Han *et al.*, 2016), facilitate K^+ efflux from

the vacuole to regulate osmotic adjustment, and some of them are involved in plant growth and development (Grabov, 2007; Osakabe *et al.*, 2013; Yang *et al.*, 2014). The *C. pepo* KUPs that were upregulated in salt-stressed *etr2b* leaf have a higher homology with Arabidopsis KUP6, an ABA responsive K^+ subfamily transporter that has a key role in osmotic adjustment and K^+ homeostasis of guard cells (Osakabe *et al.*, 2013).

C. pepo etr2b plants induced the accumulation of metabolites, such as proline, total sugars (glucose, fructose, sucrose, and trehalose) and anthocyanins at both the roots and shoots under salt stress, which demonstrates that ethylene receptors and the subsequent ethylene or ABA signal transduction pathways are mediating the production of these osmolytes and therefore the osmotic adjustment of cells under salt stress (Nahar *et al.*, 2015). These osmolytes can lower osmotic potential (Argiolas *et al.*, 2016), but can also act as stabilizers of proteins and cell components against ion toxicity and NaCl-induced oxidative damage (Nahar *et al.*, 2015; Gharsallah *et al.*, 2016). Proline is perhaps the main salinity-related osmolyte, and is considered a biochemical marker of salt stress (Hayat *et al.*, 2012). Exogenous proline treatments and transgenics plants with enhanced production of proline are more tolerant to salt, while mutants that are deficient in proline exhibited a limited growth and development under salt stress (Khedr *et al.*, 2003; Simon-Sarkadi *et al.*, 2006). The biosynthesis of proline and other osmolytes is induced by ABA in different systems (Yu *et al.*, 2020), suggesting again that the enhanced response of mutant ethylene receptors of *C. pepo* to salt stress is likely mediated by ABA.

4. The ethylene biosynthesis gene *CpACO1A*: a new player in the regulation of sex determination and female flower development in *Cucurbita pepo*

4.1. Abstract

A methanesulfonate-generated mutant has been identified in *Cucurbita pepo* that disrupts sex determination. The mutation converts female into hermaphrodite flowers and alters the growth rate and maturation of petals and carpels, delaying female flower opening, and promoting the growth rate of ovaries and the parthenocarpic development of the fruit. Whole-genome resequencing allowed identification of the causal mutation of the phenotypes as a missense mutation in the coding region of *CpACO1A*, which encodes for a type I ACO enzyme that shares a high identity with *Cucumis sativus* CsACO3 and *Cucumis melo* CmACO1. The so-called *aco1a* reduced ACO1 activity and ethylene production in the different organs where the gene is expressed, and reduced ethylene sensitivity in flowers. Other sex-determining genes, such as *CpACO2B*, *CpACS11A* and *CpACS27A*, were differentially expressed in the mutant, indicating that ethylene provided by CpACO1A but also the transcriptional regulation of *CpACO1A*, *CpACO2B*, *CpACS11A,* and *CpACS27A* are responsible for determining the fate of the floral meristem towards a female flower, promoting the development of carpels and arresting the development of stamens. The positive regulation of ethylene on petal maturation and flower opening can be mediated by inducing the biosynthesis of JA, while its negative control on ovary growth and fruit set could be mediated by its repressive effect on IAA biosynthesis.

Keywords: *ACO* gene regulation; andromonoecy; monoecy; ethylene; flower maturation; parthenocarpy.

4.2. Introduction

The cultivated species of the Cucurbitaceae family are a group of monoecious plants that have been utilized as a model for the study of the genetic control of sex determination in plants (Martínez and Jamilena, 2021). Many varieties in cultivated species are monoecious, developing male and female flower in the same plant, but some of the varieties are andromonoecious (male and hermaphroditic flowers), trimonoecious (male, female, and hermaphroditic flowers), gynoecious (only female flowers), and androecious (only male flowers). This natural variability makes this an ideal family to investigate the genetics of sex determination. The first sex-determining genes were discovered in *Cucumis sativus* (cucumber) and *Cucumis melo* (melon) (Boualem et al., 2008, 2009, 2015; Martin et al., 2009; Chen et al., 2016), but recent years have witnessed important discoveries in *Cucurbita pepo* (pumpkin and squash) (Martínez *et al*., 2014; García *et al.*, 2020*a,b*) and *Citrullus lanatus* (watermelon) (Boualem *et al*., 2016; Ji *et al*., 2016; Manzano *et a*l., 2016; Aguado *et al*., 2020; J.Zhang *et al*., 2020). Although many of the findings are similar in all species, the genetic control of sexual determination in some species differs slightly from the rest of the species (Aguado *et al*., 2020).

Ethylene is the key regulator of sex determination in cucurbits. External treatments with ethylene-releasing or -inhibiting agents have been used to determine the role of this hormone in the control of sex expression, i.e., female flowering transition and the number of female and male flowers per plant, as well as sex determination, which are the mechanisms that lead to a female or a male flower from a potentially hermaphrote floral bud (Manzano *et al*., 2013, 2014). The latter was achieved by arresting the growth of the stamens or carpels, respectively (Bai *et al*., 2004). Ethylene increases the ratio of female to male flowers in *Cucumis* and *Cucurbita* (Rudich *et al.*, 1969; Byers *et al.*, 1972; Manzano *et al*., 2011, 2013), but reduces this ratio in *Citrullus* plants. Inhibition of ethylene biosynthesis or perception, on the other hand, reduces the number of female flowers per plant in *Cucumis* and *Cucurbita*, and transforms the female flowers into bisexual or hermaphrodite ones. In *Citrullus*, this last treatment increases the number of female flowers per plant, but also transforms female flowers into hermaphroditic flowers, indicating that ethylene is required to arrest the development of stamens in female flowers of all cucurbits (Manzano *et al*.,

2014). Although gibberellins, auxins, and brassinosteroids have also been associated with sex control in cucurbits, some of their functions seem to be mediated by ethylene (Papadopoulou *et al*., 2005; Manzano *et al*., 2011; Zhang *et al*., 2014; J.Zhang *et al*., 2017).

So far, all of the discovered sex-determining genes are either in the ethylene biosynthesis and signaling pathway, or are transcriptional factors that regulate the former. The gene that regulates abortion of stamens during the formation of a female flower in all studied cucurbits encodes for an ethylene biosynthesis enzyme: cucumber *ACS2* and its orthologs (Boualem *et al*., 2008, 2009, 2016; Martínez *et al*., 2014; Ji *et al*., 2016; Manzano *et al*., 2016). This female-forming gene is negatively regulated by the transcription factor *WIP1*, which is responsible for the arrest of carpels in the formation of male flowers (Martin *et al*., 2009; Hu *et al*., 2017; J.Zhang *et al*., 2020). The male-forming *WIP1* gene is negatively regulated by *ACS11* and *ACO2/ACO3* in cucumber and melon, which are expressed very early in the floral meristem and determine the formation of a female flower. The disruption of either of these genes promotes the conversion of monoecy into androecy (Boualem *et al*., 2015; Chen *et al*., 2016). EMS mutation in ethylene receptor genes of *C. pepo* has demonstrated that ethylene perception at early and late stages of flower development is crucial for female flower determination. The *etr1a*, *etr1a-1*, *etr1b*, and *etr2b* gain of function mutations, in fact, lead to andromonoecy and androecy concomitantly with a reduced ethylene sensitivity (García *et al*., 2018, 2020*a,b*).

The role of other ethylene biosynthesis genes in sex determination is unknown. In this chapter, we demonstrate that the ethylene biosynthesis gene *CpACO1A* is involved in sex determination and flower development in *C. pepo*. Although the gene is not flower-specific, its role in ethylene biosynthesis is required for arresting stamen development, and the proper maturation and development of corolla and ovary of the female flower. *CpACO1A* and other sex-determining *ACO* and *ACS* ethylene biosynthesis genes were regulated by *CpACO1A*-producing ethylene in the female flower. The ethylene provided by CpACO1A also regulates hormonal balance in the female flowers. The increased IAA and the reduced ABA and JA contents in the *aco1a* mutant may be responsible for the parthenocarpic fruit development and the delayed flower opening of the mutant female flower.

4.3. Materials and methods

4.3.1. Plant material and isolation of mutants

The *aco1a* mutant analysed in this study was isolated from a high-throughput screening of *Cucurbita pepo* EMS collection (García *et al*., 2018). M2 plants from 600 lines were grown to maturity under standard greenhouse conditions, and alterations in reproductive developmental traits were evaluated. A mutant family was detected that produced hermaphrodite flowers, instead of female flowers. This mutant was selected for further characterization, and named *aco1a*. The monitoring of the development of the growth of the female floral organs, corolla and ovary, as well as the degree of their stamen development detected in the flowers, showed similarity with the phenotype found for other families of mutants previously described and characterized by García et al. (2020*a,b*) in *C. pepo*, which led us to deduce the possible relationship of ethylene with this new mutation. Prior to phenotyping, *aco1a* mutant plants were crossed twice with the background genotype MUC16, and the resulting BC_2 generation was selfed to obtain the BC_2S_1 generation.

4.3.2. Phenotyping for monoecy stability, sex expression, and floral traits

300 BC_2S_1 plants from wt/wt, w*t/aco1a*, and *aco1a/aco1a* were transplanted to a greenhouse and grown to maturity under local greenhouse conditions without climate control, and under standard crop management of the region, in Almería, Spain. The sex phenotype of each plant was determined according to the sex of the flowers in the first 40 nodes of each plant. A minimum of 30 wt/wt, 30 w*t/aco1a*, and 30 *aco1a/aco1a* plants were phenotyped. Phenotypic evaluations were performed in the spring-summer seasons 2019 and 2020.

The sex expression of each genotype was assessed by determining the node at which plants transitioned to pistillate flowering, and the number of male or pistillate/hermaphrodite flower nodes. The sex phenotype of each individual pistillate/hermaphrodite flower was assessed by the so-called andromonoecy index (AI) (Martínez *et al*., 2014; Manzano *et al*., 2016). Pistillate flowers were separated into three phenotypic classes that were given a score from 0 to 3 according to the degree of their stamen development: female (AI = 0), showing no stamen development; bisexual or pistillate (AI = 1; AI = 2), showing partial development of stamens and no pollen; and hermaphrodite (AI = 3), showing

complete development of stamens and pollen. The average AI of each plant and each genotype was then assessed from the resulting AI score of at least 10 individual female flowers from each plant, using a minimum of 30 plants for each genotype. To assess floral organ development, the growth rates of ovaries and petals in both female and male flowers of WT and *aco1a* mutant plants were determined by measuring the length and diameter of these floral organs every 2 d for 28 d in 20 flowers of each genotype, starting with flower buds ~2 mm in length. The anthesis time was estimated as the number of days taken for a 2 mm pistillate or male floral bud to reach anthesis.

4.3.3. Identification of *aco1a* mutation by whole-genome sequencing analysis

To identify the causal mutations of the *aco1a* phenotype, WT and mutant plants derived from BC_1S_1-segregating populations were subjected to whole-genome sequencing (WGS). In total, 120 BC_1S_1 seedlings were transplanted to a greenhouse and grown to maturity. The phenotype of those seedlings was verified in the adult plants, as wt/wt and wt/*aco1a* plants were monoecious while *aco1a/aco1a* plants were andromonoecious or partially andromonoecious. The genomic DNA from 30 WT and 30 *aco1a* plants was isolated by using the Gene JET Genomic DNA Purification Kit (Thermo Fisher®), and pooled into two different bulks: WT bulk and *aco1a* mutant bulk. DNA from each bulk was randomly sheared into short fragments of approximately 350 bp for library construction using the NEBNext® DNA Library Prep Kit (https:// international.neb.com), and fragments were briefly PCR enriched with indexed oligos. Pair-end sequencing was performed using the Illumina® sequencing platform, with a read length of PE150 bp at each end. The effective sequencing data were aligned with the reference *Cucurbita pepo* genome v.4.1 through BWA software (Li and Durbin, 2009). Single nucleotide polymorphisms (SNPs) were detected using the GATK HAPLOTYPECALLER (Depristo *et al*., 2011). ANNOVAR was used to annotate the detected SNPs (Wang, Li and Hakonarson, 2010).

Common variants between these mutant families (and other sequenced mutant families in the laboratory) were discarded, as they are likely common genomic differences with the reference genome. The genotype of the WT bulk (wt/wt and wt/*aco1a* plants) was expected to be 0/1 with an alternative allelic

frequency (AF) of 0.3, while the genotype of the mutant bulk (*aco1a/aco1a* plants) was expected to be 1/1 with an AF = 1. Therefore, the sequencing data were filtered according to the following parameters: genotype quality ≥ 90, read depth ≥ 10, AF = 1 in the mutant bulks, and AF ≤ 0.3 in the WT bulks. Once we had a set of positions that were differentially enriched in each bulk, we filtered out SNPs that were not canonical EMS changes (G > A or C > T transitions) (Till *et al*., 2004). All filters were performed with RStudio® software. The impact of this final set EMS SNPs on gene function was finally determined by using Integrative Genomics Viewer (IGV) software and the Cucurbit Genomics Database (CuGenDB) (http://cucurbit genomics.org).

4.3.4. Validation of the identified mutations by high-throughput genotyping of individual segregating plants

Segregation analysis was performed to confirm that the identified mutations were causal mutations of the *aco1a* phenotype. Approximately 300 BC_2S_1 plants segregating for the mutation were genotyped using Kompetitive allele-specific PCR (KASP) technology. Primers were synthesized by LGC Genomics® (http://www.lgcgroup.com), and the KASP assay was performed in the FX96 Touch Real-Time PCR Detection System (Bio-Rad®) using the LGC protocol (https://afly.co/xyn2). The multiplex PCRs were run with 10 µL final reaction volume containing 5 µL KASP V4.0 2x Master mix standard ROX (LCG Genomics®), 0.14 µL KASP-by-Design primer mix (LCG Genomics®), 2 µL of 10-20 ng/µL genomic DNA, and 2.86 µL of water. The PCR thermocycling conditions were 15 min at 94°C (hot-start activation) followed by 10 cycles of 94°C for 20 s and 61°C for 1 min (dropping-0.6°C per cycle to achieve a 55°C annealing temperature) followed by 26 cycles of 94°C for 20 s and 55°C for 1 min. Data were then analysed using CFX Maestro™ Software (Bio-Rad®) to identify SNP genotypes.

4.3.5. 1-aminocyclopropane-1-carboxylic acid oxidase enzyme activity

1-aminocyclopropane-1-carboxylic acid oxidase (ACO) activity was assessed following the protocol described in Bulens *et al*. (2011). The enzyme activity was quantified in leaves, stems, roots, cotyledon, and flowers in triplicate. 0.5 g of each material was pulverized in liquid nitrogen, and 1 mL of extraction buffer MOPS (pH 7.2) and 50 mg of polyvinylpolypyrrolidone (PVPP) were added

to each sample. The samples were subsequently incubated for 10 min at 4ºC and finally centrifuged for 30 min at 22,000 x g at 4ºC. 400 µL of the resulting supernatant was mixed with 3.6 mL of MOPS reaction buffer (pH 7.2) in a 20 mL glass vial. After homogenising the mixture for 5 s, samples were incubated in a water bath for 1 h at 30ºC while gently shaking. The amount of ethylene formed was determined by analysing 1 mL of gas from the headspace of the reaction tube on a Varian® 3900 gas chromatograph (GC) fitted with a flame ionisation detector (FID). A blank sample (3.6 mL reaction buffer + 400 µL DW) was used as a control for the whole process. Enzyme reactions and ethylene readings were done in triplicate. The activity of ACO was expressed as nmol * gFW^{-1} * h^{-1}.

4.3.6. Ethylene production measurements

The production of ethylene in WT and *aco1a* flowers was assessed throughout the different stages of development. Female and male floral buds of 8 to 55 mm in length (FFB / MFB) and the apical shoots of plants growing under climatic controlled conditions were collected and incubated at room temperature for 6 h in hermetic glass containers of 50-450 mL. Ethylene production was determined by analysing 1 mL of gas from the headspace in a Varian® 3900 gas chromatograph (GC) fitted with a flame ionisation detector (FID). The instrument was calibrated with standard ethylene gas. Four biological replicates were made for each one of the flower developmental stages analysed and three measurements per sample. Ethylene production was expressed as nL * gFW^{-1} * $6h^{-1}$.

4.3.7. Assessing ethylene sensitivity

To evaluate the level of sensitivity to ethylene, flower abscission was assessed for male flowers in response to an external treatment with ethylene. Male flowers from WT and *aco1a* plants were collected at two stages of development: A (anthesis) and A-2 (2 d before anthesis). For each stage, 30 WT and *aco1a* flowers were placed in glass vases with water, and incubated in two culture chambers with equal humidity and temperature, 50% RH and 20ºC. One of the chambers was used as a control (Ct), and the other was filled with 50 ppm of ethylene (ET). The tests were performed in triplicate. Both chambers remained closed for 72 h, and the percentage of abscission produced was evaluated after 24, 36, 48 and 72 h for each stage of development.

4.3.8. Hormone concentration measurements

Female flower buds of 5-8 mm from WT and *aco1a* plants were collected for hormone concentration measurements. Representative samples consisted of 3 bulks of approximately 30 female flowers each. To preserve the samples, WT and *aco1a* bulks were quickly stored on dry ice. Then, the samples were placed in a freeze dryer CRYODOS V3.1-50 (Telstar®), where they were lyophilized for 1 w and subsequently pulverized in a mixer mill MM200 (Retsch™). The concentration of salicylic acid (SA), indol-3-butyric acid (IBA), indole-3-acetic acid (IAA), gibberellic acid (GA3), 6-benzyladenine (BA), abscisic acid (ABA), and jasmonic acid (JA) were determined in each triplicated sample through ultra-performance liquid chromatography coupled with a hybrid quadrupole orthogonal time-of-flight mass spectrometer (UPLC-Q-TOF/MS/MS) according to the hormone determination method of Müller and Munné-Bosch (2011).

4.3.9. Bioinformatics and phylogenetic analysis

Alignments and protein sequences analysis were performed using the BLAST alignment tools at NCBI (https://blast.ncbi.nlm.nih.gov/Blast.cgi). Protein structure information and homology-modelling were analysed using the Protein Data Bank RCSB PDB (https://www.rcsb.org) and SWISS-MODEL (https://swissmodel. expasy.org). The phylogenetic relationships between *C. pepo*, *A. thaliana*, *S. lycopersicum*, *O. sativa*, *C. sativus*, and *C. melo* of *ACO* genes were studied using MEGA X software (Kumar *et al.*, 2018), which allowed the alignment of proteins and the construction of phylogenetic trees using MUSCLE (Edgar, 2004) and the maximum likelihood method based on the Poisson correction model (Zuckerkandl and Pauling, 1965), with 2,000 bootstrap replicates. The protein sequences (**Table S4.1**) were obtained using the Arabidopsis Information Resource (https://www.arabidopsis.org), the Cucurbit Genomics Database (CuGenDB) (http://cucurbitgenomics.org), the Rice Database Oryzabase-SHIGEN (https://shigen.nig.ac.jp/rice/oryzabase), and the Sol Genomics Network (https://solgenomics.net). Cucurbits *ACO* genes structure visualization, such as the composition and position of exons and introns, were performed with the Gene Structure Display Server (GSDS) (http://gsds.gao-lab.org/Gsds_about.php).

Finally, Delta Delta G (**ΔΔ**G), a metric for predicting how a single point mutation will affect protein stability, was assessed with the tools SNAP2 (https://rostlab.org/services/snap2web) and I-Mutant3.0 (https://folding.Biofold .org/i-mutant/i-mutant2.0.html). MUpro (http://mupro.prote omics.ics.uci.edu) and CUPSAT (http://cupsat.tu-bs.de) tools were also used to predict the stability of the CpACO1A protein.

4.3.10. Assessment of relative gene expression by quantitative RT-PCR

Gene expression analysis was carried out in samples of WT and *aco1a* plants growing in a greenhouse during the spring-summer season. The expression level was studied in male and female flowers' organs (corolla and ovaries) at different flower developmental stages, as well as in plant apical shoots, leaves, shoots, cotyledons, and roots. The analysis was performed in three biological replicates for each genotype, each of which was derived from a pool of four plants. Total RNA was isolated according to the protocol of the GeneJET Plant RNA Purification Kit (Thermo Fisher®). RNA was converted into cDNA with the ADNc RevertAid™ kit (Thermo Fisher®). The qRT-PCR was performed in 10 µl total volume with 1 × Top Green qPCR Super Mix (Bio-Rad®) in the CFX96 Touch Real-Time PCR Detection System thermocycler (Bio-Rad®). The gene expression values were calculated using the $2^{-\Delta\Delta CT}$ method (Livak and Schmittgen, 2001). The constitutive *EF1α* gene was used as the internal reference. **Table S4.2** shows the primers used for each qRT-PCR reaction.

4.3.11. Statistical analyses

Data were analysed for multiple comparisons by analysis of variance (ANOVA) using the statistical software Statgraphic Centurion XVIII. Differences between genotypes and treatments were separated by least significant difference (LSD) at a significance level of $p \leq 0.05$.

4.4. Results

4.4.1. *aco1a* impairs sex determination and petals and ovary development

The mutant *aco1a* was found in a high-throughput screening of a *C. pepo* mutant collection for alterations in flower and fruit development. To ensure accurate phenotyping, mutant plants were backcrossed with the background genotype MUC16 for two generations, and then selfed. The resulting BC_2S_1 generations segregated 3:1 for WT and *aco1a* phenotypes, indicating that the mutation is recessive (**Table S4.3**).

The sex phenotype of *aco1a* was assessed in BC_2S_1 plants growing under spring-summer conditions (**Fig. 1**). Male flowers were not affected, but most female flowers were converted into bisexual flowers with partially or totally developed stamens (**Fig. 1A**). This partial conversion of monoecy into andromonoecy, also termed unstable monoecy, partial andromonoecy or trimonoecy, indicates that *aco1a* impairs the sex determination mechanism which is responsible for arresting stamen development in the female flower. Pistillate flowers in the first 40 nodes were classified according to the andromonoecious index (AI) in either homozygous WT (wt/wt), heterozygous (wt/*aco1a*), or homozygous mutant (*aco1a/aco1a*) plants (**Fig. 1B**). The wt/wt and wt/*aco1a* plants produced only female flowers (AI = 0), indicating a complete arrest of stamen development in the pistillate flowers of these plants (**Fig. 1C**). The *aco1a/aco1a* pistillate flowers, however, exhibited different degrees of stamen development (AI ranging from 0 to 3), and plants had an average AI of 2.1 (**Fig. 1B, C**).

Figure 2 shows the effects of the *aco1a* mutation on petal and ovary/fruit development. In the bisexual and hermaphrodite flowers of *aco1a* (AI = 2-3), the petal growth rate was reduced and resembled petal development in male flowers. Petal maturity and subsequent anthesis of the flower were delayed in the mutant with respect to WT (**Fig. 2A, B**). Anthesis time, the period of time taken for a 2 mm floral bud to reach anthesis and to open, was longer in male WT flowers (average 21 d) than in female WT flowers (average 12 d) (**Fig. 2B**).

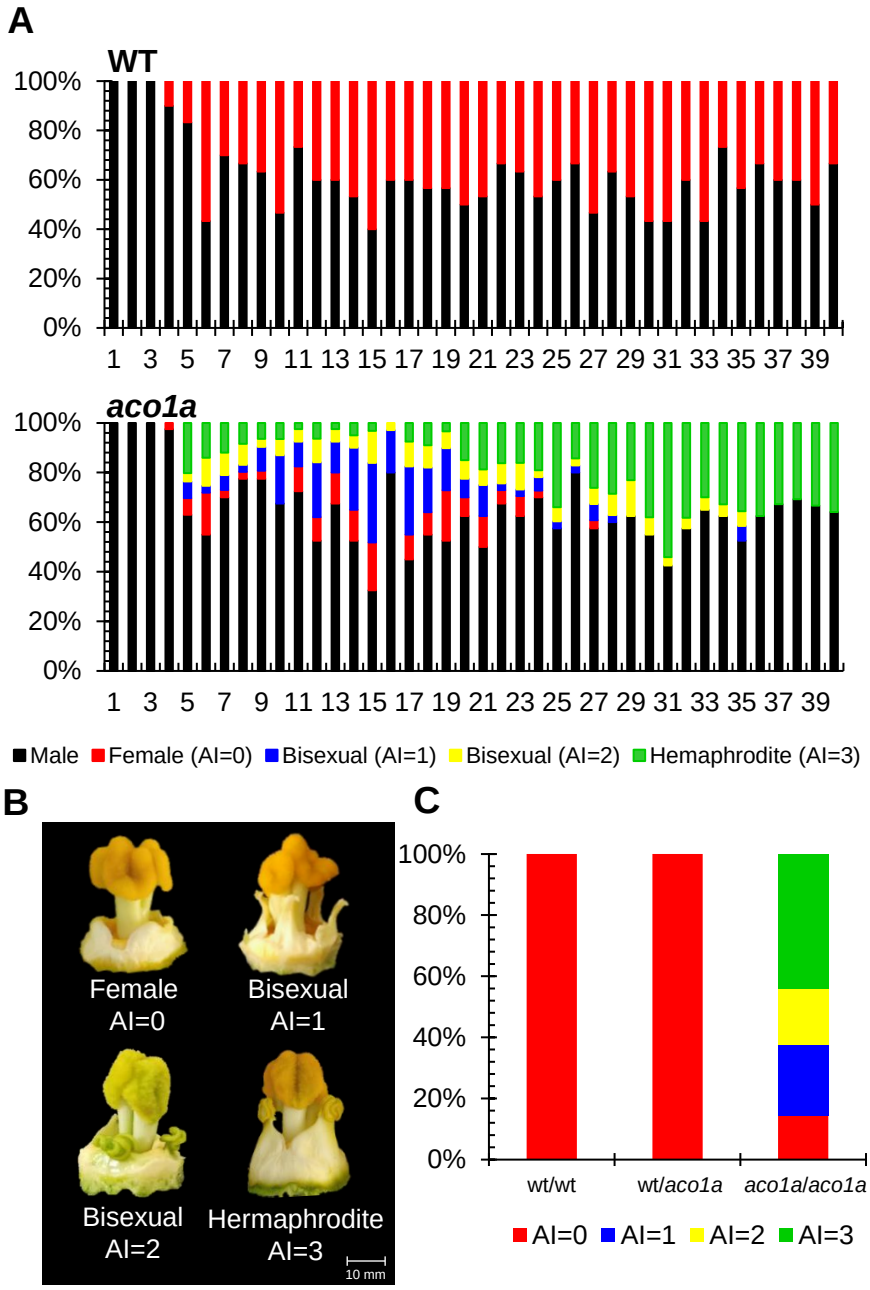

Figure 1. Sex phenotype of WT and *aco1a* plants. (**A**) Distribution of male and pistillate flowers in the first 40 nodes of the main shoot. In each node, colour bars indicate the percentages of male (black), female (red), and bisexual and hermaphrodite flowers (blue, yellow, and green) in the total number of plants analysed (n = 30 for each genotype). (**B**) Phenotype of pistillate flowers with different stamen development and AI index. Female flowers (AI = 0) develop no stamen, bisexual flowers (AI = 1-2) develop intermediate stamens, and hermaphrodite flowers (AI = 3) develop entire stamens with pollen. (**C**) Percentage of each pistillate flower in each genotype.

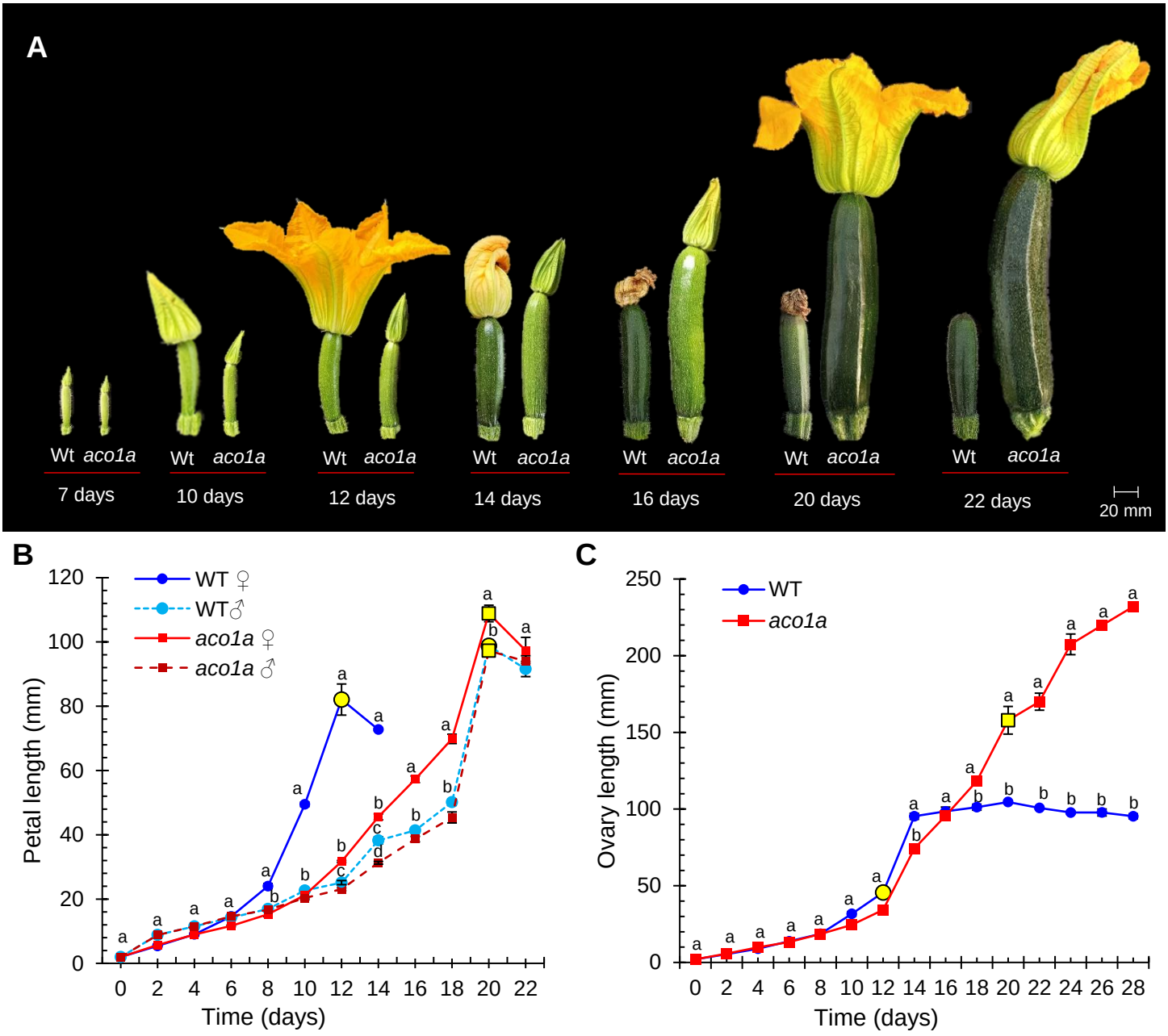

Figure 2. Comparison of WT and *aco1a* flower development. (**A**) Effect of *aco1a* mutation on the development of ovary and corolla of the pistillate flower. Note that the mutant pistillate flower reaches anthesis later than the WT, and that the ovary continues its growth until producing a parthenocarpic fruit. (**B**) Comparison of the growth rate of WT and mutant corolla. Flowers were labelled when their ovaries were 2 mm long, and then measured every 2 d for 22 d. Yellow circles indicate the time at which more than 80% of the flowers reached anthesis. (**C**) Comparison of the growth rate of WT and mutant ovaries/fruits over a period of 22 d. Error bars represent SE. Different letters indicate significant differences in flowers of the different genotypes at each developmental time ($p \leq 0.05$)

Bisexual and hermaphrodite *aco1a* flowers also took an average of 21 d to reach anthesis (range 20-25 d). No alterations in petal development or anthesis time were observed in WT and *aco1a* male flowers (**Fig. 2B**). Pollination was attempted in *aco1a* hermaphrodite flowers (AI = 2-3), but none of the fruits were able to set seeds. Since the pollen is fertile in other plants, this female sterility could be associated with the over-maturation of stigma and style because of the delayed corolla aperture. However, we were able to self *aco1a/aco1a* plants by using the few female flowers with no stamen (AI = 0). Significant differences were detected in ovary size between WT and *aco1a* pistillate flowers (**Fig. 2A, C**). At anthesis, the WT ovary reached approximately 12 cm in length and then aborted. The *aco1a* ovary, in contrast, continued to grow until it reached 18-30 cm at anthesis (**Fig. 2A, C**). The growth rate of WT and *aco1a* ovary/fruit was similar during the first 16 d. After that time, WT ovaries aborted, and those of *aco1a* maintained growth up to anthesis (**Fig. 2C**). The *aco1a* fruits can be considered parthenocarpic since they grew in the absence of pollination, as the corolla was closed.

4.4.2. *aco1a* is a missense mutation causing P5L substitution in the ethylene biosynthesis enzyme CpACO1A

To elucidate the causal mutation of *aco1a* phenotype, we performed whole-genome resequencing (WGS) of two bulked DNA samples from a BC_2S_1 segregating population: the WT bulk, having DNA from 30 WT plants (monoecious); and the *aco1a* bulk, having DNA from 30 mutant plants (partially andromonoecious). In the mutant bulk, only the plants that showed the most extreme andromonoecious phenotype were selected.

More than 98% of the sequencing reads (more than 80 million in each bulk) were mapped against the *C. pepo* reference genome version 4.1, which represented an average depth of 47.41 (**Table 1**). The identified SNPs (more than 370,000 in each of the bulks) were filtered for their mutant allele frequency (AF) in the WT and the mutant DNA bulks. For the causal mutation of the phenotype, it is expected that the genotype was 0/1 for WT bulk (alternative allele frequency AF = 0.25) and 1/1 for the mutant bulk (AF = 1).

For the non-causal SNPs, however, we expected an AF of 0.5 in both bulks. A putative causal region in chromosome 4 was found that has the expected AF in WT and mutant bulk (**Fig. 3A**). In fact, after filtering for AF = 1 in the mutant bulk and AF < 0.3 in the WT bulk, 412 SNPs were selected (**Table 1**). Among them, 145 corresponded to canonical EMS mutations (C > T and G > A), and only one on chromosome 4 was positioned on the exome and had a high impact on the protein (**Table 1; Fig. 3**).

Table 1. Summary sequencing data for WT and *aco1a*.

Sequencing				**WT**		***aco1a***
No. reads				106,448,438		84,600,742
Mapped reads (%)				98.10		98.06
Average depth				47.41		40.41
Coverage at least 4X (%)				95.81		95.41
SNPs filtering						
Total Nº. SNPs				381,666		374,917
AF (WT) < 0.3; AF (*aco1a*) = 1				412		412
EMS SNPs G > A or C > T				145		145
EMS SNPs (GQ > 90; DP > 10)				4		4
High impact SNPs				0		1
Candidate SNP						
Chr	**Position**	**Ref**	**Alt**	**Gene ID**	**Effect**	**Functional Annotation**
4	7,715,975	C	T	Cp4.1LG04g02610	P5L	1-aminocyclopropane-1-carboxylate oxidase 1

Note: AF, allelic frequency; GQ, genotype quality; DP, read depth.

The sequence surrounding the candidate *aco1a* mutation (± 500 bp) was then used in BLAST searches against the DNA and protein databases at NCBI. It was found that the C > T transition was a missense mutation changing proline by leucine at residue 5 (P5L) of the ethylene biosynthesis enzyme 1-aminocyclopropane-1-1carboxylate oxidase 1A (CpACO1A) (**Fig. 3A**). To prove that the selected EMS mutation was the one responsible for *aco1a* phenotype, we genotyped the SNP alleles in 300 plants from a BC_2S_1 population. The results demonstrated a 100% co-segregation between the *aco1a* phenotype and the C > T mutation in *CpACO1A* (**Table S4.4**). Other three EMS-induced mutations in chromosome 4 were also tested (**Table S4.5**), but none of them co-segregated with the mutant phenotype in the 300 BC_2S_1 plants analysed. The identified mutation has a deleterious effect on CpACO1A enzyme (**Fig. 3B**).

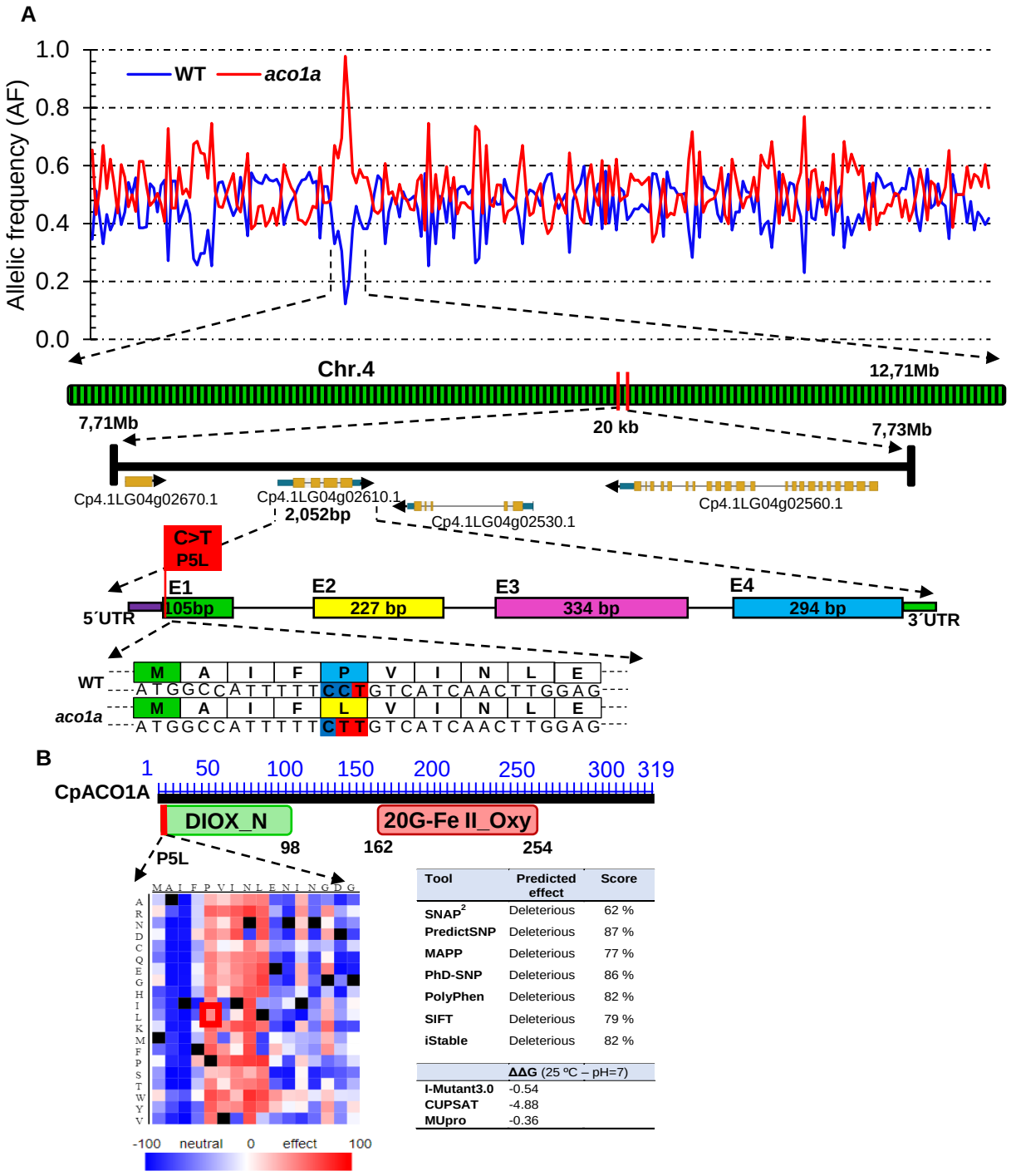

Tool	Predicted effect	Score
SNAP[2]	Deleterious	62 %
PredictSNP	Deleterious	87 %
MAPP	Deleterious	77 %
PhD-SNP	Deleterious	86 %
PolyPhen	Deleterious	82 %
SIFT	Deleterious	79 %
iStable	Deleterious	82 %

	ΔΔG (25 ºC – pH=7)
I-Mutant3.0	-0.54
CUPSAT	-4.88
MUpro	-0.36

Figure 3. Identification of *aco1a* causal mutation by BSA-sequencing. (**A**) Frequency of the alternate allele in the WT and *aco1a* bulks along the physical map of squash genome. The analysis indicates that a region of chromosome 4 is responsible for the mutant phenotype. A missense mutation on the gene *Cp4.1LG04g02610.1* (*CpACO1A*) produces a change of proline by leucine at residue 5 (P5L) of the ethylene biosynthesis enzyme CpACO1A. (**B**) Impact of P5L mutation in the N-terminal conservative non-heme dioxygenase DIOX_N region of ACO enzymes. The SNAP^2-generated heatmap of CpACO1A N-domain indicates that changes in residue 5 to have a high impact on protein function. The red box indicates the impact of the *aco1a* mutation. The table on the right shows the predicted effect of the mutation on protein function and stability by using different bioinformatics tools.

Bioinformatics analysis with the SNAP[2] tool predicted a negative effect of P5L substitution on protein function (**Fig. 3B**). Other bioinformatics tools, such as PredictSNP, MAPP and iStable, among others, showed the same evidence (**Fig. 3B**). Moreover, predicted Gibbs free energy changes (**ΔΔ**G), a metric for predicting how a single point mutation could affect protein stability, was assessed for P5L mutation by using I-mutant3.0 predictor, CUPSAT, and MUpro. The comparison of *aco1a* and WT CpACO1A resulted in negative **ΔΔ**G values, which indicated a decreased stability of the mutated protein (**Fig. 3B**).

4.4.3. Gene structure and phylogenetic relationships of *CpACO1A*

Given that the genomes of *C. pepo* are duplicated (Sun *et al*., 2017; Montero-Pau *et al.*, 2018), the gene *CpACO1A* on chromosome 4 (Cp4.1LG04g02610) has a paralog (*CpACO1B*) with more than 80% of homology on an syntenic block of chromosome 5 (Cp4.1LG05g15190). The duplicates did not maintain the same molecular structure: four exons for *CpACO1A* and three exons for *CpACO1B* (**Fig. 4A**). *ACO1*, like genes in other plants, including those of *C. maxima*, *C. moschata*, *C. melo*, *C. lanatus* and *C. sativus*, conserve the four exonic structure of *CpACO1A* (**Fig. 4A**). All ACO proteins in the NCBI database were found to conserve the proline residue on position 5, indicating that this is an essential residue for ACO activity (**Fig. 4B**). Based on residues conserved at specific positions towards the carboxylic end of the proteins, three types of ACO enzymes have been established in plants (**Fig. 4B**), which also defines its specific functionality and biological activity.

A phylogenetic tree was inferred by using ACO protein sequences from different cucurbit species, including different *Cucurbita ssp*, *Cucumis melo* and *Cucumis sativus*, together with those of the most studied model species, *Arabidopsis thaliana*, *Solanum lycopersicum*, and *Oryza sativa* (**Fig. 4B, C**). The *C. pepo* CpACO1A is a type I ACO that clustered together with melon CmACO1 and cucumber CsACO3 (also called CsACO1-like). Furthermore, the genes coding for the type I ACO1 enzymes of these three cucurbits were found to be positioned in a syntenic block of *C. pepo*, *C. melo*, and *C. sativus* genomes. The paralogous CpACO1B is also a type I ACO, but clustered separately from CpACO1A, CsACO3, and CmACO1 (**Fig. 4C**).

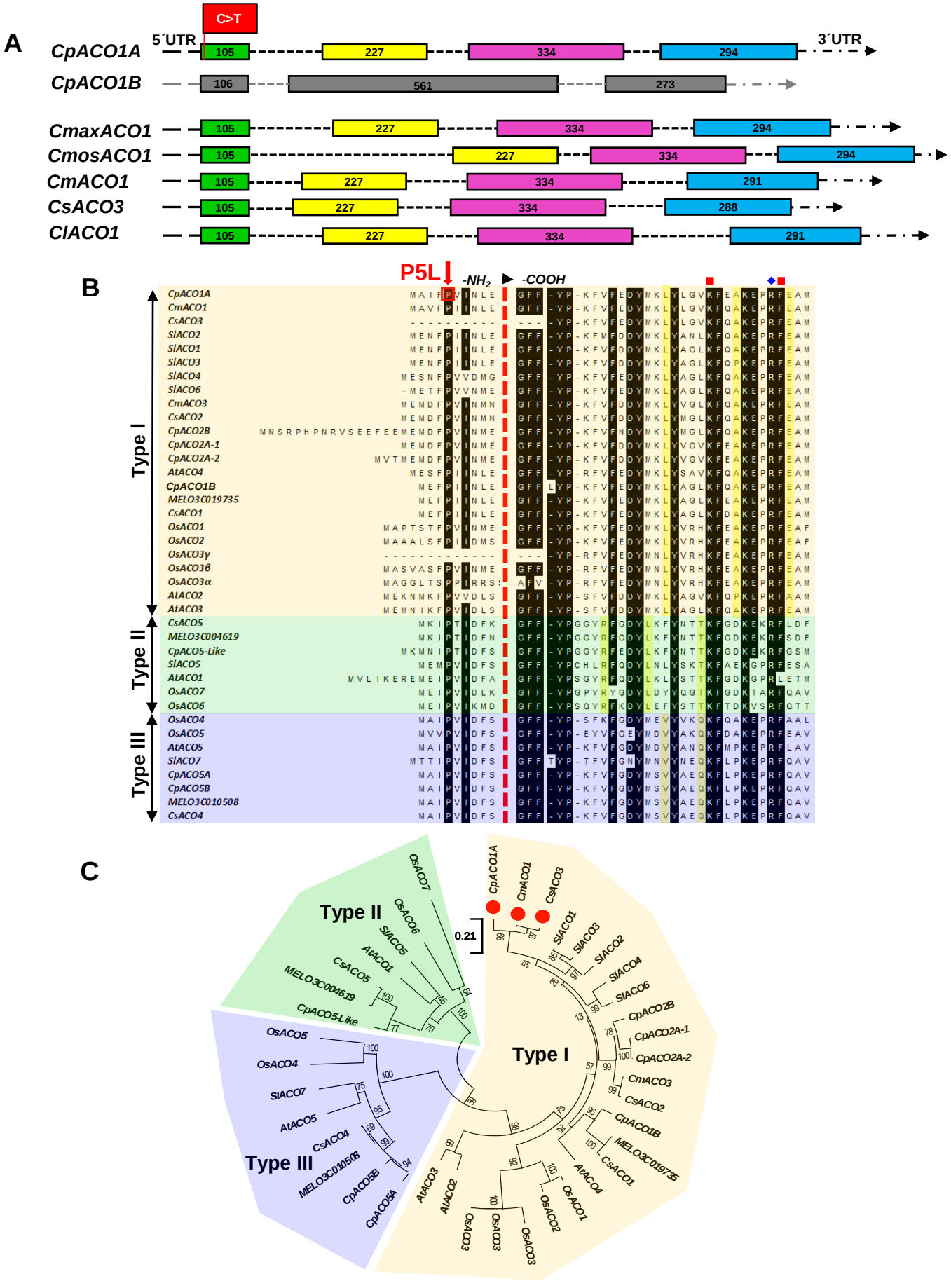
A
C>T
5´UTR
3´UTR
CpACO1A
105
227
334
294
CpACO1B
106
561
273
CmaxACO1
CmosACO1
CmACO1
291
CsACO3
288
ClACO1
B
P5L
-NH2
-COOH
Type I
Type II
Type III
CpACO1A
CmACO1
CsACO3
SlACO1
SlACO3
SlACO2
SlACO4
SlACO6
CpACO2B
CpACO2A-1
CpACO2A-2
CmACO3
CsACO2
CpACO1B
MELO3C019735
CsACO1
OsACO1
OsACO2
OsACO3
AtACO4
AtACO2
AtACO3
SlACO7
AtACO5
CsACO4
MELO3C010508
CpACO5B
CpACO5A
SlACO5
AtACO1
CsACO5
MELO3C004619
CpACO5-Like
OsACO7
OsACO6
OsACO5
OsACO4
0.21

Figure 4. Genetic relationships among ACO enzymes in different plant species. (**A**) Comparison of the gene structure of *CpACO1A* and *CpACO1B* of *C. pepo* with other homologs in cucurbit species: *Cucurbita maxima* (*CmaxACO1*), *Cucurbita moschata* (*CmosACO1*), *Cucumis melo* (*CmACO1*), *Cucumis sativus* (*CsACO3*), and *Citrullus lanatus* (*ClACO1*). (**B**) Consensus proline residue in position 5 and ACO classification according to conserved residues in a specific position towards the -COOH end of the proteins. (**C**) Phylogenetic ACO tree from different cucurbit species: *C. melo*, *C. sativus*, and *C. pepo* together with those of the most studied model species, *Arabidopsis thaliana*, *Solanum lycopersicum*, and *Oryza sativa*. Bootstrap values are depicted on the tree.

A phylogenetic tree was inferred by using ACO protein sequences from different cucurbit species, including different *Cucurbita ssp*, *Cucumis melo* and *Cucumis sativus*, together with those of the most studied model species, *Arabidopsis thaliana*, *Solanum lycopersicum*, and *Oryza sativa* (**Fig. 4B, C**). The *C. pepo* CpACO1A is a type I ACO that clustered together with melon CmACO1 and cucumber CsACO3 (also called CsACO1-like). Furthermore, the genes coding for the type I ACO1 enzymes of these three cucurbits were found to be positioned in a syntenic block of *C. pepo*, *C. melo*, and *C. sativus* genomes. The paralogous CpACO1B is also a type I ACO, but clustered separately from CpACO1A, CsACO3, and CmACO1 (**Fig. 4C**).

4.4.4. The *aco1a* mutation impairs *CpACO1A* expression, ACO activity, and ethylene production and sensitivity

The expression of *CpACO1A* and *CpACO1B* in different WT and *aco1a* tissues is shown in **Fig. 5A**. *CpACO1B* was not expressed in any of the analysed tissues, indicating that this is a non-functional paralogous gene. *CpACO1A* was found to be expressed in all tissues, except in cotyledons. Its transcript was, however, much more accumulated in roots and flowers (**Fig. 5A**). *CpACO1A* was similarly expressed in the different WT and mutant tissues, except in the female flower buds, where the gene showed a higher expression in the mutant. To understand the function of *CpACO1A* in flower development, its expression was compared in WT and *aco1a* apical shoots and female and male flowers buds (FFB / MFB) at different stages of development (**Fig. 5B**). In the apical shoot, *CpACO1A* expression was similar in WT and *aco1a* plants. In the mutant female and male flowers, *CpACO1A* transcripts are similarly more highly accumulated in the mutants, suggesting that the andromonoecious *aco1a* phenotype is not caused by a reduction of gene expression.

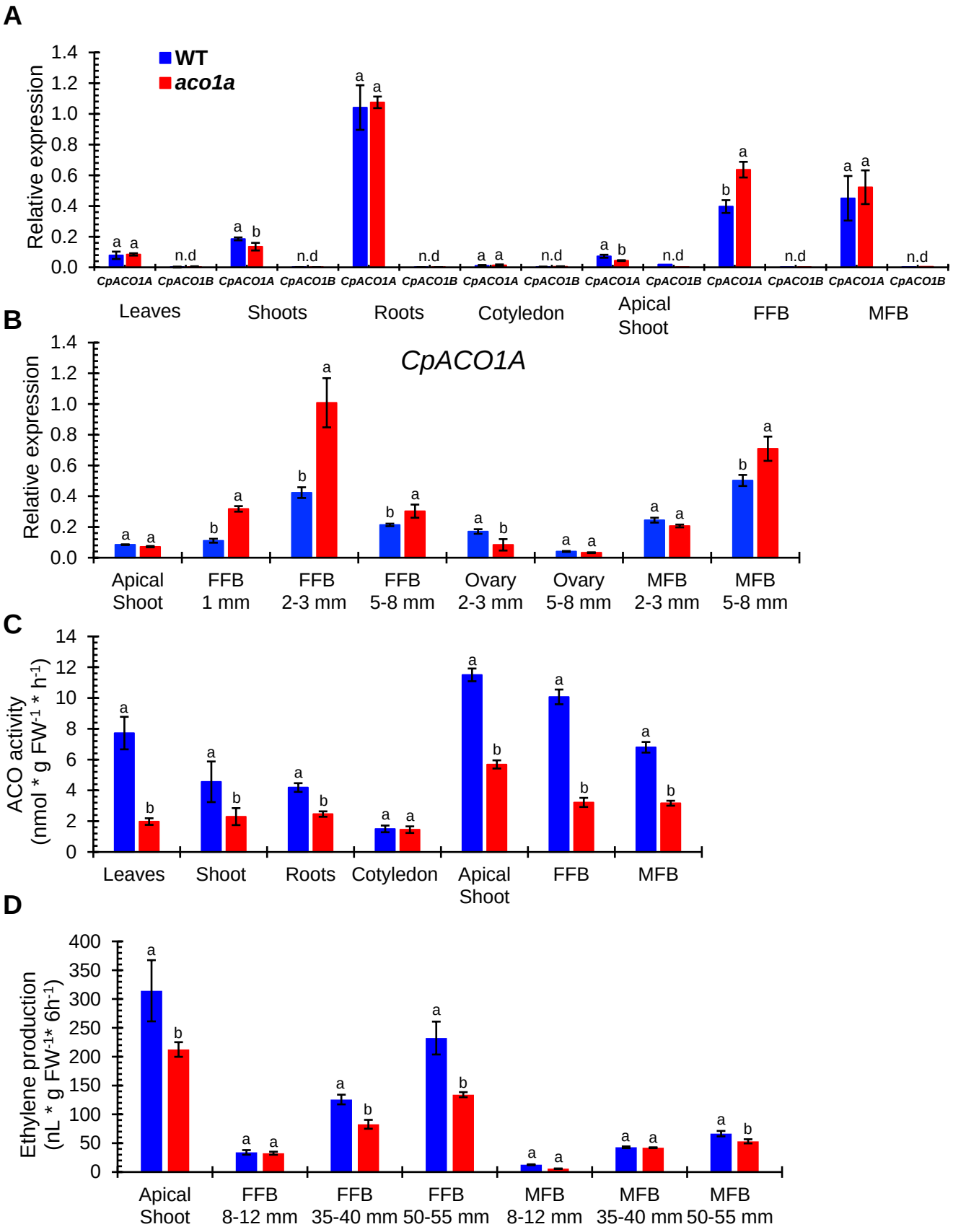
A
WT
aco1a
Relative expression
CpACO1A CpACO1B
Leaves
Shoots
Roots
Cotyledon
Apical Shoot
FFB
MFB
B
CpACO1A
Relative expression
Apical Shoot
FFB 1 mm
FFB 2-3 mm
FFB 5-8 mm
Ovary 2-3 mm
Ovary 5-8 mm
MFB 2-3 mm
MFB 5-8 mm
C
ACO activity (nmol * g FW-1 * h-1)
Leaves
Shoot
Roots
Cotyledon
Apical Shoot
FFB
MFB
D
Ethylene production (nL * g FW-1* 6h-1)
Apical Shoot
FFB 8-12 mm
FFB 35-40 mm
FFB 50-55 mm
MFB 8-12 mm
MFB 35-40 mm
MFB 50-55 mm

Figure 5. Comparison of *CpACO1A* gene expression, ACO activity, and ethylene production in WT and *aco1a* plants. (**A**) Relative gene expression of *CpACO1A* and *CpACO1B* in different WT and *aco1a* plant organs. (**B**) Relative expression of *CpACO1A* in the apical shoots and in female and male floral buds with different stages of development. (**C**) ACO1 activity in different WT and *aco1a plant* organs. (**D**) Ethylene production in the apical shoot and in female and male floral buds of WT and *aco1a* plants. FFB, female floral bud excluding the ovary; MFB, male floral bud. The assessments were performed in three independent replicates for each tissue. Error bars represent SE. Different letters indicate significant differences between WT and mutant apical shoots and flowers at the same stage of development ($p \leq 0.05$).

Although there are other ACO isoenzymes in the *C. pepo* genome, we have assessed the total ACO activity and ethylene production in different WT and *aco1*a plant tissues (**Fig. 5C**). The *aco1a* mutation was found to cause a reduction of ACO activity in all studied tissues, except in cotyledons, where the gene was not found to be expressed (**Fig. 5C**). These data suggest that the mutation *aco1a* likely impairs CpACO1A activity. The *aco1a* mutation significantly reduced the production of ethylene in the apical shoots of the plants, where a number of small floral buds are developing, and in pistillate flowers (**Fig. 5D**).

As previously reported, ethylene increased throughout the development of male, female (WT) and bisexual/hermaphrodite (*aco1a*) flowers, and pistillate flowers produced significantly more ethylene than male flowers at the same developmental stage (**Fig. 5D**). The bisexual flowers of *aco1a* showed a significant reduction of ethylene production during their development, especially those flowers with more than 35 mm in length (**Fig. 5D**). A slight reduction in ethylene production was also found in *aco1a* male flowers of 50-55 mm in length (**Fig. 5D**). Ethylene sensitivity in WT and *aco1a* plants was also assessed by measuring the abscission time of male flowers in response to external treatments with ethylene (**Fig. 6**).

The male floral buds were collected at two developmental stages: anthesis (A) and 2 d before anthesis (A-2). The flowers were put in a container with water and treated in an atmosphere with air (control) or ethylene (ET) up to 72 h, and floral abscission was evaluated every 12 h (**Fig. 6A**). Both WT and *aco1a* flowers responded to ethylene by accelerating their senescence and abscission (**Fig. 6B**). However, the increase in the percentage of flower abscission in response to ethylene was lower in *aco1a* than in WT flowers (**Fig. 6B**), indicating a partially ethylene-insensitive phenotype of the mutant *aco1a* male flowers.

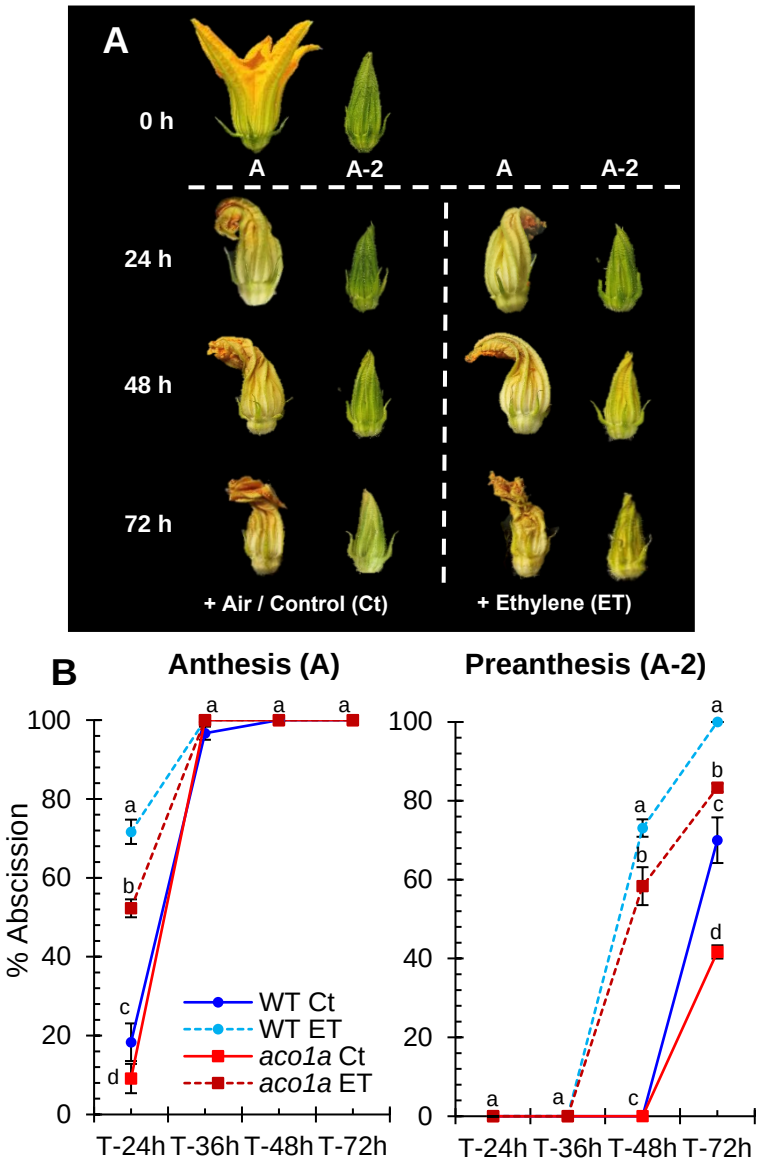

Figure 6. Ethylene sensitivity of WT and *aco1a*. The sensitivity to ethylene was determined by assessing the percentage of flower abscission in response to ethylene in male flowers at two stages of development. (**A**) Phenotype of male flowers at two stages of development: anthesis (A) and 2 d before anthesis (A-2). Photographs were taken at harvest (0 h of treatment) and 24, 48, and 72 h after the treatment with air or ethylene (ET). (**B**) Percentage of abscission in male flowers harvested at anthesis (A) or 2 d before anthesis (A-2). Error bars represent SE. Different letters indicate significant differences between flower abscission of each treatment and genotype at the same time after the treatment ($p \leq 0.05$).

4.4.5. Expression of different sex-determining genes in WT and *aco1a* flowers

The possible regulation of *CpACO1A* over other sex-determining genes was investigated by assessing the expression of those genes in WT and *aco1a* pistillate and male flowers (**Fig. 7**). The ethylene biosynthesis genes *CpACO2B*, *CpACS11A* and *CpACS27A*, which are expressed at early stages of female flower development and make the floral meristem to be determined as a female flower (Martínez and Jamilena, 2021), were differentially expressed in WT and *aco1a* pistillate flowers, but not in the apical shoots or in male flowers (**Fig. 7**).

In very small floral buds (1 mm), the *aco1a* mutation repressed the expression of the three genes. In 2-3 mm floral buds, the expression of the *CpACS11A* and *CpACS27A* was repressed in the ovary, and the expression of *CpACO2B* and *CpACS11A* was induced in the rest of the floral organs (petals, style, and stigma). In 5-8 mm female floral buds, the expressions of these three ethylene biosynthesis genes were not altered by *aco1a* (**Fig. 7**).

The mutation *aco1a* also diminished the expression of the ethylene receptor *CpETR1A* and the ethylene signaling gene *CpEIN3A* (**Fig. 7**) at early stages of female flower development (female floral buds of 1 mm and 2-3 mm in length) and in ovaries of flowers 2-3 mm in length. In the rest of the analysed tissues, including the apical shoot, female flowers at later stages of development and male flowers, no difference was found in the expression of these two ethylene signaling genes between WT and *aco1a* tissues (**Fig. 7**).

The expression *CpWIP1B*, a homolog of melon *WIP1* involved in the arrest of stamen during the development of male flowers, was unaltered by the mutation in most of the studied tissues, but in the apical shoot and in male floral buds of 5-8 mm in length, the gene was induced in the mutant.

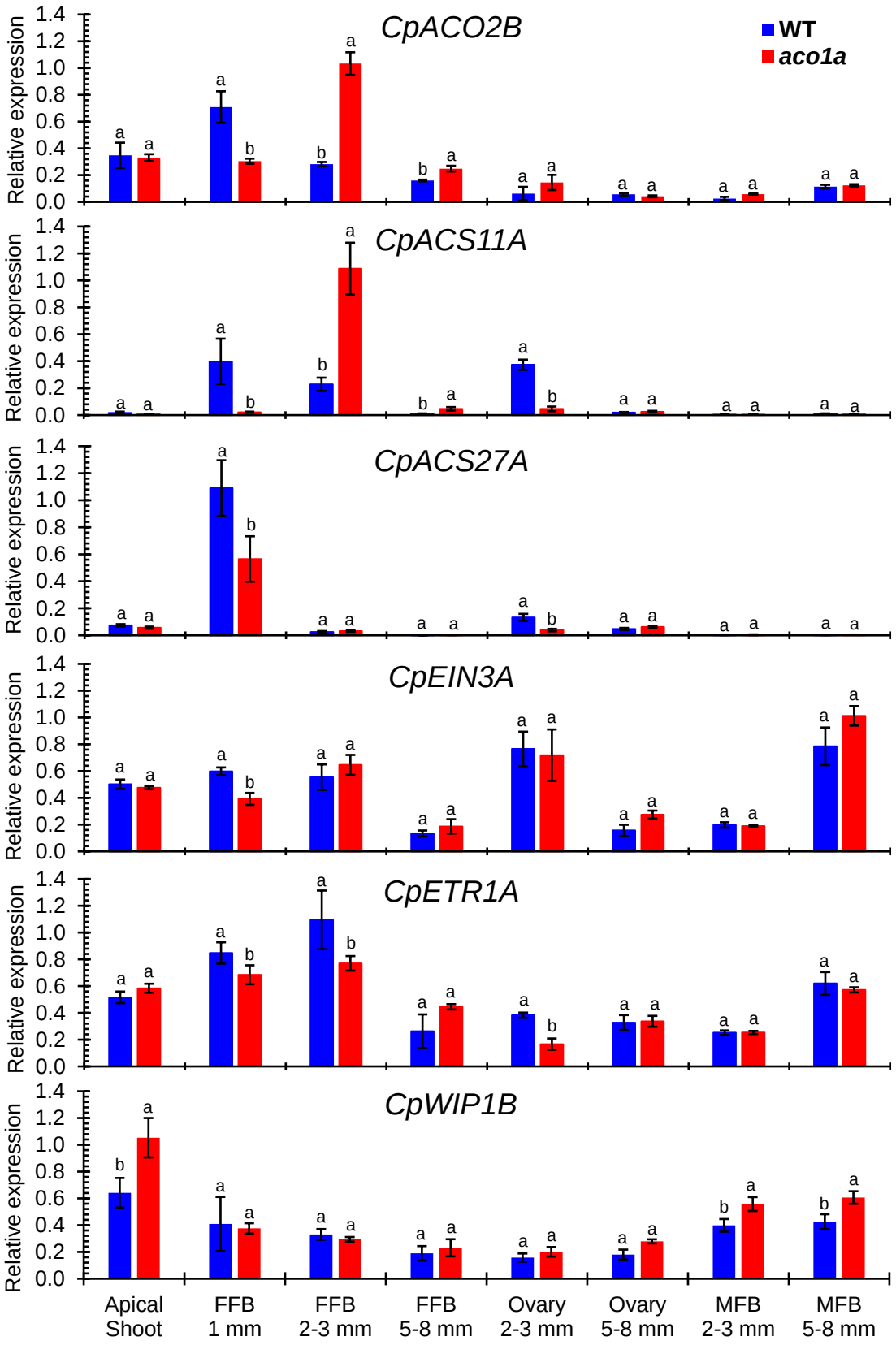
CpACO2B
CpACS11A
CpACS27A
CpEIN3A
CpETR1A
CpWIP1B
WT
aco1a
Relative expression
0.0
0.2
0.4
0.6
0.8
1.0
1.2
1.4
Apical Shoot
FFB 1 mm
FFB 2-3 mm
FFB 5-8 mm
Ovary 2-3 mm
Ovary 5-8 mm
MFB 2-3 mm
MFB 5-8 mm

Figure 7. Relative expression of different sex-determining genes in the apical shoots and flowers of WT and *aco1a* plants. The expression was assessed for genes involved in ethylene biosynthesis (*CpACO2B*, *CpACS11A*, and *CpACS27A*), ethylene perception and signaling (*CpETR1A* and *CpEIN3A*), and coding for the transcription factors (*CpWIP1B*) that are known to be involved in sex determination in cucurbit species. The relative level of each transcript was quantified by quantitative PCR in three independent replicates of each tissue. FFB, female floral bud excluding the ovary; MFB, male floral bud. Error bars represent SE. Different letters indicate significant differences between WT and mutant apical shoots and flowers at the same stage of development ($p \leq 0.05$).

4.4.6. Hormone imbalance in early female development of *aco1a* flowers

To examine whether the mutation *aco1a* can change the hormonal balance of pistillate flower, we proceeded to compare phytohormone contents of WT female flower and *aco1a* hermaphrodite flowers. **Table 2** shows phytohormone concentrations of pistillate flower buds of 5-8 mm from WT and *aco1a* plants. No difference was detected for indole-3-butyric acid (IBA), gibberellic acid (GA3), and 6-benzyladenine (BA) contents. However, the *aco1a* flowers showed a considerable reduction in the content of abscisic acid (ABA) and jasmonic acid (JA), as well as salicylic acid (SA) (**Table 2**). In contrast, the auxin (IAA) content in the *aco1a* hermaphrodite flowers was much higher than that in female WT flowers (**Table 2**).

Table 2. Hormone concentrations ng/mL (ppb).

Hormones	**WT**	***aco1a***
Salicylic acid (SA)	4661.94 ± 41.00 **a**	3196.83 ± 46.34 **b**
Indole-3-butyric acid (IBA)	n.d	n.d
Indole-3-acetic acid (IAA)	<LOQ **b**	23.25 ± 2.47 **a**
Gibberellic acid (GA3)	n.d	n.d
6-Benzyladenine (BA)	n.d	n.d
Abscisic acid (ABA)	124.81 ± 4.06 **a**	36.02 ± 2.35 **b**
Jasmonic acid (JA)	656.65 ± 19.11 **a**	248.56 ± 5.41 **b**

Different letters within the same row indicate significant differences between WT and *aco1a* hormone content ($p \leq 0.05$); n = 3. LOQ, results below the limit of quantification (5 ppb). n.d: not detected.

4.5. Discussion

It has been assumed that not ACO, but ACS, is the rate-limiting enzyme in ethylene biosynthesis. However, there is an increasing amount of evidence demonstrating the importance of ACO in controlling ethylene production in plants (Houben and Van de Poel, 2019). In cucurbits, mutations in *CmACO1* are known to inhibit fruit ripening and extend fruit shelf life (Dahmani-Mardas *et al*., 2010). An essential role of *CsACO2* and *CmACO3* orthologs in carpel development has been recently reported in cucumber and melon (Chen *et al*., 2016). In this paper, we establish that *CpACO1A* is a key regulator in sex determination and female flower development of *C. pepo*.

4.5.1. *aco1a* disrupts ethylene biosynthesis and hormonal balance during female flower development

The ACO protein family can be divided in three phylogenetic groups based on amino-acid sequence similarity (Houben and Van de Poel, 2019). At a functional level, the ACO protein has two highly-conserved and well-distinguished domains, one N-terminal, highly conservative non-heme dioxygenase DIOX_N region and a C-terminally located 2OG-FeII_Oxy region, both of which are critical for ACO activity (Ruduś *et al*., 2013). The sequence alignment and the phylogenetic tree constructed by using ACO proteins from diverse plant species have proven that CpACO1A is a type I ACO enzyme, and that the *aco1a* P5L mutation affects the first amino acid of the CpACO1A DIOX_N domain, which is a conserved proline residue in all analysed plant ACOs. The reduced ACO activity and ethylene production in *aco1a* plant organs confirmed the disfunction of P5L isoform of CpACO1A and the importance of 5P residue for its activity.

CpACO1A transcript differentially accumulated in different tissues and stages of development. Comparison of ethylene production and gene expression in WT and *aco1a* organs indicated that *CpACO1A* may be regulated by ethylene in a tissue- and temporal-specific manner. This feedback regulation could also affect other ethylene biosynthesis genes involved in flower development and sex determination, including *CpACO2B*, *CpACS11A*, and *CpACS27A*. Both positive and negative feedback ethylene-mediated regulation of *ACS* and *ACO* transcription have been reported in other systems in a tissue- and temporal-specific manner during flower and fruit development (Barry *et al*., 1996;

Nakatsuka *et al*., 1998; Inaba *et al*., 2007; Trivellini *et al*., 2011; Houben and Van de Poel, 2019; Pattyn *et al*., 2020). However, we do not exclude the possibility that the regulation of *ACS* and *ACO* genes in the female flower is mediated by other hormones, such as IAA, which was found to be highly accumulated in the ethylene-deficient *aco1a* pistillate flowers.

The hormonal imbalance detected in *aco1a* female flowers reveals the existence of crosstalk between ethylene and other hormones, such as IAA, SA, ABA and JA, during female flower development. The coaction of ethylene and auxin has been reported in various growth and developmental processes, including root elongation, lateral root formation, hypocotyl growth and fruit development and ripening, where both hormones may act synergistically or antagonistically (Stepanova *et al*., 2007; Muday *et al*., 2012; Li *et al*., 2016; Yue *et al*., 2020). The reciprocal positive regulation between auxin and ethylene is well established; elevated levels of auxin trigger transcriptional activation of subsets of *ACS* and *ACO* genes, leading to increased ethylene production; and ethylene positively controls IAA biosynthesis by the up-regulation of *Weak ET Insensitive 2* (*WEI2*) and *WEI7* (Růžička *et al*., 2007; Stepanova *et al*., 2007; Swarup *et al*., 2007; Zemlyanskaya *et al*., 2018). However, ethylene has also been reported to negatively regulate auxin biosynthesis (Harkey *et al*., 2018; S.Li *et al*., 2018).

We found that ethylene and auxin are mutually repressed, likely having an antagonistic action in squash female flower development. Auxin down-regulates the expression of ethylene biosynthesis and signaling genes in the female flower upon fruit set (Martínez *et al*., 2013), and here we demonstrated that ethylene has a negative regulation on auxin in female flowers, accumulating much higher content of IAA in ethylene-deficient *aco1a* than in WT. On the other hand, the reduced levels of ABA, JA, and SA in the ethylene-deficient mutant *aco1a* indicates that ethylene positively regulates the homeostasis of these three phytohormones in the female flower. As discussed below, all of these hormones have key functions in flower development (Chandler, 2011), and can cooperate with ethylene in the regulation of squash female flower development.

4.5.2. *CpACO1A* prevents stamen development in squash female flowers

Different sex-determining mechanisms prevent the development of either the stamens or the carpel in a primarily hermaphrodite floral meristem (Martínez and Jamilena, 2021). In Cucurbitaceae, ethylene arrests the development of stamens and promotes the development of carpels during the determination of female flowers. Early ethylene biosynthesis genes, such as *ACS11* and *ACO2*, in cucumber and melon are able to promote carpel development and determine the fate of floral meristem towards a female flower. The LOF mutation in these two ethylene biosynthesis genes leads to androecy in both cucumber and melon (Boualem *et al*., 2015; Chen *et al*., 2016), as occurs with mutation in some ethylene receptor genes (García *et al*., 2020*a,b*). Our results demonstrate that *aco1a* mutation led to a reduction in ACO activity and ethylene production, but induced the expression of *CpACO1A*. This upregulation also occurs for *CpACO2B* and *CpACS11A* in *aco1a*, but the induction of these two genes occurs in flowers where sex determination has already taken place (flowers above 2-3 mm in length). At earlier stages of female flower development (female floral buds less than 1 mm), the genes *CpACO2B* and *CpACS11A* were down-regulated in the mutant, and could not compensate for the reduced ethylene caused by *CpACO1A* disfunction. The later-acting ethylene biosynthesis gene *ACS2* is specifically expressed in female flowers at early stages of development to control the arrest of stamen development. LOF mutations for *ACS2* orthologs (*CsACS2* in cucumber, *CmACS7* in melon, *CpACS27A* in *C. pepo*, and *CitACS4* in watermelon) promote the conversion of female into hermaphrodite flowers and monoecy into andromonoecy (Boualem *et al*., 2008, 2009, 2016; Martínez *et al*., 2014; Ji *et al.*, 2016; Manzano *et al.*, 2016). The phenotype of *aco1a* mutant described in this paper resembles those of *acs2-like* mutants, indicating that *CpACO1A* is, together with *CpACS27A*, the key enzymes that produce the requisite ethylene to prevent the development of stamens in squash female flowers. The reduced expression of *CpACS27A* in *aco1a* pistillate flowers at early stages of development suggests that the regulation of these two key enzymes is coordinated, producing the required ethylene for the proper development of the female flower. This coordinated regulation may be mediated by ethylene, as occurs in other systems (Barry *et al*., 2000; Inaba *et al*., 2007).

4.5.3. *CpACO1A* controls flower opening and ovary development in the absence of pollination

The phenotype of *aco1a* flowers also indicates that ethylene regulates the growth and development of other floral organs in the pistillate flowers of squash, including the corolla and the ovary/fruit. The delayed anthesis time of the *aco1a* pistillate flower demonstrates that ethylene is a positive regulator of petal growth and maturation in squash. This was also found in squash ethylene-insensitive mutants (García *et al*., 2020*a,b*), and seems to be associated with pistillate flower masculinization. Ethylene, which is the hormone that activates the developmental program of a female flower, is also used to promote the growing rate and maturation of female corolla. In the male flower, where ethylene production is very low, petals develop slower and anthesis is markedly more delayed. Given that male flowers are produced in the first nodes of the plant, this ethylene-mediated mechanism ensures that male and female flowers reach anthesis at the same time to achieve successful pollination. JA is known to be involved in anther and pollen maturation (Stintzi and Browse, 2000; Wang *et al*., 2005; Browse and Wallis, 2019), but also participates in petal maturation and flower opening (Reeves *et al*., 2012; Oh *et al*., 2013; Niwa *et al*., 2018; Schubert *et al*., 2019*b*). The delayed flower opening and reduced JA in the ethylene-deficient hermaphrodite flowers of *aco1a* indicate that ethylene can regulate the maturation and opening of the female flower by inducing the biosynthesis of JA (**Fig. 8**).

We have previously reported that external treatments with ethylene inhibitors were able induce fruit set and early fruit development in the absence of pollination (parthenocarpic fruit), and that fruit set is concomitant with a reduction in ethylene production, ethylene biosynthesis, and signaling gene expression in the days immediately after anthesis (Martínez *et al*., 2013). Mutations in ethylene receptor genes of squash confer partial ethylene insensitivity, and also result in parthenocarpic fruits (García *et al*., 2020*a,b*). The negative role of ethylene in fruit set has been also found in tomato, where ethylene and signaling genes are down-regulated in early-developing fruit (Vriezen *et al*., 2008; Wang *et al*., 2009), and the blocking of ethylene perception, using the ethylene-insensitive mutation *Sletr1-1* or treatments with 1MCP, leads to parthenocarpic fruits through the

induction of auxin and gibberellin (Wang *et al*., 2009; Shinozaki *et al*., 2015, 2018; An *et al*., 2020).

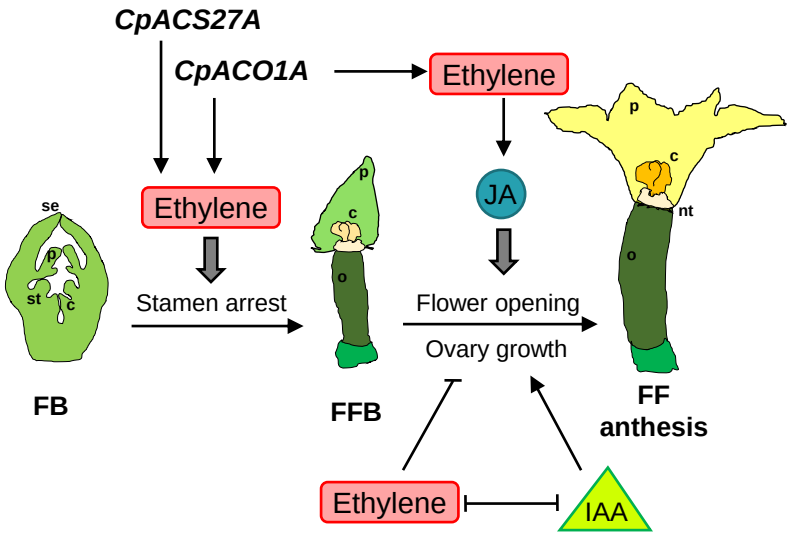

Figure. 8. Model integrating ethylene, jasmonate (JA) and auxin (IAA) in the regulation of sex determination (stamen arrest), female flower opening and ovary growth and fruit set and development in *Cucurbita pepo*. The genes *CpACO1A* and *CpACS27A* participate in the biosynthesis of the ethylene required for carpel promotion and stamen arrest at earlier stages of female floral bud (FFB) development. *CpACO1A* also participates in the ethylene produced at later stages of FFB for controlling flower opening and ovary growth and fruit set. Petal maturation and female flower opening is mediated by jasmonic acid (JA), while ovary growth and fruit set is coordinated by the antagonist action of ethylene and IAA, which are mutually repressed during the development of the female flower. se, sepal; p, petal; st, stamen; c, carpel; o, ovary; nt, nectary; FB, floral bud, FFB, female floral bud, FF, female flower.

The up-regulation of IAA in *aco1a* may be responsible for the continued growth of *aco1a* ovaries in the absence of pollination. Auxins are the key hormones regulating fruit set in the Cucurbitaceae family (Trebitsh *et al*., 1987; Kim *et al*., 1992; Martínez *et al*., 2013), and were found to be highly induced in the *aco1a* flowers. This means that auxins not only repress the production, perception and signaling of ethylene in the squash developing fruit, as reported by Martínez *et al*. (2013), but can be negatively regulated by ethylene in the developing ovary (**Fig. 8**). It is feasible that the two hormones are specifically accumulated in different floral organs, i.e., ethylene in the upper flower organs for promoting the development of carpels and petals and arresting the development of stamens, and auxin in the inferior ovary for inducing fruit set and development (**Fig. 8**)

5. Jasmonate-deficient mutant *lox3a* reveals crosstalk between JA and ET in the differential regulation of male and female flower opening and early fruit development in *Cucurbita pepo*

5.1. Abstract

JA has been found to be a relevant hormone on flower development in numerous species, but its function in cucurbit floral development and SD is unknown. Crosstalk between jasmonate (JA) and ethylene (ET) in the differential regulation of male and female flower development was addressed by using the novel JA-deficient mutant *lox3a*, and the ET-deficient and -insensitive mutants *aco1a* and *etr2b* of *Cucurbita pepo*. The *lox3a* mutation suppresses male and female flower opening and induces the development of parthenocarpic fruit. A BSA-seq and fine mapping approach allowed the identification of *lox3a* mutation in *CpLOX3A*, a *LYPOXYGENASE* gene involved in JA biosynthesis. The reduced JA content and expression of JA-signaling genes in male and female flowers of *lox3a*, and the rescue of *lox3a* phenotype by external application of MeJA, demonstrated that JA controls petal elongation and flowering opening, as well as fruit abortion in the absence of fertilization. JA can also rescue the phenotype of ET mutants *aco1a* and *etr2b*, which are specifically defective in female flower opening and fruit abortion. ET, the sex determining hormone of cucurbits, is induced in female flowers towards anthesis, activating JA production and promoting the aperture of the female flower and the abortion of the unfertilized ovary. Given the close association between flower closure and parthenocarpic fruit development, we proposed that flower opening can act as a switch that tiggers fruit set and development in fertilized ovaries, but may alternatively induce the abortion of the unfertilized ovary. Both ET and JA from mature and senescent petals can serve as remote signals that determine the alternative development of the ovary and fruit.

Keywords: anthesis; BSA-sequencing; flower maturation; lipoxygenase; parthenocarpy; petal elongation.

5.2. Introduction

Jasmonic acid (JA), together with other phytohormones such as abscisic acid (ABA), salicylic acid (SA) and ethylene (ET), integrates plant growth and development in response to changing environmental cues (Yan *et al.*, 2013; Howe *et al.*, 2018; Yang *et al.*, 2020; Delgado *et al.*, 2021). Jasmonates (JAs) are oxylipin phytohormones derived from polyunsaturated fatty acids (PUFAs), with jasmonic acid (JA) as the prototypical member. The JA biosynthesis pathway has been extensively studied in Arabidopsis (Howe *et al.*, 2018; Acosta and Przybyl, 2019; Li *et al.*, 2021). Its synthesis starts from esterified α-linolenic acid (α-LeA 18:3) in galactolipids of the chloroplast membrane or from free fatty acids released by phospholipase A (PLA). LIPOXYGENASES (LOXs), a nonheme iron containing dioxygenases that catalyse the formation fatty acid hydroperoxides from polyunsaturated substrates, followed by ALLENE OXIDE SYNTHASE (AOS) and ALLENE OXIDE CYCLASE (AOC), also participate in JA biosynthesis in the chloroplast. The resulting OPDA or dn-OPDA products leave the chloroplast and are reduced by the flavin-dependent 12-OXOPHYTODIENOATE REDUCTASES 3 (OPR3) in the peroxisome or by OPR2 in the cytosol, and then undergoes three rounds of β-oxidation by the action of ACYL-CoA OXIDASE (ACX) to produce JA. In the cytosol, JA is conjugated to Isoleucine by JASMONOYL-ISOLEUCINE SYNTHETASE (JAR1) to form JA-Ile, the most biologically active Jas (Yan *et al.*, 2013; Huang *et al.*, 2017; Wasternack and Song, 2017; Li *et al.*, 2021).

JA-Ile enters into the nucleus by JASMONATE TRANSPORTER 1 (JAT1), an ABCG-type transporter that cooperates with JAR1 to maintain a critical nuclear JA-Ile level for JA-signaling activation. Activation of the JA-signaling pathway depends on the interplay between the transcriptional activators MYC2/3/4 and MYB21/24/57 and the transcriptional repressors JASMONATE-ZIM DOMAIN proteins (JAZ). At a low JA-Ile level, JAZ represses the JA-signaling pathway by inhibiting the transcriptional activity of MYCs/MYBs. The accumulation of JA-Ile promotes the binding of JAZ to CORONATINE INSENSITIVE1 (COI1), a F-box protein component of the E3 ubiquitin ligase complex SCF^{COI1}, and the subsequent polyubiquitylation and 26S proteasomal degradation of JAZ proteins lead to the activation of JA-responsive genes (Yan *et al.*, 2013; Huang *et al.*, 2017; Wasternack and Song, 2017; Li *et al.*, 2021).

In recent years, it has been discovered that JA participates in reproductive development, controlling important processes, such as flowering time, flower opening, stamen development, and pollen fertility (Yuan and Zhang, 2015; Niwa *et al.*, 2018; Schubert *et al.*, 2019*a,b*; Acosta and Przybyl, 2019; Zhao *et al.*, 2022). The coordination of flower opening in relation to stamen/pollen and gynoecium/ovule maturation is important for successful pollination and subsequent fertilization (Niwa *et al.*, 2018; Schubert *et al.*, 2019*a,b*). Internal cues, such as pollen and ovule development and circadian rhythms, and environmental factors, such as light, temperature and humidity regulate flower opening throughout phytohormones such as IAA, GAs, ABA, ET, and JAs (Reeves *et al.*, 2012; Shakeel *et al.*, 2013; Van Doorn and Kamdee, 2014; Cho *et al.*, 2017; Niwa *et al.*, 2018).

Flower buds of the JA-deficient mutant *defective in anther dehiscence1* (*dad1*) of Arabidopsis are developed normally until 2 d before flower opening. Afterwards the development of *dad1* flowers was retarded, and unopened buds were clustered in the inflorescence. In addition, *dad1* flowers also showed male-sterility, with delayed anther dehiscence and up to 97% of pollen grain infertility (Ishiguro *et al.*, 2001; Browse and Wallis, 2019). Other JA biosynthesis mutants exhibited similar phenotypes, including *fad3 fad7 fad8* triple mutant (McConn and Browse, 1996), *lox3 lox4* double mutants (Caldelari *et al.*, 2011), *dde2-2* and *dde1* (Von Malek *et al.*, 2002; Sanders *et al*., 2000), *aos* (Park *et al.*, 2002), *opr3* and *opr3-3* (Stintzi and Browse, 2000; Chini *et al.*, 2018), and *acx1* and *acx5* (Schilmiller *et al.*, 2007). Moreover, mutants impairing JA signal transduction, such as *coi1* (Feys *et al.*, 1994) or *myb21* and *myb21 myb24* double mutants (Mandaokar *et al.*, 2006), as well as *jai3-1* (Chini *et al.*, 2007), are also male-sterile with reduced filament elongation and lack of anther dehiscence. External treatments of flower buds with JA can restore WT phenotype, providing pollen germination rates that are equivalent to WT, and abundant seed set. These data demonstrate that JA is a positive regulator of flower opening, anther dehiscence, and pollen development in Arabidopsis (Niwa *et al.*, 2018; Browse and Wallis, 2019).

The role of JA in the flower development of other plant systems is less known. In *Brassica rapa*, antisense inhibition of a nuclear gene *BrDAD1* (orthologue of *DAD1*) also causes male sterility and suppresses flower opening

(Hatakeyama *et al.*, 2003), and in wild tobacco, *Nicotiana attenuata*, transgenic plants with *AOC* and *COI1* silenced genes, showed delayed flower opening or incomplete corolla expansion phenotypes (Stitz *et al.*, 2014). The *COI1* defective mutants of tomato (*jai1* and *jai1-1*) are not male-sterile, but pollen germination and viability are lower than in WT, with premature dehydration and dehiscence of the anther and delayed petal elongation and flower opening. The *jai1* mutation, however, delayed flower opening and promoted female sterility, producing no seed upon pollination with wild type or *jai1-1* pollen, although fruit set and fruit development appear similar to WT (Li *et al.*, 2004; Schubert *et al.*, 2019*a*). The phenotype of *atmyb21 atmyb24* double mutants has also recently revealed that *SlMYB21* induces petal elongation and flower opening, pollen maturation, and gynoecium function in tomato (Niwa *et al*., 2018).

Regarding monocots, the rice mutants *eg1* (impaired in *DAD1* homologue), *eg2-1D* (impaired in *OsTIFY3/OsJAZ1*) and *ospex5* (impaired in *OsOPR7*) exhibit altered spikelet morphology with changes in floral organ identity and number, as well as defective floral meristem determinacy. In addition, *cpm2/hebiba* mutant plants (impaired in *OsAOC*) also showed complete male sterility, while other JA biosynthetic mutants were partially sterile. All of these mutants accumulated almost no OPDA, JA, and other derivatives (Riemann *et al.*, 2013; Nguyen *et al.*, 2019; You *et al.*, 2019). It has been suggested that JA mediates the expression of B- and C-class homeotic regulators of floral development. Therefore, in rice, the core JA-signaling module, JAZ/JA-Ile/COI1/MYC2, is fundamental to control spikelet and floret development from the beginning of the floral meristem, rather than being required only for the final stages of stamen and pollen maturation (Pelaz *et al.*, 2000; Wu *et al.*, 2012; Cai *et al.*, 2014; Yuan and Zhang, 2015; Browse and Wallis, 2019; Nguyen *et al.*, 2019). JA also controls flower development and sex determination in the monoecious maize. Mutations in *TASSEL SEED 1* (*TS1*), a gene encoding for the JA biosynthesis enzyme *ZmLOX8*, results in a completely feminized tassel (Acosta *et al.*, 2009; Browse, 2009; Borrego and Kolomiets, 2016; Browse and Wallis, 2019). The phenotype of *opr7 opr8* (orthologs of *OPR3*) and *ts5* (affected in the CYP94B enzyme that inactivates JA-Ile) are similar to *ts1*, suggesting that JA is necessary to control the development of male flowers and monoecy (Yan *et al.*, 2012, 2014; Lunde *et al.*, 2019).

In the monoecious cucurbits, the key hormone involved in sex determination and flower development is ET (Martínez and Jamilena, 2021). However, it has recently been reported that the silencing of cucumber *CsGL2-LIKE* delays male flowering and reduces pollen vigor and seed viability (Cai *et al.*, 2020). The reduced JA content in the ET-deficient mutant *aco1a* of squash suggests that ET can hasten the maturation and opening of the female flower by inducing the biosynthesis of JA (Cebrián *et al*., 2022). To gain insight into the role of JA in male and female flower development, in this chapter we characterise the JA-deficient mutant *lox3a*, analyse the flower and fruit development processes affected by the mutation, and reveal the interaction between JA and the sex-determining hormone ET in the differential maturation and opening of male and female flowers.

5.3. Materials and methods

5.3.1. Plant material and isolation of mutants

The *lox3a* mutant analysed in this paper was isolated from a high-throughput screening of the *Cucurbita pepo* EMS collection (García *et al*., 2018). M2 plants from 600 lines were grown to maturity under standard greenhouse conditions, and alterations in vegetative and reproductive developmental traits were evaluated. A mutant line was detected in which both male and female flowers remained closed and green throughout the development. This mutant was selected for further characterization and named *lox3a*. Prior to phenotyping, *lox3a* mutant plants were crossed with the background genotype MUC16, and the resulting BC_1 and BC_2 generations selfed to obtain the BC_1S_1 and BC_2S_1 generations, respectively (**Table S5.1**).

5.3.2. Phenotyping for sex expression and floral traits

BC_2S_1 plants from wt/wt, wt*/lox3a,* and *lox3a/lox3a* were transplanted to a greenhouse and grown to maturity under local greenhouse conditions without climate control, and under standard crop management of the region, in Almería, Spain. The sex phenotype of each plant was determined according to the sex of the flowers in the first 42 nodes of each plant. A minimum of 30 wt/wt, 30 wt*/lox3a*, and 30 *lox3a/lox3a* plants were phenotyped. Phenotypic evaluations were performed in the autumn-winter and spring-summer seasons of 2020 and 2021.

The sex expression of each genotype was assessed by determining the node at which plants transitioned to female flowering, and the number of male and female flower nodes per plant. To evaluate floral organ development, the growth rates of ovaries and petals in both male and female flowers of WT and *lox3a* mutant plants were determined by measuring the length and diameter of these floral organs every 2 d up to 28 d in 30 flowers of each genotype, starting with flower buds of ~2 mm in length. The anthesis time of WT male and female flowers was estimated as the number of days taken for a 2 mm floral bud to reach anthesis. For *lox3a*, the procedure was similar, but because of the absence of flower opening, the corolla was opened manually to check the state of the sex floral organs maturations.

5.3.3. Identification of *lox3a* mutation by WGS

To identify the causal mutations of the *lox3a* phenotype, WT and mutant plants derived from BC_1S_1-segregating populations were subjected to whole-genome sequencing (WGS). In total, 221 BC_1S_1 seedlings were transplanted to a greenhouse and grown to maturity (**Table S5.1**). The genomic DNA from 30 WT and 30 *lox3a* plants were isolated by using the Gene JET Genomic DNA Purification Kit (Thermo Fisher®) and pooled into two different bulks: WT bulk and *lox3a* mutant bulk. DNA from each bulk was randomly sheared into short fragments of approximately 350 bp for library construction using the NEBNext® DNA Library Prep Kit (https://international.neb.com), and fragments were briefly PCR-enriched with indexed oligos. Pair-end sequencing was carried out using the Illumina® sequencing platform, with a read length of PE150 bp at each end. The effective sequencing data were aligned with the reference *Cucurbita pepo* genome v.4.1 through BWA software (Li and Durbin, 2009). Single nucleotide polymorphisms (SNPs) were detected using the GATK HAPLOTYPECALLER (DePristo *et al*., 2011). ANNOVAR was used to annotate the detected SNPs (Wang, Li and Hakonarson, 2010). Common variants with other sequenced mutant lines in the laboratory were discarded, as they are likely common genomic differences with the reference genome. The genotype of the WT bulk (wt/wt and wt/*lox3a* plants) was expected to be 0/1 with an alternative allelic frequency (AF) of 0.25, while the genotype of the mutant bulk (*lox3a/lox3a* plants) was expected to be 1/1 with an AF = 1. Therefore, the sequencing data were filtered according

to the following parameters: genotype quality ≥ 90; read depth ≥ 10; AF = 1 in the *lox3a* bulks; and AF ≤ 0.3 in the WT bulks. SNPs that were not canonical EMS changes, i.e., G > A or C > T transitions, were also filtered out (Till *et al*., 2004). All filters were performed with RStudio® software. The impact of this final set EMS-SNPs on gene function was finally determined by using Integrative Genomics Viewer (IGV) software and annotations in the Cucurbit Genomics Database (CuGenDB) (http://cucurbit genomics.org).

5.3.4. High-throughput SNP genotyping for validating the *lox3a* mutation

Segregation analysis was carried out to confirm that the identified mutation was the causal mutation of the *lox3a* phenotype. 561 BC_1S_1- and 96 BC_1S_2-segregating plants were genotyped using kompetitive allele-specific PCR (KASP) technology (**Dataset S5.1**). Primers were synthesized by LGC Genomics® (http://www. lgcgroup.com), and the KASP assay was performed in the FX96 Touch Real-Time PCR Detection System (Bio-Rad®) using the LGC protocol (https://afly.co/xyn2). The multiplex PCRs were run with 10 µL final reaction volume containing 5 µL KASP V4.0 2x Master mix standard ROX (LGC Genomics®), 0.14 µL KASP-by-Design primer mix (LGC Genomics®), 2 µL of 10-20 ng/µL genomic DNA, and 2.86 µL of water. The PCR thermocycling conditions were 15 min at 94°C (hot-start activation), followed by 10 cycles of 94°C for 20 s and 61°C for 1 min (dropping-0.6°C per cycle to achieve a 55°C annealing temperature), followed by 26 cycles of 94°C for 20 s and 55°C for 1 min. Data were then analysed using CFX Maestro™ software (Bio-Rad®) to identify SNP genotypes.

5.3.5. Analysis of 5´-splicing site mutation by Sanger sequencing

Total RNA from WT and *lox3a* corollas tissues was isolated according to the protocol of the GeneJET Plant RNA Purification Kit (Thermo Fisher®) and then converted into cDNA with the ADNc RevertAid™ Kit (Thermo Fisher®). Templates for sequencing were amplified by PCR from cDNA using forward and reverse primers GAGATGATGAATTTGGCCG and CATCTTCGCGGAT GATATTG, respectively, and GoTaq® G2 Flexi DNA Polymerase (Promega). PCR products were then purified using a GeneJET PCR Purification Kit (Thermo Fisher®) and visualized in gel. Products of the sequencing reactions were purified using the BigDye XTerminator™ Purification Kit (Thermo Fisher®) and

chromatograms were obtained with the ABI 3500 Genetic Analyser (Applied Biosystem®). Sequencing results were analysed using Chromas software.

5.3.6. Assessing ET production and sensitivity

The production of ET in WT and *lox3a* flowers was assessed throughout the different stages of development, early stage (ES, corolla length < 25 mm); medium stage (MS, corolla length ~25-40 mm); and late stage (LS, corolla length ~40-55 mm). Male and female floral buds of 8 to 55 mm in length (MFB/FFB) of plants growing under climate-controlled conditions were collected and incubated at room temperature for 6 h in hermetic glass containers of 320-450 mL. ET production was determined by analysing 1 mL of gas from the headspace in a Varian® 3900 gas chromatograph (GC), fitted with a flame ionisation detector (FID). The instrument was calibrated with standard ET gas. Four biological replicates were made for each one of the flower developmental stages analysed and three measurements per sample. ET production was expressed as nL * gFW^{-1} * $6\ h^{-1}$.

To assess ET sensitivity, flower abscission was evaluated for male flowers in response to an external treatment with ET. Male flowers from WT and *lox3a* plants were collected in late stage (LS) of development 1 d before anthesis. 30 WT and 30 *lox3a* flowers were placed in glass vases with water and incubated in two culture chambers with equal humidity and temperature, 50% RH and 20 ºC. One of the chambers was used as a control (Ct), and the other was filled with 50 ppm of ET. The tests were performed in triplicate. The percentage of flower abscission was evaluated after 24, 48, 72, and 96 h for flowers in the two chambers.

5.3.7. MeJA external treatments

To elucidate the role of JA in flower opening, *lox3a* male and female flowers and *aco1a* and *etr2b* mutant female flowers were treated with 5 mM of MeJA at three developmental stages prior to anthesis: early stage (ES, corolla length < 25 mm); medium stage (MS, corolla length ~25-40 mm); and late stage (LS, corolla length ~40-55 mm). The treatments were performed in 20 flowers for each sex and stage of development, and the percentage of flowers that came to open after treatment was determined. Flowers were sprayed with 2 ml of aqueous solution of 5 mM methyl jasmonate (MeJA) (supplemented with 0.5% Tween-20).

5.3.8. JA concentration measurement

Male and female-flower buds at medium stage (MS, corolla length ~25-40 mm) and late stage of development (LS, corolla length ~40-55 mm) from WT and *lox3a* plants were collected for jasmonic acid (JA) measurement. Representative samples consisted of three bulks of 10 female- (ovary excluded) and male-flowers each. To preserve the samples, WT and *lox3a* bulks were quickly stored on dry ice. Then, the samples were placed in a freeze dryer CRYODOS V3.1-50 (Telstar®), where they were lyophilized for 5 d and subsequently pulverized in a mixer mill MM200 (Retsch™). The concentration of JA was determined in each triplicated sample through ultra-performance liquid chromatography coupled with a hybrid quadrupole orthogonal time-of-flight mass spectrometer (UPLC-Q-TOF/MS/MS), according to the hormone determination method of Müller and Munné-Bosch (2011). The JA concentrations were expressed as ng/mL (ppb).

5.3.9. Bioinformatics and phylogenetic analysis

Alignments and protein sequences analysis were performed using the BLAST alignment tools at NCBI (http://www.blast.ncbi.nlm.nih.gov). Protein structure information and homology-modelling was carried out by using the protein data bank RCSB PDB (https://www.rcsb.org), SWISS-MODEL (https://swissmodel.expasy.org) and PredSL tool (http://aias.biol.uoa.gr /PredSL/). The phylogenetic relationships between *Cucurbita pepo, Oryza sativa, Solanum lycopersicum, Zea mays, Nicotiana tabacum*, and *Arabidopsis thaliana* LOXs protein were studied using MEGA X software (Kumar *et al*., 2018), which allowed the alignment of proteins and the construction of phylogenetic trees using MUSCLE (Edgar, 2004) and the Maximum Likelihood method based on the Poisson correction model (Zuckerkandl and Pauling, 1965), with 2,000 bootstrap replicates. The protein sequences were obtained using the Cucurbit Genomics Database (http://cucurbitgenomics.org), the Rice Database Oryzabase-SHIGEN (https://shigen.nig.ac.jp/rice/oryzabase), the Sol Genomics Network (https:// solgenomics.net), the Arabidopsis Information Resource (https://www. arabidopsis.org), and the NCBI database (https://www.ncbi.nlm .nih.gov/) (**Table S5.2**). Cucurbits *LOX* genes structure visualization, such as the composition and position of exons and introns, were conducted with the Gene Structure Display

Serve (GSDS) (http://gsds.gao-lab.org/Gsds_about.php), Integrative Genomics Viewer (IGV) software and NCBI tools.

5.3.10. Assessment of gene expression by RT-qPCR

Gene expression analysis was carried out in samples of WT and *lox3a* plants growing in a greenhouse during the spring-summer season. The expression levels were studied in male and female corolla flower tissue at two different flower developmental stages close to anthesis, medium stage (MS, corolla length ~25-40 mm), and late stage (LS, corolla length ~40-55 mm), approximately. 3 and 1 d before anthesis, respectively, as well as in plant leaves and roots. The analysis was performed in three biological replicates for each genotype, each one derived from a pool of four plants. Total RNA was isolated according to the protocol of the GeneJET Plant RNA Purification Kit (Thermo Fisher®). RNA was converted into cDNA with the ADNc RevertAid™ kit (Thermo Fisher®). The RT-qPCR was performed in 10 µL total volume with 1 × Top Green qPCR Super Mix (Bio-Rad®) in the CFX96 Touch Real-Time PCR Detection System thermocycler (Bio-Rad®). The gene expression values were calculated using the $2^{-\Delta\Delta CT}$ method (Livak and Schmittgen, 2001). The constitutive *EF1α* gene was used as the internal reference. **Table S5.3** shows the primers used for each RT-qPCR reaction.

5.3.11. Statistical analyses

Data were analysed for multiple comparisons by analysis of variance (ANOVA) using the statistical software Statgraphic Centurion XVIII. Differences between genotypes and treatments were separated by the least significant difference (LSD) at the significance level $p \leq 0.05$

5.4. Results

5.4.1. *lox3a,* a new mutant, impaired the maturation of petals and flower opening

The *lox3a* mutant was found in a high-throughput screening of a *C. pepo* mutant collection for alterations in flower and fruit development. To ensure accurate phenotyping, mutant plants were backcrossed with the background genotype MUC16 for two generations, and then selfed. The resulting BC_2S_1 generations segregated 3:1 for WT and *lox3a* phenotypes, indicating that the mutation is recessive (**Table S1**). The phenotype of *lox3a* was assessed in BC_2S_1 plants growing under both autumn-winter and spring-summer seasons 2020 and 2021.

The main distinctive feature of the *lox3a* mutation was the absence of both male and female flower opening (**Fig. 1A**). WT and *lox3a* petals reached a similar length, but those of *lox3a* did not fully mature and expand to permit flower opening (**Fig. 1A, B**). Moreover, WT female petals grew faster than male flowers. Anthesis time, the period of time taken for a floral bud of ~2 mm to reach anthesis (A) and to open, was shorter in female- (average 10 d) than in male-flower petals (average 21 d) (**Fig. 1B**). The *lox3a* petals in both male and female flowers initiated their development similarly to WT ones, but their growth rate was reduced compared to WT at 1 d and 3 d before anthesis in male and female flowers, respectively (**Fig**. **1B**). Prior to anthesis, the growth rate of male and female flowers can be separated into three developmental stages (**Fig. 1B**). At the early stage (ES, corolla length < 25 mm), male and female flowers had the same petal growth rate. At the medium developmental stage (MS, corolla length ~25-40 mm), however, female petals grew faster than male ones. The later developmental phase (LS, corolla length ~40-55 mm) coincided with 1 d before anthesis in female flowers and 3 d before anthesis in male flowers, and was characterised by petal elongation and maturation (**Fig. 1B**). Furthermore, petal growth rate in *lox3a* was slightly decreased relative to WT in MS and LS, but not in ES (**Fig. 1B**). Despite the absence of flower opening, the *lox3a* male and female flowers were fertile, developing mature stamens and carpels with viable pollen and ovules (**Fig. 1C**).

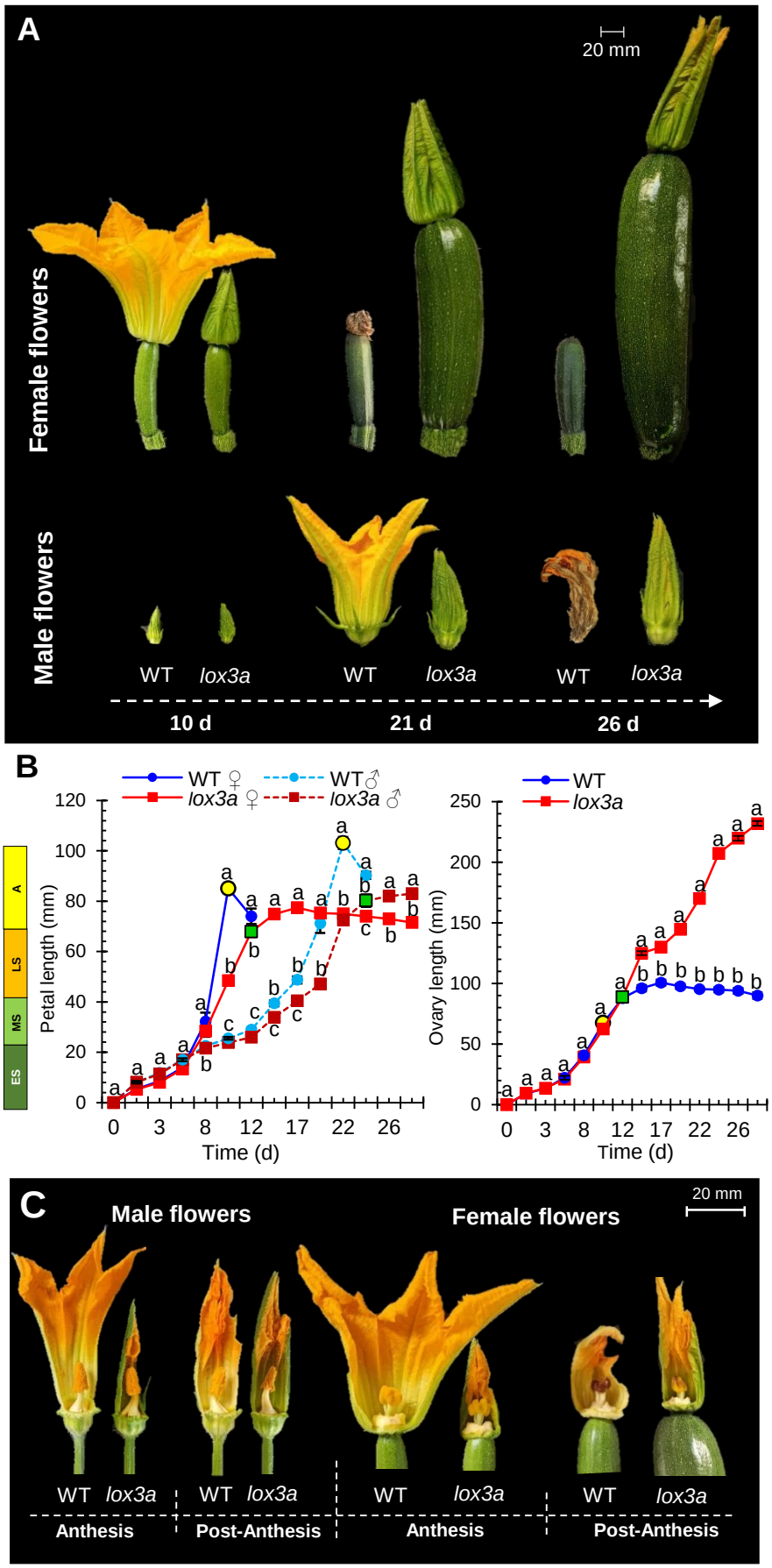
A
20 mm
Female flowers
Male flowers
WT
lox3a
WT
lox3a
WT
lox3a
10 d
21 d
26 d
B
WT ♀
lox3a ♀
WT ♂
lox3a ♂
A
LS
MS
ES
Petal length (mm)
Time (d)
WT
lox3a
Ovary length (mm)
Time (d)
C
Male flowers
Female flowers
20 mm
WT
lox3a
WT
lox3a
WT
lox3a
WT
lox3a
Anthesis
Post-Anthesis
Anthesis
Post-Anthesis

Figure 1. Comparison of WT and *lox3a* flower development. (**A**) Effect of *lox3a* mutation on the development of male and female flowers. Note the absence of both male and female flower opening in *lox3a,* and that the ovary continues its growth until producing a parthenocarpic fruit. (**B**) Comparison of the growth rate of WT and *lox3a* corolla and ovary/fruit. Flowers were labeled when their corolla were 2 mm long, and then measured every 2 d up to 28 d. Yellow circles indicate the time at which more than 80% of the WT flowers reached anthesis. Green squares indicate when *lox3a* male and female flowers were fertile. According to petal growth rate, pre-anthesis male and female flowers can be separated into three developmental stages: early (ES, male and female petals have the same growth rate); medium (MS, female petals growth faster than male ones); and late (LS, petal elongation just before flower opening). (**C**) Development of reproductive organs. Note that senescent stamens and carpels were found in the unopen *lox3a* flowers with viable pollen and ovules. Error bars represent SE. Different letters indicate significant differences between flowers of the different genotypes at each developmental time ($p \leq 0.05$).

The lack of corolla maturation caused the sexual organs to develop out of sync with the petals. When the unopen *lox3a* flowers reached a similar size to WT flowers just prior to anthesis, they showed both mature stamens and carpels with pollen and receptive stigma (**Fig. 1C**). In subsequent days, the still unopen flowers showed senescent stamens and carpels (**Fig. 1C**). The *lox3a* ovary, however, was capable of growing in the absence of pollination and fertilization, demonstrating that *lox3a* also induced parthenocarpy (**Fig**. **1A**). During the first 10-12 d of flower development (anthesis time in WT female flowers), the growth rates of WT and *lox3a* ovaries were similar. Afterwards, WT ovaries of approximately 100 mm in length aborted, which occurred 1 d after anthesis; whereas, those of *lox3a* flowers retained their growth, reaching a fruit commercial size of 200 mm after 22-25 d of flower initiation (**Fig. 1B**). Unfertilized *lox3a* fruit can even complete its development and mature without seeds. Therefore, the mutation *lox3a* abolished the abortion of the ovary in the absence of fertilization.

Given that the unopen *lox3a* female flower resembled that of the ET-deficient and -insensitive mutants (García *et al*., 2020*a,b*; Cebrián *et al*., 2022), we evaluated whether the *lox3a* mutation could also affect sex determination and sex expression mechanisms. No change was observed in sex determination, as stamen and carpel primordia arrested their development normally, thus determining a regular development of male and female flowers, respectively. Furthermore, the sex expression of *lox3a* plants was similar to that of WT, showing that *lox3a* and WT plants had the same female flowering transition and the same number of male and female flowers per plant (**Fig. S5.1**).

5.4.2. *lox3a* is a 5´-splicing site mutation in the JA biosynthesis gene *CpLOX3A*

To elucidate the causal mutation of *lox3a* phenotype, a whole-genome resequencing (WGS) was performed of two bulked DNA samples from a BC_1S_1 segregating population: a WT bulk, having DNA from 30 WT plants, and a *lox3a* bulk, having DNA from 30 *lox3a* plants. The more than 80 million reads resulting from either WT or *lox3a* bulks sequencing were mapped against the *C. pepo* reference genome version 4.1, which covered approximately 97% of the reference genome with an average depth of 37.70 (**Table 1**).

Table 1. Summary sequencing data for WT and *lox3a* DNA bulks

Sequencing	**WT**	***lox3a***
Number of reads	81,081,404	87,715,354
Mapped reads (%)	97.98	97.76
Average depth	37.70	41.86
Coverage at least 4X (%)	95.22	95.37
SNPs filtering		
Total number SNPs	387,948	391,081
AF (WT) < 0.3; AF (*lox3a*) = 1	971	971
EMS SNPs G > A or C > T	291	291
EMS SNPs (GQ > 90; DP > 10)	3	3
High impact SNPs	0	1

Candidate SNP

Chr	**Position**	**Ref**	**Alt**	**Gene ID**	**Effect**	**Functional Annotation**
12	5,883,147	G	A	Cp4.1LG12g09270.1	5´splicing	Lipoxygenase
12	5,803,670	G	A	Cp4.1LG12g09310.1	P281L	Jasmonate-zim-domain protein
12	3,782,831	G	A	Cp4.1LG12g04490.1	Q587Stop	Elongation factor G mitochondrial

Note: AF, allelic frequency; GQ, genotype quality; DP, read depth

The more than 380,000 identified SNPs in each of the bulks were filtered by their mutant allele frequency (AF) in the WT and the *lox3a* DNA bulks. For the causal mutation of the phenotype, it is expected that the genotype of the WT bulks was 0/1 (alternative allele frequency AF ≤ 0.3) and 1/1 for the *lox3a* bulk (AF = 1). For the non-causal SNPs, however, an AF of 0.5 in both bulks is anticipated. A putative causal region on chromosome 12 was found that has the expected AF in WT and *lox3a* bulk (**Fig. 2**). After filtering for AF, 971 SNPs were selected (**Table 1**). Among them, 291 corresponded to canonical EMS mutations (G > A and C > T), and three of them (SNP1, SNP2, and SNP3) had genotype

quality ≥ 90 and read depth ≥ 10, and were closed together in chromosome 12 (**Table 1**). SNP1, SNP2, and SNP3 correspond to G > A mutations located in the coding regions of genes for the lipoxygenase *CpLOX3A*, the jasmonate-zim-domain protein *CpJAZ1A,* and the mitochondrial elongation factor G *CpEFG1A*, respectively (**Table 1, Fig. 2**).

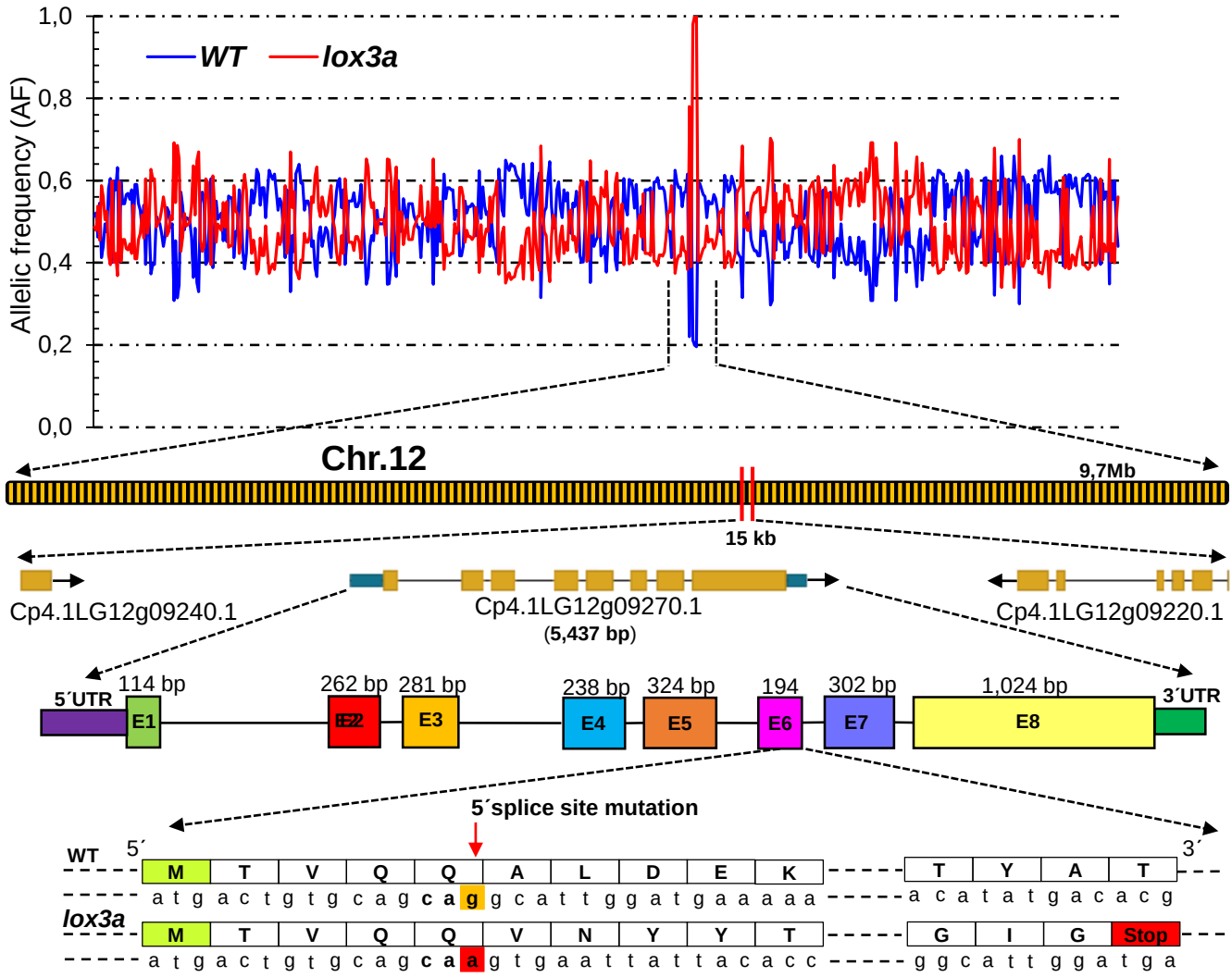

Figure 2. Identification of *lox3a* causal mutation by BSA-sequencing. Frequency of the alternate allele in the WT and *lox3a* bulks along the physical map of squash genome. The BSA-seq analysis indicated that a region of chromosome 12 is responsible for the mutant phenotype. The subsequent fine mapping of the genome region demonstrated that a mutation on the gene *Cp4.1LG12g09270.1* (*CpLOX3A*) produces a 5´-splicing site mutation of intron 6. The mutant CpLOX3A transcript is 91 nucleotides longer than the WT, thus generating a premature stop codon and a truncated CpLOX3A protein.

A fine mapping approach was conducted with the three SNP positions in 561 individual plants from the segregating population BC_1S_1. Results demonstrated that only SNP1 co-segregated 100% with the mutant phenotype (**Dataset S5.1**). Moreover, only 0.18% recombination was found between SNP1 and SNP2, and 47% recombination between SNP2 and SNP3. Given that SNP2 was located in a gene coding for jasmonate-zim-domain protein (*CpJAZ1A*), we validated the mapping results in three BC_1S_2 populations that only segregated for one of the three SNPs. Only the population segregating for SNP1 was again co-segregating with the *lox3a* phenotype, but all BC_1S_2 plants segregating for either SNP2 or SNP3 had a WT phenotype (**Dataset S5.1**). In addition, we found that *CpJAZ1A* showed no expression in any of the analysed tissues, suggesting that it is a non-functional paralog in the duplicated genome of *C. pepo*. Since those three EMS mutations were the only ones in that chromosome 12 region, we concluded that SNP1 was the causal mutation of the *lox3a* phenotype.

5.4.3. *CpLOX3A* structure and phylogeny

The mutation of SNP1 did not change the residue of the protein in that position (**Fig. 2**), but given that it was positioned in the last nucleotide of exon 5, we investigated whether it could affect the 5´-splicing site of intron 6. The transcripts of WT and mutant *CpLOX3A* were amplified by PCR and sequenced. The mutant *CpLOX3A* transcript was 91 nucleotides longer than the WT (**Fig. S5.2**), and its sequence demonstrated that the G > A transition prevented intron 6 splicing, thus generating a premature stop codon and a putative truncated CpLOX3A protein (**Fig. 2, Fig. S5.2**).Given that the genome of *C. pepo* is duplicated (Sun *et al.*, 2017; Montero-Pau *et al.*, 2018), the gene *CpLOX3A* on chromosome 12 (*Cp4.1LG12g09270.1)* has a paralog (*CpLOX3B*) with more than 90% of homology on an syntenic block of chromosome 17 (*Cp4.1LG17g04130.1*). The duplicate transcripts had highly similar structures, although *CpLOX3A* had eight exons and *CpLOX3B* only seven (**Fig. 3A**). The CpLOX3A protein displays more than 70% similarity to plant lipoxygenases, and contains two conserved distinctive domains of this family: a beta-barrel (PLAT/LH2) and a catalytic lipoxygenase helical bundle at the C-terminus; and a predicted chloroplast transit peptide (cTP) at the N-terminus of the protein **(Fig. 3B**). CpLOX3A was also slightly shorter (912 amino acids) than CpLOX3B (922 amino acids) (**Fig. 3B**).

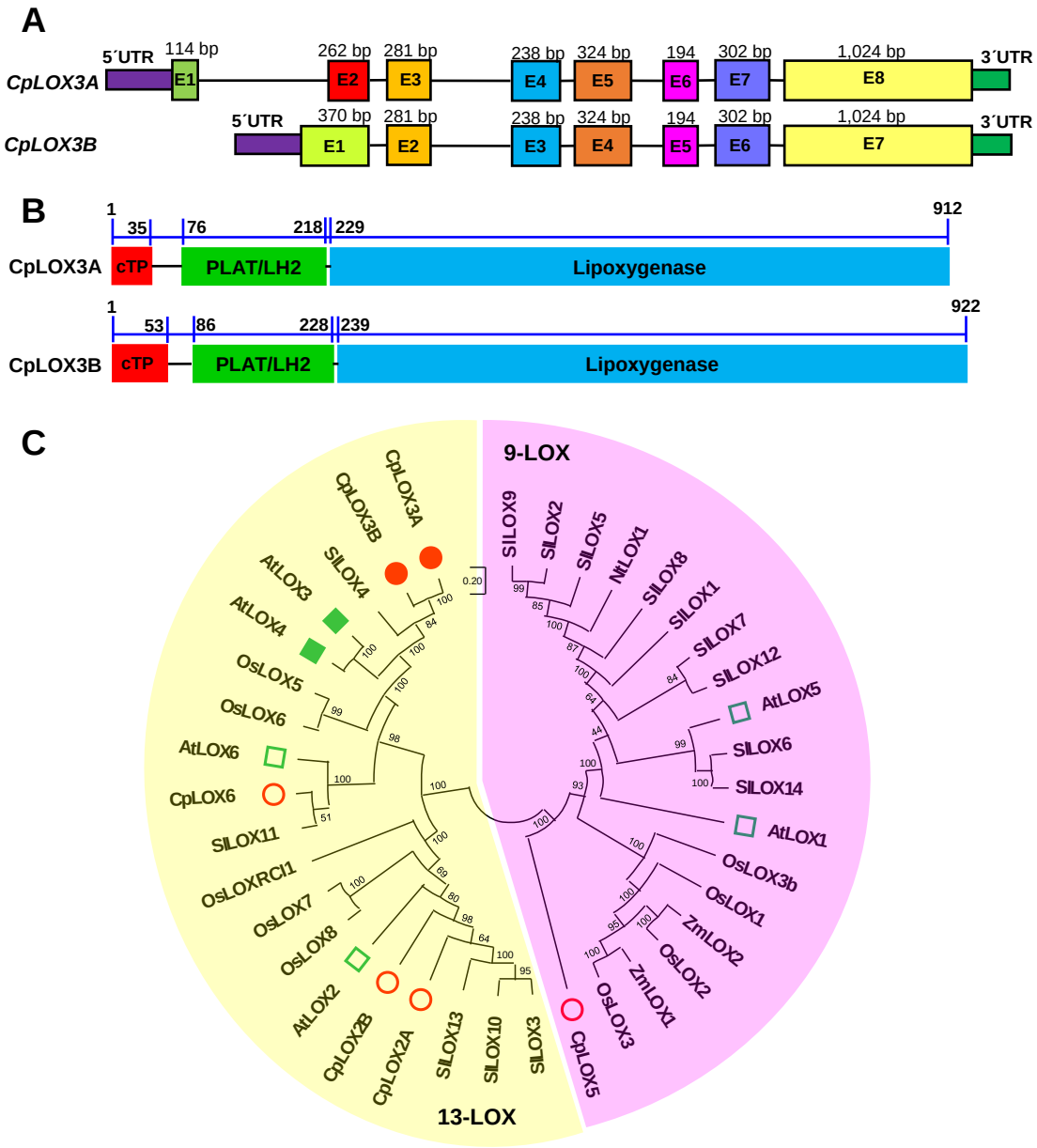

Figure 3. Genetic structure and phylogeny relationships among LOX enzymes in different plant species. (**A**) Comparison of the gene structure of *CpLOX3A* and *CpLOX3B* of *C. pepo.* (**B**) Comparison of CpLOX3A and CpLOX3B protein conserved distinctive domains: a beta-barrel (PLAT/LH2) and a catalytic lipoxygenase helical bundle at the C-terminus; and a predicted chloroplast transit peptide (cTP) at the N-terminus of the protein. (**C**) Phylogenetic LOXs tree from *C. pepo* together with those of the most studied model species, *Arabidopsis thaliana*, *Solanum lycopersicum*, *Oryza sativa, Zea mays,* and *Nicotiana tabacum*. Bootstrap values for the main branches are depicted on the tree.

Lipoxygenases are nonheme iron-containing fatty acid dioxygenases that catalyse the peroxidation of polyunsaturated fatty acids such as linoleic acid, α-linolenic acid, and arachidonic acid. They are classified according to the positional specificity of linoleic acid oxygenation, which occurs at carbon 9 of the hydrocarbon backbone for the 9-LOX types, and at carbon 13 for the 13-LOX types. 13-LOX can be further classified into type I and type II based on the absence or the presence of a chloroplast transit peptide (cTP), respectively (**Fig. 3B, C**). According to the PredSL tool, a neural network-based method for predicting cTPs, the N-terminus of both CpLOX3A and CpLOX3B had a cTP of 35 and 53 residues, respectively (**Fig. 3B**). The primary structure of CpLOX3A and CpLOX3B indicated that they were members of class II plastid-localized 13-lipoxygenases. That prediction was supported by Bayesian and maximum parsimony phylogenetic analyses of plant lipoxygenases (**Fig. 3C**). The phylogenetic tree was inferred by using six LOX protein sequences of *C. pepo* with those from five different model plant species; *Arabidopsis thaliana*; *Solanum lycopersicum*; *Oryza sativa*; *Zea mays*; and *Nicotiana tabacum* (**Fig. 3C**; **Table S5.2**). The *C. pepo* CpLOX3A and CpLOX3B clustered with type II 13-LOXs, including the tomato SlLOX4 and Arabidopsis AtLOX3/AtLOX4. CpLOX6 and CpLOX2A/CpLOX2B were also part of the 13-LOX cluster, together with AtLOX6 and AtLOX2. Only CpLOX5 was found to belong to the 9-LOX cluster (**Fig. 3C**).

5.4.4. JA rescues the phenotype of the JA-deficient *lox3a*

To examine whether *lox3a* affected JA homeostasis, hormone content, expression of JA biosynthesis and signaling genes, and the response to MeJA of male and female flowers were assessed. JA content was evaluated in petals of male and female flowers at early (MS, corolla length ~25-40 mm) and later stage of development (LS, corolla length ~40-55 mm). WT female corolla had two times more JA than that of WT male flowers at both stages, with the highest content in LS, approximately 1 d before anthesis (**Fig. 4A**). The *lox3a* male and female flowers showed an average reduction in JA content of 90% and 99%, respectively, for both stages (**Fig 4A**), which indicates a high deficiency of JA from the early stage of flower development.

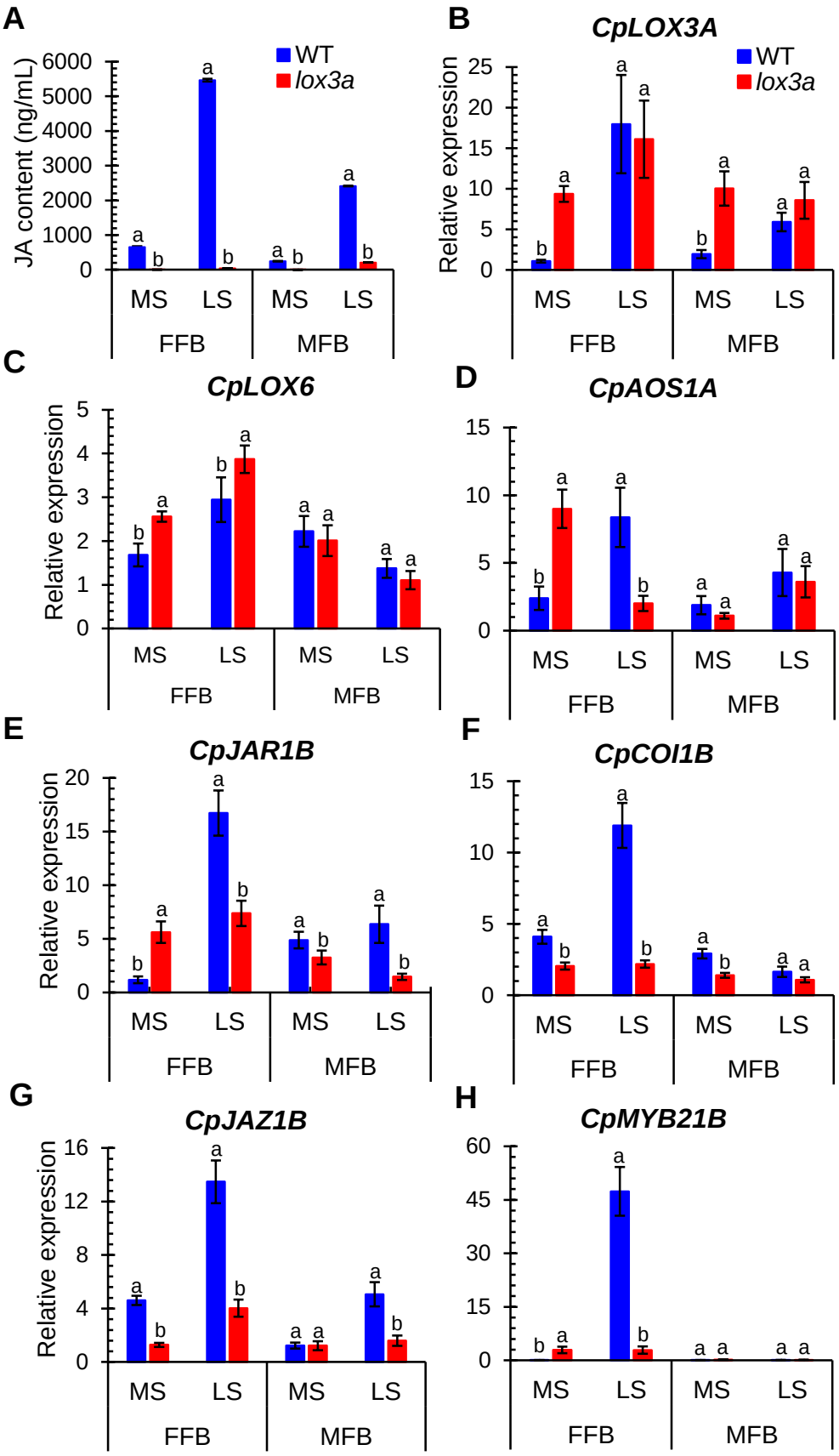
A
JA content (ng/mL)
6000
5000
4000
3000
2000
1000
0
WT
lox3a
MS
LS
MS
LS
FFB
MFB
B
CpLOX3A
Relative expression
25
20
15
10
5
0
C
CpLOX6
Relative expression
D
CpAOS1A
E
CpJAR1B
Relative expression
F
CpCOI1B
G
CpJAZ1B
Relative expression
H
CpMYB21B

Figure 4. Comparison of JA content and JA biosynthesis and signaling gene expression in WT and *lox3a*. (**A**) JA content in WT and *lox3a* male and female flowers in medium (MS) and late stage (LS). (**B-E**) Relative expression of JA biosynthesis genes *CpLOX3A*, *CpLOX6*, *CpAOS1A,* and C*pJAR1B* and (**F-H**) relative expression of JA-signaling genes *CpCOI1B*, *CpJAZ1B*, and *CpMYB21B* in WT and *lox3a* male and female corolla flowers in medium (MS) and late stage (LS). FFB, female flower buds; MFB, male flower buds. The assessments were performed in three independent replicates for each tissue. Error bars represent SE. Different letters indicate significant differences between WT and *lox3a* tissues at the same stage of development ($p \leq 0.05$).

Fig. 4 also shows the relative expression of JA biosynthesis and signaling genes in petals of male and female flowers at MS and LS developmental stages. *CpLOX3A* was induced upon anthesis in both WT male and female flowers, although the induction was higher in female flowers (**Fig. 4B**). No expression was found for the paralogs *CpLOX3B* and *CpLOX2A* in any of the analysed tissues, suggesting that they might be non-functional pseudogenes (data not shown). Expression of *CpLOX3A*, *CpLOX2B,* and *CpLOX6* was detected in leaves and roots, and expression of *CpLOX3A* and *CpLOX6* was detected in flowers (**Fig. S5.3**). Other JA biosynthesis genes, including those coding for lipoxygenase *CpLOX6*, allene oxide synthase *CpAOS1A* and jasmonyl-isoleucine synthetase *CpJAR1B*, exhibited similar expression profiles to *CpLOX3A* in WT flowers (**Fig. 4C, D, E**). Gene expression in *lox3a* indicated that JA biosynthesis genes were regulated in a manner that was dependent on the sex and/or the developmental stage of the flower. *CpLOX3A* expression was similar in WT and mutant flowers at LS, but it was induced in flowers at MS (**Fig. 4B**), indicating a negative feedback regulation of *CpLOX3A* by JA in the early developmental stage. The mutation *lox3a* also up-regulated *CpLOX6* in female flowers, but not in male flowers (**Fig. 4C**).

CpAOS1A was also induced in mutant female flowers at MS but repressed in female flowers at LS (**Fig 4D**). The expression of *CpJAR1B* was down-regulated in *lox3a* male flowers and in female flowers at LS, but it was up-regulated by the mutation in female flowers at MS (**Fig. 4E**). No flower expression was detected for the paralogs *CpAOS1B* and *CpJAR1A* (data not shown). Taken together, all of these data suggest a negative feedback regulation of JA biosynthesis genes at the early stage, but a positive feedback regulation at floral stages closer to anthesis. The JA signaling genes *CpCOI1B*, *CpJAZ1B,* and

CpMYB21B were specifically induced in WT female flowers upon anthesis, but not in WT male flowers (**Fig. 4F, G, H**). Moreover, the *lox3a* mutation caused a down-regulation of the three genes in all analysed tissues, indicating a repression of the JA-signaling pathway in *lox3a* petals prior anthesis. No flower expression was observed for the paralogs *CpCOI1A*, *CpJAZ1A*, and *CpMYB21A* in flowers (data not shown).

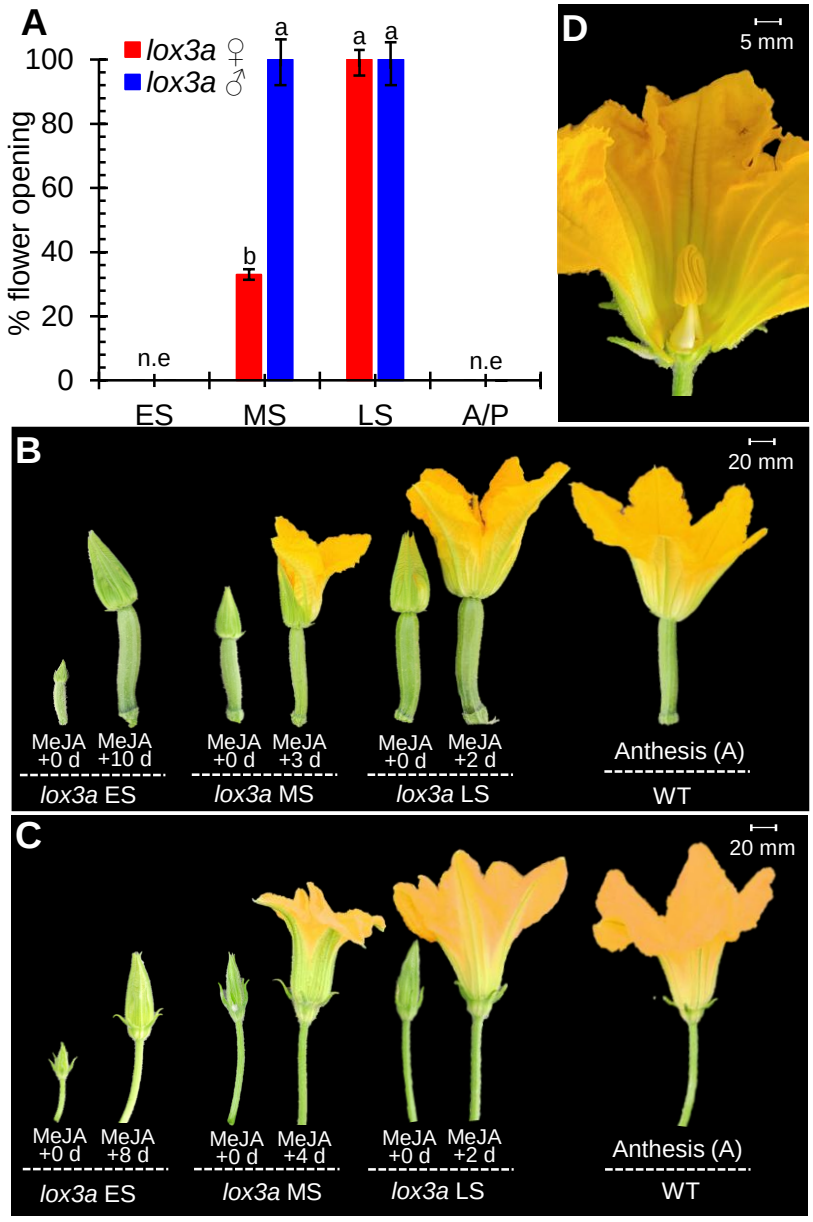

Figure 5. Effect of MeJA treatment on male and female flower opening in *C. pepo*. (**A**) Percentage of flower opening in *lox3a* flowers at early (ES), medium (MS), late (LS), anthesis (A), and post-anthesis (P) developmental stages in *lox3a* flowers. (**B, C**) Phenotypic effect of MeJA treatment on male and female flowers at three developmental stages before anthesis: early (ES); medium (MS); and late (LS). Flowers are shown untreated (left) and several days after treatment (right).

WT flowers at anthesis (A) are shown for comparison. (**D**) Lack of synchronization of reproductive organ and petals in MeJA-treated *lox3a* male flowers. ES, corolla length < 25 mm; MS, corolla length ~25-40 mm; LS, corolla length ~40-55 mm; A, corolla length > 55 mm; MeJA, methyl jasmonate. Error bars represent SE. Different letters indicate significant differences between WT and *lox3a* tissues at the same stage of development ($p \leq 0.05$). n.e, no expression.

To confirm the deficiency in JA of *lox3a*, mutant flowers were treated with 5 mM of MeJA, and floral organ development, maturation, and flower opening in subsequent days after the treatment were assessed. MeJA was applied to flowers at early, medium, and late stages of development (ES, MS, and LS, respectively, before anthesis, A), but also to closed flowers with a corolla length greater that 55 mm, which coincided with flowers at anthesis (A) (dehiscent anthers or receptive stigma) or at post-anthesis (P) (overmature stamens and stigma). MeJA application was able to rescue the phenotype of *lox3a* male and female flowers, although the response to MeJA depended on the sex of the flower and the stage of flower development (**Fig. 5**).

Female flowers were less sensitive to MeJA than male flowers, and only responded to the treatment when they had a size close to anthesis (A). Therefore, 100% of *lox3a* male and female flowers at LS responded to the treatment and were able to complete their maturation and to open 2 d after MeJA application. However, while 100% of MS male flowers opened in response to MeJA, only 30% of female flowers at the same stages reached petal elongation and opening (**Fig. 5A, B, C**). In addition, none of the male or female flowers at ES or at anthesis (A) or post-anthesis (P) were able to open in response to MeJA (**Fig. 5A, B, C**). The maturation of reproductive organs was independent of MeJA treatment. In fact, the JA-induced aperture on male and female *lox3a* flowers at MS was normally associated with immature stamens or carpels, indicating that JA accelerated petal elongation and flower opening, but did not coordinate the maturation of reproductive organs in either male or female flowers (**Fig. 5D**).

5.4.5. Crosstalk between JA and ET in flower maturation and opening

Given that female flowers of the ET-deficient and -insensitive mutants of *C. pepo* delay their opening, remain attached to parthenocarpic fruits and are deficient in JA (García *et al*., 2020*a,b*; Cebrián *et al*., 2022), we investigated the role of ET in these developmental processes. For this, WT and *lox3a* plants were compared for production and sensitivity to ET, and for expression of ET biosynthesis and signaling genes in male and female flowers of WT and *lox3a* plants at either ES, MS, or LS pre-anthesis stages of development. The effect of MeJA treatment on female flower opening of the ET biosynthesis and signaling mutants *aco1a* and *etr2b* was also evaluated.

ET production was much higher in female than in male flowers, and its production profile increased throughout flower development until flower maturation and anthesis (**Fig. 6A**). At the pre-anthesis stage LS, female flowers produced seven times more ET than male flowers (**Fig. 6A**). Furthermore, the *lox3a* mutation delayed the production of ET in the female flower, but ET production at the late development stage (LS) was found to be slightly higher in the *lox3a* flower. In the male flower, *lox3a* did not change the production of ET, except in LS, where it was also higher in *lox3a* than in WT (**Fig. 6A**). ET sensitivity, assessed by male flower abscission in response to external treatments with ET, was not affected by the *lox3a* mutation (**Fig. 6B**). Detached male flowers at LS developmental stages were treated in an atmosphere with air (control, Ct) or ET up to 96 h, and flower abscission was evaluated every 12 h after treatment initiation (**Fig. 6B**). The lack of maturation and opening of *lox3a* flowers slightly delayed male flower abscission, but both WT and *lox3a* flowers accelerated their abscission in response to ET (**Fig. 6B**).

The expression profiles of ET biosynthesis and signaling genes in WT and *lox3a* petals demonstrated that JA regulates the transcription of genes in the ET pathway during flower maturation and opening. The *lox3a* mutation decreased the expression of the ET biosynthesis gene *CpACO1A* in female flowers at the late stage of development (LS) but increased the expression of ET signaling genes *CpETR1A* and *CpEIN3A* in both male and female flowers at MS and LS developmental stages (**Fig. 6C**).

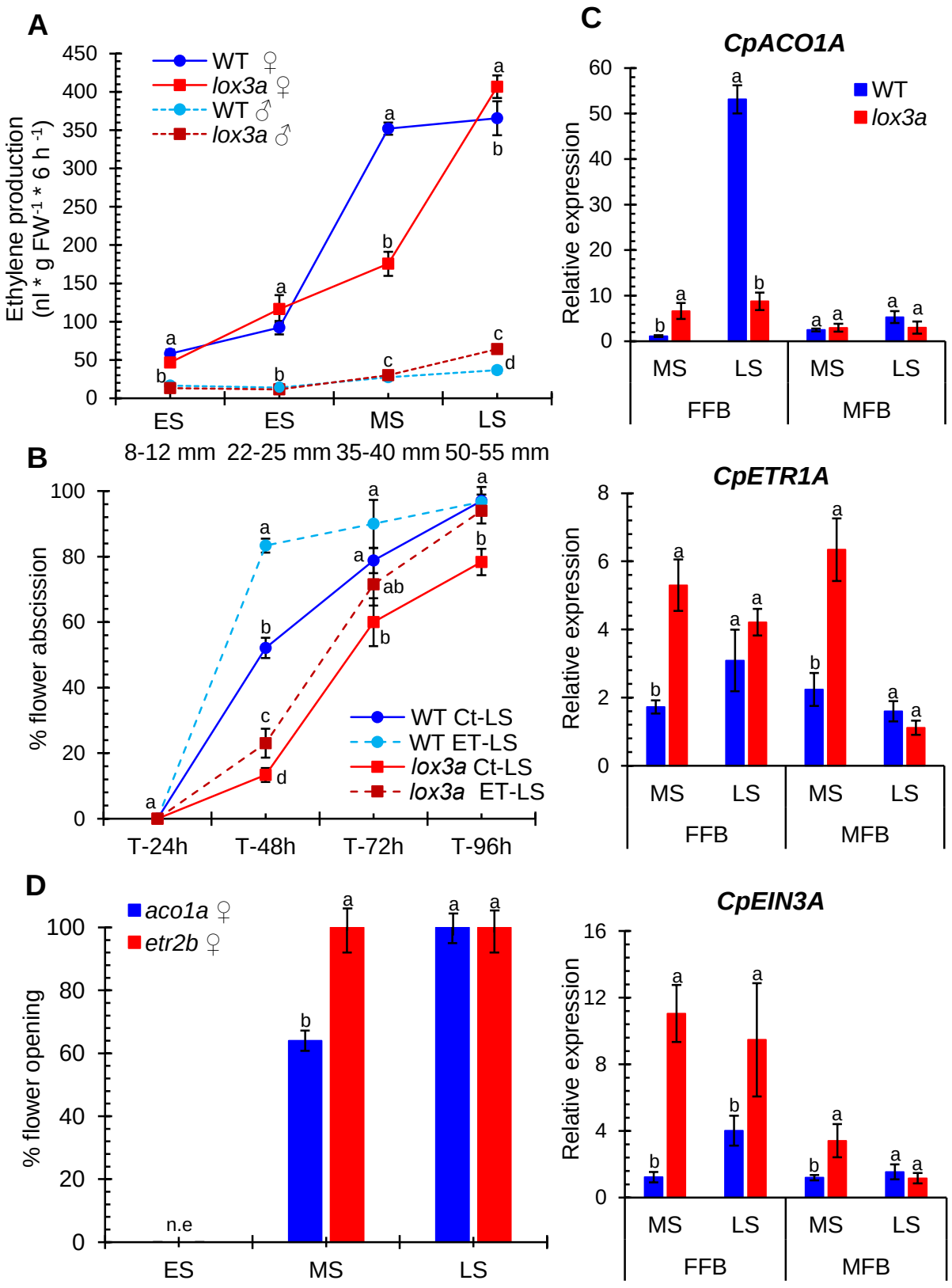
A
Ethylene production (nl * g FW-1 * 6 h-1)
WT ♀
lox3a ♀
WT ♂
lox3a ♂
ES
ES
MS
LS
8-12 mm
22-25 mm
35-40 mm
50-55 mm
B
% flower abscission
WT Ct-LS
WT ET-LS
lox3a Ct-LS
lox3a ET-LS
T-24h
T-48h
T-72h
T-96h
C
CpACO1A
Relative expression
WT
lox3a
MS
LS
MS
LS
FFB
MFB
CpETR1A
CpEIN3A
D
% flower opening
aco1a ♀
etr2b ♀
n.e
ES
MS
LS

Figure 6. Comparison of ET production, ET sensitivity, and ET gene expression in WT and *lox3a*, and effect of MeJA treatment on *aco1a* and *etr2b* female flower opening in *C. pepo.* (**A**) ET production in male and female floral buds of WT and *lox3a* plants in ES, MS, and LS development stage. (**B**) Percentage of abscission in male WT and *lox3a* flowers harvested at late stage (LS), 1 d before anthesis, and evaluated at 24, 48, 72 and 96 h after no treatment, air (Ct), or treatment with ethylene (ET). (**C**) Relative expression of *CpACO1A, CpETR1A*, and *CpEIN3A* in male and female floral buds at medium (MS) and late (LS) stages of development. (**D**) Percentage of flower opening in *aco1a* and *etr2b* MeJA-treated female flowers at early (ES), medium (MS), and late (LS) developmental stages. FFB, female floral bud; MFB, male floral bud. The assessments were performed in three independent replicates for each tissue. Error bars represent SE. Different letters indicate significant differences between WT and *lox3a* tissues at the same stage of development ($p \leq 0.05$).

Although *CpACO1A* seems to be activated by JA, the increased ET content and the higher expression of ET-signaling genes indicated that JA represses ET biosynthesis and response at the petal elongation stage LS immediately prior to flower opening (**Fig. 6C**).

The effect of MeJA on female flower opening of the ET-deficient *aco1a* and the ET -insensitive *etr2b* mutants is shown in **Fig. 6D**. The reduced ET production and response in those mutants was accompanied by the occurrence of stamens in the carpel bearing flowers (female flowers are converted into hermaphrodite flowers), and by a delay in flower opening and the lack of ovary abortion until flower opening. Male flowers opened normally (**Fig. 7A**; García *et al*., 2020*a,b*; Cebrián *et al*., 2022). JA rescued flower opening and ovary abortion when it was applied to the hermaphrodite flowers of *aco1a* and *etr2b* plants at medium (MS) or late (LS) developmental stages, but not in flowers at the early stage (ES) of development (**Fig. 6D**). These data confirm that the ET mutants *aco1a* and *etr2b* are also deficient in JA, and that ET up-regulated the production of the JA required for female-flower opening and ovary abortion. Therefore, the delayed female-flower opening and ovary abortion in the squash ET mutants (García *et al*., 2020*a,b*; Cebrián *et al*., 2022) seems to result from a reduction of JA, which makes petal elongation and flower opening occur more slowly in male flowers.

5.5. Discussion

The JA biosynthesis and signaling pathway has been extensively studied in Arabidopsis, and to some extent in other species, such as tomato, rice, and maize (Upadhyay and Mattoo, 2018; An *et al.*, 2019; Pak *et al.*, 2021). Mutants for JA biosynthesis and signaling genes have revealed that JA not only plays an important role in the response of plants to biotic and abiotic stresses, but is also a regulator of development, controlling flowering time and floral organ development and fertility (Acosta and Przybyl, 2019; Browse and Wallis, 2019; Schubert *et al.*, 2019*a,b*). In cucurbits, the role of JA in flower development is barely known. To gain insight into the role of JA in squash flower development, in this paper, we identified and characterized a squash JA-deficient mutant, demonstrating that JA regulates flower maturation and opening, and participates in the abortion of unfertilized ovaries. We also revealed that ET, the female sex-determining hormone in cucurbits (Martínez and Jamilena, 2021), accelerates female-flower opening and promotes ovary abortion throughout the activation of JA.

5.5.1. *lox3a* is a JA-deficient mutant that affects flower opening and ovary development

The combination of BSA-seq analysis and fine mapping allowed the identification of a loss-of-flower-opening mutation of squash (*lox3a*) into a *LIPOXYGENASE* gene called *CpLOX3A*. The sequence alignment and the phylogenetic tree constructed by using LOXs protein from diverse plant species proved that CpLOX3A is a 13-type lipoxygenase (13-LOX), clustered together with Arabidopsis LOX3 and LOX4, two of the four plastid-localized Arabidopsis 13-LOXs. These enzymes catalyse the oxidation of polyunsaturated fatty acids into functionally-diverse oxylipins, including JAs (Bannenberg *et al*., 2009). The protein domains, with an N-terminal chloroplast transit peptide (cTP), also suggest that CpLOX3A is a plastid-localized type II 13-LOX. In accordance with this, the 5´-splicing site mutation *lox3a*, causing the retention of intron 6 in the mRNA and the generation of a premature stop codon and a truncated enzyme, was expected to be a high-impact mutation resulting in JA deficiency. The results not only confirmed a lower JA production in squash *lox3a* male and female flowers, but also proved that external MeJA was able to rescue the *lox3a*

phenotype, thus demonstrating that *CpLOX3A* is responsible for JA biosynthesis in flowers, and that the *lox3a* phenotype is caused by a deficiency in JA. External treatments of plants and flower buds with JAs were also able to restore WT phenotypes of JA-deficient mutants in Arabidopsis, rice, and maize (Schilmiller *et al.*, 2007; Caldelari *et al.*, 2011; Xiao *et al.*, 2014; Pak *et al.*, 2021).

The widespread expression of squash *CpLOX3A*, *CpLOX2B* and *CpLOX6* suggests that these 13-LOXs may play different developmental functions in different tissues, including flowers, leaves and roots. However, the phenotype of *lox3a* indicates that *CpLOX3A* has a specific and indispensable role in squash flower development, a function that cannot be complemented by other *13-LOX* genes, such as *CpLOX6*, which are also expressed at the same flower developmental stages. The broad expression of *TASSEL SEED 1* (*TS1*), a gene encoding for enzyme ZmLOX8, also contradicts its specific role in carpel abortion during sex determination of the maize male flower (Acosta *et al.*, 2009; Browse, 2009). Similarly, Arabidopsis *13-LOX* genes also exhibit a specific function in flower development. For the four 13-LOX of Arabidopsis, only LOX3 and LOX4, but not LOX2 and LOX6, have been found to be indispensable and sufficient for stamen maturation and pollen fertility. In fact, double mutants *lox3 lox4* are male sterile (Caldelari *et al.*, 2011), while *lox2*, *lox3*, and *lox6* single mutants, and *lox2 lox4 lox6* triple mutants are fully fertile (Chauvin *et al*., 2013).

The mutant phenotype clearly indicates that *lox3a* impaired only the late stage of pre-anthesis male and female flower development (LS, **Fig. 7A**), suppressing petal elongation and flower opening. Furthermore, the lack of flower opening in *lox3a* suppresses the abortion of unfertilized ovary, which leads to the development of parthenocarpic fruits. This positive role of *CpLOX3A* and JA in squash petal elongation and flower opening is also supported by the induction of *CpLOX3A* and other JA biosynthesis genes in the corolla of WT male and female flowers towards anthesis. We also found that, as occurs in Arabidopsis (Sanders *et al.*, 2000; Ishiguro *et al.*, 2001), *lox3a* flowers were able to respond to MeJA and to open when they were at a developmental stage closer to anthesis, but not the early stage (ES) or at post-anthesis (unopen flowers with overmature stigma or anthers). The high induction of JA-signaling components, including *CpCOI1B*, *CpJAZ1B* and *CpMYB21B*, at the late stage (LS) of pre-anthesis petal development, may account for this specific “time-window” response to MeJA

(Sanders *et al*., 2000). Therefore, JA produced in petals (and possibly in other floral organs) will be only receptive in a corolla with an activated JA-signaling pathway. We cannot rule out, however, as reported in Arabidopsis (Acosta and Przybyla, 2019), that the competence of petal cells to respond to JA requires the previous actuation of hormones, such as auxin (IAA) and gibberellin (GAs).

The positive feedback regulation of JA biosynthesis and signaling genes at developmental stages closer to anthesis, as shown by the diminished expression of *CpAOS1A*, *CpJAR1B*, *CpCOI1B*, *CpJAZ1B* and *CpMYB21B* in *lox3a* flowers, may be responsible for the rapid induction of JA biosynthesis and signaling in the corolla of flowers immediately prior to anthesis. A positive feedback regulation of JA biosynthesis has been also found in tomato flower development (Schubert *et al*., 2019*a*), but a negative feedback regulation was found in Arabidopsis (Reeves *et al*., 2012; Huang *et al*., 2017). In Arabidopsis and tomato, it has been reported that JA can control the elongation of both petals and stamens by inducing sugar transporters that facilitate water uptake and cell elongation (Stadler *et al*., 1999; Ishiguro *et al*., 2001; Schubert *et al*., 2019*a,b*), but whether or not this mechanism of action also works in squash remains to be elucidated.

Petal maturation and flower opening seem to be a widespread JA function that has been demonstrated by the phenotypes of JA-deficient and -insensitive mutants in Arabidopsis, rice, tomato, and Nicotiana (Ishiguro *et al*., 2001; Liu *et al*., 2009; Xiao *et al*., 2014; Liu *et al*., 2017; Niwa *et al*., 2018), but the function of JA in reproductive organ development has diversified during the flowering plant evolution. In Arabidopsis, JA-deficiency or -insensitivity results in male sterility, characterized by delayed anther dehiscence and flower opening, insufficient filament elongation, and production of unviable pollen (Acosta and Przybyl, 2019). In contrast, JA insensitivity in tomato leads to a female-sterile phenotype; the development of stamen and pollen is also affected, but to a lesser extent (Dobritzsch *et al.*, 2015). These differences between tomato and Arabidopsis were observed even when the mutations affect the same orthologous JA genes, including *COI1* (Feys *et al.*, 1994; Li *et al.*, 2004) and *MYB21* (Mandaokar *et al*., 2006; Schubert *et al.*, 2019*a*). In maize, the JA-deficient mutations *ts1* and *opr7 opr8* produce a conversion of male into female flowers in the tassel, indicating that JA is necessary for the suppression of carpel primordia during male flower

determination in the tassel (Acosta *et al*., 2009, Browse *et al*., 2009; Yang *et al*., 2012). In rice, JA regulates spikelet morphogenesis, with JA-deficient mutants exhibiting changes in floral organ identity and number, as well as defective floral meristem determinacy (Cai *et al*., 2014). In squash, the normal development of sexual organs and the male and female fertility of *lox3a* suggest that JA does not participate in stamen and pollen development, either in the development of style, stigma, or ovules. However, the enhanced growth of the *lox3a* ovary in the absence of flower opening and pollination indicate that JA could be a negative regulator of fruit set and early fruit development, a function that has been also reported for ET (Martínez *et al*., 2014).

5.5.2. Crosstalk between ET and JA in the differential regulation of male and female flower development and opening

ET is the key hormone controlling sex determination in squash and other cucurbits (Martínez and Jamilena, 2021). Early ET production is crucial to arrest stamen primordia development in the floral meristem that will be determined as a female flower (Boualem *et al*., 2008; 2009; Martínez *et al*., 2014; Manzano *et al*., 2016). As confirmed in this paper, ET is also induced in already-determined male and female flowers, increasing its production towards anthesis, and markedly more in female- than in male-flowers (Manzano *et al*., 2010). This late-produced ET appears to be responsible for the higher growth rate and the quicker maturation and opening of female flowers in comparison with male flowers. In fact, the growth rate of the pistillate in the ET biosynthesis *aco1a* mutant (Cebrián *et al*., 2022) and in the ET-insensitive mutants *etr1a* and *etr2b* (García *et al*., 2020*a*) resembled that of male flowers during both MS and LS, delaying their opening to the same time as male flowers (**Fig. 7A**). This growth slowdown of ET mutant pistillate flowers affects petals, stamens, stile and stigma, which impairs female fertility (García *et al*., 2020*a*; Cebrián *et al*., 2022).

The reduced JA production in female flowers of the ET biosynthesis mutant *aco1a* of squash suggests that ET could regulate female-flower development and opening through JA (Cebrián *et al*., 2022). In this paper, we demonstrate that MeJA can rescue petal elongation and flower opening defects of *aco1a* and *etr2b* pistillate flowers, but it did not restore their diminished growth rate, or prevent abnormal stamen occurrence.

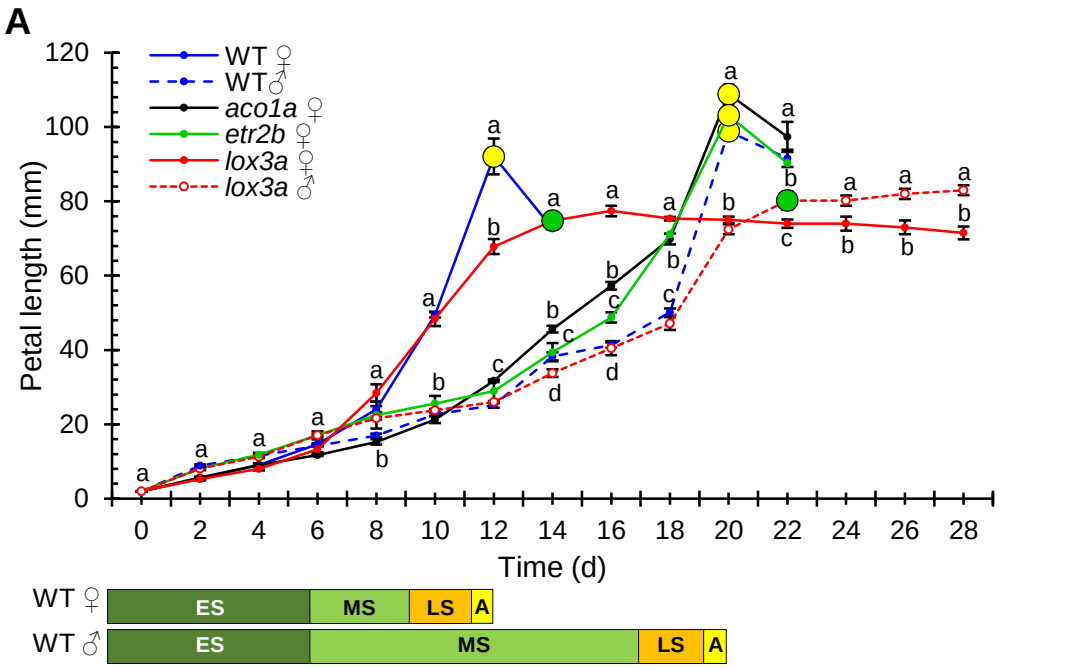
A
Petal length (mm)
Time (d)
WT ♀
WT ♂
aco1a ♀
etr2b ♀
lox3a ♀
lox3a ♂
WT ♀
WT ♂
ES
MS
LS
A

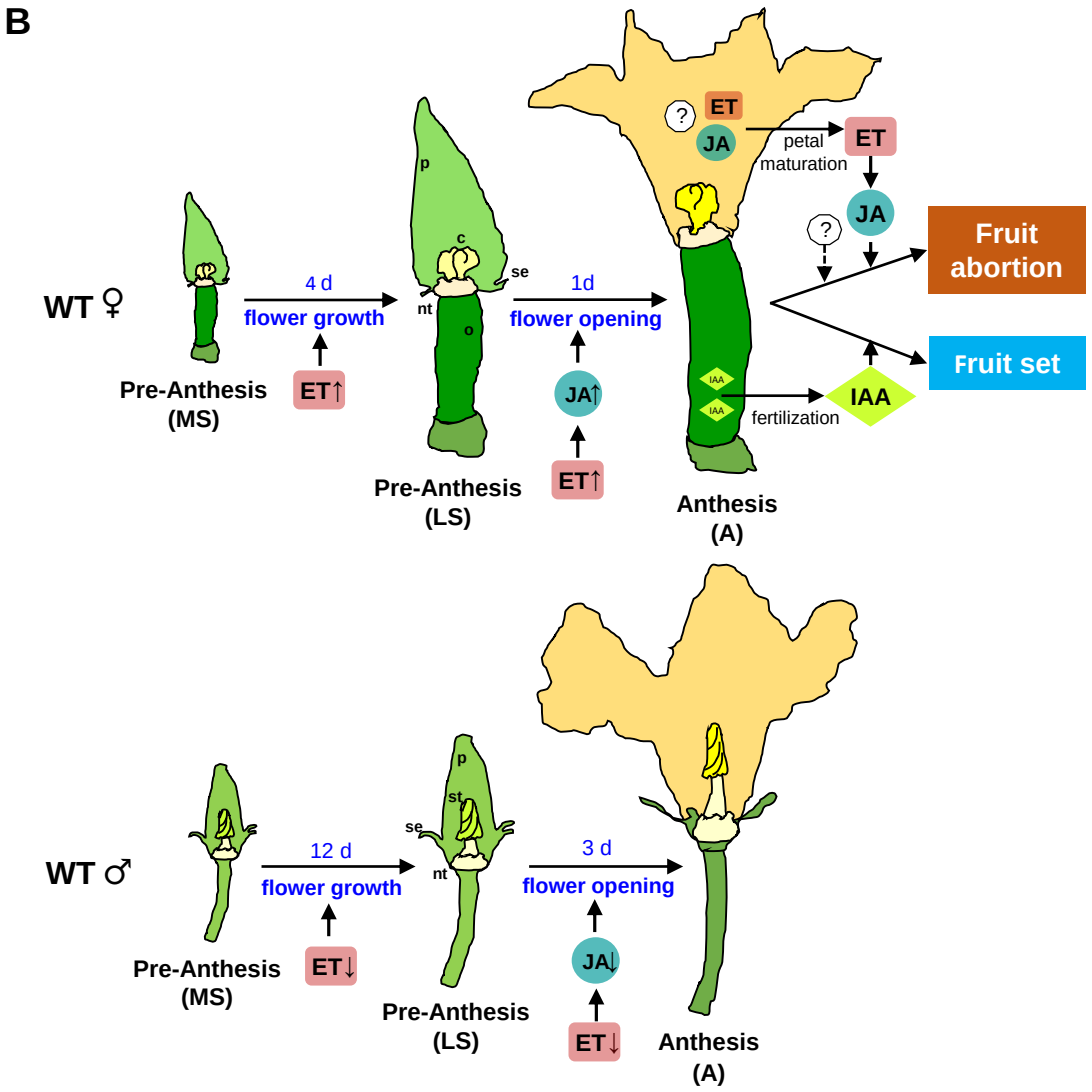
B
WT ♀
4 d
flower growth
ET↑
Pre-Anthesis
(MS)
Pre-Anthesis
(LS)
1d
flower opening
JA↑
ET↑
Anthesis
(A)
ET
JA
petal
maturation
ET
JA
Fruit
abortion
Fruit set
IAA
fertilization
WT ♂
12 d
flower growth
ET↓
Pre-Anthesis
(MS)
Pre-Anthesis
(LS)
3 d
flower opening
JA↓
ET↓
Anthesis
(A)

Figure 7. (**A**) Comparison of the growth rate of WT, *aco1a*, *etr2b* and *lox3a* corolla development. Yellow circles indicate flower opening at anthesis (A), while green circles indicate the time at which unopen male and female flowers of *lox3a* are fertile. (**B**) Model integrating the role of ethylene (ET), jasmonate (JA), and auxin (IAA) in the male and female flower growth/opening, and in fruit set and development in *C. pepo*. The higher growth rate of female flowers at MS is directly regulated by ET, while the quicker petal elongation and female flower opening at LS depend on the crosstalk between ET and JA. After flower opening, fruit set and development is coordinated by IAA and other hormones derived from the fertilized ovules. In the absence of fertilization, an alternative developmental program is activated from signals coming from sepals, which may include ET and JA. se, sepal; p, petal; st, stamen; c, carpel; o, ovary; nt, nectary; MS, medium stage; LS, late stage; A, anthesis. Error bars represent SE. Different letters indicate significant differences between flowers of the different genotypes at each developmental time ($p \leq 0.05$).

These data demonstrate that JA mediates the action of ET in female petal elongation and female-flower opening, but not in flower growth, or sex determination (**Fig. 7**). The higher production of JA and ET in female flowers in comparison with male flowers (10 times more JA and seven times more ET towards flower opening), and the higher expression of JA biosynthesis and signaling genes towards female-flower anthesis, suggests that ET of female flowers induces the production and response of JA to hasten flower opening in female but not in male flowers (**Fig. 7**). The higher ET production and the up-regulation of ET-signaling genes *CpETR1A* and *CpEIN3A* in *lox3a* female petals towards anthesis also indicate that JA represses ET biosynthesis and response in petals towards anthesis, which could prevent the premature senescence of petals.

5.5.3. Crosstalk between ET and JA in parthenocarpic fruit development

The regulation of flower opening and its synchronization with stamen and carpel maturation not only ensures sexual reproduction, but may also act as a trigger for the subsequent flower developmental program, including fruit set and fruit abortion (**Fig. 7B**). The parthenocarpy in JA- and ET-deficient and insensitive mutants of squash (García *et al*., 2020*a*; Cebrián *et al*., 2022) may indicate that ET and JA are negative regulators of fruit set and development. However, given that this parthenocarpic development of the fruit was associated with unopen female flowers, and it finishes once the flower opens, it is likely that parthenocarpy is caused by the lack of JA, ET, and maybe other signaling factors

occurring in mature or senescent petals after flower opening (**Fig. 7B**). Floral opening would thus act as a developmental switch that triggers fruit set and fruit development by hormones, such IAA and GAs, coming from fertilized ovules; in the absence of fertilization, however, flower opening may also activate an alternative program that results in abortion of the ovary. Ovary abortion would be, therefore, a positively-regulated process that is activated from mature or senescent petals after flower opening (**Fig. 7B**). In accordance with this hypothesis, the results showed that ovary and early fruit development in *lox3a* female flowers are independent of pistil and stigma development, which are senescent in the still-growing ovary, but are rather coordinated by petals, ending when corolla reaches maturation and opens. Likewise, the induced flower opening in MeJA-treated female flowers of *lox3a*, *etr2b* and *aco1a* mutants is synchronized with fruit abortion, but pistil and stigma are still immature. Moreover, the delayed flower opening squash ET-deficient and -signaling mutants also delayed fruit abortion until the flower is open (García *et al*., 2020*a*, Cebrián *et al*., 2022).

Parthenocarpy has been found to be associated with defective mutants in petal development. The LOF mutation in *MdPI*, a *PISTILLATA*-like MADS-box transcription factor of apple, not only produces apetalous flowers with homeotic conversions of petals and stamens into sepals and carpels, but also confers parthenocarpic fruit development in apple (Yao *et al*., 2001). Parthenocarpic fruits are also exhibited by the B-class *AP3* homeotic mutants of tomato (Gómez *et al*., 1999; Quinet *et al*., 2014; Okabe *et al*., 2019). *PeMADS6*, a *PI*-like gene of *Phalaenopsis equestris*, is not only required to confer petal and stamen identity, but seems to repress ovary development in orchids (Tsai *et al*., 2005). On the other hand, the ectopic expression of *PI* represses fruit development and results in small berries in both apple and grape (Fernandez *et al*., 2013; Yao *et al*., 2018). Other floral organ identity genes were also found to be involved in ovary/fruit development. Thus, the down-regulation of *TM29*, a tomato *SEPALLATA* homolog, causes a partial conversion of petals and stamens into sepals, and parthenocarpic tomato fruits (Ampomah-Dwamena *et al*., 2002), and the strawberry mutant for the MADS-box *FveSEP3* gene also develop green flowers with sepaloid petal, stamen, and carpel, as well as parthenocarpic fruits (Pi *et al*., 2021).

The mechanisms that regulate parthenocarpic fruit development in homeotic mutants with aberrant floral organ development, including those in JA and ET genes of squash, is largely undetermined. It has been proposed that parthenocarpy was associated with abnormal stamens in AP3 tomato mutants (Okabe *et al*., 2019). Squash ET mutants are also defective in stamen development (they develop partial developed stamens), but the jasmonate *lox3a* mutant female flowers exhibits no stamen development. Nevertheless, these and other floral homeotic mutants were defective in mature petals, supporting our hypothesis that mature and senescent petals induce a positive signal that activates ovary/fruit abortion in the absence of fertilization (**Fig. 7B**). Whether JA, ET, and possibly other signaling molecules derived from mature/senescent petals, can activate squash fruit abortion awaits further investigation, but it is likely that they can act as repressors of IAA and/or GAs (Martínez *et al*., 2013; Shinozaki *et al*., 2015).

6. General conclusions

FIRST. The ET receptor mutations *etr1a*, *etr1b* and *etr2b* enhance salt tolerance in *Cucurbita pepo* during both germination and vegetative growth, demonstrating that the ET receptors ETR1A, ETR1B and ETR2B play a positive role in salt tolerance.

SECOND. The enhanced salt tolerance response of the *etr2b* plants is associated with a reduced accumulation of Na^+ in shoots and leaves, an induction of genes that exclude Na^+ in photosynthetic organs, while maintaining K^+/Na^+ homoeostasis and osmotic adjustment, and with a higher accumulation of compatible solutes, including proline, total carbohydrates and anthocyanin.

THIRD. The higher upregulation of genes involved in Ca^{2+} signalling (*CpCRCK2A* and *CpCRCK2B*) and ABA biosynthesis (*CpNCED3A* and *CpNCED3B*) in *etr2b* leaves under salt stress likely indicates that the function of ET receptors in salt stress response in *C. pepo* can be mediated by Ca^{2+} and ABA signalling pathways.

FOURTH. The combination of Bulk Segregant Analysis (BSA) and next-generation sequencing (NGS) enabled the identification of *aco1a* and *lox3a*, two EMS mutations disrupting flower and fruit development in *C. pepo*.

FIFTH. The mutant *aco1a* is defective in female sex determination mechanism, promoting the conversion of female into bisexual flowers, and monoecy into andromonoecy. The mutation also disrupts the growth rate and maturation of petals and carpels, delaying female flower opening, and promoting the growth rate of ovaries and the parthenocarpic development of the fruit.

SIXTH. The *aco1a* phenotype is caused by a missense mutation in the coding region of *CpACO1A*, a gene coding for a type I ACO enzyme that shares a high identity with *Cucumis sativus* CsACO3 and *Cucumis melo* CmACO1. This enzyme is responsible of the ET biosynthesis that is required to arrest stamen development during early stages of female flower development in *C. pepo*.

SEVENTH. The contents of JA and IAA in *aco1a* female flowers suggests that ET activates petal maturation and female-flower opening by inducing the biosynthesis of JA, but suppresses fruit set and development by repressing the biosynthesis of IAA.

EIGHTH. The mutation *lox3a* suppresses *C. pepo* male- and female-flower opening, and promotes the parthenocarpic development of the fruit.

NINTH. The *lox3a* mutation affects *CpLOX3A*, a *LYPOXYGENASE* gene involved in JA biosynthesis. The reduced JA content and the diminished expression of JA signalling genes in female- and male-flowers of *lox3a*, and the rescue of *lox3a* phenotype by external application of MeJA, demonstrated that JA controls petal elongation and flowering opening, as well as fruit abortion in absence of fertilization.

TENTH. The effect of JA on ET-biosynthesis and -signalling mutants revealed a JA-ET crosstalk in the differential regulation of female- and male-flower opening in *C. pepo.* ET is up-regulating JA biosynthesis and signalling only in the female flower, promoting so the faster opening of female flowers in comparison with male flowers.

ELEVENTH. The phenotypes of ET and JA mutants demonstrated that these two hormones have a negative role on fruit set and development. Given the close association between flower opening and fruit abortion, we have suggested a model in which flower opening acts as a switch that triggers fruit set and development in the fertilized ovary, but may alternatively induce the abortion of the unfertilized ovary. To perform this function, both ET and JA from mature and senescent petals in open flowers can serve as remote signals that activate ovary/fruit abortion in absence of fertilization.

7. References

Abrahám E, Hourton-Cabassa C, Erdei L, Szabados L. 2010. Methods for determination of proline in plants. *Methods in Molecular Biology* **639**, 317-331.

Achard P, Cheng H, De Grauwe L, Decat J, Schoutteten H, *et al*. 2006. Integration of plant responses to environmentally activated phytohormonal signals. *Science* **311**, 91-94.

Acosta IF, Laparra H, Romero SP, Schmelz E, Hamberg M, *et al*. 2009. *tasselseed1* is a lipoxygenase affecting jasmonic acid signaling in sex determination of maize. *Science* **323**, 262-265.

Acosta IF, Przybyl M. 2019. Jasmonate signaling during Arabidopsis stamen maturation. *Plant and Cell Physiology* **60**, 2648-2659.

Adams DO, Yang SF, Stumpf PK. 1979. Ethylene biosynthesis: identification of 1-aminocyclopropane-1-carboxylic acid as an intermediate in the conversion of methionine to ethylene. *Proceedings of the National Academy of Sciences* **76**, 170-174.

Aguado E, García A, Iglesias-Moya J, Romero J, Wehner TC, *et al.* 2020. Mapping a partial andromonoecy locus in *Citrullus lanatus* using BSA-Seq and GWAS approaches. *Frontiers in Plant Science* **11**, 1243.

Ahmad RM, Cheng C, Sheng J, Wang W, Ren H, Aslam M, Yan Y. 2019. Interruption of jasmonic acid biosynthesis causes differential responses in the roots and shoots of maize seedlings against salt stress. *International Journal of Molecular Sciences* **20**, 6202.

Akagi T, Henry IM, Ohtani H, Morimoto T, Beppu K, Kataoka I, Tao R. 2018. A Y-encoded suppressor of feminization arose via lineage-specific duplication of a cytokinin response regulator in kiwifruit. *The Plant Cell* **30**, 780-795.

Albacete A, Martínez-Andújar C, Ghanem ME, Acosta M, Sánchez-Bravo J, *et al.* 2009. Rootstock-mediated changes in xylem ionic and hormonal status are correlated with delayed leaf senescence, and increased leaf area and crop productivity in salinized tomato. *Plant, Cell & Environment* **32**, 928-938.

Alonso JM, Hirayama T, Roman G, Nourizadeh S, Ecker JR. 1999. EIN2, a bifunctional transducer of ethylene and stress responses in Arabidopsis. *Science* **284**, 2148-2152.

Amini M. 2014. Ethyl methanesulfonate. Encyclopedia of Toxicology: Third Edition. Academic Press, 522-524.

Ampomah-Dwamena C, Morris BA, Sutherland P, Veit B, Yao JL. 2002. Down-regulation of *TM29*, a tomato *SEPALLATA* homolog, causes parthenocarpic fruit development and floral reversion. *Plant Physiology* **130**, 605-617.

An J, Althiab Almasaud R, Bouzayen M, Zouine M, Chervin C. 2020. Auxin and ethylene regulation of fruit set. *Plant Science* **292**, 110381.

An L, Ahmad RM, Ren H, Qin J, Yan Y. 2019. Jasmonate signal receptor gene family *ZmCOIs* restore male fertility and defense response of Arabidopsis mutant *coi1-1*. *Journal of Plant Growth Regulation* **38**, 479-493.

Apse MP, Aharon GS, Snedden WA, Blumwald E. 1999. Salt tolerance conferred by overexpression of a vacuolar Na^+/H^+ antiport in Arabidopsis. *Science* **285**, 1256-1258.

Argiolas A, Puleo GL, Sinibaldi E, Mazzolai B. 2016. Osmolyte cooperation affects turgor dynamics in plants. *Scientific Reports* **6**, 1-8.

Aroca R, Ruiz-Lozano JM, Zamarreño AM, Paz JA, García-Mina JM, Pozo MJ, López-Ráez JA. 2013. Arbuscular mycorrhizal symbiosis influences strigolactone production under salinity and alleviates salt stress in lettuce plants. *Journal of Plant Physiology* **1**, 47-55.

Arraes FBM, Beneventi MA, Lisei de Sa ME, Paixao JFR, Albuquerque EVS *et al*. 2015. Implications of ethylene biosynthesis and signaling in soybean drought stress tolerance. *BMC Plant Biology* **15**, 1-20.

Bachman GR, McMahon MJ. 1997. Light quality effects on flower sex expression in cucumber and spinach. *HortScience* **32**, 464.

Bai SL, Peng YB, Cui JX, Gu HT, Xu LY, *et al.* 2004. Developmental analyses reveal early arrests of the spore-bearing parts of reproductive organs in unisexual flowers of cucumber (*Cucumis sativus* L.). *Planta* **220**, 230-240.

Bakshi A, Piy S, Fernandez JC, Chervin C, Hewezi T, Binder BM. 2018. Ethylene receptors signal via a noncanonical pathway to regulate abscisic acid responses. *Plant Physiology* **176**, 910-929.

Bakshi A, Wilson RL, Lacey RF, Kim H, Wuppalapati SK, Binder BM. 2015. Identification of regions in the receiver domain of the ETHYLENE RESPONSE1 ethylene receptor of arabidopsis important for functional divergence. *Plant Physiology* **169**, 219-232.

Bannenberg G, Martínez M, Hamberg M, Castresana C. 2009. Diversity of the enzymatic activity in the lipoxygenase gene family of *Arabidopsis thaliana*. *Lipids* **44**, 85.

Barry CS, Blume B, Bouzayen M, Cooper W, Hamilton AJ, Grierson D. 1996. Differential expression of the 1-aminocyclopropane-1-carboxylate oxidase gene family of tomato. *The Plant Journal* **9**, 525-535.

Barry CS, Llop-Tous MI, Grierson D. 2000. The regulation of 1-aminocyclopropane-1-carboxylic acid synthase gene expression during the transition from system-1 to system-2 ethylene synthesis in tomato. *Plant Physiology* **123**, 979-986.

Bassil E, Tajima H, Liang YC, Ohto MA, Ushijima K, *et al.* 2011. The Arabidopsis Na^+/H^+ antiporters NHX1 and NHX2 control vacuolar pH and K^+ homeostasis to regulate growth, flower development, and reproduction. *The Plant Cell* **23**, 3482-3497.

Beaudoin N, Serizet C, Gosti F, Giraudat J. 2000. Interactions between abscisic acid and ethylene signaling cascades. *The Plant Cell* **12**, 1103-1115.

Berthomieu P, Conéjéro G, Nublat A, Brackenbury WJ, Lambert C, *et al.* 2003. Functional analysis of *AtHKT1* in Arabidopsis shows that Na^+ recirculation by the phloem is crucial for salt tolerance. *EMBO Journal* **22**, 2004-2014.

Binder BM. 2020. Ethylene signaling in plants. *Journal of Biological Chemistry* **295**, 7710-7725.

Binder BM, Chang C, Schaller GE. 2012. Perception of ethylene by plants - ethylene receptors. *Annual Plant Reviews* **44**, 117-145.

Binder BM, Walker JM, Gagne JM, Emborg TJ, Hemmann G, Bleecker AB, Vierstra RD. 2007. The Arabidopsis EIN3 binding F-Box proteins EBF1 and EBF2 have distinct but overlapping roles in ethylene signaling. *The Plant Cell* **19**, 509-523.

Bisognin DA. 2002. Origin and evolution of cultivated cucurbits. *Ciência Rural* **32**, 715-723.

Bisson MMA, Groth G. 2010. New insight in ethylene signaling: autokinase activity of ETR1 modulates the interaction of receptors and EIN2. *Molecular Plant* **3**, 882-889.

Bleecker AB, Estelle MA, Somerville C, Kende H. 1988. Insensitivity to ethylene conferred by a dominant mutation in *Arabidopsis thaliana*. *Science* **241**, 1086-1089.

Bleecker AB, Kende H. 2000. Ethylene: a gaseous signal molecule in plant. *Annual Review of Cell and Developmental Biology* **16**, 1-18.

Boller T, Herner RC, Kende H. 1979. Assay for and enzymatic formation of an ethylene precursor, 1-aminocyclopropane-1-carboxylic acid. *Planta* **145**, 293-303.

Borrego EJ, Kolomiets MV. 2016. Synthesis and functions of jasmonates in maize. *Plants* **5**, 41.

Böttcher C, Burbidge CA, Boss PK, Davies C. 2013. Interactions between ethylene and auxin are crucial to the control of grape (*Vitis vinifera* L.) berry ripening. *BMC Plant Biology* **13**, 1-14.

Boualem A, Fergany M, Fernandez R, Troadec C, Martín A *et al.* 2008. A conserved mutation in an ethylene biosynthesis enzyme leads to andromonoecy in melons. *Science* **321**, 836-838.

Boualem A, Fleurier S, Troadec C, Audigier P, Kumar AP *et al.* 2014. Development of a *Cucumis sativus* TILLinG platform for forward and reverse genetics. *PLoS ONE* **9**, e97963.

Boualem A, Lemhemdi A, Sari MA, Pignoly S, Troadec C, *et al*. 2016. The andromonoecious sex determination gene predates the separation of *Cucumis* and *Citrullus* genera. *PLoS ONE* **11**, e0155444.

Boualem A, Troadec C, Camps C, Lemhemdi, A, Morin H, *et al.* 2015. A cucurbit androecy gene reveals how unisexual flowers develop and dioecy emerges. *Science* **350**, 688-691.

Boualem A, Troadec C, Kovalski I, Sari MA, Perl-Treves R, Bendahmane A. 2009. A conserved ethylene biosynthesis enzyme leads to andromonoecy in two *Cucumis* species. *PLoS ONE* **4**, e6144.

Browse J. 2009. Jasmonate: preventing the maize tassel from getting in touch with his feminine side. *Science Signaling* **2**, pe9

Browse J, Wallis JG. 2019. Arabidopsis flowers unlocked the mechanism of jasmonate signaling. *Plants* **8**, 285

Bulens I, Van de Poel B, Hertog ML, De Proft MP, Geeraerd AH, Nicolaï BM. 2011. Protocol: an updated integrated methodology for analysis of metabolites and enzyme activities of ethylene biosynthesis. *Plant Methods* **7**, 1-10.

Byers RE, Baker LR, Sell HM, Herner RC, Dilley DR. 1972. Ethylene: a natural regulator of sex expression of *Cucumis melo* L. *Proceedings of the National Academy of Sciences* **69**, 717-720.

Cai Q, Yuan Z, Chen M, Yin C, Luo Z, *et al.* 2014. Jasmonic acid regulates spikelet development in rice. *Nature Communications* **5**, 1-13.

Cai S, Chen G, Wang Y, Huang Y, Marchant DB, *et al.* 2017. Evolutionary conservation of ABA signaling for stomatal closure. *Plant Physiology* **174**, 732-747.

Cai Y, Bartholomew ES, Dong M, Zhai X, Yin S, *et al.* 2020. The HD-ZIP IV transcription factor GL2-LIKE regulates male flowering time and fertility in cucumber. *Journal of Experimental Botany* **71**, 5425-5437.

Cajamar. F. 2021. *Análisis de la Campaña Hortofrutícola de Almería, Campaña 2020/2021*. Cajamar, Almería, Spain.

Cantliffe DJ. 1981 Alteration of sex expression in cucumber due to changes in temperature, light intensity, and photoperiod. *HortScience* **106**, 133-136.

Caldelari D, Wang G, Farmer EE, Dong X. 2011. Arabidopsis *lox3 lox4* double mutants are male sterile and defective in global proliferative arrest. *Plant Molecular Biology* **75**, 25-33.

Cao WH, Liu J, Chen T, Cao YR, He XJ, *et al.* 2007*a*. Ethylene receptor signaling and plant salt-stress responses. In *Advances in Plant Ethylene Research*. Springer, Dordrecht, 333-339.

Cao WH, Liu J, He XJ, Mu RL, Zhou HL, Chen SY, Zhang JS. 2007*b*. Modulation of ethylene responses affects plant salt-stress responses. *Plant Physiology* **143**, 707-719.

Caseys C. 2018. *Shy Girl* gives kiwifruit male flowers. *The Plant Cell* **30**, 739-740.

Cebrián G, Iglesias-Moya J, Romero J, Martínez C, Garrido D, Jamilena M. 2022. The ethylene biosynthesis gene *CpACO1A*: a new player in the regulation of sex determination and female flower development in *Cucurbita pepo*. *Frontiers in Plant Science* **12**, 3399.

Chandler JW. 2011. The hormonal regulation of flower development. *Journal of Plant Growth Regulation* **30**, 242-254.

Chang C, Kwok SF, Bleecker AB, Meyerowitz EM. 1993. Arabidopsis ethylene-response gene *ETR1*: similarity of product to two-component regulators. *Science* **262**, 539-544.

Chao Q, Rothenberg M, Solano R, Roman G, Terzaghi W, Ecker JR. 1997. Activation of the ethylene gas response pathway in Arabidopsis by the nuclear protein ETHYLENE-INSENSITIVE3 and related proteins. *Cell* **89**, 1133-1144.

Chauvin A, Caldelari D, Wolfender JL, Farmer EE. 2013. Four 13-lipoxygenases contribute to rapid jasmonate synthesis in wounded *Arabidopsis thaliana* leaves: a role for lipoxygenase 6 in responses to long-distance wound signals. *New Phytologist* **197**, 566-575.

Chen D, Ma X, Li C, Zhang W, Xia G, Wang M. 2014. A wheat aminocyclopropane-1-carboxylate oxidase gene, *TaACO1*, negatively regulates salinity stress in *Arabidopsis thaliana*. *Plant Cell Reports* **33**, 1815-1827.

Chen H, Sun J, Li S, Cui Q, Zhang H, *et al*. 2016. An ACC oxidase gene essential for cucumber carpel development. *Molecular Plant* **9**, 1315-1327.

Chen K, Li GJ, Bressan RA, Song CP, Zhu JK, Zhao Y. 2020. Abscisic acid dynamics, signaling, and functions in plants. *Journal of Integrative Plant Biology* **62**, 25-54.

Chen L, Hao L, Parry MAJ, Phillips AL, Hu YG. 2014. Progress in TILLING as a tool for functional genomics and improvement of crops. *Journal of Integrative Plant Biology* **56**, 425-443.

Chen R, Jiang H, Li L, Zhai Q, Qi L, *et al.* 2012. The Arabidopsis mediator subunit MED25 differentially regulates jasmonate and abscisic acid signaling through interacting with the MYC2 and ABI5 transcription factors. *The Plant Cell* **24**, 2898-2916.

Chen YF, Randlett MD, Findell JL, Schallert GE. 2002. Localization of the ethylene receptor ETR1 to the endoplasmic reticulum of Arabidopsis. T*he Journal of Biological Chemistry* **277**, 19861-19866.

Chen YH. 2012. *CsACO4*, an ACC oxidase gene regulating male differentiation in cucumber. *African Journal of Biotechnology* **11**, 13069-13074.

Chini A, Fonseca S, Fernández G, Adie B, Chico JM, *et al.* 2007. The JAZ family of repressors is the missing link in jasmonate signaling. *Nature* **448**, 666-671.

Chini A, Monte I, Zamarreño AM, Hamberg M, Lassueur S *et al.* 2018. An OPR3-independent pathway uses 4,5-didehydrojasmonate for jasmonate synthesis. *Nature Chemical Biology* **14**, 171-178.

Chiwocha SDS, Cutler AJ, Abrams SR, Ambrose SJ, Yang J, Ross ARS, Kermode AR. 2005. The *etr1-2* mutation in *Arabidopsis thaliana* affects the abscisic acid, auxin, cytokinin and gibberellin metabolic pathways during maintenance of seed dormancy, moist-chilling and germination. *The Plant Journal* **42**, 35-48.

Cho LH, Yoon J, An G. 2017. The control of flowering time by environmental factors. *The Plant Journal* **90**, 708-719.

Choi WG, Toyota M, Kim SH, Hilleary R, Gilroy S. 2014. Salt stress-induced Ca^{2+} waves are associated with rapid, long-distance root-to-shoot signaling in plants. *Proceedings of the National Academy of Sciences* **111**, 6497-6502.

Chomicki G, Schaefer H, Renner SS. 2020. Origin and domestication of Cucurbitaceae crops: insights from phylogenies, genomics and archaeology. *New Phytologist* **226**, 1240-1255.

Choudhary P, Pramitha L, Rana S, Verma S, Aggarwal PR, Muthamilarasan M. 2021. Hormonal crosstalk in regulating salinity stress tolerance in graminaceous crops. *Physiologia Plantarum* **173**, 1587-1596.

Chow PS, Landhäusser SM. 2004. A method for routine measurements of total sugar and starch content in woody plant tissues. T*ree Physiology* **24**, 1129-1136.

Dahmani-Mardas F, Troadec C, Boualem A, Lévêque S, Alsadon AA, *et al*. 2010. Engineering melon plants with improved fruit shelf life using the TILLING approach. *PLoS ONE* **5**, e15776

De Jong M, Wolters-Arts M, García-Martínez JL, Mariani C, Vriezen WH. 2011. The *Solanum lycopersicum* AUXIN RESPONSE FACTOR 7 (SlARF7) mediates cross-talk between auxin and gibberellin signaling during tomato fruit set and development. *Journal of Experimental Botany* **62**, 617.

Decker DS. 1988. Origin(s), evolution, and systematics of *Cucurbita pepo* (Cucurbitaceae). *Economic Botany* **42**, 4-15.

DeFalco TA, Bender KW, Snedden WA. 2010. Breaking the code: Ca^{2+} sensors in plant signaling. *Biochemical Journal* **425**, 27-40.

Delgado C, Mora-poblete F, Ahmar S, Chen JT, Figueroa CR. 2021. Jasmonates and plant salt stress: molecular players, physiological effects, and improving tolerance by using genome-associated tools. *International Journal of Molecular Sciences* **22**, 1-26.

Demidchik V, Maathuis FJM. 2007. Physiological roles of nonselective cation channels in plants: from salt stress to signaling and development. *New Phytologist* **175**, 387-404.

DePristo MA, Banks E, Poplin R, Garimella KV, Maguire JR, *et al.* 2011. A framework for variation discovery and genotyping using next-generation DNA sequencing data. *Nature Genetics* **43**, 491-501.

Diggle PK, Di Stilio VS, Gschwend AR, Golenberg EM, Moore RC, Russell JRW, Sinclair JP. 2011. Multiple developmental processes underlie sex differentiation in angiosperms. *Trends in Genetics* **27**, 368-376.

Ding H, Lai J, Wu Q, Zhang S, Chen L, *et al.* 2016. Jasmonate complements the function of Arabidopsis lipoxygenase3 in salinity stress response. *Plant Science* **244**, 1-7.

Ding J, Chen B, Xia X, Mao W, Shi K, Zhou Y, Yu J. 2013. Cytokinin-induced parthenocarpic fruit development in tomato is partly dependent on enhanced gibberellin and auxin biosynthesis. *PLoS ONE* **8**, 70080.

Dobritzsch S, Weyhe M, Schubert R, Dindas J, Hause G, Kopka J, Hause B. 2015. Dissection of jasmonate functions in tomato stamen development by transcriptome and metabolome analyses. *BMC Biology* **13**, 1-18.

Dong H, Zhen Z, Peng J, Chang L, Gong Q, Wang NN. 2011. Loss of *ACS7* confers abiotic stress tolerance by modulating ABA sensitivity and accumulation in Arabidopsis. *Journal of Experimental Botany* **62**, 4875-4887.

Dubois M, Van den Broeck L, Inzé D. 2018. The pivotal role of ethylene in plant growth. *Trends in Plant Science* **23**, 311-323

Edgar RC. 2004. MUSCLE: multiple sequence alignment with high accuracy and high throughput. *Nucleic Acids Research* **32**, 1792-1797.

Elhakem AH. 2020. Salicylic acid ameliorates salinity tolerance in maize by regulation of phytohormones and osmolytes. *Plant, Soil and Environment* **66**, 533-541.

Esteras C, Gómez P, Monforte AJ, Blanca J, Vicente-Dólera N, *et al.* 2012. High-throughput SNP genotyping in *Cucurbita pepo* for map construction and quantitative trait loci mapping. *BMC Genomics* **13**, 1-21.

Farmer EE, Goossens A. 2019. Jasmonates: what ALLENE OXIDE SYNTHASE does for plants. *Journal of Experimental Botany* **70**, 3373-3378.

Fernandez L, Chäib J, Martinez-Zapater JM, Thomas MR, Torregrosa L. 2013. Mis-expression of a *PISTILLATA*-like MADS box gene prevents fruit development in grapevine. *The Plant Journal* **73**, 918-928.

Fernández-Calvo P, Chini A, Fernández-Barbero G, Chico JM, Gimenez-Ibañez S, *et al.* 2011. The Arabidopsis bHLH transcription factors MYC3 and MYC4 are targets of JAZ repressors and act additively with MYC2 in the activation of jasmonate responses. *The Plant Cell* **23**, 701-715.

Ferrándiz C, Fourquin C, Prunet N, Scutt CP, Sundberg E, Trehin C, Vialette-Guiraud ACM. 2010. Carpel development. *Advances in Botanical Research* **55**, 1-73.

Feys BJF, Benedetti CE, Penfold CN, Turner JG. 1994. Arabidopsis mutants selected for resistance to the phytotoxin coronatine are male sterile, insensitive to methyl jasmonate, and resistant to a bacterial pathogen. *The Plant Cell* **6**, 751-759.

Fukuda A, Nakamura A, Hara N, Toki S, Tanaka Y. 2011. Molecular and functional analyses of rice NHX-type Na^+/H^+ antiporter genes. *Planta* **233**, 175-188.

Galun E. 1959. The role of auxins in the sex expression of the cucumber. *Physiologia Plantarum* **12**, 48-61.

Galun E. 1962. Study of the inheritance of sex expression in the cucumber. The interaction of major genes with modifying genetic and non-genetic factors. *Genetica* **32**, 134-163.

Gamble RL, Coonfield ML, Schaller GE. 1998. Histidine kinase activity of the ETR1 ethylene receptor from Arabidopsis. *Proceedings of the National Academy of Sciences* **95**, 7825-7829.

García A, Aguado E, Martínez C, Loska D, Beltrán S, *et al.* 2020*a*. The ethylene receptors *CpETR1A* and *CpETR2B* cooperate in the control of sex determination in *Cucurbita pepo*. *Journal of Experimental Botany* **71**, 154-167.

García A, Aguado E, Garrido D, Martínez C, Jamilena M. 2020*b*. Two androecious mutations reveal the crucial role of ethylene receptors in the initiation of female flower development in *Cucurbita pepo*. *The Plant Journal* **103**, 1548-1560.

García A. (2019). Identification and molecular characterization of ethylene-insensitive mutants in *Cucurbita pepo.*

García A, Aguado E, Parra G, Manzano S, Martínez C, *et al.* 2018. Phenomic and genomic characterization of a mutant platform in *Cucurbita pepo*. *Frontiers in Plant Science* **9**, 1049.

Garciadeblás B, Senn ME, Bañuelos MA, Rodríguez-Navarro A. 2003. Sodium transport and HKT transporters: the rice model. *The Plant Journal* **34**, 788-801.

Ghanem ME, Albacete A, Martínez-Andújar C, Acosta M, Romero-Aranda R, *et al*. 2008. Hormonal changes during salinity-induced leaf senescence in tomato (*Solanum lycopersicum* L.). *Journal of Experimental Botany* **59**, 3039-3050.

Gharbi E, Martínez JP, Benahmed H, Lepoint G, Vanpee B, Quinet M, Lutts S. 2017. Inhibition of ethylene synthesis reduces salt-tolerance in tomato wild relative species *Solanum chilense*. *Journal of Plant Physiology* **210**, 24-37.

Gharsallah C, Fakhfakh H, Grubb D, Gorsane F. 2016. Effect of salt stress on ion concentration, proline content, antioxidant enzyme activities and gene expression in tomato cultivars. *AoB PLANTS* **8**.

Girek Z, Prodanovic S, Zdravkovic J, Zivanovic T, Ugrinovic M, Zdravkovic M. 2013. The effect of growth regulators on sex expression in melon (*Cucumis melo* L.). *Crop Breeding and Applied Biotechnology* **13**, 165-171.

Gómez P, Jamilena M, Capel J, Zurita S, Angosto T, Lozano R. 1999. Stamenless, a tomato mutant with homeotic conversions in petals and stamens. *Planta* **209**, 172-179.

Grabov A. 2007. Plant KT/KUP/HAK potassium transporters: single family - multiple functions. *Annals of Botany* **99**, 1035-1041.

Grbić V, Bleecker AB. 1995. Ethylene regulates the timing of leaf senescence in Arabidopsis. *The Plant Journal* **8**, 595-602.

Gull A, Ahmad Lone A, Ul Islam Wani N. 2019. Biotic and abiotic stresses in plants. Abiotic and Biotic Stress in Plants. IntechOpen, 1-19

Guo J, Xu W, Hu Y, Huang J, Zhao Y, *et al.* 2020. Phylotranscriptomics in Cucurbitaceae reveal multiple whole-genome duplications and key morphological and molecular innovations. *Molecular Plant* **13**, 1117-1133.

Guzmán P, Ecker JR. 1990. Exploiting the triple response of Arabidopsis to identify ethylene-related mutants. *The Plant Cell* **2**, 513-523.

Han M, Wu W, Wu WH, Wang Y. 2016. Potassium transporter KUP7 is involved in K^+ acquisition and translocation in Arabidopsis root under K^+-limited conditions. *Molecular Plant* **9**, 437-446.

Harkey AF, Watkins JM, Olex AL, DiNapoli KT, Lewis DR, *et al.* 2018. Identification of transcriptional and receptor networks that control root responses to ethylene. *Plant Physiology* **176**, 2095-2118.

Harloff HJ, Lemcke S, Mittasch J, Frolov A, Wu JG, *et al.* 2012. A mutation screening platform for rapeseed (*Brassica napus* L.) and the detection of sinapine biosynthesis mutants. *Theoretical and Applied Genetics* **124**, 957-969.

Hatakeyama K, Ishiguro S, Okada K, Takasaki T, Hinata K. 2003. Antisense inhibition of a nuclear gene, *BrDAD1*, in Brassica causes male sterility that is restorable with jasmonic acid treatment. *Molecular Breeding* **11**: 325-336.

Hayat S, Hayat Q, Alyemeni MN, Wani AS, Pichtel J, Ahmad A. 2012. Role of proline under changing environments: a review. *Plant Signaling and Behavior* **7**, 1456.

Hazman M, Hause B, Eiche E, Nick P, Riemann M. 2015. Increased tolerance to salt stress in OPDA-deficient rice *ALLENE OXIDE CYCLASE* mutants is linked to an increased ROS-scavenging activity. *Journal of Experimental Botany* **66**, 3339-3352.

Heslop-Harrison J. 1957. The experimental modification of sex expression in flowering plants. *Biological Reviews* **32**, 38-90.

Hoppen C, Müller L, Hänsch S, Uzun B, Milić D, *et al*. 2019. Soluble and membrane-bound protein carrier mediate direct copper transport to the ethylene receptor family. *Scientific Reports* **9**, 1-11.

Horie T, Hauser F, Schroeder JI. 2009. HKT transporter-mediated salinity resistance mechanisms in Arabidopsis and monocot crop plants. *Trends in Plant Science* **14**, 660-668.

Horie T, Motoda J, Kubo M, Yang H, Yoda K, *et al.* 2005. Enhanced salt tolerance mediated by AtHKT1 transporter-induced Na^+ unloading from xylem vessels to xylem parenchyma cells. *The Plant Journal* **44**, 928-938.

Houben M, Van de Poel B. 2019. 1-aminocyclopropane-1-carboxylic acid oxidase (ACO): the enzyme that makes the plant hormone ethylene. *Frontiers in Plant Science* **10**, 695

Howe GA, Major IT, Koo AJ. 2018. Modularity in jasmonate signaling for multistress resilience. *Annual Review of Plant Biology* **69**, 387-415.

Hu B, Li D, Liu X, Qi J, Gao D, *et al.* 2017. Engineering non-transgenic gynoecious cucumber using an improved transformation protocol and optimized CRISPR/Cas9 system. *Molecular Plant* **10**, 1575-1578.

Hua J, Sakai H, Nourizadeh S, Chen QG, Bleecker AB, Ecker JR, Meyerowitz EM. 1998. *EIN4* and *ERS2* are members of the putative ethylene receptor gene family in Arabidopsis. *The Plant Cell* **10**, 1321-1332.

Huang H, Liu B, Liu L, Song S. 2017. Jasmonate action in plant growth and development. *Journal of Experimental Botany* **68**, 1349-1359.

Hussain S, Bai Z, Huang J, Cao X, Zhu L, *et al*. 2019. 1-Methylcyclopropene modulates physiological, biochemical, and antioxidant responses of rice to different salt stress levels. *Frontiers in Plant Science* **10,** 124

Hussain S, Zhong C, Bai Z, Cao X, Zhu L, *et al.* 2018. Effects of 1-methylcyclopropene on rice growth characteristics and superior and inferior spikelet development under salt stress. *Journal of Plant Growth Regulation* **37**, 1368-1384.

Iglesias MJ, Terrile MC, Bartoli CG, D'Ippólito S, Casalongué CA. 2010. Auxin signaling participates in the adaptative response against oxidative stress and salinity by interacting with redox metabolism in Arabidopsis. *Plant Molecular Biology* **74**, 215-222.

Ikram MMM, Esyanti RR, Dwivany FM. 2017. Gene expression analysis related to ethylene induced female flowers of cucumber (*Cucumis sativus* L.) at different photoperiod. *Journal of Plant Biotechnology* **44**, 229-234.

Inaba A, Liu X, Yokotani N, Yamane M, Lu WJ, Nakano R, Kubo Y. 2007. Differential feedback regulation of ethylene biosynthesis in pulp and peel tissues of banana fruit. *Journal of Experimental Botany* **58**, 1047-1057.

Isayenkov SV, Maathuis FJM. 2019. Plant salinity stress: many unanswered questions remain. *Frontiers in Plant Science* **10**, 80.

Ishiguro S, Kawai-Oda A, Ueda J, Nishida I, Okada K. 2001. The *DEFECTIVE IN ANTHER DEHISCENCE1* gene encodes a novel phospholipase A1 catalyzing the initial step of jasmonic acid biosynthesis, which synchronizes pollen maturation, anther dehiscence, and flower opening in Arabidopsis. *The Plant Cell* **13**, 2191-2209.

Jabbour F, Espinosa F, Dejonghe Q, Péchon TL. 2022. Development and evolution of unisexual flowers: a review. *Plants* **11**, 155.

Ji G, Zhang J, Gong G, Shi J, Zhang H, *et al*. 2015. Inheritance of sex forms in watermelon (*Citrullus lanatus*). *Scientia Horticulturae* **193**, 367-373.

Ji G, Zhang J, Zhang H, Sun H, Gong G, *et al.* 2016. Mutation in the gene encoding *1-aminocyclopropane-1-carboxylate synthase 4* (*CitACS4*) led to andromonoecy in watermelon. *Journal of Integrative Plant Biology* **58**, 762-765.

Jiang K, Moe-Lange J, Hennet L, Feldman LJ. 2016. Salt stress affects the redox status of Arabidopsis root meristems. *Frontiers in Plant Science* **7**, 81.

Jiang Z, Zhou X, Tao M, Yuan F, Liu L, *et al.* 2019. Plant cell-surface GIPC sphingolipids sense salt to trigger Ca^{2+} influx. *Nature* **572**, 341-346.

Jin J, Duan J, Shan C, Mei Z, Chen H, *et al.* 2020. Ethylene insensitive3-like2 (OsEIL2) confers stress sensitivity by regulating *OsBURP16*, the *β* subunit of polygalacturonase (PG1*β*-like) subfamily gene in rice. *Plant Science* **292**, 110353.

Joshi R, Sahoo KK, Tripathi AK, Kumar R, Gupta BK, Pareek A, Singla-Pareek SL. 2018. Knockdown of an inflorescence meristem-specific cytokinin oxidase - OsCKX2 in rice reduces yield penalty under salinity stress condition. *Plant, Cell & Environment* **41**, 936-946.

Ju C, Chang C. 2015. Mechanistic insights in ethylene perception and signal transduction. *Plant Physiology* **169**, 85-95.

Ju C, Chang C. 2012. Advances in ethylene signaling: protein complexes at the endoplasmic reticulum membrane. *AoB PLANTS* **2012,** pls031.

Ju C, Yoon GM, Shemansky JM, Lin DY, Ying ZI, *et al.* 2012. CTR1 phosphorylates the central regulator EIN2 to control ethylene hormone signaling from the ER membrane to the nucleus in Arabidopsis. *Proceedings of the National Academy of Sciences* **109**, 19486-19491.

Kahana A, Silberstein L, Kessler N, Goldstein RS, Perl-Treves R. 1999. Expression of ACC oxidase genes differs among sex genotypes and sex phases in cucumber. *Plant Molecular Biology* **41**, 517-528.

Kai W, Fu Y, Wang J, Liang B, Li Q, Leng P. 2019*a*. Functional analysis of *SlNCED1* in pistil development and fruit set in tomato (*Solanum lycopersicum* L.). *Scientific Reports* **9**, 1-13.

Kai W, Wang J, Liang B, Fu Y, Zheng Y, Zhang W, Li Q, Leng P. 2019*b*. PYL9 is involved in the regulation of ABA signaling during tomato fruit ripening. *Journal of Experimental Botany* **70**, 6305-6319.

Kamachi S, Sekimoto H, Kondo N, Sakai S. 1997. Cloning of a cDNA for a 1-aminocyclopropane-1-carboxylate synthase that is expressed during development of female flowers at the apices of *Cucumis sativus* L. *Plant and Cell Physiology* **38**, 1197-206.

Kates HR, Soltis PS, Soltis DE. 2017. Evolutionary and domestication history of *Cucurbita* (pumpkin and squash) species inferred from 44 nuclear loci. *Molecular Phylogenetics and Evolution* **111**, 98-109.

Kawai Y, Ono E, Mizutani M. 2014. Evolution and diversity of the 2-oxoglutarate-dependent dioxygenase superfamily in plants. *The Plant Journal* **78**, 328-343.

Kazan K. 2015. Diverse roles of jasmonates and ethylene in abiotic stress tolerance. *Trends in Plant Science* **20**, 219-229.

Keunen E, Peshev D, Vangronsveld J, Van Den Ende W, Cuypers A. 2013. Plant sugars are crucial players in the oxidative challenge during abiotic stress: extending the traditional concept. *Plant, Cell & Environment* **36**, 1242-1255.

Khan NA, Khan MIR, Ferrante A, Poor P. 2017. Ethylene: a key regulatory molecule in plants. *Frontiers in Plant Science* **8**, 1782.

Khedr AHA, Abbas MA, Abdel Wahid AA, Quick WP, Abogadallah GM. 2003. Proline induces the expression of salt-stress-responsive proteins and may improve the adaptation of *Pancratium maritimum* L. to salt-stress. *Journal of Experimental Botany* **54**, 2553-2562.

Kim IS, Okubo H, Fujieda K. 1992. Endogenous levels of IAA in relation to parthenocarpy in cucumber (*Cucumis sativus* L.). *Scientia Horticulturae* **52**, 1-8.

Knopf RR, Trebitsh T. 2006. The female-specific *Cs-ACS1G* gene of cucumber. A case of gene duplication and recombination between the non-sex-specific 1-aminocyclopropane-1-carboxylate synthase gene and a branched-chain amino acid transaminase gene. *Plant and Cell Physiology* **47**, 1217-1228.

Kobayashi NI, Yamaji N, Yamamoto H, Okubo K, Ueno H, *et al*. 2017. OsHKT1;5 mediates Na^+ exclusion in the vasculature to protect leaf blades and reproductive tissues from salt toxicity in rice. *The Plant Journal* **91**, 657-670.

Kombrink E. 2012. Chemical and genetic exploration of jasmonate biosynthesis and signaling paths. *Planta* **236**, 1351-1366.

Kubicki, B. 1969*a*. Investigations of sex determination in cucumber (*Cucumis sativus* L.), V. Genes controlling intensity of femaleness. *Genetica Polonica* **10**, 69-86.

Kubicki, B. 1969*b*. Investigations of sex determination in cucumber (*Cucumis sativus* L.). VII. Trimonoecism. *Genetica Polonica* **10**, 123-143.

Kubicki, B. 1969*c*. Investigations on sex determination in cucumbers (*Cucumis sativus* L.). VI. Androecism. *Genetica Polonica* **10**, 87-99.

Kumar S, Stecher G, Li M, Knyaz C, Tamura K. 2018. MEGA X: molecular evolutionary genetics analysis across computing platforms. *Molecular Biology and Evolution* **35**, 1547-1549.

Kurowska M, Daszkowska-Golec A, Gruszka D, Marzec M, Szurman M, Szarejko I, Maluszynski M. 2011. TILLING - a shortcut in functional genomics. *Journal of Applied Genetics* **52**, 371-390.

Lai YS, Shen D, Zhang W, Zhang X, Qiu Y, *et al.* 2018*a*. Temperature and photoperiod changes affect cucumber sex expression by different epigenetic regulations. *BMC Plant Biology* **18**, 1-13.

Lai YS, Zhang W, Zhang X, Shen D, Wang H, *et al.* 2018*b*. Integrative analysis of transcriptomic and methylomic data in photoperiod-dependent regulation of cucumber sex expression. *G3: Genes, Genomes, Genetics* **8**, 3981-3991.

Lai YS, Zhang X, Zhang W, Shen D, Wang H, *et al.* 2017. The association of changes in DNA methylation with temperature-dependent sex determination in cucumber. *Journal of Experimental Botany* **68**, 2899-2912.

Lee S, Kim SG, Park CM. 2010. Salicylic acid promotes seed germination under high salinity by modulating antioxidant activity in Arabidopsis. *New Phytologist* **188**, 626-637.

Lefebvre V, North H, Frey A, Sotta B, Seo M, *et al*. 2006. Functional analysis of Arabidopsis *NCED6* and *NCED9* genes indicates that ABA synthesized in the endosperm is involved in the induction of seed dormancy. *The Plant Journal* **45**, 309-319.

Lei G, Shen M, Li ZG, Zhang B, Duan K, *et al.* 2011. EIN2 regulates salt stress response and interacts with a MA3 domain-containing protein ECIP1 in Arabidopsis. *Plant, Cell & Environment* **34**, 1678-1692.

Leidi EO, Barragán V, Rubio L, El-Hamdaoui A, Ruiz MT, *et al.* 2010. The AtNHX1 exchanger mediates potassium compartmentation in vacuoles of transgenic tomato. *The Plant Journal* **61**, 495-506.

Leyser O. 2018. Auxin signaling. *Plant Physiology* **176**, 465-479.

Li C, Hao M, Wang W, Wang H, Chen F, *et al*. 2018. An efficient CRISPR/Cas9 platform for rapidly generating simultaneous mutagenesis of multiple gene homoeologs in allotetraploid oilseed rape.

Frontiers in Plant Science **9**, 442.

Li CH, Wang G, Zhao JL, Zhang LQ, Ai LF, *et al*. 2014. The receptor-like kinase SIT1 mediates salt sensitivity by activating MAPK3/6 and regulating ethylene homeostasis in rice. *The Plant Cell* **26**, 2538-2553.

Li D, Sheng Y, Niu H, Li Z. 2019. Gene Interactions regulating sex determination in cucurbits. *Frontiers in Plant Science* **10**, 1231.

Li H, Durbin R. 2009. Fast and accurate short read alignment with Burrows-Wheeler transform. *Bioinformatics* **25**, 1754-1760.

Li J, Li Y, Yin Z, Jiang J, Zhang M, *et al*. 2017. *OsASR5* enhances drought tolerance through a stomatal closure pathway associated with ABA and H_2O_2 signaling in rice. *Plant Biotechnology Journal* **15**, 183-196.

Li L, Zhao Y, McCaig BC, Wingerd BA, Wang J *et al.* 2004. The tomato homolog of CORONATINE-INSENSITIVE1 is required for the maternal control of seed maturation, jasmonate-signaled defense responses, and glandular trichome development. *The Plant Cell* **16**, 126-143.

Li M, Yu G, Cao C, Liu P. 2021. Metabolism, signaling, and transport of jasmonates. *Plant Communications* **2**, 100231.

Li S, Xu H, Ju Z, Cao D, Zhu H, *et al.* 2018. The RIN-MC fusion of MADs-box transcription factors has transcriptional activity and modulates expression of many ripening genes. *Plant Physiology* **176**, 891-909

Li SB, Xie ZZ, Hu CG, Zhang JZ. 2016. A review of auxin response factors (ARFs) in plants. *Frontiers in Plant Science* **7**, 47.

Li X, Chen R, Chu Y, Huang J, Jin L, Wang G, Huang J. 2018. Overexpression of *RCc3* improves root system architecture and enhances salt tolerance in rice. *Plant Physiology and Biochemistry* **130**, 566-576.

Li Y, Pearl SA, Jackson SA. 2015. Gene networks in plant biology: approaches in reconstruction and analysis. T*rends in Plant Science* **20**, 664-675.

Li Z, Han Y, Niu H, Wang Y, Jiang B, Weng Y. 2020. Gynoecy instability in cucumber (*Cucumis sativus* L.) is due to unequal crossover at the copy number variation-dependent *Femaleness* (*F*) locus. *Horticulture Research* **7**, 32.

Li Z, Peng J, Wen X, Guo H. 2013. *ETHYLENE-INSENSITIVE3* is a senescence-associated gene that accelerates age-dependent leaf senescence by directly repressing miR164 transcription in Arabidopsis. *The Plant Cell* **25**, 3311-3328.

Liu F, Jiang H, Ye S, Chen WP, Liang W, *et al.* 2010. The Arabidopsis P450 protein CYP82C2 modulates jasmonate-induced root growth inhibition, defense gene expression and indole glucosinolate biosynthesis. *Cell Research* **20**, 539-552.

Liu L, Zou Z, Qian K, Xia C, He Y, *et al.* 2017. Jasmonic acid deficiency leads to scattered floret opening time in cytoplasmic male sterile rice Zhenshan 97A. *Journal of Experimental Botany* **68**, 4613-4625.

Liu S, Zhang Y, Feng Q, Qin L, Pan C, Lamin-Samu AT, Lu G. 2018. Tomato AUXIN RESPONSE FACTOR 5 regulates fruit set and development via the mediation of auxin and gibberellin signaling. *Scientific Reports* **8**, 1-16.

Liu W, Li RJ, Han TT, Cai W, Fu ZW, Lu YT. 2015. Salt stress reduces root meristem size by nitric oxide-mediated modulation of auxin accumulation and signaling in Arabidopsis. *Plant Physiology* **168**, 343-356.

Livak KJ, Schmittgen TD. 2001. Analysis of relative gene expression data using real-time quantitative PCR and the $2^{-\Delta\Delta CT}$ method. *Methods* **25**, 402-408.

Lockhart J. 2013. Salt of the earth: ethylene promotes salt tolerance by enhancing Na/K homeostasis. *The Plant Cell* **25**, 3150.

Loenen WAM. 2018. S-adenosylmethionine metabolism and aging. In *Epigenetics of Aging and Longevity*, Academic Press, 59-93.

Long TA, Brady SM, Benfey PN. 2008. Systems approaches to identifying gene regulatory networks in plants. *Annual Review of Cell and Developmental Biology* **24**, 81-103.

Lu C, Chen MX, Liu R, Zhang L, Hou X, *et al.* 2019. Abscisic acid regulates auxin distribution to mediate maize lateral root development under salt stress. *Frontiers in Plant Science* **10**, 716.

Lunde C, Kimberlin A, Leiboff S, Koo AJ, Hake S. 2019. *Tasselseed5* overexpresses a wound-inducible enzyme, ZmCYP94B1, that affects jasmonate catabolism, sex determination, and plant architecture in maize. *Communications Biology* **2**, 1-11.

Luo Y, Pan BZ, Li L, Yang CX, Xu ZF. 2020. Developmental basis for flower sex determination and effects of cytokinin on sex determination in *Plukenetia volubilis* (Euphorbiaceae). *Plant Reproduction* **33**, 21.

Ma N, Hu C, Wan L, Hu Q, Xiong J, Zhang C. 2017. Strigolactones improve plant growth, photosynthesis, and alleviate oxidative stress under salinity in rapeseed (*Brassica napus* L.) by regulating gene expression. *Frontiers in Plant Science* **8**, 1671.

Mancinelli AL. 1990. Interaction between light quality and light quantity in the photoregulation of anthocyanin production. *Plant Physiology* **92**, 1191-1195.

Mandaokar A, Thines B, Shin B, Markus Lange B, Choi G, *et al.* 2006. Transcriptional regulators of stamen development in Arabidopsis identified by transcriptional profiling. *The Plant Journal* **46**, 984-1008.

Manishankar P, Wang N, Köster P, Alatar AA, Kudla J. 2018. Calcium signaling during salt stress and in the regulation of ion homeostasis. *Journal of Experimental Botany* **69**, 4215-4226.

Manzano S, Aguado E, Martínez C, Megías Z, García A, Jamilena M. 2016. The ethylene biosynthesis gene *CitACS4* regulates monoecy/andromonoecy in watermelon (*Citrullus lanatus*). *PLoS ONE* **11**, e0154362.

Manzano S, Martínez C, García JM, Megías Z, Jamilena M. 2014. Involvement of ethylene in sex expression and female flower development in watermelon (*Citrullus lanatus*). *Plant Physiology and Biochemistry* **85**, 96-104.

Manzano S, Martínez C, Gómez P, Garrido D, Jamilena M. 2010. Cloning and characterisation of two *CTR1*-like genes in *Cucurbita pepo*: regulation of their expression during male and female flower development. *Sexual Plant Reproduction* **23**, 301-313.

Manzano S, Martínez C, Megías Z, Garrido D, Jamilena M. 2013. Involvement of ethylene biosynthesis and signaling in the transition from male to female flowering in the monoecious *Cucurbita pepo*. *Journal of Plant Growth Regulation* **32**, 789-798.

Manzano S, Martínez C, Megías Z, Gómez P, Garrido D, Jamilena M. 2011. The role of ethylene and brassinosteroids in the control of sex expression and flower development in *Cucurbita pepo*. *Plant Growth Regulation* **65**, 213-221.

Martin A, Troadec C, Boualem A, Rajab M, Fernandez R, *et al.* 2009. A transposon-induced epigenetic change leads to sex determination in melon. *Nature* **461**, 1135-1138.

Martínez C, Jamilena M. 2021. To be a male or a female flower, a question of ethylene in cucurbits. *Current Opinion in Plant Biology* **59**, 101981.

Martínez C, Manzano S, Megías Z, Barrera A, Boualem A, *et al.* 2014. Molecular and functional characterization of *CpACS27A* gene reveals its involvement in monoecy instability and other associated traits in squash (*Cucurbita pepo* L.). *Planta* **239**, 1201-1215.

Martínez C, Manzano S, Megías Z, Garrido D, Picó B, Jamilena M. 2013. Involvement of ethylene biosynthesis and signaling in fruit set and early fruit development in zucchini squash (*Cucurbita pepo* L.). *BMC Plant Biology* **13**, 139.

Martínez-Fernández I, Sanchís S, Marini N, Balanzá V, Ballester P, *et al.* 2014. The effect of NGATHA altered activity on auxin signaling pathways within the Arabidopsis gynoecium. *Frontiers in Plant Science* **5**, 210**.**

Martínez-González C, Castellanos-Morales G, Barrera-Redondo J, Sánchez-De La Vega, G, Hernández-Rosales, H, *et al.* 2021. Recent and historical gene flow in cultivars, landraces, and a wild taxon of *Cucurbita pepo* in Mexico. *Frontiers in Ecology and Evolution* **9**, 307.

Maynard D, Chibani K, Schmidtpott S, Seidel T, Spross J, Viehhauser A, Dietz KJ. 2021. Biochemical characterization of 13-lipoxygenases of *Arabidopsis thaliana*. *International Journal of Molecular Sciences* **22**, 10237.

McConn M, Browse J. 1996. The critical requirement for linolenic acid is pollen development, not photosynthesis, in an Arabidopsis mutant. *The Plant Cell* **8**, 403-416.

Mian A, Oomen RJ, Isayenkov S, Sentenac H, Maathuis FJM, Véry AA. 2011. Over-expression of an Na^+- and K^+-permeable HKT transporter in barley improves salt tolerance. *The Plant Journal* **68**, 468-479.

Miao M, Yang X, Han X, Wang K. 2011. Sugar signaling is involved in the sex expression response of monoecious cucumber to low temperature. *Journal of Experimental Botany* **62**, 797-804.

Montero-Pau J, Blanca J, Bombarely A, Ziarsolo P, Esteras C, *et al.* 2018. *De novo* assembly of the zucchini genome reveals a whole-genome duplication associated with the origin of the *Cucurbita* genus. *Plant Biotechnology Journal* **16**, 1161-1171.

Montero-Pau J, Esteras C, Blanca J, Ziarsolo P, Cañizares J, Picó B. 2016. Genetics and genomics of *Cucurbita* spp. In *Genetics and Genomics of* Cucurbitaceae, Springer, Cham, 211-227.

Moussatche P, Klee HJ. 2004. Autophosphorylation activity of the Arabidopsis ethylene receptor multigene family. *Journal of Biological Chemistry* **279**, 48734-48741.

Muchate NS, Nikalje GC, Rajurkar NS, Suprasanna P, Nikam TD. 2016. Plant salt stress: adaptive responses, tolerance mechanism and bioengineering for salt tolerance. *Botanical Review* **82**, 371-406.

Muday GK, Rahman A, Binder BM. 2012. Auxin and ethylene: collaborators or competitors? *Trends in Plant Science* **17**, 181-195.

Müller M, Munné-Bosch S. 2011. Rapid and sensitive hormonal profiling of complex plant samples by liquid chromatography coupled to electrospray ionization tandem mass spectrometry. *Plant Methods* **7**, 1-11.

Müller M, Munné-Bosch S. 2015. Ethylene response factors: a key regulatory hub in hormone and stress signaling. *Plant Physiology* **169**, 32-41.

Munns R, Gilliham M. 2015. Salinity tolerance of crops - what is the cost? *New Phytologist* **208**, 668-673.

Munns R, Tester M. 2008. Mechanisms of salinity tolerance. *Annual Review of Plant Biology* **59**, 651-681.

Nahar K, Hasanuzzaman M, Fujita M. 2015. Roles of osmolytes in plant adaptation to drought and salinity. In *Osmolytes and plants acclimation to changing environment: emerging omics technologies*. Springer, New Delhi, 37-68.

Nakatsuka A, Murachi S, Okunishi H, Shiomi S, Nakano R, Kubo Y, Inaba A. 1998. Differential expression and internal feedback regulation of 1-aminocyclopropane-1-carboxylate synthase, 1-aminocyclopropane-1-carboxylate oxidase, and ethylene receptor genes in tomato fruit during development and ripening. *Plant Physiology* **118**, 1295-1305.

Nguyen HT, To HTM, Lebrun M, Bellafiore S, Champion A. 2019. Jasmonates—the master regulator of rice development, adaptation and defense. *Plants* **8**, 339.

Nishiyama R, Watanabe Y, Fujita Y, Le DT, Kojima M, *et al.* 2011. Analysis of cytokinin mutants and regulation of cytokinin metabolic genes reveals important regulatory roles of cytokinins in drought, salt and abscisic acid responses, and abscisic acid biosynthesis. *The Plant Cell* **23**, 2169-2183.

Niu M, Huang Y, Sun S, Sun J, Cao H, Shabala S, Bie Z. 2018. Root respiratory burst oxidase homologue-dependent H_2O_2 production confers salt tolerance on a grafted cucumber by controlling Na^+ exclusion and stomatal closure. J*ournal of Experimental Botany* **69**, 3465-3476.

Niwa T, Suzuki T, Takebayashi Y, Ishiguro R, Higashiyama T, Sakakibaraa H, Ishiguro S. 2018. Jasmonic acid facilitates flower opening and floral organ development through the upregulated expression of *SlMYB21* transcription factor in tomato. *Bioscience, Biotechnology and Biochemistry* **82**, 292-303.

Oh Y, Baldwin IT, Galis I. 2013. A jasmonate ZIM-domain protein NaJAZd regulates floral jasmonic acid levels and counteracts flower abscission in *Nicotiana attenuata* plants. *PLoS ONE* **8**, e57868.

Ohkama-Ohtsu N, Sasaki-Sekimoto Y, Oikawa A, Jikumaru Y, Shinoda S, *et al.* 2011. 12-oxo-phytodienoic acid–glutathione conjugate is transported into the vacuole in Arabidopsis. *Plant and Cell Physiology* **52**, 205-209.

Okabe Y, Ariizumi T, Ezura H. 2013. Updating the micro-tom TILLING platform. *Breeding Science* **63**, 42-48.

Okabe Y, Yamaoka T, Ariizumi T, Ushijima K, Kojima M, *et al.* 2019. Aberrant stamen development is associated with parthenocarpic fruit set through up-regulation of gibberellin biosynthesis in tomato. *Plant and Cell Physiology* **60**, 38-51.

Osakabe Y, Arinaga N, Umezawa T, Katsura S, Nagamachi K, *et al.* 2013. Osmotic stress responses and plant growth controlled by potassium transporters in Arabidopsis. *The Plant Cell* **25**, 609-624.

Owens KW, Peterson CE, Tolla GE. 1980. Induction of perfect flowers on gynoecious muskmelon by silver nitrate and aminoethoxyvinylglycine. *HortScience* **15**, 654-655

Pak H, Wang H, Kim Y, Song U, Tu M, Wu D, Jiang L. 2021. Creation of male-sterile lines that can be restored to fertility by exogenous methyl jasmonate for the establishment of a two-line system for the hybrid production of rice (*Oryza sativa* L.). *Plant Biotechnology Journal* **19**, 365-374.

Pan J, Wang G, Wen H, Du H, Lian H, *et al.* 2018. Differential gene expression caused by the f and m loci provides insight into ethylene-mediated female flower differentiation in cucumber. *Frontiers in Plant Science* **9**, 1091.

Pannell JR. 2017. Plant sex determination. *Current Biology* **27**, R191-R197.

Papadopoulou E, Grumet R. 2005. Brassinosteriod-induced femaleness in cucumber and relationship to ethylene production. *HortScience* **40**, 1763-1767.

Papadopoulou E, Little HA, Hammar SA, Grumet R. 2005. Effect of modified endogenous ethylene production on sex expression, bisexual flower development and fruit production in melon (*Cucumis melo* L.). *Sexual Plant Reproduction* **18**, 131-142.

Pardo JM. 2010. Biotechnology of water and salinity stress tolerance. *Current Opinion in Biotechnology* **21**, 185-196.

Paris HS. 2010. History of the cultivar-groups of *Cucurbita pepo*. *Horticultural Reviews* **25**, 71-170.

Paris HS. 2016*a*. Genetic resources of pumpkins and squash, *Cucurbita spp*. In *Genetics and genomics of Cucurbitaceae*. Springer, Cham, 111-154.

Paris HS. 2016*b*. Overview of the origins and history of the five major cucurbit crops: issues for ancient DNA analysis of archaeological specimens. *Vegetation History and Archaeobotany* **25**, 405-414.

Paris HS. 2018. Consumer-oriented exploitation and conservation of genetic resources of pumpkins and squash, *Cucurbita*. *Israel Journal of Plant Sciences* **65**, 202-221.

Paris HS, Lebeda A, Křistkova E, Andres TC, Nee MH. 2012. Parallel evolution under domestication and phenotypic differentiation of the cultivated subspecies of *Cucurbita pepo* (Cucurbitaceae). *Economic Botany* **66**, 71-90.

Park JH, Halitschke R, Kim HB, Baldwin IT, Feldmann KA, Feyereisen R. 2002. A knock-out mutation in allene oxide synthase results in male sterility and defective wound signal transduction in Arabidopsis due to a block in jasmonic acid biosynthesis. *The Plant Journal* **31**, 1-12.

Pattyn J, Vaughan-Hirsch J, Van de Poel B. 2021. The regulation of ethylene biosynthesis: a complex multilevel control circuitry. *New Phytologist* **229**, 770-782.

Pawełkowicz ME, Skarzyńska A, Pląder W, Przybecki Z. 2019. Genetic and molecular bases of cucumber (*Cucumis sativus* L.) sex determination. *Molecular Breeding* **39**, 1-27.

Pelaz S, Ditta GS, Baumann E, Wisman E, Yanofsky MF. 2000. B and C floral organ identity functions require *SEPALLATA MADS*-box genes. *Nature* **405**, 200-203.

Peng J, Li Z, Wen X, Li W, Shi H, *et al.* 2014. Salt-induced stabilization of EIN3/EIL1 confers salinity tolerance by deterring ROS accumulation in Arabidopsis. *PLoS Genetics* **10**, e1004664.

Peterson CE, Anhder LMD. 1960. Induction of staminate flowers on gynoecious cucumbers with gibberellin A3. *Science* **131**, 1673-1674.

Pi M, Hu S, Cheng L, Zhong R, Cai Z, *et al*. 2021. The MADS-box gene *FveSEP3* plays essential roles in flower organogenesis and fruit development in woodland strawberry. *Horticulture Research* **8**, 1-15.

Potuschak T, Lechner E, Parmentier Y, Yanagisawa S, Grava S, Koncz C, Genschik P. 2003. EIN3-dependent regulation of plant ethylene hormone signaling by two Arabidopsis F-box proteins: EBF1 and EBF2. *Cell* **115**, 679-689.

Qiao H, Chang KN, Yazaki J, Ecker JR. 2009. Interplay between ethylene, ETP1/ETP2 F-box proteins, and degradation of EIN2 triggers ethylene responses in Arabidopsis. *Genes and Development* **23**, 512-521.

Qiu D, Hu W, Zhou Y, Xiao J, Hu R, *et al.* 2021. TaASR1-D confers abiotic stress resistance by affecting ROS accumulation and ABA signaling in transgenic wheat. *Plant Biotechnology Journal* **19**, 1588-1601.

Qiu L, Xie F, Yu J, Wen CK. 2012. Arabidopsis RTE1 is essential to ethylene receptor ETR1 amino-terminal signaling independent of CTR1. *Plant Physiology* **159**, 1263-1276.

Qiu ZB, Guo JL, Zhu AJ, Zhang L, Zhang MM. 2014. Exogenous jasmonic acid can enhance tolerance of wheat seedlings to salt stress. *Ecotoxicology and Environmental Safety* **104**, 202-208.

Quinet M, Bataillel G, Dobrev PI, Capel C, Gómez P, *et al.* 2014. Transcriptional and hormonal regulation of petal and stamen development by *STAMENLESS,* the tomato (*Solanum lycopersicum* L.) orthologue to the B-class *APETALA3* gene. *Journal of Experimental Botany* **65**, 2243-2256.

Rahneshan Z, Nasibi F, Moghadam AA. 2018. Effects of salinity stress on some growth, physiological, biochemical parameters and nutrients in two pistachio (*Pistacia vera* L.) rootstocks. *Journal of Plant Interactions* **13**, 73-82.

Ranal MA, De Santana DG. 2006. How and why to measure the germination process? *Revista Brasileira de Botanica* **29**, 1-11.

Reeves PH, Ellis CM, Ploense SE, Wu MF, Yadav V, *et al.* 2012. A regulatory network for coordinated flower maturation. *PLoS Genetics* **8**, e1002506.

Reguera M, Bassil E, Tajima H, Wimmer M, Chanoca A, *et al.* 2015. Ph regulation by NHX-type antiporters is required for receptor-mediated protein trafficking to the vacuole in Arabidopsis. *The Plant Cell* **27**, 1200-1217.

Riemann M, Haga K, Shimizu T, Okada K, Ando S *et al.* 2013. Identification of rice allene oxide cyclase mutants and the function of jasmonate for defence against *Magnaporthe oryzae*. *The Plant Journal* **74**, 226-238.

Riyazuddin R, Verma R, Singh K, Nisha N, Keisham M, *et al.* 2020. Ethylene: a master regulator of salinity stress tolerance in plants. *Biomolecules* **10**, 1-22.

Rodríguez-Rosales MP, Gálvez FJ, Huertas R, Aranda MN, Baghour M, Cagnac O, Venema K. 2009. Plant NHX cation/proton antiporters. *Plant Signaling and Behavior* **4**, 265-276.

Romera FJ, Smith AP, Pérez-Vicente R. 2016. Ethylene's role in plant mineral nutrition. *Frontiers in Plant Science* **7**, 911.

Rudich J, Halevy AH, Kedar N. 1969. Increase in femaleness of three cucurbits by treatment with ethrel, an ethylene releasing compound. *Planta* **86**, 69-76.

Ruduś I, Sasiak M, Kępczyński J. 2013. Regulation of ethylene biosynthesis at the level of 1-aminocyclopropane-1-carboxylate oxidase (ACO) gene. *Acta Physiologiae Plantarum* **35**, 295-307.

Růžička K, Ljung K, Vanneste S, Podhorská R, Beeckman T, Friml J, Benková E. 2007. Ethylene regulates root growth through effects on auxin biosynthesis and transport-dependent auxin distribution. *The Plant Cell* **19**, 2197-2212.

Ryu H, Cho YG. 2015. Plant hormones in salt stress tolerance. *Journal of Plant Biology* **58**, 147-155.

Saito S, Fujii N, Miyazawa Y, Yamasaki S, Matsuura S, *et al.* 2007. Correlation between development of female flower buds and expression of the *CS-ACS2* gene in cucumber plants. *Journal of Experimental Botany* **58**, 2897-2907.

Sanders PM, Lee PY, Biesgen C, Boone JD, Beals TP, Weiler EW, Goldberg RB. 2000. The Arabidopsis *DELAYED DEHISCENCE1* gene encodes an enzyme in the jasmonic acid synthesis pathway. *The Plant Cell* **12**, 1041-1061.

Sanjur OI, Piperno DR, Andres TC, Wessel-Beaver L. 2002. Phylogenetic relationships among domesticated and wild species of *Cucurbita* (Cucurbitaceae) inferred from a mitochondrial gene: Implications for crop plant evolution and areas of origin. *Proceedings of the National Academy of Sciences* **99**, 535.

Schaller F, Zerbe P, Reinbothe S, Reinbothe C, Hofmann E, Pollmann S. 2008. The allene oxide cyclase family of *Arabidopsis thaliana* – localization and cyclization. T*he FEBS Journal* **275**, 2428-2441.

Scharein B, Groth G. 2011. Phosphorylation alters the interaction of the Arabidopsis phosphotransfer protein AHP1 with its sensor kinase ETR1. *PloS ONE* **6**, e24173.

Scharein B, Voet-van-Vormizeele J, Harter K, Groth G. 2008. Ethylene signaling: identification of a putative ETR1-AHP1 phosphorelay complex by fluorescence spectroscopy. *Analytical Biochemistry* **377**, 72-76.

Schilmiller AL, Koo AJK, Howe GA. 2007. Functional diversification of acyl-coenzyme A oxidases in jasmonic acid biosynthesis and action. *Plant Physiology* **143**, 812-824.

Schott-Verdugo S, Müller L, Classen E, Gohlke H, Groth G. 2019. Structural model of the ETR1 ethylene receptor transmembrane sensor domain. *Scientific Reports* **9**, 1-14.

Schubert R, Dobritzsch S, Gruber C, Hause G, Athmer B, *et al.* 2019*a*. Tomato MYB21 acts in ovules to mediate jasmonate-regulated fertility. *The Plant Cell* **31**, 1043-1062.

Schubert R, Grunewald S, Sivers L Von, Hause B. 2019*b*. Effects of jasmonate on ethylene function during the development of tomato stamens. *Plants* **8**, 277.

Sega GA. 1984. A review of the genetic effects of ethyl methanesulfonate. *Mutation Research/Reviews in Genetic Toxicology* **134**, 113-142.

Seifikalhor M, Aliniaeifard S, Shomali A, Azad N, Hassani B, Lastochkina O, Li T. 2019. Calcium signaling and salt tolerance are diversely entwined in plants. *Plant Signaling & Behavior* **14**, 1665455.

Shakeel SN, Gao Z, Amir M, Chen YF, Rai MI, Haq NU, Schaller GE. 2015. Ethylene regulates levels of ethylene receptor CTR1 signaling complexes in *Arabidopsis thaliana*. *Journal of Biological Chemistry* **290**, 12415-12424.

Shakeel SN, Wang X, Binder BM, Schaller GE. 2013. Mechanisms of signal transduction by ethylene: overlapping and non-overlapping signaling roles in a receptor family. *AoB PLANTS* **5**, plt010.

Sharma A, Kumar V, Sidhu GPS, Kumar R, Kohli SK, *et al.* 2019*a*. Abiotic stress management in plants: role of ethylene. *Molecular Plant Abiotic Stress*, 185-208.

Sharma A, Shahzad B, Kumar V, Kohli SK, Sidhu GPS, *et al.* 2019*b*. Phytohormones regulate accumulation of osmolytes under abiotic stress. *Biomolecules* **9**, 285.

Sheard LB, Tan X, Mao H, Withers J, Ben-Nissan G, *et al.* 2010. Jasmonate perception by inositol-phosphate-potentiated COI1-JAZ co-receptor. *Nature* **468**, 400-405.

Shifriss O, George WL. 1964. Sensitivity of female inbreds of *Cucumis sativus* to sex reversion by gibberellin. *Science* **143**, 1452-1453.

Shinozaki Y, Beauvoit BP, Takahara M, Hao S, Ezura K, *et al.* 2020. Fruit setting rewires central metabolism via gibberellin cascades. *Proceedings of the National Academy of Sciences* **117**, 23970-23981.

Shinozaki Y, Ezura H, Ariizumi T. 2018*a*. The role of ethylene in the regulation of ovary senescence and fruit set in tomato (*Solanum lycopersicum*). *Plant Signaling & Behavior* **13**.

Shinozaki Y, Nicolas P, Fernandez-Pozo N, Ma Q, Evanich DJ, *et al*. 2018*b*. High-resolution spatiotemporal transcriptome mapping of tomato fruit development and ripening. *Nature Communications* **9**, 1-13.

Shinozaki Y, Hao S, Kojima M, Sakakibara H, Ozeki-Lida Y, *et al.* 2015. Ethylene suppresses tomato (*Solanum lycopersicum*) fruit set through modification of gibberellin metabolism. *The Plant Journal* **83**, 237-251.

Shiomi S, Yamamoto M, Ono T, Kakiuchi K, Nakamoto J, *et al.* 1998. cDNA cloning of ACC synthase and ACC oxidase genes in cucumber fruit and their differential expression by wounding and auxin. *Journal of the Japanese Society for Horticultural Science* **67**, 685-692.

Sikora P, Chawade A, Larsson M, Olsson J, Olsson O. 2011. Mutagenesis as a tool in plant genetics, functional genomics, and breeding. *International Journal of Plant Genomics* **2011**, 314829.

Simon-Sarkadi L, Kocsy G, Várhegyi Á, Galiba G, De Ronde JA. 2006. Stress-induced changes in the free amino acid composition in transgenic soybean plants having increased proline content. *Biologia Plantarum* **50**, 793-796.

Slama I, Abdelly C, Bouchereau A, Flowers T, Savouré A. 2015. Diversity, distribution and roles of osmoprotective compounds accumulated in halophytes under abiotic stress. *Annals of Botany* **115**, 433-447.

Smith BD. 1997. The initial domestication of *Cucurbita pepo* in the Americas 10,000 years ago. *Science* **276**, 932-934.

Smith BD. 2006. Eastern North America as an independent center of plant domestication. *Proceedings of the National Academy of Sciences* **103**, 12223-12228.

Stadler R, Truernit E, Gahrtz M, Sauer N. 1999. The AtSUC1 sucrose carrier may represent the osmotic driving force for anther dehiscence and pollen tube growth in Arabidopsis. *The Plant Journal* **19**, 269-278.

Staswick PE, Tiryaki I. 2004. The oxylipin signal jasmonic acid is activated by an enzyme that conjugates it to isoleucine in Arabidopsis. *The Plant Cell* **16**, 2117-2127.

Stenzel I, Otto M, Delker C, Kirmse N, Schmidt D, *et al.* 2012. *ALLENE OXIDE CYCLASE* (*AOC*) gene family members of *Arabidopsis thaliana*: tissue- and organ-specific promoter activities and in vivo heteromerization. *Journal of Experimental Botany* **63**, 6125-6138.

Stepanova AN, Yun J, Likhacheva AV, Alonso JM. 2007. Multilevel interactions between ethylene and auxin in Arabidopsis roots. *The Plant Cell* **19**, 2169.

Stintzi A, Browse J. 2000. The Arabidopsis male-sterile mutant, *opr3*, lacks the 12-oxophytodienoic acid reductase required for jasmonate synthesis. *Proceedings of the National Academy of Sciences* **97**, 10625-10630.

Stitz M, Hartl M, Baldwin IT, Gaquerel E. 2014. Jasmonoyl-L-isoleucine coordinates metabolic networks required for anthesis and floral attractant emission in wild tobacco (*Nicotiana attenuata*). *The Plant Cell* **26**, 3964-3983.

Sun H, Wu S, Zhang G, Jiao C, Guo S, *et al.* 2017. Karyotype stability and unbiased fractionation in the paleo-allotetraploid *Cucurbita* genomes. *Molecular Plant* **10**, 1293-1306.

Swarup R, Perry P, Hagenbeek D, Van Der Straeten D, Beemster GTS, *et al*. 2007. Ethylene upregulates auxin biosynthesis in Arabidopsis seedlings to enhance inhibition of root cell elongation. *The Plant Cell* **19**, 2186-2196.

Tadele Z. 2016. Mutagenesis and TILLING to dissect gene function in plants. *Current Genomics* **17**, 499-508.

Tai TH. 2013. Generation of rice mutants by chemical mutagenesis. *Methods in Molecular Biology* **956**, 29-37.

Takahashi H, Suge H. 1980. Sex expression in cucumber plants as affected by mechanical stress. *Plant and Cell Physiology* **21**, 303-310

Tanveer M, Shahzad B, Sharma A, Biju S, Bhardwaj R. 2018. 24-Epibrassinolide; an active brassinolide and its role in salt stress tolerance in plants: a review. *Plant Physiology and*

Biochemistry **130**, 69-79.

Tao JJ, Chen HW, Ma B, Zhang WK, Chen SY, Zhang JS. 2015. The role of ethylene in plants under salinity stress. *Frontiers in Plant Science* **6**, 1059.

Tao Q, Niu H, Wang Z, Zhang W, Wang H, *et al.* 2018. Ethylene responsive factor ERF110 mediates ethylene-regulated transcription of a sex determination-related orthologous gene in two *Cucumis* species. *Journal of Experimental Botany* **69**, 2953-2965.

Tavladoraki P, Cona A, Federico R, Tempera G, Viceconte N, *et al.* 2011. Polyamine catabolism: target for antiproliferative therapies in animals and stress tolerance strategies in plants. *Amino Acids* **42**, 411-426.

Theodoulou FL, Job K, Slocombe SP, Footitt S, Holdsworth M, *et al*. 2005. Jasmonic acid levels are reduced in COMATOSE ATP-binding cassette transporter mutants. Implications for transport of jasmonate precursors into peroxisomes. *Plant Physiology* **137**, 835-840.

Thines B, Katsir L, Melotto M, Niu Y, Mandaokar A, *et al.* 2007. JAZ repressor proteins are targets of the SCFCOI1 complex during jasmonate signaling. *Nature* **448**, 661-665.

Tholen D, Voesenek LACJ, Poorter H. 2004. Ethylene insensitivity does not increase leaf area or relative growth rate in Arabidopsis, *Nicotiana tabacum*, and *Petunia x hybrida*. *Plant Physiology* **134**, 1803-1812.

Till BJ, Datta S, Jankowicz-Cieslak J. 2018. TILLING: The next generation. In *Advances in biochemical engineering/biotechnology*. Springer Science and Business Media, Deutschland GmbH, 139-160.

Till BJ, Reynolds SH, Weil C, Springer N, Burtner C, *et al*. 2004. Discovery of induced point mutations in maize genes by TILLING. *BMC Plant Biology* **4**, 1-8.

Trebitsh T, Rudich J, Riov J. 1987. Auxin, biosynthesis of ethylene and sex expression in cucumber (*Cucumis sativus*). *Plant Growth Regulation* **5**, 105-113.

Trebitsh T, Staub JE, O'Neill SD. 1997. Identification of a 1-aminocyclopropane-1-carboxylic acid synthase gene linked to the *Female* (*F*) locus that enhances female sex expression in cucumber. *Plant Physiology* **113**, 987-995.

Trivellini A, Ferrante A, Vernieri P, Serra G. 2011. Effects of abscisic acid on ethylene biosynthesis and perception in *Hibiscus rosa-sinensis* L. flower development. *Journal of Experimental Botany* **62**, 5437-5452.

Tsai WC, Lee PF, Chen HI, Hsiao YY, Wei WJ, *et al.* 2005. *PeMADS6*, a *GLOBOSA/PISTILLATA*-like gene in *Phalaenopsis equestris* involved in petaloid formation, and correlated with flower longevity and ovary development. *Plant and Cell Physiology* **46**, 1125-1139.

Upadhyay RK, Mattoo AK. 2018. Genome-wide identification of tomato (*Solanum lycopersicum* L.) lipoxygenases coupled with expression profiles during plant development and in response to methyl-jasmonate and wounding. *Journal of Plant Physiology* **231**, 318-328.

Urao T, Miyata S, Yamaguchi-Shinozaki K, Shinozaki K. 2000. Possible His to Asp phosphorelay signaling in an Arabidopsis two-component system. *FEBS Letters* **478**, 227-232.

Van den Broeck L, Gordon M, Inzé D, Williams C, Sozzani R. 2020. Gene regulatory network inference: connecting plant biology and mathematical modeling. *Frontiers in Genetics* **11**, 457.

Van Doorn WG, Kamdee C. 2014. Flower opening and closure: an update. *Journal of Experimental Botany* **65**, 5749-5757.

Van Zelm E, Zhang Y, Testerink C. 2020. Salt tolerance mechanisms of plants. *Annual Review of Plant Biology* **71**, 403-433.

Verma RK, Santosh Kumar VV, Yadav SK, Pushkar S, Rao MV, Chinnusamy V. 2019. Overexpression of ABA receptor *PYL10* gene confers drought and cold tolerance to indica rice. *Frontiers in Plant Science* **10**, 1488.

Verslues PE, Bray EA. 2006. Role of abscisic acid (ABA) and *Arabidopsis thaliana* ABA-insensitive loci in low water potential-induced ABA and proline accumulation. *Journal of Experimental Botany* **57**, 201-212.

Vicente-Dólera N, Troadec C, Moya M, Del Río-Celestino M, Pomares-Viciana T, *et al.* 2014. First TILLING platform in *Cucurbita pepo*: a new mutant resource for gene function and crop improvement. *PLoS ONE* **9**, e112743.

Virdi AS, Singh S, Singh P. 2015. Abiotic stress responses in plants: roles of calmodulin-regulated proteins. *Frontiers in Plant Science* **6**, 809.

Von Malek B, Van Der Graaff E, Schneitz K, Keller B. 2002. The Arabidopsis male-sterile mutant *dde2-2* is defective in the *ALLENE OXIDE SYNTHASE* gene encoding one of the key enzymes of the jasmonic acid biosynthesis pathway. *Planta* **216**, 187-192.

Vriezen WH, Feron R, Maretto F, Keijman J, Mariani C. 2008. Changes in tomato ovary transcriptome demonstrate complex hormonal regulation of fruit set. *New Phytologist* **177**, 60-76.

Wang C, Xin M, Zhou X, Liu C, Li S, *et al.* 2017. The novel ethylene-responsive factor CsERF025 affects the development of fruit bending in cucumber. *Plant Molecular Biology* **95**, 519-531.

Wang DH, Li F, Duan QH, Han T, Xu ZH, Bai SN. 2010. Ethylene perception is involved in female cucumber flower development. *The Plant Journal* **61**, 862-872.

Wang H, Li S, Li YA, Xu Y, Wang Y, *et al.* 2019. MED25 connects enhancer–promoter looping and MYC2-dependent activation of jasmonate signaling. *Nature Plants* **5**, 616-625.

Wang H, Schauer N, Usadel B, Frasse P, Zouine M, *et al.* 2009. Regulatory features underlying pollination-dependent and-independent tomato fruit set revealed by transcript and primary metabolite profiling. *The Plant Cell* **21**, 1428-1452.

Wang J, Qin H, Zhou S, Wei P, Zhang H, *et al.* 2020. The ubiquitin-binding protein OsDSK2a mediates seedling growth and salt responses by regulating gibberellin metabolism in rice. *The Plant Cell* **32**, 414-428.

Wang K, Li M, Hakonarson H. 2010. ANNOVAR: functional annotation of genetic variants from high-throughput sequencing data. *Nucleic Acids Research* **38**, e164.

Wang W, Esch JJ, Shiu SH, Agula H, Binder BM, *et al.* 2006. Identification of important regions for ethylene binding and signaling in the transmembrane domain of the ETR1 ethylene receptor of Arabidopsis. *The Plant Cell* **18**, 3429-3442.

Wang W, Hall AE, O'Malley R, Bleecker AB. 2003. Canonical histidine kinase activity of the transmitter domain of the ETR1 ethylene receptor from Arabidopsis is not required for signal transmission. *Proceedings of the National Academy of Sciences* **100**, 352-357.

Wang Y, Diao P, Kong L, Yu R, Zhang M, *et al.* 2020. Ethylene enhances seed germination and seedling growth under salinity by reducing oxidative stress and promoting chlorophyll content via ETR2 pathway. *Frontiers in Plant Science* **11**, 1066.

Wang Y, Wang T, Li K, Li X. 2008. Genetic analysis of involvement of ETR1 in plant response to salt and osmotic stress. *Plant Growth Regulation* **54**, 261-269.

Wang Z, Dai L, Jiang Z, Peng W, Zhang L, Wang G, Xie D. 2005. *GmCOI1*, a soybean F-box protein gene, shows ability to mediate jasmonate-regulated plant defense and fertility in Arabidopsis. *Molecular Plant-Microbe Interactions* **18**, 1285-1295.

Wasternack C, Feussner I. 2018. The oxylipin pathways: biochemistry and function. *Annual Review oPlant Biology* **69**, 363–386.

Wasternack C, Hause B. 2018. A bypass in jasmonate biosynthesis – the OPR3-independent formation. *Trends in Plant Science* **23**, 276-279.

Wasternack C, Song S. 2017. Jasmonates: biosynthesis, metabolism, and signaling by proteins activating and repressing transcription. *Journal of Experimental Botany* **68**, 1303-1321.

Wasternack C. 2007. Oxylipins: biosynthesis, signal transduction and action. *Annual Plant Reviews* **24**, 185-228.

Weeden NF. 1984. Isozyme studies indicate that the genus *Cucurbita* is an ancient tetraploid. *Report/Cucurbit Genetics Cooperative* **7**, 84-85.

Wei LJ, Deng XG, Zhu T, Zheng T, Li PX, *et al*. 2015. Ethylene is involved in brassinosteroids induced alternative respiratory pathway in cucumber (*Cucumis sativus* L.) seedlings response to abiotic stress. *Frontiers in Plant Science* **6**, 982.

Wilson RL, Bakshi A, Binder BM. 2014*a*. Loss of the ETR1 ethylene receptor reduces the inhibitory effect of far-red light and darkness on seed germination of *Arabidopsis thaliana*. *Frontiers in Plant Science* **5**, 433.

Wilson RL, Kim H, Bakshi A, Binder BM. 2014*b*. The ethylene receptors ETHYLENE RESPONSE1 and ETHYLENE RESPONSE2 have contrasting roles in seed germination of arabidopsis during salt stress. *Plant Physiology* **165**, 1353-1356.

Whitaker, TW, Davis GN. 1962. Cucurbits. Botany, cultivation, and utilization. *Interscience Publishers Inc*: New York, USA.

Wu MF, Sang Y, Bezhani S, Yamaguchi N, Han SK, *et al.* 2012. SWI2/SNF2 chromatin remodeling ATPases overcome polycomb repression and control floral organ identity with the LEAFY and SEPALLATA3 transcription factors. *Proceedings of the National Academy of Sciences* **109**, 3576-3581.

Xanthopoulou A, Montero-Pau J, Mellidou I, Kissoudis C, Blanca J, *et al.* 2019. Whole-genome resequencing of *Cucurbita pepo* morphotypes to discover genomic variants associated with morphology and horticulturally valuable traits. *Horticulture Research* **6**, 1-17.

Xiao Y, Chen Y, Charnikhova T, Mulder PPJ, Heijmans J, *et al.* 2014. OsJAR1 is required for JA-regulated floret opening and anther dehiscence in rice. *Plant Molecular Biology* **86**, 19-33.

Yamasaki S, Fujii N, Takahashi H. 2003. Characterization of ethylene effects on sex determination in cucumber plants. *Sexual Plant Reproduction* **16**, 103-111.

Yan J, Guan L, Sun Y, Zhu Y, Liu L, *et al.* 2015. Calcium and ZmCCaMK are involved in brassinosteroid-induced antioxidant defense in maize leaves. *Plant and Cell Physiology* **56**, 883-896.

Yan J, Li S, Gu M, Yao R, Li Y, *et al.* 2016. Endogenous bioactive jasmonate is composed of a set of (+)-7-iso-JA-amino acid conjugates. *Plant Physiology* **172**, 2154-2164.

Yan Y, Borrego E, Kolomiets MV. 2013. Jasmonate biosynthesis, perception and function in plant development and stress responses. *Lipid Metabolism. InTech*, 393-442.

Yan Y, Christensen S, Isakeit T, Engelberth J, Meeley R, *et al.* 2012. Disruption of OPR7 and OPR8 reveals the versatile functions of jasmonic acid in maize development and defense. *The Plant Cell* **24**, 1420-1436.

Yan Y, Huang PC, Borrego E, Kolomiets M. 2014. New perspectives into jasmonate roles in maize. *Plant Signaling and Behavior* **9**, 1-5.

Yang C, Lu X, Ma B, Chen SY, Zhang JS. 2015*a*. Ethylene signaling in rice and Arabidopsis: Conserved and diverged aspects. *Molecular Plant **8***, 495-505.

Yang C, Ma B, He SJ, Xiong Q, Duan KX, *et al.* 2015*b*. *MAOHUZI6/ETHYLENE INSENSITIVE3-LIKE1* and *ETHYLENE INSENSITIVE3-LIKE2* regulate ethylene response of roots and coleoptiles and negatively affect salt tolerance in rice. *Plant Physiology* **169**, 148-165.

Yang J, Duan G, Li C, Liu L, Han G, Zhang Y, Wang C. 2019. The crosstalks between jasmonic acid and other plant hormone signaling highlight the involvement of jasmonic acid as a core component in plant response to biotic and abiotic stresses. *Frontiers in Plant Science* **10**, 1349.

Yang L, Zu YG, Tang ZH. 2013. Ethylene improves Arabidopsis salt tolerance mainly via retaining K^+ in shoots and roots rather than decreasing tissue Na^+ content. *Environmental and Experimental Botany* **86**, 60-69.

Yang T, Zhang S, Hu Y, Wu F, Hu Q, *et al.* 2014. The role of a potassium transporter OsHAK5 in potassium acquisition and transport from roots to shoots in rice at low potassium supply levels. *Plant Physiology* **166**, 945-959.

Yang TH, Lenglet-Hilfiker A, Stolz S, Glauser G, Farmer EE. 2020. Jasmonate precursor biosynthetic enzymes LOX3 and LOX4 control wound-response growth restriction. *Plant Physiology* **184**, 1172-1180.

Yao JL, Xu J, Tomes S, Cui W, Luo Z, *et al.* 2018. Ectopic expression of the *PISTILLATA* homologous *MdPI* inhibits fruit tissue growth and changes fruit shape in apple. *Plant Direct* **2**, e00051.

Yau CP, Wang L, Yu M, Zee SY, Yip WK. 2004. Differential expression of three genes encoding an ethylene receptor in rice during development, and in response to indole-3-acetic acid and silver ions. *Journal of Experimental Botany* **55**, 547-556.

Yin T, Quinn JA. (1995). Tests of a mechanistic model of one hormone regulating both sexes in *Cucumis sativus* (Cucurbitaceae). *American Journal of Botany* **82**, 1537-1546.

You X, Zhu S, Zhang W, Zhang J, Wang C, *et al.* 2019. OsPEX5 regulates rice spikelet development through modulating jasmonic acid biosynthesis. *New Phytologist* **224**, 712-724.

Yu Z, Duan X, Luo L, Dai S, Ding Z, Xia G. 2020. How plant hormones mediate salt stress responses. *Trends in Plant Science* **25**, 1117-1130.

Yuan Z, Zhang D. 2015. Roles of jasmonate signaling in plant inflorescence and flower development. *Current Opinion in Plant Biology* **27**, 44-51.

Yue P, Lu Q, Liu Z, Lv T, Li X, *et al.* 2020. Auxin-activated MdARF5 induces the expression of ethylene biosynthetic genes to initiate apple fruit ripening. *New Phytologist* **226**, 1781-1795.

Zemlyanskaya EV, Omelyanchuk NA, Ubogoeva EV, Mironova VV. 2018. Deciphering auxin-ethylene crosstalk at a systems level. *International Journal of Molecular Sciences* **19**, 4060.

Zhang HX, Blumwald E. 2001. Transgenic salt-tolerant tomato plants accumulate salt in foliage but not in fruit. *Nature Biotechnology* **19**, 765-768.

Zhang J, Guo S, Ji G, Zhao H, Sun H, *et al.* 2020. A unique chromosome translocation disrupting *ClWIP1* leads to gynoecy in watermelon. *The Plant Journal* **101**, 265-277.

Zhang J, Shi J, Ji G, Zhang H, Gong G, *et al*. 2017. Modulation of sex expression in four forms of watermelon by gibberellin, ethephone and silver nitrate. *Horticultural Plant Journal* **3**, 91-100

Zhang LB, Simmons MP, Kocyan A, Renner SS. 2006. Phylogeny of the *Cucurbitales* based on DNA sequences of nine loci from three genomes: Implications for morphological and sexual system evolution. *Molecular Phylogenetics and Evolution* **39**, 305-322.

Zhang P, Zhang J, Chen M. 2017. Economic impacts of climate change on agriculture: the importance of additional climatic variables other than temperature and precipitation. *Journal of Environmental Economics and Management* **83**, 8-31.

Zhang S, Gu X, Shao J, Hu Z, Yang W, *et al*. 2021. Auxin metabolism is involved in fruit set and early fruit development in the parthenocarpic tomato “R35-P”. *Frontiers in Plant Science* **12**, 1611.

Zhang Y, Wang Y, Xing J, Wan J, Wang X, *et al.* 2020. Copalyl diphosphate synthase mutation improved salt tolerance in maize (*Zea mays.* L) via enhancing vacuolar Na^+ sequestration and maintaining ROS homeostasis. *Frontiers in Plant Science* **11**, 457.

Zhang Y, Zhang X, Liu B, Wang W, Liu X, *et al*. 2014. A GAMYB homologue CsGAMYB1 regulates sex expression of cucumber via an ethylene-independent pathway. *Journal of Experimental Botany* **65**, 3201-3213.

Zhang Y, Zhao G, Li Y, Mo N, Zhang J, Liang Y. 2017. Transcriptomic analysis implies that GA regulates sex expression via ethylene-dependent and ethylene-independent pathways in cucumber (*Cucumis sativus* L.). *Frontiers in Plant Science* **8**, 10.

Zhao L, Li X, Chen W, Xu Z, Chen M, Wang H, Yu D. 2022. The emerging role of jasmonate in the control of flowering time. *Journal of Experimental Botany* **73**, 11-21.

Zheng Y, Wu S, Bai Y, Sun H, Jiao C, *et al.* 2019. Cucurbit Genomics Database (CuGenDB): a central portal for comparative and functional genomics of cucurbit crops. *Nucleic Acids Research* **47**, D1128-D1136.

Zhou J, Li Z, Xiao G, Zhai M, Pan X, Huang R, Zhang H. 2020. CYP71D8L is a key regulator involved in growth and stress responses by mediating gibberellin homeostasis in rice. *Journal of Experimental Botany* **71**, 1160-1170.

Zhu T, Deng X, Zhou X, Zhu L, Zou L, *et al.* 2016. Ethylene and hydrogen peroxide are involved in brassinosteroid-induced salt tolerance in tomato. *Scientific Reports* **6**, 35392-35392.

Zhu X, Pan T, Zhang X, Fan L, Quintero FJ, *et al*. 2018. K^+ efflux antiporters 4, 5, and 6 mediate pH and K^+ homeostasis in endomembrane compartments. *Plant Physiology* **178**, 1657-1678.

Zuckerkandl E, Pauling L. 1965. Molecules as documents of evolutionary history. *Journal of Theoretical Biology* **8**, 357-366.

8. Supplementary material

8.1. Supplementary tables

3. Involvement of ethylene receptors in the salt tolerance response of *Cucurbita pepo*

Table S3.1. Primers and TaqMan probes used for genotyping *etr1a*, *etr1b* and *etr2b* mutations.

***etr1a* family**	**Sequence**	**Tm (ºC)**
Forward	GTTCAGTTTGGTGCTTTCAT	54.3
Reverse	ACAAGCATAAGCGCAGTC	53.8
Probe C	FAM — TAACCG**C**TGTGGTATCGTGTGC — BHQ1	64.2
Probe T	HEX— TAACCG**T**TGTGGTATCGTGTGC —BHQ1	64.2
***etr1b* family**		
Forward	GGTTCTTGTTCAGTTTGGTG	56.4
Reverse	ATAATATGTACAAGCATAAGGGCA	58.3
Probe C	FAM—TTTAA**C**CGCTGTGGTATCGTGTGCAA—BHQ1	66.2
Probe T	HEX—TTTAA**T**CGCTGTGGTATCGTGTGCAA—BHQ1	64.2
***etr2b* family**		
Forward	TAGCTTGGCTTGCCATCA	53.8
Reverse	TCTTGGAGTAACCAGGAAC	55.0
Probe C	FAM —AGCTGGGACT**C**CTCCAGAAG— BHQ1	62.5
Probe T	HEX—AGCTGGGACT**T**CTCCAGAAG—BHQ1	60.5

Table S3.2. List of primer sequences used for qRT-PCR analysis.

Genes	**Forward Primer**	**Reverse Primer**	**Transcript Name (CuGenDB)**
CpKUP6-1A	GCTCCCTTCCAAATCATCAA	CGTTCCGTAATGTTGCAATG	Cp4.1LG13g08840
CpKUP6-1B	TTCATCCGATCCGAGAAAAC	GATCGGCAAAGAACACGATT	Cp4.1LG01g23230
CpKUP6-2A	AAACGGGGAGGCTGTTTAGT	TGACCCCCAATAGCACTCTC	Cp4.1LG03g07680
CpKUP6-2B	CGAGTTCGAGAAGGACTTGG	ACATCCATTTGTGGGCTCTC	Cp4.1LG04g05290
CpKEA4-1A	TCAACCCACTCGGAGTCAC	AAATGGAAAGGGAAGGGAAA	Cp4.1LG18g03650
CpKEA4-1B	ATTGGACCCGGAGGTTTAAG	CCTCCTAGAACAGCCACTGC	Cp4.1LG04g10710
CpKEA4-2A	CCCCTACCGTCTCTCTTCCAC	AAGATGAAAATGCGGACAGG	Cp4.1LG11g00130
CpKEA4-2B	ATCGGCACCCTTATCTTGC	GCAGAATGCCACTGATGCTA	Cp4.1LG07g06210
CpHKT1A	CCTAAAACTCGCTCCGACTG	TTGGCACAAACCCACAACTA	Cp4.1LG18g06540
CpNHK1-3B	CACTCAACTGATCGGGAGGT	CAAATGAGAGCGTTGCAAAA	Cp4.1LG12g05410
CpCRCK2A	CCTCCTTTCCATAGCTTTGAAGT	CGGGTCGGGTGGACTATTAT	Cp4.1LG16g06470
CpCRCK2B	GCTCATGCTATCACCTATCTTCA	TAACTTGGGTCGAGACATGC	Cp4.1LG05g09620
CpNCED3A	CTTCGTGGGTCAAATCTGGT	GACACTGAAGGAGGCGAAAC	Cp4.1LG14g03280
CpNCED3B	CTGCTCCCTCCGTGTCTTC	ACAAGTGATGACCGGAAACC	Cp4.1LG01g00800
EF1α	CGTCAAGAAGAAATAAGCCA	CTACTACGAGAGAGAGAGCCG	

4. The ethylene biosynthesis gene *CpACO1A*: a new player in the regulation of sex determination and female flower development in *Cucurbita pepo*

Table S4.1. List of the *ACO* genes and proteins used in phylogenetic analysis.

Species	GeneID	Gene	Type	Protein (aa)
Cucurbita pepo	Cp4.1LG04g02610	*CpACO1A*	1	319
	Cp4.1LG05g15190	*CpACO1B*	1	311
	Cp4.1LG10g09730	*CpACO2A-1*	1	316
	Cp4.1LG00g09300	*CpACO2A-2*	1	334
	Cp4.1LG19g08030	*CpACO2B*	1	336
	Cp4.1LG02g03090	*CpACO5A*	3	311
	Cp4.1LG06g06110	*CpACO5B*	3	309
	Cp4.1LG07g10650	*CpACO5-Like*	2	299
Cucumis melo	MELO3C014437	*CmACO1*	1	318
	MELO3C007425	*CmACO3*	1	327
	MELO3C019735	-	1	314
	MELO3C010508	-	3	309
	MELO3C004619	-	2	300
Cucumis sativus	Csa6G160180	*CsACO1*	1	314
	Csa6G511860	*CsACO2*	1	320
	Csa6G421630	*CsACO3*	1	317
	Csa4G361270	*CsACO4*	3	309
	Csa2G000520	*CsACO5*	2	300
Arabidopsis thaliana	AT2G19590.1	*AtACO1*	2	308
	AT1G62380.1	*AtACO2*	1	320
	AT1G12010.1	*AtACO3*	1	320
	AT1G05010.1	*AtACO4*	1	323
	AT1G77330.1	*AtACO5*	3	307
Solanum lycopersicum	Solyc07g049530.2.1	*SlACO1*	1	315
	Solyc12g005940.1.1	*SlACO2*	1	316
	Solyc07g049550.2.1	*SlACO3*	1	316
	Solyc02g081190.2.1	*SlACO4*	1	320
	Solyc07g026650.2.1	*SlACO5*	2	301
	Solyc02g036350.2.1	*SlACO6*	1	319
	Solyc06g060070.2.1	*SlACO7*	3	314
Oryza sativa	LOC_Os09g27750.1	*OsACO2*	1	323
	LOC_Os02g53180.1	*OsACO3α*	1	345
	LOC_Os02g53180.2	*OsACO3β*	1	322
	LOC_Os02g53180.3	*OsACO3γ*	1	284
	LOC_Os06g37590.1	*OsACO6*	2	294
	LOC_Os01g39860.1	*OsACO7*	2	313
	LOC_Os11g08380.1	*OsACO4*	3	310
	LOC_Os05g05680.1	*OsACO5*	3	309

Table S4.2. Primers used for gene expression analysis by qPCR.

Gene	Primer	Sequence
CpACO1A	F	CATAGAGTGATGACTCAGACAAGC
	R	CCATTGGACCCAAATTAGCA
CpACO1B	F	CAGTTGCTGAAAGACGACCA
	R	TGGTCATATATTCCCCTGAGTTG
CpACS11A	F	CGTCGTCTTAAGGCCTTTG
	R	GGTGTACCTAATTTAACGCAAC
CpACS27A	F	CCAATACGGACGGTGAA
	R	GGAGAAGCTGAAGAAGGAAG
CpACO2B	F	GGAGGGAGAGGAAGATAAGG
	R	TGGGTTATTGGAAAATGGAG
CpWIP1B	F	TCCCTACTCCATGCTTCAC
	R	TCCTCCTCATTCACAACAAC
CpETR1A	F	AAAGGAGAGCTGCCTGAGAGTC
	R	CACGACGCTCTATAAGTTCCGA
CpEIN3A	F	TAGCAGCCAATTCAACCAGTTTAAGCC
	R	CGGTAAAGCATCGAATTGAGATCAGG
CpEf-1α	F	CGTCAAGAAGAAATAAGCCA
	R	CTACTACGAGAGAGAGAGCCG

Table S4.3. Inheritance of *aco1a* mutant in the backcrossing and selfing generations.

	Number of plants				
Generation	**WT**	***aco1a***	**Expected segregation**	**X_c^2**	**p-value**
BC_1	43	-	1:0	-	-
BC_1S_1	163	57	3:1	0.10	> 0.05
BC_2S_1	219	81	3:1	0.64	> 0.05

Table S4.4. Validation of the identified mutations by high-throughput genotyping of individual segregating plants.

Plant	Phenotype	Genotype	Andromonoecius Index (AI)									
1	WT	wt/wt	0	0	0	0	0	0	0	0	0	0
2	WT	wt/*aco1a*	0	0	0	0	0	0	0	0	0	0
3	*aco1a*	*aco1a/aco1a*	**1,5**	**0,5**	**0,5**	**0,5**	**2,5**	**2,8**	**2**	**1,8**	**2,8**	**3**
4	WT	wt/wt	0	0	0	0	0	0	0	0	0	0
5	WT	wt/*aco1a*	0	0	0	0	0	0	0	0	0	0
6	WT	wt/*aco1a*	0	0	0	0	0	0	0	0	0	0
7	WT	wt/wt	0	0	0	0	0	0	0	0	0	0
8	*aco1a*	*aco1a/aco1a*	**3**	**3**	**0,5**	**1**	**1**	**2**	**1**	**3**	**3**	**3**
9	WT	wt/*aco1a*	0	0	0	0	0	0	0	0	0	0
10	WT	wt/*aco1a*	0	0	0	0	0	0	0	0	0	0
11	WT	wt/wt	0	0	0	0	0	0	0	0	0	0
12	WT	wt/wt	0	0	0	0	0	0	0	0	0	0
13	WT	wt/*aco1a*	0	0	0	0	0	0	0	0	0	0
14	WT	wt/*aco1a*	0	0	0	0	0	0	0	0	0	0
15	WT	wt/wt	0	0	0	0	0	0	0	0	0	0
16	*aco1a*	*aco1a/aco1a*	**3**	**3**	**0,5**	**0,5**	**1**	**1,5**	**2,5**	**2**	**1,5**	**2,5**
17	WT	wt/*aco1a*	0	0	0	0	0	0	0	0	0	0
18	WT	wt/*aco1a*	0	0	0	0	0	0	0	0	0	0
19	WT	wt/*aco1a*	0	0	0	0	0	0	0	0	0	0
20	WT	wt/wt	0	0	0	0	0	0	0	0	0	0
21	WT	wt/wt	0	0	0	0	0	0	0	0	0	0
22	*aco1a*	*aco1a/aco1a*	**3**	**3**	**1**	**1,5**	**0,5**	**2,8**	**3**	**3**	**3**	**3**
23	WT	wt/*aco1a*	0	0	0	0	0	0	0	0	0	0
24	WT	wt/*aco1a*	0	0	0	0	0	0	0	0	0	0
25	WT	wt/wt	0	0	0	0	0	0	0	0	0	0
26	WT	wt/*aco1a*	0	0	0	0	0	0	0	0	0	0
27	WT	wt/wt	0	0	0	0	0	0	0	0	0	0
28	*aco1a*	*aco1a/aco1a*	**2**	**2**	**2,5**	**1**	**2,5**	**2**	**2,5**	**3**	**3**	**3**
29	*aco1a*	*aco1a/aco1a*	**0,5**	**1**	**1**	**1**	**1**	**2**	**3**	**1,8**	**2,5**	**2,3**
30	WT	wt/*aco1a*	0	0	0	0	0	0	0	0	0	0
31	WT	wt/wt	0	0	0	0	0	0	0	0	0	0
32	WT	wt/*aco1a*	0	0	0	0	0	0	0	0	0	0
33	*aco1a*	*aco1a/aco1a*	**0**	**1**	**1,5**	**2**	**1,5**	**1**	**2,5**	**1**	**2**	**3**
34	WT	wt/*aco1a*	0	0	0	0	0	0	0	0	0	0
35	WT	wt/*aco1a*	0	0	0	0	0	0	0	0	0	0
36	WT	wt/wt	0	0	0	0	0	0	0	0	0	0
37	*aco1a*	*aco1a/aco1a*	**1,5**	**1**	**1**	**1,5**	**2,5**	**1**	**3**	**3**	**3**	**3**
38	WT	wt/*aco1a*	0	0	0	0	0	0	0	0	0	0
39	*aco1a*	*aco1a/aco1a*	**0**	**1,5**	**0,5**	**1**	**1,5**	**0,5**	**1**	**2**	**2,5**	**2**
40	WT	wt/*aco1a*	0	0	0	0	0	0	0	0	0	0
41	WT	wt/wt	0	0	0	0	0	0	0	0	0	0
42	WT	wt/wt	0	0	0	0	0	0	0	0	0	0
43	WT	wt/*aco1a*	0	0	0	0	0	0	0	0	0	0
44	WT	wt/*aco1a*	0	0	0	0	0	0	0	0	0	0
45	WT	wt/*aco1a*	0	0	0	0	0	0	0	0	0	0
46	*aco1a*	*aco1a/aco1a*	**3**	**2**	**1**	**1**	**1**	**1,5**	**2**	**3**	**2,8**	**3**
47	WT	wt/*aco1a*	0	0	0	0	0	0	0	0	0	0
48	WT	wt/*aco1a*	0	0	0	0	0	0	0	0	0	0
49	*aco1a*	*aco1a/aco1a*	**0,5**	**0,5**	**2**	**0,5**	**0,5**	**1**	**1,5**	**1**	**0,5**	**1,5**
50	*aco1a*	*aco1a/aco1a*	**0,5**	**1**	**2**	**1**	**0,5**	**0,5**	**1**	**2,5**	**0,5**	**0,5**
51	WT	wt/*aco1a*	0	0	0	0	0	0	0	0	0	0
52	*aco1a*	*aco1a/aco1a*	**2,5**	**1,5**	**2**	**0,5**	**0,5**	**2,5**	**0,5**	**3**	**3**	**3**
53	WT	wt/*aco1a*	0	0	0	0	0	0	0	0	0	0
54	WT	wt/*aco1a*	0	0	0	0	0	0	0	0	0	0

55	*aco1a*	*aco1a/aco1a*	**2,5**	**2**	**1**	**0,5**	**1**	**1**	**1**	**1,5**	**1,5**	**2**
56	WT	wt/*aco1a*	0	0	0	0	0	0	0	0	0	0
57	*aco1a*	*aco1a/aco1a*	**3**	**1,5**	**1**	**1**	**0,5**	**0,5**	**0,5**	**3**	**3**	**3**
58	WT	wt/wt	0	0	0	0	0	0	0	0	0	0
59	WT	wt/*aco1a*	0	0	0	0	0	0	0	0	0	0
60	WT	wt/wt	0	0	0	0	0	0	0	0	0	0
61	*aco1a*	*aco1a/aco1a*	**2,5**	**0,5**	**0,5**	**0,5**	**0,5**	**2**	**1,5**	**2,5**	**1,5**	**2,8**
62	*aco1a*	*aco1a/aco1a*	**0**	**0,5**	**1**	**0,5**	**1**	**1**	**0,5**	**0,5**	**1**	**2,8**
63	*aco1a*	*aco1a/aco1a*	**0,5**	**3**	**2,5**	**1,5**	**1**	**3**	**3**	**3**	**2,8**	**3**
64	WT	wt/wt	0	0	0	0	0	0	0	0	0	0
65	WT	wt/*aco1a*	0	0	0	0	0	0	0	0	0	0
66	WT	wt/*aco1a*	0	0	0	0	0	0	0	0	0	0
67	*aco1a*	*aco1a/aco1a*	**2**	**1**	**0,5**	**0,5**	**0,5**	**3**	**2,8**	**3**	**3**	**2,8**
68	*aco1a*	*aco1a/aco1a*	**2,5**	**1**	**1**	**0,5**	**1,5**	**3**	**2,5**	**2,8**	**3**	**2,5**
69	*aco1a*	*aco1a/aco1a*	**1**	**1,5**	**1,5**	**1**	**1**	**0,5**	**1,5**	**1**	**2**	**2,5**
70	WT	wt/*aco1a*	0	0	0	0	0	0	0	0	0	0
71	*aco1a*	*aco1a/aco1a*	**0,5**	**2**	**0,5**	**1**	**0,5**	**0,5**	**0**	**1**	**0,5**	**2,5**
72	WT	wt/*aco1a*	0	0	0	0	0	0	0	0	0	0
73	WT	wt/*aco1a*	0	0	0	0	0	0	0	0	0	0
74	WT	wt/*aco1a*	0	0	0	0	0	0	0	0	0	0
75	WT	wt/wt	0	0	0	0	0	0	0	0	0	0
76	*aco1a*	*aco1a/aco1a*	**3**	**3**	**2,5**	**2,5**	**2**	**1,8**	**2,8**	**2,5**	**2,8**	**3**
77	WT	wt/wt	0	0	0	0	0	0	0	0	0	0
78	WT	wt/wt	0	0	0	0	0	0	0	0	0	0
79	WT	wt/*aco1a*	0	0	0	0	0	0	0	0	0	0
80	*aco1a*	*aco1a/aco1a*	**3**	**1**	**1**	**2,5**	**1,8**	**1,8**	**2**	**1,8**	**1,8**	**2,8**
81	WT	wt/*aco1a*	0	0	0	0	0	0	0	0	0	0
82	*aco1a*	*aco1a/aco1a*	**1,5**	**2**	**1**	**0,5**	**1**	**1**	**1,5**	**1,8**	**2,5**	**3**
83	WT	wt/wt	0	0	0	0	0	0	0	0	0	0
84	WT	wt/*aco1a*	0	0	0	0	0	0	0	0	0	0
85	*aco1a*	*aco1a/aco1a*	**1,5**	**1,5**	**2**	**2**	**2**	**3**	**3**	**3**	**3**	**2**
86	WT	wt/*aco1a*	0	0	0	0	0	0	0	0	0	0
87	*aco1a*	*aco1a/aco1a*	**2,5**	**0,5**	**1**	**1,5**	**1,5**	**0,5**	**3**	**2,8**	**1,5**	**3**
88	WT	wt/*aco1a*	0	0	0	0	0	0	0	0	0	0
89	WT	wt/wt	0	0	0	0	0	0	0	0	0	0
90	WT	wt/*aco1a*	0	0	0	0	0	0	0	0	0	0
91	WT	wt/wt	0	0	0	0	0	0	0	0	0	0
92	WT	wt/*aco1a*	0	0	0	0	0	0	0	0	0	0
93	WT	wt/*aco1a*	0	0	0	0	0	0	0	0	0	0
94	WT	wt/wt	0	0	0	0	0	0	0	0	0	0
95	*aco1a*	*aco1a/aco1a*	**1**	**1,5**	**1**	**2**	**1,5**	**3**	**2**	**1,5**	**1**	**3**
96	*aco1a*	*aco1a/aco1a*	**3**	**3**	**1**	**1**	**1,5**	**1**	**1**	**3**	**2,5**	**3**
97	WT	wt/*aco1a*	0	0	0	0	0	0	0	0	0	0
98	WT	wt/wt	0	0	0	0	0	0	0	0	0	0
99	WT	wt/wt	0	0	0	0	0	0	0	0	0	0
100	*aco1a*	*aco1a/aco1a*	**0,5**	**1**	**3**	**0,5**	**1,5**	**0,5**	**0,5**	**3**	**2,8**	**3**
101	WT	wt/*aco1a*	0	0	0	0	0	0	0	0	0	0
102	WT	wt/wt	0	0	0	0	0	0	0	0	0	0
103	WT	wt/*aco1a*	0	0	0	0	0	0	0	0	0	0
104	*aco1a*	*aco1a/aco1a*	**3**	**0,5**	**0,5**	**2,8**	**3**	**3**	**3**	**3**	**3**	**3**
105	WT	wt/*aco1a*	0	0	0	0	0	0	0	0	0	0
106	WT	wt/*aco1a*	0	0	0	0	0	0	0	0	0	0
107	*aco1a*	*aco1a/aco1a*	**0**	**1**	**0,5**	**0,8**	**0,8**	**3**	**3**	**1,8**	**3**	**3**
108	*aco1a*	*aco1a/aco1a*	**3**	**1,5**	**1**	**1,5**	**1,5**	**2,8**	**2,8**	**3**	**1,5**	**2**
109	WT	wt/*aco1a*	0	0	0	0	0	0	0	0	0	0
110	*aco1a*	*aco1a/aco1a*	**1**	**1**	**1,5**	**1,5**	**2,8**	Determinate				
111	WT	wt/*aco1a*	0	0	0	0	0	0	0	0	0	0
112	WT	wt/wt	0	0	0	0	0	0	0	0	0	0
113	WT	wt/wt	0	0	0	0	0	0	0	0	0	0
114	WT	wt/*aco1a*	0	0	0	0	0	0	0	0	0	0
115	*aco1a*	*aco1a/aco1a*	**2,5**	**1**	**1**	**0,5**	**0,5**	**0,5**	**3**	**3**	**2,8**	**3**

116	WT	wt/*aco1a*	0	0	0	0	0	0	0	0	0	0
117	WT	wt/*aco1a*	0	0	0	0	0	0	0	0	0	0
118	*aco1a*	*aco1a/aco1a*	**1,5**	**2**	**1**	**1**	**1**	**0,5**	**1**	**1,8**	**3**	**2,8**
119	WT	wt/*aco1a*	0	0	0	0	0	0	0	0	0	0
120	*aco1a*	*aco1a/aco1a*	**3**	**2**	**1**	**2,5**	**2**	**3**	**3**	**3**	**3**	**3**
121	WT	wt/wt	0	0	0	0	0	0	0	0	0	0
122	WT	wt/*aco1a*	0	0	0	0	0	0	0	0	0	0
123	WT	wt/wt	0	0	0	0	0	0	0	0	0	0
124	WT	wt/*aco1a*	0	0	0	0	0	0	0	0	0	0
125	WT	wt/wt	0	0	0	0	0	0	0	0	0	0
126	*aco1a*	*aco1a/aco1a*	**3**	**2,5**	**3**	**3**	**2,5**	**2,5**	**3**	**3**	**3**	**3**
127	WT	wt/*aco1a*	0	0	0	0	0	0	0	0	0	0
128	WT	wt/*aco1a*	0	0	0	0	0	0	0	0	0	0
129	WT	wt/*aco1a*	0	0	0	0	0	0	0	0	0	0
130	*aco1a*	*aco1a/aco1a*	**3**	**3**	**3**	**3**	**1**	**3**	**3**	**3**	**3**	**3**
131	*aco1a*	*aco1a/aco1a*	**2**	**2,5**	**2,5**	**1,5**	**1**	**2,5**	**2,8**	**3**	**0,5**	**2,5**
132	WT	wt/*aco1a*	0	0	0	0	0	0	0	0	0	0
133	WT	wt/wt	0	0	0	0	0	0	0	0	0	0
134	WT	wt/*aco1a*	0	0	0	0	0	0	0	0	0	0
135	*aco1a*	*aco1a/aco1a*	**3**	**3**	**2**	**3**	**3**	**2,8**	**3**	**3**	**3**	**3**
136	WT	wt/*aco1a*	0	0	0	0	0	0	0	0	0	0
137	WT	wt/wt	0	0	0	0	0	0	0	0	0	0
138	WT	wt/*aco1a*	0	0	0	0	0	0	0	0	0	0
139	WT	wt/*aco1a*	0	0	0	0	0	0	0	0	0	0
140	WT	wt/wt	0	0	0	0	0	0	0	0	0	0
141	WT	wt/wt	0	0	0	0	0	0	0	0	0	0
142	WT	wt/*aco1a*	0	0	0	0	0	0	0	0	0	0
143	WT	wt/*aco1a*	0	0	0	0	0	0	0	0	0	0
144	*aco1a*	*aco1a/aco1a*	**3**	**1**	**3**	**2**	**2,8**	**3**	**3**	**3**	**3**	**3**
145	*aco1a*	*aco1a/aco1a*	**2**	**1,5**	**1,5**	**3**	**3**	**3**	**3**	**1,5**	**2,8**	**3**
146	WT	wt/*aco1a*	0	0	0	0	0	0	0	0	0	0
147	WT	wt/*aco1a*	0	0	0	0	0	0	0	0	0	0
148	WT	wt/wt	0	0	0	0	0	Determinate				
149	WT	wt/*aco1a*	0	0	0	0	0	0	0	0	0	0
150	*aco1a*	*aco1a/aco1a*	**1**	**3**	**2,5**	**3**	**3**	**2,5**	**3**	**3**	**3**	**3**
151	WT	wt/*aco1a*	0	0	0	0	0	0	0	0	0	0
152	WT	wt/*aco1a*	0	0	0	0	0	0	0	0	0	0
153	WT	wt/wt	0	0	0	0	0	0	0	0	0	0
154	WT	wt/*aco1a*	0	0	0	Determinate						
155	WT	wt/*aco1a*	0	0	0	0	0	0	0	0	0	0
156	*aco1a*	*aco1a/aco1a*	**0**	**1**	**2,5**	**2**	**2,5**	**3**	**3**	**3**	**2,8**	**3**
157	WT	wt/*aco1a*	0	0	0	0	0	0	0	0	0	0
158	WT	wt/*aco1a*	0	0	0	0	0	0	0	0	0	0
159	*aco1a*	*aco1a/aco1a*	**0,5**	**2**	**1**	**0,5**	**2**	**2**	**0,8**	**3**	**3**	**3**
160	WT	wt/*aco1a*	0	0	0	0	0	0	0	0	0	0
161	*aco1a*	*aco1a/aco1a*	**2**	**2**	**1**	**0,5**	**1**	**3**	**3**	**3**	**2,8**	**2,8**
162	WT	wt/*aco1a*	0	0	0	0	0	0	0	0	0	0
163	WT	wt/*aco1a*	0	0	0	0	0	0	0	0	0	0
164	*aco1a*	*aco1a/aco1a*	**3**	**3**	**1**	**1,5**	**3**	**3**	**3**	**2,8**	**3**	**3**
165	*aco1a*	*aco1a/aco1a*	**2,5**	**1,5**	**2**	**1,5**	**1,5**	**3**	**3**	**3**	**3**	**3**
166	*aco1a*	*aco1a/aco1a*	**2,5**	**1**	**1**	**1,5**	**1,5**	**2,8**	**3**	**3**	**3**	**2,5**
167	WT	wt/wt	0	0	0	0	0	0	0	0	0	0
168	*aco1a*	*aco1a/aco1a*	**3**	**3**	**3**	**3**	**3**	**3**	**3**	**3**	**2,8**	**3**
169	WT	wt/*aco1a*	0	0	0	0	0	0	0	0	0	0
170	*aco1a*	*aco1a/aco1a*	**1**	**1,5**	**0,5**	**3**	**3**	**2**	**3**	**2,8**	**3**	**3**
171	*aco1a*	*aco1a/aco1a*	**2**	**0,5**	**0**	**2,8**	**1,8**	**1,5**	**1,5**	**2,8**	**3**	**3**
172	WT	wt/wt	0	0	0	0	0	0	0	0	0	0
173	WT	wt/*aco1a*	0	0	0	0	0	0	0	0	0	0
174	*aco1a*	*aco1a/aco1a*	**2,5**	**3**	**0,5**	**3**	**3**	**2**	**3**	**3**	**3**	**2,8**
175	WT	wt/*aco1a*	0	0	0	0	0	0	0	0	0	0
176	WT	wt/*aco1a*	0	0	0	0	0	0	0	0	0	0

177	*aco1a*	*aco1a/aco1a*	**1,5**	**1**	**1**	**2**	**3**	**3**	**2**	**2,5**	**2,5**	**3**
178	WT	wt/wt	0	0	0	0	0	0	0	0	0	0
179	*aco1a*	*aco1a/aco1a*	**3**	**3**	**2**	**3**	**3**	**3**	**2,5**	**3**	**1,5**	**2,8**
180	WT	wt/*aco1a*	0	0	0	0	0	0	0	0	0	0
181	WT	wt/*aco1a*	0	0,5	0	0	0	0	0	0	0	0
182	WT	wt/*aco1a*	0	0	0	0	0	0	0	0	0	0
183	*aco1a*	*aco1a/aco1a*	**2,5**	**0,5**	**2**	**1**	**2,5**	**2,5**	**3**	**3**	**3**	**3**
184	WT	wt/*aco1a*	0	0	0	0	0	0	0	0	0	0
185	WT	wt/*aco1a*	0	0	0	0	0	0	0	0	0	0
186	WT	wt/wt	0	0	0	0	0	0	0	0	0	0
187	WT	wt/*aco1a*	0	0	0	0	0	0	0	0	0	0
188	WT	wt/*aco1a*	0	0	0	0	0	0	0	0	0	0
189	WT	wt/wt	0	0	0	0	0	0	0	0	0	0
190	WT	wt/wt	0	0	0	0	0	0	0	0	0	0
191	WT	wt/wt	0	0	0	0	0	0	0	0	0	0
192	WT	wt/wt	0	0	0	0	0	0	0	0	0	0
193	WT	wt/wt	0	0	0	0	0	0	0	0	0	0
194	WT	wt/wt	0	0	0	0	0	0	0	0	0	0
195	WT	wt/*aco1a*	0	0	0	0	0	0	0	0	0	0
196	*aco1a*	*aco1a/aco1a*	**3**	**0,5**	**0,5**	**1**	**2**	**2,8**	**1**	**2,8**	**3**	**2,8**
197	*aco1a*	*aco1a/aco1a*	**0,5**	**1**	**0,5**	**3**	**0,5**	**2**	**2,5**	**3**	**2,8**	**3**
198	WT	wt/*aco1a*	0	0	0	0	0	0	0	0	0	0
199	WT	wt/*aco1a*	0	0	0	0	0	0	0	0	0	0
200	WT	wt/wt	0	0	0	0	0	0	0	0	0	0
201	WT	wt/wt	0	0	0	0	0	0	0	0	0	0
202	*aco1a*	*aco1a/aco1a*	**2**	**3**	**2,5**	**0,5**	**1**	**2,8**	**3**	**2,8**	**3**	**2,8**
203	WT	wt/*aco1a*	0	0	0	0	0	0	0	0	0	0
204	*aco1a*	*aco1a/aco1a*	**3**	**2,5**	**2**	**2,5**	**3**	**2,8**	**3**	**2,8**	**3**	**2**
205	WT	wt/wt	0	0	0	0	0	0	0	0	0	0
206	WT	wt/*aco1a*	0	0	0	0	0	0	0	0	0	0
207	WT	wt/*aco1a*	0	0	0	0	0	0	0	0	0	0
208	*aco1a*	*aco1a/aco1a*	**3**	**0,5**	**1**	**1**	**2,5**	**3**	**0,5**	**2,5**	**2,8**	**3**
209	*aco1a*	*aco1a/aco1a*	**3**	**0,5**	**0,5**	**0,5**	**0,5**	**3**	**1,8**	**1,5**	**1,8**	**1,8**
210	WT	wt/*aco1a*	0	0	0	0	0	0	0	0	0	0
211	WT	wt/wt	0	0	0	0	0	0	0	0	0	0
212	WT	wt/*aco1a*	0	0	0	0	0	0	0	0	0	0
213	WT	wt/wt	0	0	0	0	0	0	0	0	0	0
214	WT	wt/*aco1a*	0	0	0	0	0	0	0	0	0	0
215	*aco1a*	*aco1a/aco1a*	**2,5**	**3**	**0,5**	**1,5**	**3**	**2,5**	**2,8**	**3**	**3**	**2,8**
216	*aco1a*	*aco1a/aco1a*	**1,5**	**1**	**1**	**1**	**1,5**	**3**	**3**	**2,8**	**3**	**2,8**
217	*aco1a*	*aco1a/aco1a*	**3**	**2**	**3**	**3**	**3**	**3**	**3**	**3**	**3**	**3**
218	WT	wt/*aco1a*	0	0	0	0	0	0	0	0	0	0
219	WT	wt/*aco1a*	0	0	0	0	0	0	0	0	0	0
220	*aco1a*	*aco1a/aco1a*	3	3	3	3	3	3	3	3	3	3
221	WT	wt/*aco1a*	0	0	0	0	0	0	0	0	0	0
222	WT	wt/wt	0	0	0	0	0	0	0	0	0	0
223	WT	wt/*aco1a*	0	0	0	0	0	0	0	0	0	0
224	WT	wt/wt	0	0	0	0	0	0	0	0	0	0
225	WT	wt/*aco1a*	0	0	0	0	0	0	0	0	0	0
226	WT	wt/*aco1a*	0	0	0	0	0	0	0	0	0	0
227	*aco1a*	*aco1a/aco1a*	**3**	**1,5**	**2**	**2,5**	**1,5**	**3**	**1,8**	**2**	**0,3**	**2,8**
228	WT	wt/*aco1a*	0	0	0	0	0	0	0	0	0	0
229	WT	wt/wt	0	0	0	0	0	0	0	0	0	0
230	WT	wt/*aco1a*	0	0	0	0	0	0	0	0	0	0
231	WT	wt/*aco1a*	0	0	0	Determinate						
232	WT	wt/*aco1a*	0	0	0	0	0	0	0	0	0	0
233	WT	wt/wt	0	0	0	0	0	0	0	0	0	0
234	WT	wt/*aco1a*	0	0	0	0	0	0	0	0	0	0
235	*aco1a*	*aco1a/aco1a*	**0**	**1**	**0,5**	**0,8**	**0,8**	**3**	**3**	**1,8**	**3**	**3**
236	*aco1a*	*aco1a/aco1a*	**0,5**	**1**	**1**	**1**	**1**	**2**	**3**	**1,8**	**2,5**	**2,3**
237	WT	wt/*aco1a*	0	0	0	0	0	0	0	0	0	0

238	WT	wt/wt	0	0	0	0	0	0	0	0	0	0
239	WT	wt/*aco1a*	0	0	0	0	0	0	0	0	0	0
240	WT	wt/*aco1a*	0	0	0	0	0	0	0	0	0	0
241	WT	wt/*aco1a*	0	0	0	0	0	0	0	0	0	0
242	WT	wt/wt	0	0	0	0	0	0	0	0	0	0
243	WT	wt/wt	0	0	0	0	0	0	0	0	0	0
244	*aco1a*	*aco1a/aco1a*	**3**	**2**	**1**	**2,5**	**2**	**3**	**3**	**3**	**3**	**3**
245	WT	wt/wt	0	0	0	0	0	0	0	0	0	0
246	WT	wt/*aco1a*	0	0	0	0	0	0	0	0	0	0
247	WT	wt/*aco1a*	0	0	0	0	0	0	0	0	0	0
248	WT	wt/*aco1a*	0	0	0	0	0	0	0	0	0	0
249	WT	wt/*aco1a*	0	0	0	0	0	0	0	0	0	0
250	*aco1a*	*aco1a/aco1a*	**3**	**1**	**1**	**2,5**	**1,8**	**1,8**	**2**	**1,8**	**1,8**	**2,8**
251	WT	wt/*aco1a*	0	0	0	0	0	0	0	0	0	0
252	WT	wt/*aco1a*	0	0	0	0	0	0	0	0	0	0
253	WT	wt/wt	0	0	0	0	0	0	0	0	0	0
254	WT	wt/wt	0	0	0	0	0	0	0	0	0	0
255	WT	wt/wt	0	0	0	0	0	0	0	0	0	0
256	WT	wt/*aco1a*	0	0	0	0	0	0	0	0	0	0
257	WT	wt/*aco1a*	0	0	0	0	0	0	0	0	0	0
258	WT	wt/*aco1a*	0	0	0	0	0	0	0	0	0	0
259	*aco1a*	*aco1a/aco1a*	**2**	**3**	**2,5**	**0,5**	**1**	**2,8**	**3**	**2,8**	**3**	**2,8**
260	*aco1a*	*aco1a/aco1a*	**3**	**3**	**0,5**	**1**	**1**	**2**	**1**	**3**	**3**	**3**
261	WT	wt/wt	0	0	0	0	0	0	0	0	0	0
262	WT	wt/wt	0	0	0	0	0	0	0	0	0	0
263	WT	wt/*aco1a*	0	0	0	0	0	0	0	0	0	0
264	WT	wt/*aco1a*	0	0	0	0	0	0	0	0	0	0
265	WT	wt/*aco1a*	0	0	0	0	0	0	0	0	0	0
266	WT	wt/wt	0	0	0	0	0	0	0	0	0	0
267	WT	wt/*aco1a*	0	0	0	0	0	0	0	0	0	0
268	WT	wt/*aco1a*	0	0	0	0	0	0	0	0	0	0
269	*aco1a*	*aco1a/aco1a*	**2,5**	**3**	**1,5**	**2**	**2,5**	**3**	**1,5**	**1**	**2,8**	**3**
270	WT	wt/*aco1a*	0	0	0	0	0	0	0	0	0	0
271	WT	wt/*aco1a*	0	0	0	0	0	0	0	0	0	0
272	*aco1a*	*aco1a/aco1a*	**1,5**	**2**	**1**	**2,5**	**3**	**1,5**	**2,8**	**3**	**3**	**2**
273	*aco1a*	*aco1a/aco1a*	**3**	**2,5**	**2,5**	**2**	**1**	**1**	**1,5**	**2**	**2,5**	**1,8**
274	*aco1a*	*aco1a/aco1a*	**3**	**3**	**1**	**2**	**1,5**	**1**	**3**	**2,8**	**3**	**2,8**
275	WT	wt/*aco1a*	0	0	0	0	0	0	0	0	0	0
276	WT	wt/*aco1a*	0	0	0	0	0	0	0	0	0	0
277	WT	wt/wt	0	0	0	0	0	0	0	0	0	0
278	WT	wt/*aco1a*	0	0	0	0	0	0	0	0	0	0
279	WT	wt/wt	0	0	0	0	0	0	0	0	0	0
280	WT	wt/*aco1a*	0	0	0	0	0	0	0	0	0	0
281	WT	wt/*aco1a*	0	0	0	0	0	0	0	0	0	0
282	WT	wt/wt	0	0	0	0	0	0	0	0	0	0
283	WT	wt/wt	0	0	0	0	0	0	0	0	0	0
284	WT	wt/*aco1a*	0	0	0	0	0	0	0	0	0	0
285	WT	wt/*aco1a*	0	0	0	0	0	0	0	0	0	0
286	WT	wt/wt	0	0	0	0	0	0	0	0	0	0
287	WT	wt/*aco1a*	0	0	0	0	0	0	0	0	0	0
288	WT	wt/*aco1a*	0	0	0	0	0	0	0	0	0	0
289	*aco1a*	*aco1a/aco1a*	**1,5**	**3**	**3**	**2,8**	**3**	**3**	**3**	**3**	**3**	**3**
290	*aco1a*	*aco1a/aco1a*	**3**	**3**	**3**	**3**	**3**	**3**	**2,5**	**2,8**	**3**	**3**
291	WT	wt/*aco1a*	0	0	0	0	0	0	0	0	0	0
292	WT	wt/wt	0	0	0	0	0	0	0	0	0	0
293	WT	wt/*aco1a*	0	0	0	0	0	0	0	0	0	0
294	*aco1a*	*aco1a/aco1a*	**1**	**0,5**	**2,5**	**1,5**	**3**	**3**	**3**	**3**	**3**	**2**
295	*aco1a*	*aco1a/aco1a*	**0**	**0**	**0,5**	**1**	**1**	**0,5**	**0,5**	**3**	**3**	**3**
296	WT	wt/*aco1a*	0	0	0	0	0	0	0	0	0	0
297	WT	wt/*aco1a*	0	0	0	0	0	0	0	0	0	0
298	WT	wt/wt	0	0	0	0	0	0	0	0	0	0

299	WT	wt/wt	0	0	0	0	0	0	0	0	0	0
300	WT	wt/wt	0	0	0	0	0	0	0	0	0	0

Table S4.5. EMS mutations in chromosome 4 of *aco1a* mutant line.

Chr	Position	Ref	Alt	Gene ID	Impact	Functional Annotation
4	3,982,041	G	A	Cp4.1LG04g07570	Intron	ATP-dependent Clp protease proteolytic subunit
4	5,341,391	C	T	Cp4.1LG04g06230	3´UTR	Shikimate kinase
4	7,603,991	C	T	Intergenic	intergenic	between Cp4.1LG04g02740 and Cp4.1LG04g02810
4	7,715,975	C	T	Cp4.1LG04g02610	Exon, P5L	1-aminocyclopropane-1-carboxylate oxidase 1 (ACO1)

The SNPs were genotyped in a BC_2S_1 population segregating for the *aco1a* phenotype. Only the mutation C > T in *Cp4.1LG04g02610* co-segregated with the mutant phenotype in a total of 300 plant analysed.

5. Jasmonate-deficient mutant *lox3a* reveals crosstalk between JA and ET in the differential regulation of male and female flower opening and early fruit development in *Cucurbita pepo*

Table S5.1. Inheritance of *lox3a* mutant in the backcrossing and selfing generations.

	Number of plants				
Generation	**WT**	***lox3a***	**Expected segregation**	**X_c^2**	**p-value**
BC_1	50	-	1:0	-	-
BC_1S_1	168	53	3:1	0.12	> 0.05
BC_2S_1	220	80	3:1	0.44	> 0.05

Table S5.2. List of the *LOX* genes and proteins used in phylogenetic analysis.

Species	Gene ID	Gene	Type	Protein (aa)
Cucurbita pepo	Cp4.1LG16g09120	*CpLOX2A*	13	898
	Cp4.1LG05g05220	*CpLOX2B*	13	901
	Cp4.1LG12g09270	*CpLOX3A*	13	912
	Cp4.1LG17g04130	*CpLOX3B*	13	922
	Cp4.1LG17g05900	*CpLOX5*	9	835
	Cp4.1LG01g16060	*CpLOX6*	13	925
Arabidopsis thaliana	AT1G55020	*AtLOX1*	9	859
	AT3G45140	*AtLOX2*	13	896
	AT1G17420	*AtLOX3*	13	919
	AT1G72520	*AtLOX4*	13	926
	AT3G22400	*AtLOX5*	9	886
	AT1G67560	*AtLOX6*	13	917
Solanum lycopersicum	Solyc08g014000	*SlLOX1*	9	860
	Solyc01g099190	*SlLOX2*	9	859
	Solyc01g006540	*SlLOX3*	13	896
	Solyc03g122340	*SlLOX4*	13	908
	Solyc01g099160	*SlLOX5*	9	862
	Solyc09g075860	*SlLOX6*	9	877
	Solyc01g099200	*SlLOX7*	9	841
	Solyc08g029000	*SlLOX8*	9	861
	Solyc01g099180	*SlLOX9*	9	854
	Solyc12g011040	*SlLOX10*	13	892
	Solyc05g014790	*SlLOX11*	13	911
	Solyc01g099210	*SlLOX12*	9	863
	Solyc01g006560	*SlLOX13*	13	902
	Solyc09g075870	*SlLOX14*	9	854
Oryza sativa	Os03g0699700	*OsLOX1*	9	863
	Os03g0738600	*OsLOX2*	9	870
	Os03g0700400	*OsLOX3*	9	866
	Os03g0700700	*OsLOX3B*	9	877
	Os04g0447100	*OsLOX5*	13	899
	Os03g0179900	*OsLOX6*	13	918
	Os08g0508800	*OsLOX7*	13	924
	Os08g0509100	*OsLOX8*	13	941
	RCI-1	*OsLOXRCI1*	13	922
Zea mays	ZEAMMB73_Zm00001d033623	*ZmLOX1*	9	864
	ZEAMMB73_Zm00001d042541	*ZmLOX2*	9	873
Nicotiana tabacum	LOC107806322	*NtLOX1*	9	862

Table S5.3. Primers used for gene expression analysis by qPCR.

Gene	Primer	Sequence
CpLOX6	F	TAGAAGGGGTATGGCTGTGG
	R	GTTTAGGCCACCAAGGTTCA
CpLOX2A	F	GTCAGAGCAGAGGGGTGAAG
	R	TCGTCCGCTTAATGCTTCTT
CpLOX3A	F	AACGCGCACAATCTTCTTCT
	R	AGCTGCCATATCCAATTGCT
CpAOS1A	F	CGGAGTCTCCTCCTCCTCTT
	R	CACAACTCGAGAATCGTTGG
CpJAR1B	F	ACTCTCAGTCTGCTACCGGC
	R	TGATAAACAAGCGGGACACA
CpCOI1B	F	GTTGAGACAAGTTGTGGTGTCC
	R	GGAGAGATTATCGTTGTCGATG
CpJAZ1B	F	CCATACCAAATGAACCAGCAG
	R	GGGGATAGATATGAAAAACCACG
CpMYB21B	F	ACTCAGCCGAAGGTGTGGT
	R	ATGTTGCCTCGTCGAACATT
CpACO1A	F	CATAGAGTGATGACTCAGACAAGC
	R	CCATTGGACCCAAATTAGCA
CpETR1A	F	AAAGGAGAGCTGCCTGAGAGTC
	R	CACGACGCTCTATAAGTTCCGA
CpEIN3A	F	TAGCAGCCAATTCAACCAGTTTAAGCC
	R	CGGTAAAGCATCGAATTGAGATCAGG
CpEf-1α	F	CGTCAAGAAGAAATAAGCCA
	R	CTACTACGAGAGAGAGAGCCG

8.2. Supplementary figures

3. Involvement of ethylene receptors in the salt tolerance response of *Cucurbita pepo*

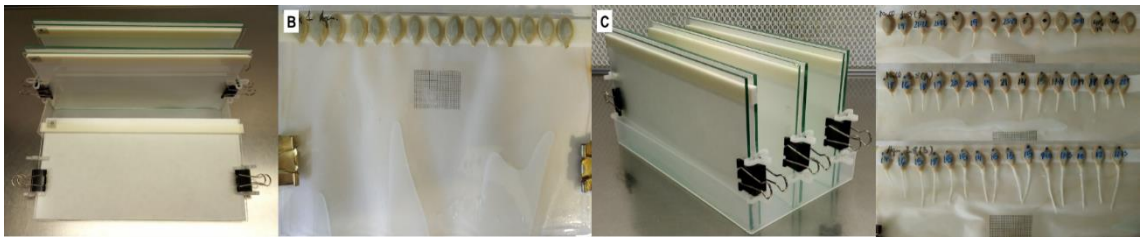

Figure S3.1. (**A**) Device designed to study *C. pepo* seed germination between two sandwich glasses. (**B**) Seeds were put in a foam strip placed between two pieces of filter papers and two panes of glass of 12 x 20 cm and secured with two paperclips. (**C**) The device is situated vertically in a recipient with treatment solutions for seeds to germinate and grow vertically and placed in an environmentally controlled growth chamber. (**D**) Germinated seeds at different times.

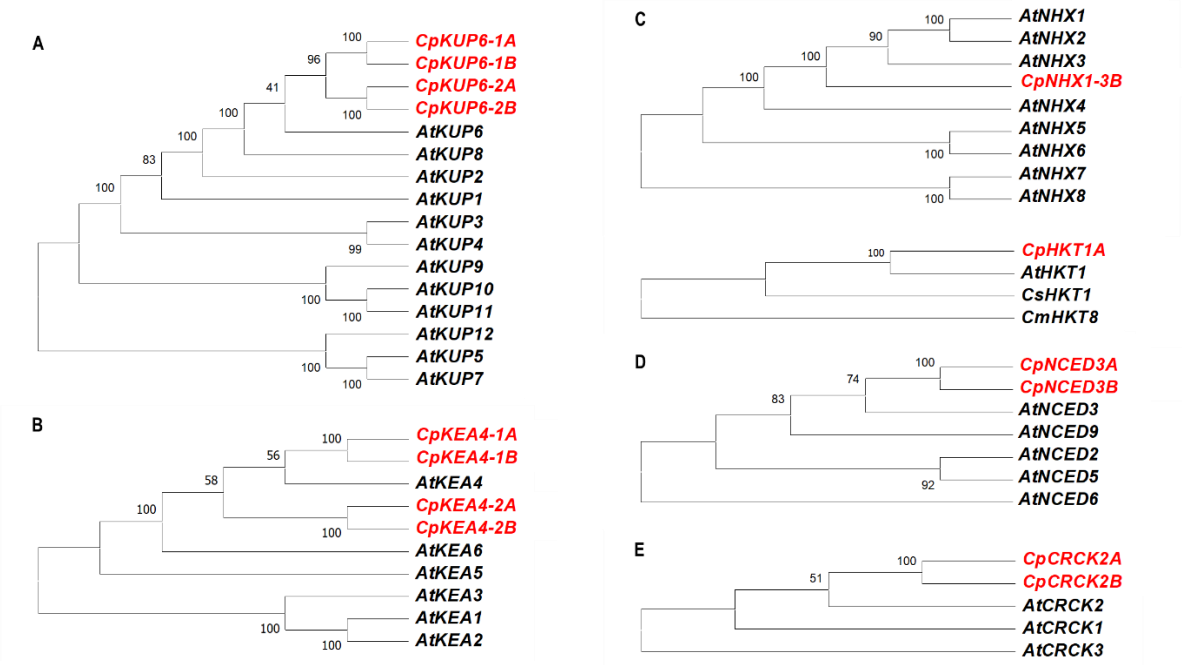

Figure S3.2. Phylogenetic relationships for different gene families in *Cucurbita pepo* and *Arabidopsis*. (**A**) Potassium transporters (*KUPs*). (**B**) K^+/H^+ antiporters (*KEAs*). (**C**) Na^+ transporter (*HKTs*) and Na^+/H^+ exchangers (*NHXs*). In this case, *Cucumis sativus* and *Cucumis melo HKT* genes were also included. (**D**) 9-cis-epoxycarotenoid dioxygenase (*NCEDs*). (**E**) Calmodulin-binding receptor-like cytoplasmic kinase (*CRCKs*).

5. Jasmonate-deficient mutant *lox3a* reveals crosstalk between JA and ET in the differential regulation of male and female flower opening and early fruit development in *Cucurbita pepo*

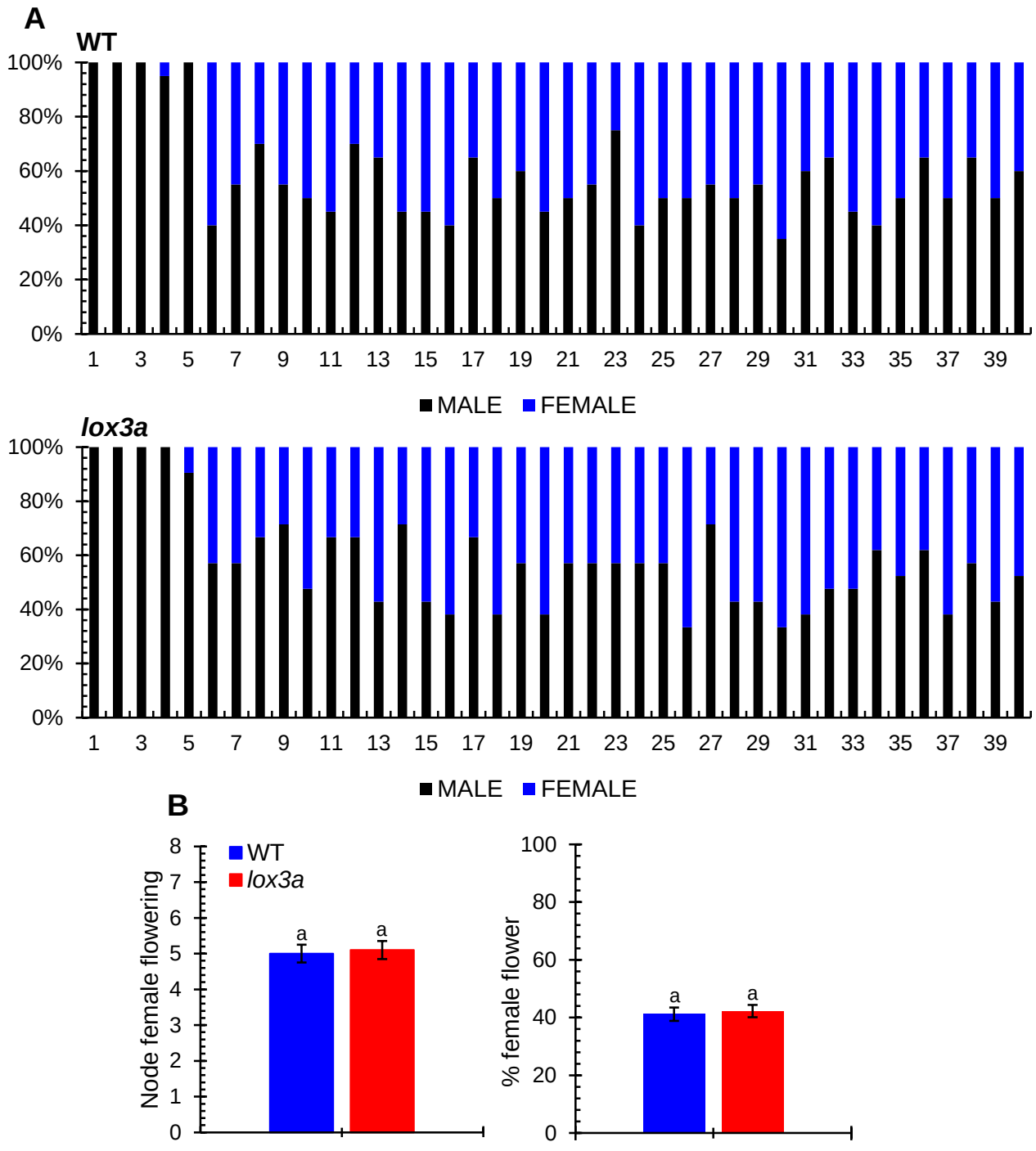

Figure S5.1. (**A**) Distribution of male and female flowers on the first 40 nodes of the main shoot of WT and *lox3a* plants. Each column represent one plant node, indicating the percentage of plants having female or male flowers in that specific node. A minimum of 10 plants was used for each genotype. (**B**) Female flowering transition and percentage of female flowers per plant in WT and *lox3a* plants. Different letters indicate significant differences between WT and *lox3a* at the same stage of development ($p \leq 0.05$).

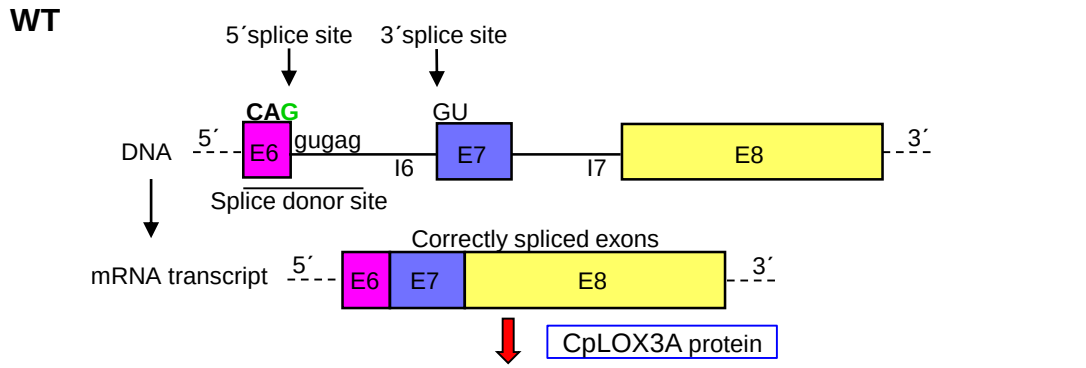

Met K L W D H L F F T K H L W F L S P S C F K E A I L R S S S G H F G G Y L E K Q F R P F R V V P Met E K K R I V Met N
L R K A V N G P V A A I S K D L V K A V P L A E K P V K F K V R A V V T I R N K N K E D I K E T I V K N L D A F T D R I G Q
N V V L Q L I S T E I D P K T N T P K K S N E A V L K D W S K K T N L K V E K V N Y I A E F L L T S D F G E P G A I T I T N
K H Q Q E F F L E T I T I E Q L A S D P I H F P C N S W V Q S R K D H P A K R I F F S N K S Y L P G E T P A G I K A L R E
Q E L K D I R G D G K G E R K L S D R V Y D F D V Y N D L G N P D K G I E F S R P R L G G E K I P Y P R R C R T G R A P
S D T D I T A E S R V E K P L P Met Y V P R D E Q F E E S K Q T T F S L G R L K A V L Y N L I P S L K A S I L S N K H D F
H G F S D I D S L Y S K G V L L K L G L Q D K L L K K L P L P R V V S E S S Q G L L R Y N T P K I L S K D K F A W L R D D
E F G R Q A I A G V N P V N I E R L K V F P P V S N L D P D V Y G P Q E S A L K E E H I L G Q L N G Met T V Q Q A L D E
K K L F I V D Y H D V Y L P F I D R I N A L D G R K T Y A T R T I F F L T P L G T L K P I A I E L S L P S T A P S S R S K R V
V T P P V E A T S N W I W Q L A K A H V C S N D A G V H Q L V N H W L R T H A S L E P F I L A A H R Q L S A Met H P I F
K L L D P H Met R Y T Met E I N A L A R Q S L V N G E G V I E S C F T P G R Y C Met E I S A A A Y K N F W R F D Met E G
L P A D L I R R G Met A E P D P T K P H G L K L L I E D Y P Y A S D G L L I W D A I E N W V K T Y V T H Y Y P N A N I I R E
D E E L Q T W Y R E S V N V G H A D L R H E T W W P Q L N N G D D L V S I L T T L I W L S S A Q H A A L N F G Q Y P Y
G G Y V P N R P P L Met R R L I P D E N D P E Y A I F L N D P Q K Y F L S A L P S V L Q A T K F Met A V V D T L S T H S P
D E E Y L G E R Q Q P S I W T G D A E Met V E A F Y E F S A E I G R I E K E I D R R N S D G R L K N R C G A G V L A Y E
L L A P S S E P G V T C R G V P N S V S I Stop

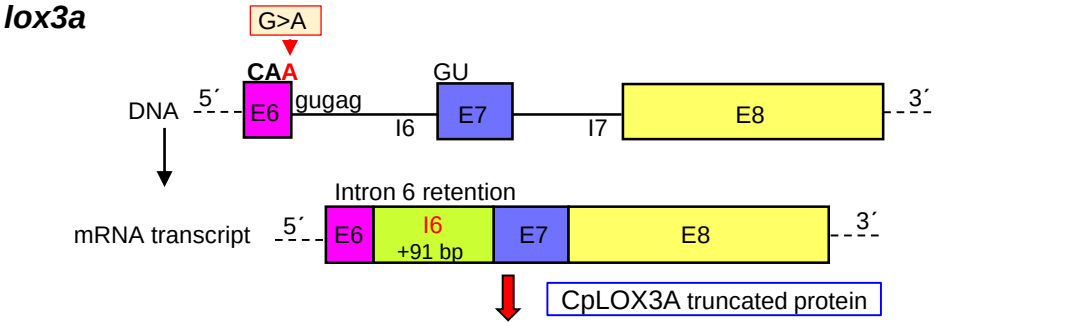

Met K L W D H L F F T K H L W F L S P S C F K E A I L R S S S G H F G G Y L E K Q F R P F R V V P Met E K K R I V Met N
L R K A V N G P V A A I S K D L V K A V P L A E K P V K F K V R A V V T I R N K N K E D I K E T I V K N L D A F T D R I G Q
N V V L Q L I S T E I D P K T N T P K K S N E A V L K D W S K K T N L K V E K V N Y I A E F L L T S D F G E P G A I T I T N
K H Q Q E F F L E T I T I E Q L A S D P I H F P C N S W V Q S R K D H P A K R I F F S N K S Y L P G E T P A G I K A L R E
Q E L K D I R G D G K G E R K L S D R V Y D F D V Y N D L G N P D K G I E F S R P R L G G E K I P Y P R R C R T G R A P
S D T D I T A E S R V E K P L P Met Y V P R D E Q F E E S K Q T T F S L G R L K A V L Y N L I P S L K A S I L S N K H D F
H G F S D I D S L Y S K G V L L K L G L Q D K L L K K L P L P R V V S E S S Q G L L R Y N T P K I L S K D K F A W L R D D
E F G R Q A I A G V N P V N I E R L K V F P P V S N L D P D V Y G P Q E S A L K E E H I L G Q L N G Met T V Q Q V N Y Y
T K Met L T H H S D F F S N P N N I L P Q I A L I V T G I G Stop

Figure S5.2. Schematic representation of the effects of G > A transition on the 5´-splicing site of intron 6 in the JA biosynthesis gene *CpLOX3A*. Note that the mutation prevented intron 6 splicing, generating a 91 nucleotide larger mRNA, a premature stop codon, and a truncated CpLOX3A protein.

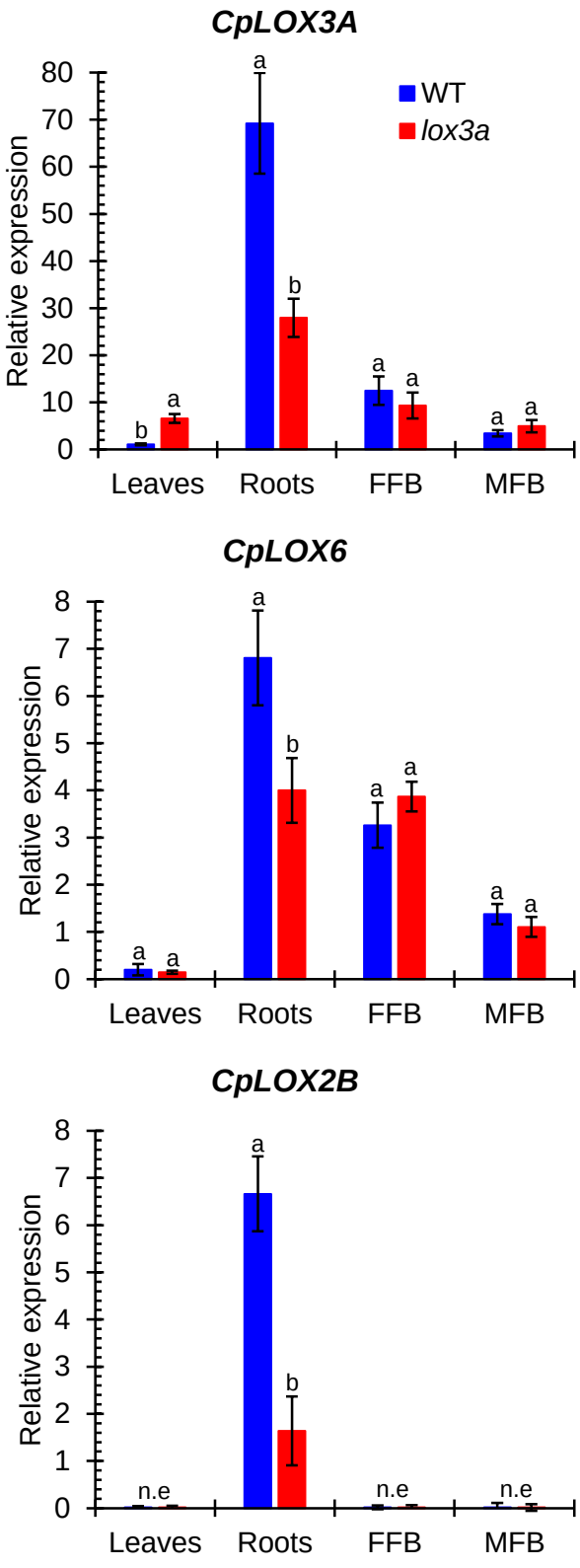

Figure S5.3. Relative gene expression of *LOX* genes *CpLOX3A*, *CpLOX6,* and *CpLOX2B* in vegetative and reproductive organs of WT and *lox3a* plants: leaves, roots, female floral buds (FFB), and male floral buds (MFB) at the early stage of development. The assessments were performed in three independent replicates for each tissue. Different letters indicate significant differences between WT and *lox3a* tissues at the same stage of development ($p \leq 0.05$). n.e, no expression.

8.3. Supplementary dataset.

5. Jasmonate-deficient mutant l*ox3a* reveals crosstalk between JA and ET in the differential regulation of male and female flower opening and early fruit development in *Cucurbita pepo*

Dataset S5.1. Fine mapping of the three identified mutations (SNP1, SNP2 and SNP3) in chromosome 12 by high-throughput genotyping of individual plants in segregating BC_1S_1 and BC_1S_2 populations. Recombinant BC_1S_1 plants between SNP1 and SNP2 are highlighted in red. These plants demonstrate that SNP1, but not SNP2, is the identified mutation that co-segregates with the mutant phenotype.

PHENOTYPE

WT
lox3a

GENOTYPE

0/0 homozygous for reference allele
1/1 homozygous for alternative allele
0/1 heterozygous

SNP1: position 5,883,147. Lipoxygenase *(CpLOX3A)*
SNP2: position 5,803,670. Jasmonate-zim-domain protein (*CpJAZ1A*)
SNP3: position 3,782,831. Elongation factor G mitochondrial (*CpEFG1A*)

			GENOTYPE		
POPULATION	PLANT	PHENOTYPE	SNP1	SNP2	SNP3
BC1S1	1	WT	0/1	0/1	0/0
	2	WT	0/1	0/1	0/1
	3	WT	0/1	0/1	0/1
	4	WT	0/1	0/1	0/1
	5	WT	0/1	0/1	0/1
	6	*lox3a*	1/1	1/1	1/1
	7	WT	0/0	0/0	0/1
	8	WT	0/1	0/1	1/1
	9	*lox3a*	1/1	1/1	1/1
	10	WT	0/1	0/1	0/1
	11	WT	0/0	0/0	0/1
	12	WT	0/1	0/1	0/1
	13	WT	0/0	0/0	0/1
	14	*lox3a*	1/1	1/1	1/1
	15	*lox3a*	1/1	1/1	1/1
	16	WT	0/1	0/1	0/1
	17	WT	0/0	0/0	0/0
	18	WT	0/0	0/0	0/1
	19	*lox3a*	1/1	1/1	0/1
	20	*lox3a*	1/1	1/1	1/1
	21	WT	0/1	0/1	0/1
	22	WT	0/1	0/1	0/1
	23	WT	0/1	0/1	0/1
	24	WT	0/1	0/1	0/1
	25	*lox3a*	1/1	1/1	1/1
	26	WT	0/1	0/1	0/1
	27	WT	0/1	0/1	1/1
	28	WT	0/1	0/1	0/1
	29	WT	0/0	0/0	0/1
	30	WT	0/1	0/1	0/0

			GENOTYPE		
POPULATION	PLANT	PHENOTYPE	SNP1	SNP2	SNP3
BC1S1	31	*lox3a*	1/1	1/1	1/1
	32	WT	0/1	0/1	0/1
	33	*lox3a*	1/1	1/1	0/1
	34	WT	0/1	0/1	0/1
	35	*lox3a*	1/1	0/1	0/1
	36	WT	0/0	0/0	0/0
	37	WT	0/1	0/1	0/1
	38	*lox3a*	1/1	1/1	1/1
	39	WT	0/1	0/1	0/1
	40	WT	0/1	0/1	0/1
	41	WT	0/1	0/1	0/1
	42	WT	0/0	0/0	0/1
	43	WT	0/1	0/1	0/1
	44	WT	0/1	0/1	0/0
	45	*lox3a*	1/1	1/1	1/1
	46	WT	0/0	0/0	0/1
	47	*lox3a*	1/1	1/1	1/1
	48	WT	0/1	0/1	0/1
	49	WT	0/1	0/1	0/1
	50	*lox3a*	1/1	1/1	0/1
	51	WT	0/0	0/0	0/1
	52	WT	0/1	0/1	1/1
	53	WT	0/0	0/0	0/0
	54	WT	0/1	0/1	0/0
	55	WT	0/1	0/1	0/1
	56	*lox3a*	1/1	1/1	1/1
	57	WT	0/1	0/1	0/1
	58	WT	0/0	0/0	0/0
	59	WT	0/0	0/0	0/0
	60	WT	0/1	0/1	0/1

POPULATION	PLANT	PHENOTYPE	GENOTYPE SNP1	SNP2	SNP3
BC1S1	61	*lox3a*	1/1	1/1	1/1
	62	*lox3a*	1/1	1/1	0/1
	63	WT	0/1	1/1	0/1
	64	WT	0/0	0/1	0/1
	65	*lox3a*	1/1	1/1	1/1
	66	*lox3a*	1/1	1/1	0/1
	67	WT	0/1	0/1	0/1
	68	*lox3a*	1/1	1/1	1/1
	69	*lox3a*	1/1	1/1	1/1
	70	WT	0/0	0/0	0/0
	71	*lox3a*	1/1	1/1	0/0
	72	WT	0/0	0/0	0/1
	73	WT	0/1	0/1	0/0
	74	WT	0/0	0/0	0/1
	75	WT	0/0	0/1	0/0
	76	WT	0/1	0/1	0/1
	77	*lox3a*	1/1	1/1	0/0
	78	*lox3a*	1/1	1/1	0/1
	79	WT	0/0	0/0	0/1
	80	WT	0/1	0/1	1/1
	81	*lox3a*	1/1	1/1	0/1
	82	*lox3a*	1/1	1/1	1/1
	83	WT	0/1	0/1	0/1
	84	WT	0/1	0/1	0/0
	85	*lox3a*	1/1	1/1	0/1
	86	WT	0/1	0/1	0/0
	87	WT	0/1	0/1	0/1
	88	WT	0/1	0/1	0/1
	89	WT	0/0	0/0	0/1
	90	WT	0/0	0/0	0/1
	91	WT	0/0	0/0	0/1
	92	WT	0/1	0/1	0/0
	93	WT	0/1	0/1	0/1
	94	WT	0/1	0/1	0/1
	95	*lox3a*	1/1	1/1	0/1
	96	*lox3a*	1/1	1/1	0/1
	97	WT	0/1	0/1	0/0
	98	WT	0/1	0/1	0/1
	99	WT	0/0	0/0	0/1
	100	WT	0/0	0/1	0/1
	101	WT	0/1	0/1	0/1
	102	WT	0/1	0/1	0/1
	103	WT	0/1	0/1	0/1
	104	WT	0/1	0/1	0/1
	105	WT	0/1	0/1	0/0
	106	WT	0/1	0/1	0/1
	107	WT	0/1	0/1	1/1
	108	WT	0/1	0/1	1/1
	109	*lox3a*	1/1	1/1	1/1
	110	WT	0/1	0/1	0/1
	111	WT	0/1	0/1	0/0
	112	*lox3a*	1/1	1/1	0/1
	113	WT	0/0	0/0	0/1
	114	*lox3a*	1/1	1/1	0/0
	115	WT	0/0	0/0	0/1
	116	WT	0/0	0/0	1/1
	117	*lox3a*	1/1	1/1	1/1
	118	WT	0/1	0/1	1/1
	119	WT	0/0	0/0	0/0
	120	WT	0/1	0/1	1/1
	121	WT	0/1	0/1	0/0
	122	WT	0/1	0/1	0/1
	123	*lox3a*	1/1	1/1	0/1
	124	WT	0/0	0/0	0/0
	125	WT	0/1	0/1	1/1
	126	WT	0/0	0/0	0/1
	127	WT	0/0	0/0	0/1
	128	WT	0/1	0/1	0/1
	129	WT	0/0	0/0	1/1
	130	WT	0/0	0/0	0/1
	131	WT	0/1	0/1	0/1
	132	WT	0/0	0/0	0/1
	133	WT	0/1	0/1	1/1
	134	*lox3a*	1/1	0/1	0/1
	135	WT	0/1	0/1	0/1
	136	WT	0/0	0/0	0/1
	137	WT	0/1	0/1	0/1
	138	WT	0/1	0/1	0/1
	139	WT	0/1	0/1	0/1
	140	WT	0/1	0/1	0/0

POPULATION	PLANT	PHENOTYPE	GENOTYPE SNP1	SNP2	SNP3
BC1S1	141	WT	0/0	0/0	1/1
	142	*lox3a*	1/1	1/1	0/0
	143	WT	0/1	0/1	0/0
	144	WT	0/1	0/1	0/1
	145	WT	0/1	0/1	0/0
	146	WT	0/1	0/1	1/1
	147	WT	0/1	0/1	1/1
	148	WT	0/0	0/0	0/1
	149	*lox3a*	1/1	1/1	1/1
	150	*lox3a*	1/1	1/1	0/1
	151	WT	0/0	0/0	0/1
	152	WT	0/1	0/1	0/0
	153	WT	0/0	0/0	0/1
	154	*lox3a*	1/1	1/1	1/1
	155	WT	0/1	0/1	1/1
	156	WT	0/0	0/0	1/1
	157	WT	0/0	0/0	1/1
	158	WT	0/1	0/1	0/1
	159	*lox3a*	1/1	1/1	0/1
	160	WT	0/1	0/1	1/1
	161	WT	0/1	0/1	0/0
	162	WT	0/1	0/1	1/1
	163	*lox3a*	1/1	1/1	0/1
	164	*lox3a*	1/1	1/1	0/1
	165	*lox3a*	1/1	1/1	0/1
	166	WT	0/0	0/0	0/0
	167	WT	0/0	0/0	1/1
	168	*lox3a*	1/1	1/1	1/1
	169	WT	0/1	0/1	0/1
	170	WT	0/1	0/1	1/1
	171	WT	0/1	0/1	0/1
	172	WT	0/1	0/1	0/1
	173	WT	0/0	0/0	0/0
	174	WT	0/1	0/1	0/1
	175	WT	0/1	0/1	1/1
	176	WT	0/1	0/1	1/1
	177	WT	0/1	0/1	1/1
	178	WT	0/1	0/1	1/1
	179	WT	0/1	0/1	0/1
	180	WT	0/1	0/1	0/1
	181	WT	0/1	0/1	1/1
	182	WT	0/0	0/0	0/0
	183	*lox3a*	1/1	1/1	0/1
	184	WT	0/1	0/1	0/1
	185	WT	0/1	0/1	0/1
	186	WT	0/1	0/1	0/1
	187	WT	0/0/	0/0	0/1
	188	WT	0/0	0/0	0/0
	189	WT	0/1	0/1	0/1
	190	*lox3a*	1/1	1/1	1/1
	191	WT	0/1	0/1	0/0
	192	WT	0/1	0/1	0/0
	193	WT	0/1	0/1	0/1
	194	WT	0/0	0/0	0/0
	195	WT	0/1	0/1	0/1
	196	WT	0/0	0/0	0/0
	197	WT	0/1	0/1	0/1
	198	WT	0/1	0/1	0/0
	199	WT	0/1	0/1	0/1
	200	WT	0/1	0/1	0/1
	201	WT	0/1	0/1	1/1
	202	WT	0/1	0/1	0/1
	203	*lox3a*	1/1	1/1	1/1
	204	*lox3a*	1/1	1/1	0/1
	205	WT	0/0	0/0	0/0
	206	*lox3a*	1/1	1/1	0/1
	207	WT	0/1	0/1	0/0
	208	*lox3a*	1/1	1/1	0/1
	209	WT	0/1	0/1	0/1
	210	WT	0/1	0/1	0/1
	211	*lox3a*	1/1	1/1	1/1
	212	WT	0/1	0/1	0/1
	213	WT	0/0	0/0	0/0
	214	*lox3a*	1/1	1/1	0/1
	215	WT	0/1	0/1	0/1
	216	WT	0/0	0/1	0/0
	217	WT	0/1	0/1	0/1
	218	WT	0/0	0/0	0/0
	219	WT	0/1	0/1	0/1
	220	WT	0/1	0/1	0/1

POPULATION	PLANT	PHENOTYPE	GENOTYPE SNP1	SNP2	SNP3
BC1S1	221	WT	0/1	0/1	0/1
	222	WT	0/1	0/1	0/1
	223	*lox3a*	1/1	1/1	0/1
	224	*lox3a*	1/1	1/1	0/1
	225	WT	0/1	0/1	0/1
	226	WT	0/0	0/0	0/0
	227	WT	0/1	0/1	0/1
	228	*lox3a*	1/1	1/1	1/1
	229	*lox3a*	1/1	1/1	1/1
	230	*lox3a*	1/1	1/1	1/1
	231	WT	0/1	0/1	0/1
	232	WT	0/1	0/1	0/0
	233	WT	0/1	0/1	0/1
	234	WT	0/1	0/1	0/1
	235	WT	0/1	0/0	0/0
	236	WT	0/1	0/1	0/1
	237	WT	0/1	0/1	1/1
	238	*lox3a*	1/1	1/1	1/1
	239	*lox3a*	1/1	1/1	1/1
	240	WT	0/0	0/0	0/0
	241	*lox3a*	1/1	1/1	1/1
	242	WT	0/0	0/0	0/0
	243	WT	0/1	0/1	0/1
	244	WT	0/0	0/0	0/1
	245	WT	0/0	0/0	0/0
	246	WT	0/1	0/1	1/1
	247	WT	0/1	0/1	0/1
	248	WT	0/1	0/1	1/1
	249	WT	0/1	0/1	0/1
	250	*lox3a*	1/1	1/1	1/1
	251	*lox3a*	1/1	1/1	0/1
	252	WT	0/1	0/1	0/1
	253	*lox3a*	1/1	1/1	1/1
	254	WT	0/1	1/1	1/1
	255	WT	0/1	0/1	0/1
	256	WT	0/1	0/1	0/1
	257	*lox3a*	1/1	1/1	1/1
	258	WT	0/1	0/1	0/1
	259	*lox3a*	1/1	1/1	0/1
	260	WT	0/0	0/0	0/1
	261	*lox3a*	1/1	1/1	0/0
	262	*lox3a*	1/1	1/1	1/1
	263	WT	0/0	0/0	0/0
	264	WT	0/0	0/0	0/0
	265	WT	0/1	0/1	0/1
	266	WT	0/1	0/1	0/0
	267	WT	0/1	0/1	1/1
	268	*lox3a*	1/1	1/1	1/1
	269	WT	0/1	0/1	0/1
	270	*lox3a*	1/1	1/1	1/1
	271	WT	0/1	0/1	0/1
	272	WT	0/1	0/1	0/1
	273	WT	0/1	0/1	0/0
	274	WT	0/1	0/1	0/1
	275	*lox3a*	1/1	1/1	1/1
	276	WT	0/1	0/1	1/1
	277	*lox3a*	1/1	1/1	1/1
	278	*lox3a*	1/1	1/1	1/1
	279	*lox3a*	1/1	1/1	0/1
	280	WT	0/1	0/1	0/1
	281	*lox3a*	1/1	1/1	1/1
	282	WT	0/0	0/0	0/0
	283	WT	0/1	0/1	0/1
	284	WT	0/0	0/0	0/0
	285	WT	0/0	0/1	0/0
	286	WT	0/0	0/0	0/0
	287	WT	0/0	0/0	1/1
	288	WT	0/0	0/0	0/1
	289	WT	0/0	0/0	0/0
	290	*lox3a*	1/1	1/1	1/1
	291	WT	0/0	0/0	0/0
	292	WT	0/0	0/0	0/0
	293	*lox3a*	1/1	1/1	0/1
	294	WT	0/0	0/0	0/1
	295	WT	0/1	0/1	0/1
	296	*lox3a*	1/1	1/1	1/1
	297	WT	0/1	0/1	0/1
	298	WT	0/1	0/1	0/1
	299	*lox3a*	1/1	1/1	0/1
	300	WT	0/0	0/0	0/1

POPULATION	PLANT	PHENOTYPE	GENOTYPE SNP1	SNP2	SNP3
BC1S1	301	*lox3a*	1/1	1/1	1/1
	302	WT	0/1	0/1	0/1
	303	WT	0/1	0/1	0/1
	304	WT	0/0	1/1	0/0
	305	WT	0/0	0/0	0/1
	306	WT	0/0	0/0	0/1
	307	WT	0/1	0/1	0/1
	308	*lox3a*	1/1	1/1	0/0
	309	*lox3a*	1/1	1/1	1/1
	310	WT	0/1	0/1	0/1
	311	WT	0/1	0/1	0/1
	312	WT	0/0	0/0	0/1
	313	WT	0/1	0/1	0/1
	314	WT	0/1	0/1	0/1
	315	WT	0/1	0/1	0/1
	316	WT	0/1	0/1	0/1
	317	*lox3a*	1/1	1/1	0/1
	318	WT	0/0	0/0	0/0
	319	*lox3a*	1/1	1/1	0/1
	320	WT	0/1	0/1	0/1
	321	WT	0/1	0/1	0/1
	322	*lox3a*	1/1	1/1	0/1
	323	WT	0/0	0/0	0/0
	324	*lox3a*	1/1	0/1	0/0
	325	WT	0/0	0/0	0/0
	326	WT	0/0	0/0	0/0
	327	*lox3a*	1/1	1/1	0/1
	328	WT	0/0	0/0	1/1
	329	WT	0/0	0/0	0/0
	330	WT	0/1	0/1	0/1
	331	*lox3a*	1/1	1/1	1/1
	332	WT	0/1	0/1	0/0
	333	*lox3a*	1/1	1/1	1/1
	334	WT	0/1	0/1	0/1
	335	*lox3a*	1/1	1/1	0/0
	336	WT	0/1	0/1	0/1
	337	*lox3a*	1/1	1/1	0/1
	338	*lox3a*	1/1	1/1	0/1
	339	WT	0/0	0/0	0/0
	340	WT	0/1	0/1	1/1
	341	WT	0/1	0/1	0/0
	342	WT	0/1	0/1	0/1
	343	*lox3a*	1/1	1/1	1/1
	344	*lox3a*	1/1	1/1	1/1
	345	*lox3a*	1/1	1/1	0/1
	346	WT	0/0	0/0	0/0
	347	*lox3a*	1/1	1/1	1/1
	348	WT	0/1	0/1	0/1
	349	WT	0/1	0/1	0/1
	350	WT	0/0	0/0	0/1
	351	*lox3a*	1/1	1/1	1/1
	352	WT	0/1	0/1	1/1
	353	WT	0/1	0/1	1/1
	354	*lox3a*	1/1	1/1	0/1
	355	WT	0/1	0/1	0/1
	356	*lox3a*	1/1	1/1	0/1
	357	*lox3a*	1/1	1/1	0/1
	358	WT	0/0	0/0	0/1
	359	WT	0/0	0/0	0/1
	360	WT	0/1	0/1	0/1
	361	WT	0/1	0/1	1/1
	362	WT	0/1	0/1	0/1
	363	WT	0/0	0/0	0/1
	364	*lox3a*	1/1	1/1	1/1
	365	WT	0/1	0/1	0/1
	366	WT	0/1	0/0	0/0
	367	WT	0/1	0/1	1/1
	368	WT	0/0	0/0	1/1
	369	WT	0/1	0/1	0/0
	370	*lox3a*	1/1	1/1	1/1
	371	WT	0/1	0/1	0/1
	372	*lox3a*	1/1	1/1	1/1
	373	WT	0/0	0/0	0/0
	374	WT	0/0	0/0	0/0
	375	*lox3a*	1/1	1/1	1/1
	376	*lox3a*	1/1	1/1	1/1
	377	*lox3a*	1/1	1/1	1/1
	378	WT	0/1	0/1	0/1
	379	WT	0/1	0/1	0/1
	380	WT	0/0	0/0	0/0

POPULATION	PLANT	PHENOTYPE	GENOTYPE SNP1	SNP2	SNP3
BC1S1	381	WT	0/1	0/1	0/1
	382	*lox3a*	1/1	1/1	0/0
	383	*lox3a*	1/1	1/1	0/1
	384	WT	0/1	0/1	0/1
	385	*lox3a*	1/1	1/1	0/1
	386	WT	0/0	0/0	0/0
	387	*lox3a*	1/1	1/1	1/1
	388	WT	0/1	0/1	1/1
	389	*lox3a*	1/1	1/1	1/1
	390	WT	0/1	0/1	1/1
	391	WT	0/1	0/1	0/0
	392	WT	0/0	0/0	0/1
	393	WT	0/1	0/1	0/1
	394	WT	0/1	0/1	0/1
	395	WT	0/1	0/1	0/1
	396	*lox3a*	1/1	1/1	1/1
	397	WT	0/1	0/1	0/1
	398	WT	0/0	0/0	0/0
	399	WT	0/0	0/0	0/1
	400	WT	0/0	0/1	0/1
	401	WT	0/0	0/0	0/1
	402	WT	0/1	0/1	0/1
	403	WT	0/0	0/0	0/1
	404	WT	0/1	0/1	0/0
	405	WT	0/0	0/0	0/1
	406	WT	0/1	0/1	0/1
	407	WT	0/1	0/1	1/1
	408	*lox3a*	1/1	1/1	0/0
	409	WT	0/0	0/0	0/1
	410	WT	0/0	0/0	1/1
	411	WT	0/1	0/1	0/0
	412	WT	0/1	0/1	1/1
	413	WT	0/1	0/1	0/1
	414	WT	0/0	0/0	1/1
	415	*lox3a*	1/1	1/1	0/1
	416	*lox3a*	1/1	1/1	0/1
	417	WT	0/1	0/1	0/1
	418	WT	0/0	0/0	0/0
	419	*lox3a*	1/1	1/1	1/1
	420	WT	0/0	0/0	0/0
	421	WT	0/1	0/1	0/1
	422	WT	0/1	0/1	1/1
	423	WT	0/1	0/1	1/1
	424	WT	0/1	0/1	0/1
	425	WT	0/1	0/1	0/0
	426	WT	0/1	0/1	1/1
	427	WT	0/1	0/1	0/1
	428	WT	0/1	0/1	0/1
	429	WT	0/1	0/1	0/1
	430	WT	0/1	0/1	1/1
	431	*lox3a*	1/1	1/1	1/1
	432	WT	0/1	0/1	1/1
	433	WT	0/1	0/1	0/1
	434	WT	0/1	0/1	0/1
	435	WT	0/1	0/1	0/1
	436	*lox3a*	1/1	1/1	0/0
	437	WT	0/1	0/1	0/1
	438	WT	0/1	0/1	0/1
	439	*lox3a*	1/1	1/1	0/1
	440	*lox3a*	1/1	0/1	0/1
	441	WT	0/1	0/1	0/1
	442	*lox3a*	1/1	1/1	0/1
	443	WT	0/1	0/1	1/1
	444	WT	0/1	0/1	0/1
	445	WT	0/1	0/1	0/1
	446	WT	0/1	0/1	1/1
	447	WT	0/1	0/1	1/1
	448	WT	0/1	0/1	0/0
	449	WT	0/1	0/1	1/1
	450	*lox3a*	1/1	1/1	0/1
	451	WT	0/1	0/1	1/1
	452	WT	0/1	0/1	0/1
	453	WT	0/1	0/1	0/0
	454	WT	0/0	0/0	0/1
	455	WT	0/1	0/1	0/0
	456	WT	0/0	0/0	0/1
	457	WT	0/1	0/1	0/1
	458	WT	0/0	0/0	1/1
	459	WT	0/0	0/0	0/1
	460	WT	0/0	0/0	1/1

POPULATION	PLANT	PHENOTYPE	GENOTYPE SNP1	SNP2	SNP3
BC1S1	461	*lox3a*	1/1	1/1	0/1
	462	WT	0/1	0/1	0/0
	463	*lox3a*	1/1	1/1	0/1
	464	WT	0/0	0/0	0/0
	465	WT	0/0	0/0	0/1
	466	WT	0/1	0/1	0/1
	467	WT	0/1	0/1	0/1
	468	WT	0/0	0/0	1/1
	469	WT	0/1	0/1	0/1
	470	*lox3a*	1/1	1/1	0/0
	471	WT	0/0	0/0	0/1
	472	WT	0/1	0/1	0/1
	473	WT	0/0	0/0	0/0
	474	*lox3a*	1/1	1/1	0/1
	475	WT	0/1	0/1	0/0
	476	WT	0/1	0/1	0/1
	477	WT	0/1	0/1	0/1
	478	WT	0/0	0/0	0/1
	479	WT	0/0	0/0	0/1
	480	WT	0/0	0/0	0/1
	481	WT	0/1	0/1	0/1
	482	WT	0/1	0/1	0/1
	483	WT	0/1	0/0	0/0
	484	WT	0/0	0/0	0/1
	485	*lox3a*	1/1	1/1	1/1
	486	WT	0/1	0/1	1/1
	487	WT	0/1	0/1	1/1
	488	*lox3a*	1/1	1/1	0/1
	489	WT	0/0	0/0	0/0
	490	WT	0/0	0/0	0/1
	491	WT	0/0	0/0	0/1
	492	WT	0/1	0/1	0/0
	493	*lox3a*	1/1	1/1	0/1
	494	*lox3a*	1/1	1/1	1/1
	495	WT	0/1	0/1	1/1
	496	WT	0/1	0/1	1/1
	497	WT	0/0	0/0	0/0
	498	WT	0/1	0/1	1/1
	499	WT	0/1	0/1	0/0
	500	WT	0/1	0/1	0/1
	501	WT	0/0	0/0	0/1
	502	WT	0/0	0/0	0/1
	503	*lox3a*	1/1	1/1	1/1
	504	*lox3a*	1/1	1/1	0/1
	505	WT	0/1	0/1	0/1
	506	WT	0/1	0/1	1/1
	507	WT	0/1	0/1	0/1
	508	WT	0/1	0/1	0/1
	509	*lox3a*	1/1	0/1	1/1
	510	WT	0/1	0/1	1/1
	511	WT	0/0	0/0	0/0
	512	WT	0/0	0/0	1/1
	513	*lox3a*	1/1	1/1	0/1
	514	WT	0/1	0/1	1/1
	515	WT	0/1	0/1	0/0
	516	WT	0/0	0/0	0/0
	517	WT	0/1	0/1	1/1
	518	*lox3a*	1/1	1/1	1/1
	519	WT	0/1	0/1	1/1
	520	WT	0/1	0/1	0/1
	521	*lox3a*	1/1	1/1	0/1
	522	*lox3a*	1/1	1/1	0/0
	523	*lox3a*	1/1	0/1	0/1
	524	WT	0/0	0/0	0/0
	525	*lox3a*	1/1	1/1	0/1
	526	WT	0/1	0/1	0/1
	527	WT	0/0	0/0	0/1
	528	WT	0/1	0/1	0/0
	529	WT	0/1	0/1	1/1
	530	WT	0/1	0/1	1/1
	531	WT	0/1	0/1	1/1
	532	WT	0/1	0/1	1/1
	533	*lox3a*	1/1	1/1	0/0
	534	WT	0/1	0/1	0/1
	535	*lox3a*	1/1	1/1	0/1
	536	WT	0/1	0/1	0/1
	537	*lox3a*	1/1	1/1	0/1
	538	WT	0/1	0/1	1/1
	539	WT	0/1	0/1	0/1
	540	WT	0/0	0/0	0/0

POPULATION	PLANT	PHENOTYPE	GENOTYPE SNP1	SNP2	SNP3
BC1S1	541	WT	0/0	0/0	0/1
	542	WT	0/1	0/1	0/0
	543	*lox3a*	1/1	1/1	0/1
	544	*lox3a*	1/1	1/1	0/1
	545	WT	0/0	0/0	0/1
	546	WT	0/1	0/1	0/0
	547	WT	0/1	0/1	0/1
	548	WT	0/1	0/1	0/1
	549	WT	0/1	0/1	1/1
	550	*lox3a*	1/1	1/1	0/0
	551	WT	0/1	0/1	0/1
	552	WT	0/1	0/1	1/1
	553	WT	0/0	0/0	0/0
	554	WT	0/0	0/0	1/1
	555	WT	0/0	0/0	0/1
	556	WT	0/1	0/1	0/0
	557	*lox3a*	1/1	0/1	0/1
	558	*lox3a*	1/1	1/1	0/1
	559	WT	0/1	0/1	0/1
	560	*lox3a*	1/1	1/1	1/1
	561	WT	0/0	0/0	0/0

POPULATION	PLANT	PHENOTYPE	GENOTYPE SNP1	SNP2	SNP3
BC1S2 / Selfed offspring of BC1S1 plant 0/1 0/0 0/0	1	*lox3a*	1/1	0/0	0/0
	2	*lox3a*	1/1	0/0	0/0
	3	WT	0/1	0/0	0/0
	4	WT	0/0	0/0	0/0
	5	WT	0/1	0/0	0/0
	6	WT	0/1	0/0	0/0
	7	WT	0/1	0/0	0/0
	8	WT	0/1	0/0	0/0
	9	*lox3a*	1/1	0/0	0/0
	10	*lox3a*	1/1	0/0	0/0
	11	WT	0/1	0/0	0/0
	12	WT	0/1	0/0	0/0
	13	WT	0/1	0/0	0/0
	14	WT	0/0	0/0	0/0
	15	WT	0/1	0/0	0/0
	16	WT	0/1	0/0	0/0
	17	WT	0/1	0/0	0/0
	18	WT	0/0	0/0	0/0
	19	WT	0/1	0/0	0/0
	20	WT	0/1	0/0	0/0
	21	WT	0/0	0/0	0/0
	22	*lox3a*	1/1	0/0	0/0
	23	WT	0/1	0/0	0/0
	24	WT	0/0	0/0	0/0
	25	*lox3a*	1/1	0/0	0/0
	26	WT	0/0	0/0	0/0
	27	WT	0/1	0/0	0/0
	28	WT	0/1	0/0	0/0
	29	WT	0/1	0/0	0/0
	30	WT	0/1	0/0	0/0
	31	WT	0/0	0/0	0/0
	32	WT	0/0	0/0	0/0
	33	WT	0/1	0/0	0/0
	34	WT	0/0	0/0	0/0
	35	WT	0/1	0/0	0/0
	36	WT	0/0	0/0	0/0

POPULATION	PLANT	PHENOTYPE	GENOTYPE SNP1	SNP2	SNP3
BC1S2 / Selfed offspring of BC1S1 plant 0/0 0/1 0/0	1	WT	0/0	0/1	0/0
	2	WT	0/0	1/1	0/0
	3	WT	0/0	0/1	0/0
	4	WT	0/0	0/0	0/0
	5	WT	0/0	0/1	0/0
	6	WT	0/0	0/1	0/0
	7	WT	0/0	0/0	0/0
	8	WT	0/0	0/1	0/0
	9	WT	0/0	0/1	0/0
	10	WT	0/0	0/1	0/0
	11	WT	0/0	1/1	0/0
	12	WT	0/0	0/1	0/0
	13	WT	0/0	0/0	0/0
	14	WT	0/0	0/1	0/0
	15	WT	0/0	0/1	0/0
	16	WT	0/0	1/1	0/0
	17	WT	0/0	1/1	0/0
	18	WT	0/0	0/0	0/0
	19	WT	0/0	0/1	0/0
	20	WT	0/0	0/0	0/0
	21	WT	0/0	0/1	0/0
	22	WT	0/0	0/1	0/0
	23	WT	0/0	0/1	0/0
	24	WT	0/0	0/1	0/0
	25	WT	0/0	1/1	0/0
	26	WT	0/0	0/1	0/0
	27	WT	0/0	0/0	0/0
	28	WT	0/0	0/1	0/0
	29	WT	0/0	1/1	0/0
	30	WT	0/0	1/1	0/0

POPULATION	PLANT	PHENOTYPE	GENOTYPE SNP1	SNP2	SNP3
BC1S2 / Selfed offspring of BC1S1 plant 0/0 0/0 0/1	1	WT	0/0	0/0	0/1
	2	WT	0/0	0/0	0/1
	3	WT	0/0	0/0	0/1
	4	WT	0/0	0/0	0/0
	5	WT	0/0	0/0	0/0
	6	WT	0/0	0/0	0/1
	7	WT	0/0	0/0	0/1
	8	WT	0/0	0/0	0/0
	9	WT	0/0	0/0	0/1
	10	WT	0/0	0/0	0/1
	11	WT	0/0	0/0	0/0
	12	WT	0/0	0/0	1/1
	13	WT	0/0	0/0	1/1
	14	WT	0/0	0/0	0/0
	15	WT	0/0	0/0	0/1
	16	WT	0/0	0/0	0/0
	17	WT	0/0	0/0	0/1
	18	WT	0/0	0/0	0/1
	19	WT	0/0	0/0	0/1
	20	WT	0/0	0/0	0/1
	21	WT	0/0	0/0	1/1
	22	WT	0/0	0/0	0/1
	23	WT	0/0	0/0	1/1
	24	WT	0/0	0/0	0/1
	25	WT	0/0	0/0	1/1
	26	WT	0/0	0/0	1/1
	27	WT	0/0	0/0	0/1
	28	WT	0/0	0/0	0/0
	29	WT	0/0	0/0	0/0
	30	WT	0/0	0/0	0/0

9. Annexes

Cebrián et al. *Horticulture Research* (2021)8:73
https://doi.org/10.1038/s41438-021-00508-z

Horticulture Research
www.nature.com/hortres

ARTICLE Open Access

Involvement of ethylene receptors in the salt tolerance response of *Cucurbita pepo*

Gustavo Cebrián[1], Jessica Iglesias-Moya[1], Alicia García[1], Javier Martínez[1], Jonathan Romero[1], José Javier Regalado[1], Cecilia Martínez[1], Juan Luis Valenzuela[1] and Manuel Jamilena[1]

Abstract

Abiotic stresses have a negative effect on crop production, affecting both vegetative and reproductive development. Ethylene plays a relevant role in plant response to environmental stresses, but the specific contribution of ethylene biosynthesis and signalling components in the salt stress response differs between Arabidopsis and rice, the two most studied model plants. In this paper, we study the effect of three gain-of-function mutations affecting the ethylene receptors *CpETR1B*, *CpETR1A*, and *CpETR2B* of *Cucurbita pepo* on salt stress response during germination, seedling establishment, and subsequent vegetative growth of plants. The mutations all reduced ethylene sensitivity, but enhanced salt tolerance, during both germination and vegetative growth, demonstrating that the three ethylene receptors play a positive role in salt tolerance. Under salt stress, *etr1b*, *etr1a*, and *etr2b* germinate earlier than WT, and the root and shoot growth rates of both seedlings and plants were less affected in mutant than in WT. The enhanced salt tolerance response of the *etr2b* plants was associated with a reduced accumulation of Na^+ in shoots and leaves, as well as with a higher accumulation of compatible solutes, including proline and total carbohydrates, and antioxidant compounds, such as anthocyanin. Many membrane monovalent cation transporters, including Na^+/H^+ and K^+/H^+ exchangers (NHXs), K^+ efflux antiporters (KEAs), high-affinity K^+ transporters (HKTs), and K^+ uptake transporters (KUPs) were also highly upregulated by salt in *etr2b* in comparison with WT. In aggregate, these data indicate that the enhanced salt tolerance of the mutant is led by the induction of genes that exclude Na^+ in photosynthetic organs, while maintaining K^+/Na^+ homoeostasis and osmotic adjustment. If the salt response of *etr* mutants occurs via the ethylene signalling pathway, our data show that ethylene is a negative regulator of salt tolerance during germination and vegetative growth. Nevertheless, the higher upregulation of genes involved in Ca^{2+} signalling (*CpCRCK2A* and *CpCRCK2B*) and ABA biosynthesis (*CpNCED3A* and *CpNCED3B*) in *etr2b* leaves under salt stress likely indicates that the function of ethylene receptors in salt stress response in *C. pepo* can be mediated by Ca^{2+} and ABA signalling pathways.

Introduction

One of the great challenges facing agriculture today is the development of production systems that mitigate the deleterious effects of climate change, including drought and salinity[1]. In arid and semi-arid areas, soil and water salinity constitute two of the most important abiotic stresses that limit crop production. At present, >1 billion hectares worldwide are affected by soil salinity[2].

Crop development and performance is severely affected by salinity. The primary effects of salinity are very similar to those caused by drought. A high concentration of salt in the soil reduces the plant's ability to absorb water, known as the osmotic effect due to salinity. This not only leads to reduced absorption of essential elements, such as K^+, Ca^{2+} and NO_3^-, but also a toxic accumulation of Na^+ and Cl^- in aerial parts of the plant[3]. The accumulation of salt in leaf cells inhibits cell expansion and photosynthetic

Correspondence: Manuel Jamilena (mjamille@ual.es)
[1]Department of Biology and Geology, Agri-food Campus of International Excellence (CeiA3) and Research Center CIAMBITAL, University of Almería, 04120 Almería, Spain

activity, which ultimately leads to a reduction in crop yield[4].

The entrance and the perception of Na^+ in roots are little known processes. Sodium can enter the root through non-selective cation channels (NSCCs)[5], although extracellular cation receptors, such as MONOCATION INDUCED [Ca^{2+}] and INCREASES 1 (MOCA1), have been detected, which are capable of sensing sodium and other cations, as well as promoting the influx of Ca^{2+} into the cell[6,7]. The perception of the stress signal triggers a secondary signalling by reactive oxygen species (ROS) and abscisic acid (ABA), which also regulate the intracellular level of Ca^{2+}. The cytosolic calcium activates phosphorylation cascades of Ca^{2+}-dependent proteins or calcium sensors, including calmodulins (CaM), CaM-like (CML) and calcineurin B-like proteins (CBL), which leads to regulation of stress response genes[8,9].

To deal with salinity, plants have implemented three general mechanisms that improve plant tolerance to salt stress: (i) restoration of ion homoeostasis (Na^+/K^+ homoeostasis); (ii) restoration of osmotic homoeostasis; and (iii) prevention and repair of cell damage. Ionic homoeostasis mediated by membrane ion transporters constitutes the main response mechanism against salt stress. Plasma membrane Na^+/H^+ antiporters, such SALT OVERLY SENSITIVE 1 (SOS1/AtNHX7) and AtNHX8, extrude Na^+ into the extracellular medium in response to an increase in intracellular Ca^{2+}. HIGH-AFFINITY K^+ TRANSPORTER1-like (HTK1-like) also has a strong affinity for Na^+[9], which excludes the translocation of Na^+[10,11]. Tonoplast Na^+/H^+ antiporters, such as Na^+/H^+ EXCHANGER 1–4 of Arabidopsis (NHX1-4), are also activated by Ca^{2+}, transporting Na^+ (and K^+) into the vacuole[12–14], reducing toxic Na^+ in the cytoplasm, and decreasing the osmotic potential of the cell. The overexpression of both plasma membrane and tonoplast antiporters results in a greater tolerance to salinity in a wide range of plant species[15–17]. K^+ transporters, including the high-affinity transporter family HAK/KT/KUP, the HKT family of high-affinity K^+ transporters and the KEA family of K^+ efflux antiporters, are also involved in salt tolerance by maintaining K^+/Na^+ homoeostasis[10,17]. To restore osmotic homoeostasis and cell volume and turgor, salt also activates the production of compatible solutes or osmolytes, including proline, sugar alcohols, sorbitol and anthocyanins, among others[18,19]. These osmolytes also function as protectors of membranes and proteins by reducing oxidative damage[20,21].

The phytohormones ABA and ethylene play key roles in the defensive response of plants against abiotic stresses[7,22]. ABA is a positive regulator of plant defensive response. Under both salinity and water deficit, plants induce the production of ABA biosynthesis genes, such as *NINE-CIS-EPOXYCAROTENOID DIOXYGENASES* (*NCEDs*) and *ABA DEFICIENTS* (*ABAs*). ABA is then perceived by the ABA receptors PYRABACTIN RESISTANCE/PYR-ABACTIN RESISTANCE LIKE (PYR/PYL), which induce phosphorylation activity of the ABA-dependent SUCROSE NON-FERMENTING RELATED PROTEIN KINASES (SnRKs) family, and the activation of the ABA-dependent transcriptional network involved in ionic and osmotic adjustments in response to salt stress[7,23].

The function of ethylene in salt stress response is, however, more controversial[24]. It is generally presumed that ethylene improves the response of plants to salt stress[25]. However, other authors supported a negative role of ethylene during salt stress, at least in certain growth stages in which its induction can activate oxidative stress and leaf senescence[26]. In Arabidopsis, ethylene positively regulates salinity response, and both ethylene biosynthesis and signalling genes are required for salt tolerance[27,28]. The biosynthesis *ACS* and *ACO* genes in Arabidopsis are induced under salinity conditions, but certain individual members can play a negative role in salt tolerance[29–31]. The ethylene signalling elements also participate in the response of plant to salt stress, but their functions are also unclear[24]. In Arabidopsis, the positive elements of the ethylene response are generally upregulated in response to salt and are positive regulators of salt tolerance; whereas, negative elements are downregulated by salt and are considered to be negative regulators of salt tolerance[24]. In contrast, orthologous ethylene positive signalling genes, including *MHZ7/OsEIN2*, *MHZ6/OSEIL1* and *OsEIL2*, have an opposite function in rice, since their suppression produces salinity tolerance, while their individual overexpression enhances salt sensitivity[32].

The five ethylene receptors of Arabidopsis, ETR1, ERS1, ETR2, ERS2 and EIN4, are negative regulators of the ethylene signal pathway, but play a contrasting role in salt tolerance. They possess highly similar amino acid sequences and domain structures. The ethylene binding property of all of the receptors resides in three or four N-terminal transmembrane helices that are located within the membrane of the endoplasmic reticulum[33,34]. These N domains are connected by a GAF domain to a C-terminal His protein kinase domain that is positioned in the cytoplasm[33,34]. ETR1, ETR2, and EIN4 have an additional C-terminal receiver domain[34]. Both gain-of-function and loss-of-function mutants have been described for the five Arabidopsis ethylene receptor genes. Dominant gain-of-function mutations in a single receptor gene lead to ethylene insensitivity; whereas, recessive loss-of-function mutations confer little or no phenotype, but the combination of two or three loss-of-function ethylene receptor mutations confers constitutive ethylene responses[35]. The function of the five Arabidopsis ethylene receptor genes in salt tolerance has been investigated in loss-of-function mutants during germination, finding that ETR1 and EIN4

inhibit, while ETR2 stimulates and ERS1 and ERS2 have no effect on, seed germination under salt stress[36–38]. These contrasting roles do not appear to require an ethylene canonical signalling pathway, but occur by regulating ABA signal transduction[24,25,36,39]. Silencing of alfalfa *MsETR2* abolishes ethylene-triggered tolerance to salt stress, indicating that this ethylene receptor is a positive regulator of salt tolerance in alfalfa[40].

Recently, García et al.[41] isolated four *Cucurbita pepo* mutants, *etr1a, etr1a-1, etr1b* and *etr2b*, all exhibiting a reduced response to ethylene, as well as concomitant changes in developmental traits regulated by ethylene[41–43]. The four mutations affected sex determination in this monoecious species, as well as female fertility. They convert female into male or female-sterile hermaphrodite flowers, which prevents self-fertilisation of homozygous mutant plants, and forces the maintenance of mutations in segregating populations[42,43]. The duplicated genome of *C. pepo*[44] contains six ethylene receptor genes, two paralogs for either *ETR1* (*CpETR1A* and *CpETR1B*), *ERS1* (*CpERS1A* and *CpERS1B*) and *ETR2* (*CpETR2A* and *CpETR2B*), and the identified mutations affect three of the ethylene receptor genes. *etr1a-1* and *etr1a* are A95V and P36L amino acid exchanges in the first and third transmembrane helix of CpETR1A, respectively, *etr1b* is a T94I amino acid exchange in the third transmembrane helix of CpETR1B, and *etr2b* is an E340K amino acid exchange in the coiled-coil domain between the GAF and histidine-kinase domains of CpETR2B[42,43].

In this paper, we investigated the response of *etr1b*, *etr1a*, and *etr2b* gain-of-function mutants to salt stress during germination, seedling establishment, and subsequent vegetative growth. Since the three mutants showed enhanced salt tolerance response during all studied developmental stages and reduced content of Na^+ in photosynthetic organs, we also analysed the molecular mechanisms involved in the enhanced salt tolerance of the *Cucurbita etr* mutants, including accumulation of osmoprotectants and activation of gene networks involved in the biosynthesis of ABA, Ca^{2+} signalling elements, and Na^+ and K^+ membrane transporters reducing the accumulation of toxic Na^+ in shoots and leaves.

Results

Tolerance of *etr1b*, *etr1a*, and *etr2b* to salt stress during germination and early stages of seedling development

To determine the ability of *etr* mutants to germinate in the presence of NaCl, WT and *etr1b*, *etr1a*, and *etr2b* mutant seeds were germinated in both water and 100 mM of NaCl up to 55 h, recording the initiation of seed germination every 2 h. The results are shown in Fig. 1. In water, both WT and the three *etr* mutants showed a similar germination rate, although the mutant seed was slightly delayed with respect to WT (Fig. 1A). The NaCl treatment delayed germination of both WT and *etrs*, but the delayed time was much higher in the WT, meaning that the three *etr* mutants germinated faster than WT under salt stress.

The salt treatment affected WT and mutant seed differently for different germination parameters, including germination initiation, average time for 50% germination, and average germination time (Fig. 1B, D). In water, the assessment of the three germination parameters in *etr* seeds was highly similar to that of WT. Under salt stress, however, there was a significant increase in germination initiation, 50% of germination and average germination time in WT and mutant seeds, but the percentage of increase of these three parameters in NaCl with respect to water was significantly lower in the three mutants compared with their corresponding WT genotypes (Fig. 1B). Taken together, the data revealed that the three *etr* mutants are all more tolerant to salt stress than their corresponding WT during germination.

Seedling growth was also differentially reduced by salinity in WT and ethylene-insensitive mutants (Fig. 2). Radicle and hypocotyl growth rates were both reduced in response to NaCl treatments in WT and *etr* mutants, but the mutant seedlings were always less affected than WT ones (Fig. 2). When germinated and grown in water, the length of the radicle 48 h after germination was similar in WT and mutants, but the reduction of the radicle length under salt stress conditions was much more noticeable in the WT seedlings (Fig. 2A). The same was true for the length of the hypocotyl 3 days after germination, a parameter that was much more reduced in WT than in *etr* mutants (Fig. 2B). Under salt stress, in fact, WT seedlings reduced the length of their hypocotyls by approximately 50%, while *etr* mutants exhibited a reduction of only 20–35% (Fig. 2A, B).

Figure 3A, B shows the effect of salt stress on the root and shoot growth, and root balls of WT and *etr* mutants, 20 days post-germination. Under control conditions, the root and leaf biomass of mutant seedlings was much higher than that of WT, indicating a higher vigour in the three mutant plants (Fig. 3C, D). Although root biomass was decreased considerably under salt stress, that of mutant plants was similar to that of the WT control plants grown in water (Fig. 3C). The biomass of the aerial part of the plant was also significantly higher in the *etr* mutants, and although reduced by the NaCl treatment, the leaf biomass of the mutant plants under salt stress was also higher than that of the WT (Fig. 3D). The reduction in leaf and root biomass in response to salt stress was not significantly different between WT and mutant plants (Fig. 3C, D). These data demonstrate that *etr1b*, *etr1a* and *etr2b* seedlings were more vigorous than those of WT under control and salt conditions, but the responsiveness of WT and mutant plants to salt stress did not

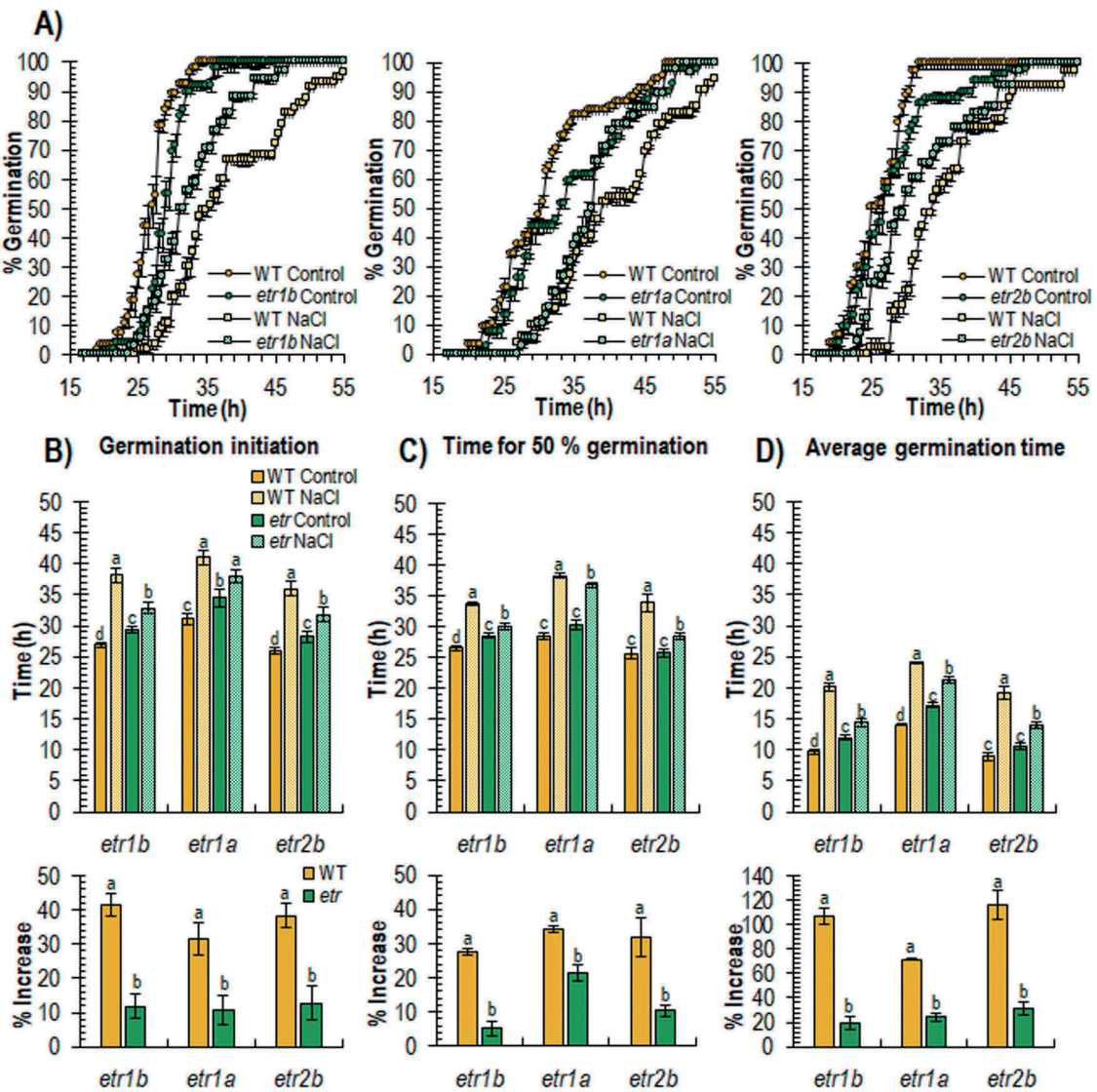

Fig. 1 Effect of salt stress on germination parameters of WT and *etr1b*, *etr1a*, and *etr2b*. **A** Germination rates of WT and *etr1b*, *etr1a*, and *etr2b* ethylene receptor mutants under control and NaCl conditions. The percentage of germination was analysed every 2â€‰h at the indicated time points. The data represent means of three independent replicates with at least 50 seeds counted per replicate. **B**, **C**, and **D** Effect of NaCl stress treatment on germination initiation, time at which 50% of seed is germinated, and average germination time. The bottom graphs show the percentage of increase of each parameter in response to salt stress in WT and mutant plants with respect to plants of the same genotype grown under control conditions. Means were obtained from four independent replicates with at least 50 seeds per replicate. Different letters indicate statistically significant differences (*P*â€‰<â€‰0.05) between samples

significantly differ, at least during the first 20 days of vegetative development.

Growth and ionic balance of WT and *etr2b* plant in response to salt stress

The separation of WT and *etr2b* offspring (see Materials and Methods) allowed further analyses of this ethylene receptor mutant. WT and *etr2b* plants were grown under control and saline conditions up to 45 days after sowing (DAS) (Fig. 4).

The growth of roots, shoots and leaves was always higher in the mutant (Fig. 4) under both control and salt stress, which confirmed the higher vigour of the ethylene receptor mutants observed in previous experiments, and the higher salt tolerance of the mutant. However, the relative response of WT and mutant plants to salt stress differed throughout plant development. At early stages (5 and 10 DAS) *etr2b* and WT responded similarly to salt stress, reducing both plant height and root length (Fig. 4A, B). The reduction in leaf and root biomass

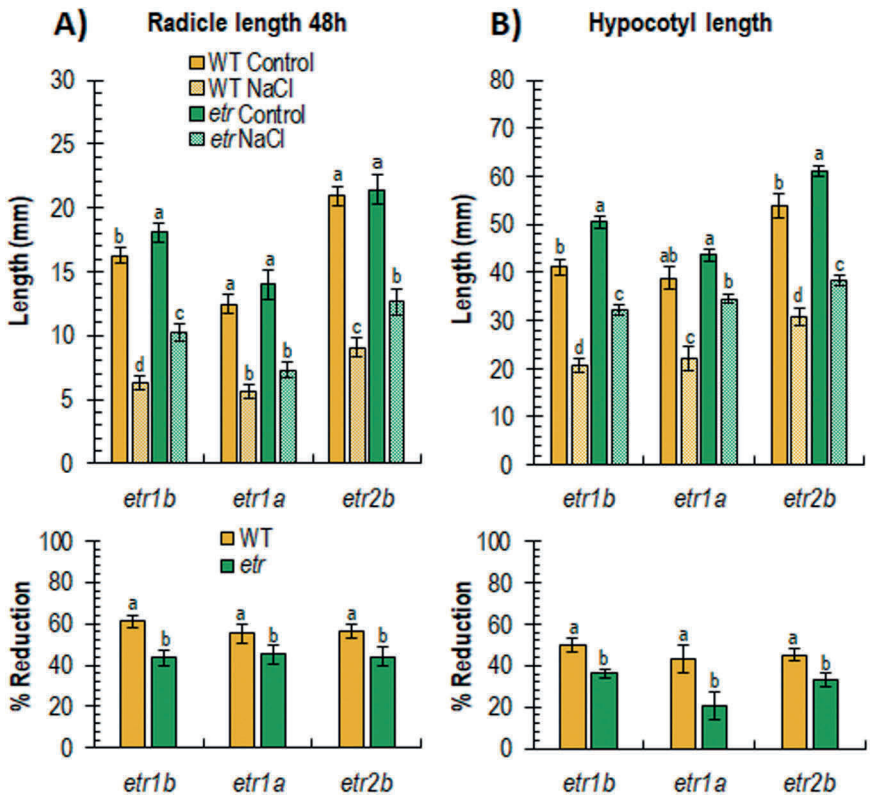

Fig. 2 Effect of salt stress on growth parameters of WT and *etr1b*, *etr1a*, and *etr2b* seedlings. A Effect of salt stress on radicle length at 48 h. **B** Effect of salt stress on hypocotyl length in seedlings growing in darkness for 72 h. The bottom graphs of each figure show the percentage of reduction of each parameter in response to salt stress in WT and mutant plants with respect to plants of the same genotype growing under control conditions. Different letters indicate statistically significant differences ($P < 0.05$) between samples

between 5 and 30 DAS was also similar in WT and mutant plants (Fig. 4C, D). At 45 DAS, however, the salt sensitivity of the mutant was significantly lower than that of the WT, with *etr2b* exhibiting a significantly lower percentage of reduction in leaf and root biomass than WT (Fig. 4C, D). These data indicate that *etr2b*, and probably the other two ethylene receptor mutants, have an enhanced tolerance to salt stress not only during germination, but also during plant vegetative development.

Table 1 shows the effect of salinity on the nutrient content of WT and *etr2b* leaves and roots. For most of the nutrients, no significant differences were found between WT and *etr2b* plants in either roots or in leaves. For K and Ca, no differences were identified between WT and *etr2b*, except that the Ca content was slightly lower in the mutant under non-saline conditions. The total N content was reduced in response to salt stress in both WT and mutant leaves, but no difference was detected between the response of the two genotypes. As expected, salt-stressed plants increased their content of the phytotoxic elements Cl^- and Na. In leaves of salt-stressed plants, Na accumulated at least 4.5 mg/kg more in WT than in *etr2b*, but Cl^- content was found to be similar in the two genotypes. In roots, however, no significant difference was found between WT and *etr2b* for either Na or Cl^- (Table 1).

Comparison of stress metabolites and gene expression in WT and *etr2b* in response to salt stress

To gain insight into the mechanisms that regulate the enhanced salt tolerance of *etr2b*, the content of some metabolites and the expression of genes related to salt stress in different plant systems were measured. Figure 5 shows the contents of proline, total carbohydrate, and anthocyanin in leaves and roots of WT and mutant plants grown under either control or salinity conditions for 45 days. Under control conditions, most of the assessments were similar in WT and *etr2b* plants, although *etr2b* roots showed a decreased content of proline, and *etr2b* leaves reduced their content in total carbohydrates (Fig. 5). In salt-stressed plants, the response of WT and mutant plants was completely dissimilar. Salt induced the accumulation of proline, total carbohydrates and anthocyanins in both roots and leaves of the mutant plants, but hardly changed their contents in WT in either roots or in leaves (Fig. 5A–C).

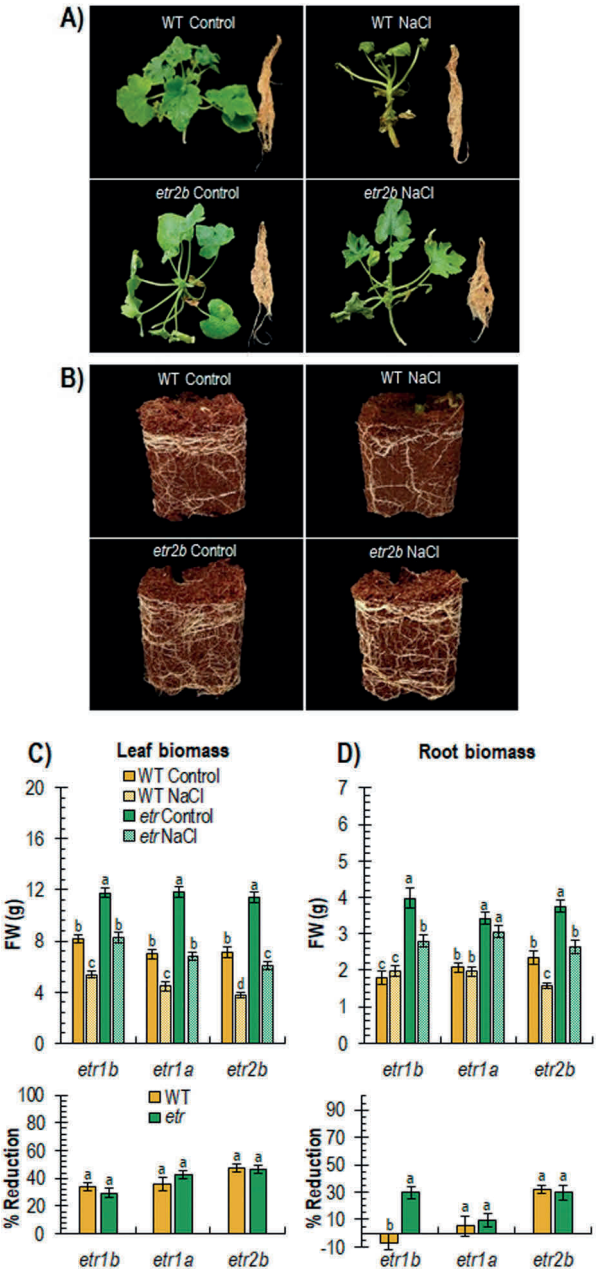

Fig. 3 Effect of salt stress on the growth of WT and *etr1b*, *etr1a*, and *etr2b* plants grown for 20 days under control and NaCl conditions. A WT and *etr2b* shoots and roots. **B** Root balls of WT and *etr2b* plants. **C**, **D** Effect of salt stress on leaf and root biomass. The bottom graphs of each figure show the percentage of reduction of each parameter in response to salt stress in WT and mutant plants with respect to plants of the same genotype growing under control conditions. Different letters indicate statistically significant differences ($P < 0.05$) between samples

The expression of genes associated with abiotic stress tolerance was also compared in WT and *etr2b* plants grown over 45 days under standard and saline stress conditions. Since the *C. pepo* genome is duplicated, we investigated the expression of paralogs from both A and B subgenomes (indicated by the letter A or B at the end of the gene name, respectively). The phylogenetic relationship between *C. pepo* selected genes (Supplementary Table S2) and Arabidopsis homologues with known functions was previously examined for each gene family (Supplementary Fig. S2), thus providing a likely function of the analysed genes in *C. pepo*. In fact, the name that we assigned to each *C. pepo* gene corresponds to the Arabidopsis gene, which had the most conserved protein identity (Supplementary Fig. S2).

The expression of most of the genes associated with salt tolerance was much more induced in the mutant than in the WT plants, indicating an enhanced response of *etr2b* plants to salt stress (Fig. 6). K^+ transporter genes, including K^+ uptake permeases or KUPs (*CpKUP6-1A, CpKUP6-1B and CpKUP6-2A, CpKUP6-2B*), and K^+/H^+ efflux antiporters or KEAs (*CpKEA4-1A, CpKEA4-1B* and *CpKEA4-2A, CpKEA4-2B*), with the exception of *CpKUP6-2A*, were upregulated by NaCl in both WT and *etr2b*, but the upregulation in the mutant was between 2 and 25 times higher than in the WT (Fig. 6A, B). Under control conditions, some of them, including, *CpKEA4-1A*, *CpKEA4-1B*, were also more expressed in mutant than in WT plants.

The same is true for genes encoding Na^+/H^+ exchanger *CpNHX1-3B* and Na^+ transporter *CpHKT1A*, which were only upregulated in *etr2b* plants when grown under saline conditions (Fig. 6C). Of particular interest is the *CpHKT1A* gene, whose expression was already highest in non-stressed mutant plants, and was upregulated more than 300-fold in response to salinity in only the *etr2b* mutant (Fig. 6C). Genes involved in abiotic stress signalling pathways, including Ca^{2+} signalling gene Calmodulin-binding receptor-like kinases *CpCRCK2A* and *CpCRCK2B*, and ABA biosynthesis genes *CpNCED3A* and *CpNCED3B*, were also more highly induced in *etr2b* plants than in WT in response to salt stress (Fig. 6D, E).

Discussion

Ethylene is a key modulator of plant response to salt stress, but its specific role in different plant species and plant developmental stages is unclear[24,27,32]. In Arabidopsis and other plants, including maize and tomato, ethylene positively regulates salt stress tolerance[25,45–47], however, in other plant species, such as rice and tobacco, ethylene plays a negative role in salinity stress response[24,32]. In this paper, we demonstrate that ethylene is also involved in the salt stress response of *C. pepo*. All of the physiological and molecular data presented in this paper indicate that gain-of-function mutations in three *C. pepo* ethylene receptor genes increase salt stress tolerance at germination and during seedling and plant vegetative development, suggesting that ethylene is a negative regulator of salt tolerance in *C. pepo*.

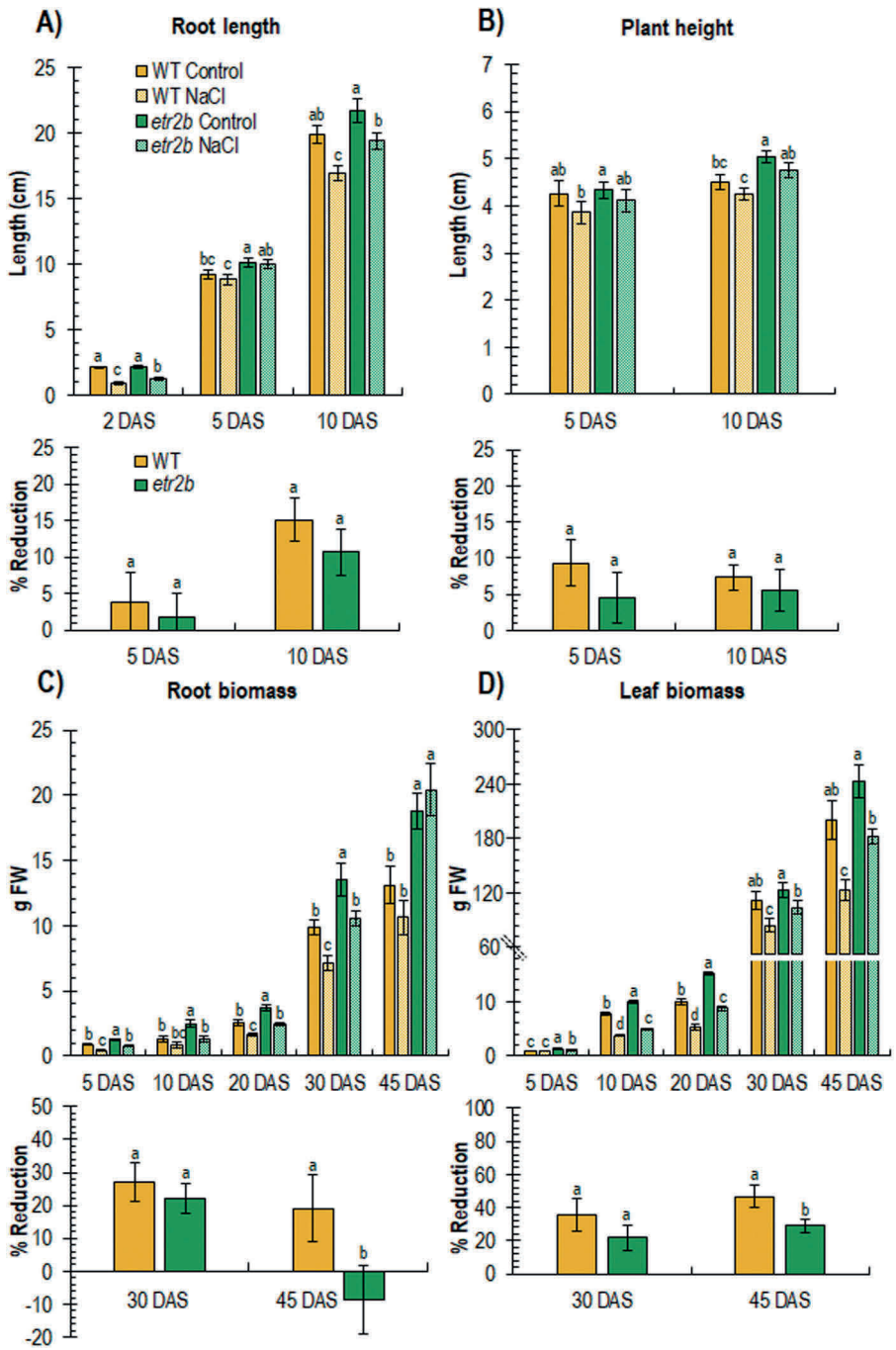

Fig. 4 Effect of salt stress on root and leaf development of WT and ethylene receptor *etr2b* mutant of *C. pepo* at different days after sowing (DAS). The graphs at the top in **A**, **B**, **C** and **D** show the growth rates of root length and plant height, as well as root and leaf biomass, in plants growing under control and NaCl conditions. The graphs at the bottom show the percentage of reduction of the same parameters in response to salt stress in WT and mutant plants with respect to plants growing under control conditions. Different letters indicate statistically significant differences ($P < 0.05$) between samples

ETR receptors modulate salt tolerance response at germination and during seedling and plant vegetative growth

Seed germination is severely affected by salinity, being the first process involved in the stress tolerance response[7]. The phenotypes of loss-of-function mutants in Arabidopsis have demonstrated that ETR1 and EIN4 inhibit, while ETR2 enhances, seed germination under salt stress, and ERS1 and ERS2 have no significant effect on seed

Table 1 Content of macronutrients, micronutrients, and phytotoxic elements in WT and etr2b mutant leaves and roots of plants grown under Control and NaCl conditions for a total of 45 days after sowing (DAS)

	Macronutrients (%)						Micronutrients (mg/kg)					Phytotoxic elements (mg/kg)	
	N total	P	K	Ca	Mg	S	Fe	Mn	Cu	Zn	B	Cl^-	Na
Leaves													
WT control	5.23 a	1.40 a	7.19 a	4.16 ab	0.50 a	0.38 a	187.67 a	202.33 a	5.91 c	77.73 b	131.33 a	45.85 c	1.92 c
WT NaCl	4.54 c	1.20 a	6.85 a	4.06 ab	0.44 a	0.39 a	245.33 a	219.67 a	15.73 a	100.20 a	117.67 a	86.05 a	14.19 a
etr2b control	5.08 b	1.54 a	8.24 a	3.72 b	0.43 a	0.40 a	235.00 a	220.33 a	6.69 c	85.23 ab	125.50 a	63.71 b	1.76 c
etr2b NaCl	4.56 c	1.18 a	7.23 a	4.50 a	0.46 a	0.38 a	199.67 a	240.33 a	10.10 b	86.80 ab	110.00 a	82.73 a	9.61 b
Root													
WT control	3.23 b	1.66 a	2.00 a	1.47 a	0.17 a	0.28 a	319.00 a	165.67 b	8.29 b	69.23 ab	33.80 ab	7.37 b	7.32 b
WT NaCl	3.19 b	1.32 c	2.40 a	0.81 b	0.16 a	0.33 a	292.00 a	212.50 ab	8.57 ab	59.85 b	30.35 bc	20.78 a	13.92 a
etr2b control	3.29 ab	1.58 ab	2.35 a	1.27 ab	0.16 a	0.33 a	312.33 a	178.00 b	9.28 ab	62.77 ab	35.47 a	10.76 b	8.32 b
etr2b NaCl	3.47 a	1.41 bc	2.33 a	1.12 ab	0.16 a	0.33 a	289.67 a	232.00 a	10.95 a	76.50 a	30.33 c	18.82 a	12.91 a

Different letters within the same column indicate significant differences between means ($P < 0.05$)

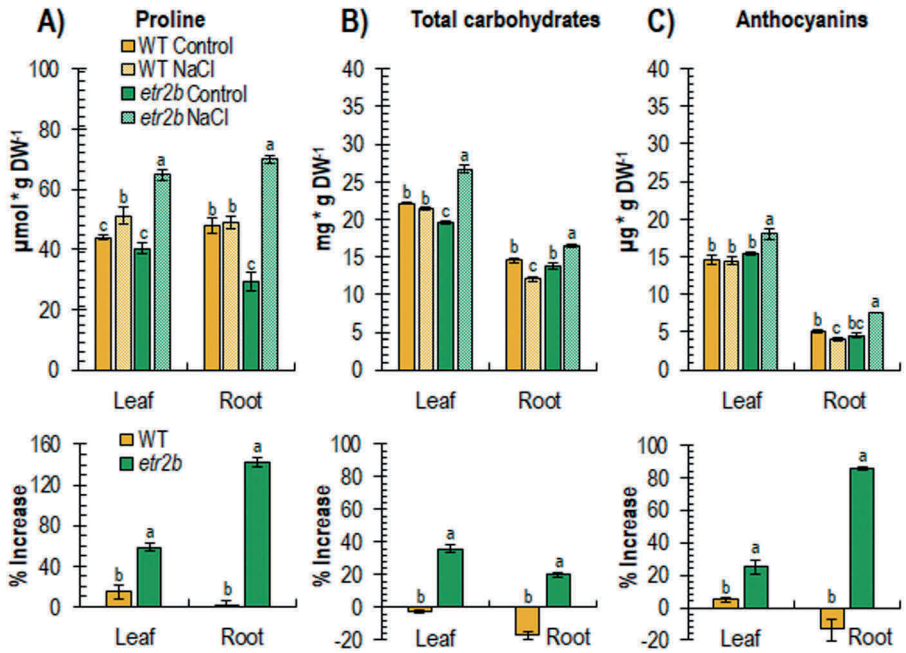

Fig. 5 Content of stress metabolites in WT and *etr2b* mutant leaves of plants growing under control and NaCl conditions for a total of 45 days after sowing (DAS). A, **B** and **C** shows the content of proline, total carbohydrates and anthocyanins, respectively. The bottom graphs show the increment in metabolite content in response to salt stress in WT and mutant plants. DW, dry weight. Different letters indicate statistically significant differences ($P < 0.05$) between samples

germination[36,37,39]. Accordingly, Arabidopsis loss-of-function mutations for ETR1, including *etr1-6* and *etr1-7*, are more tolerant to salt stress and germinate before WT; whereas, gain-of-function mutants for ETR1, including *etr1-1*, *etr1-2* and *etr1-3*, are more sensitive to salt stress and germinate later than WT under salt stress[48–50]. The accelerated germination of the three analysed gain-of-function *etr1b, etr1a*, and *etr2b* of *C. pepo* under salt stress indicate that CpETR1B, CpETR1A, and CpETR2B are positive regulators of squash seed germination under salt stress. If this function is dependent on ethylene and the ethylene signal transduction pathway, ethylene would play a negative role in *C. pepo* salt tolerance, which is similar to what occurs in rice[24]. However, given that in Arabidopsis the function of ETRs in seed germination can take place independently of the canonical

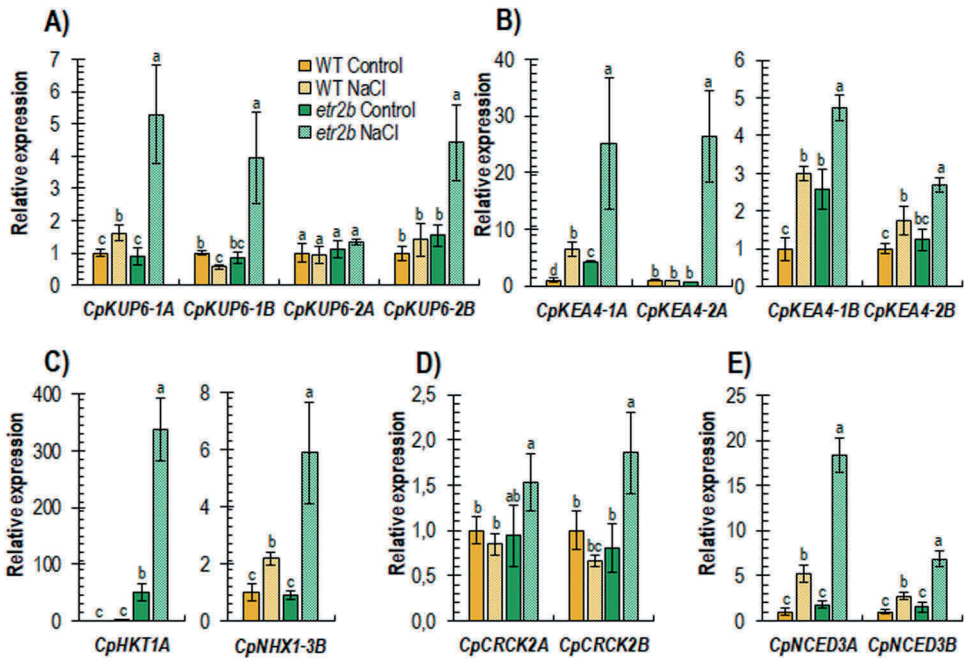

Fig. 6 Relative expression of genes encoding for ion transporters, salt stress signalling and ABA biosynthesis in leaves of WT and etr2b plants grown for 45 days under control and NaCl conditions. A Potassium transporters CpKUPs. **B** K+/H+ efflux antiporters CpKEAs. **C** Sodium transporter CpHKT1A and Na+/H+ exchanger CpNHX1-3B. **D** Calmodulin-binding receptor-like cytoplasmic kinase, CpCRCKs. **E** 9-cis-epoxycarotenoid dioxygenase CpNCEDs, involved in ABA biosynthesis. In each gene family, the number of each gene corresponds to that of Arabidopsis with the highest identity at the protein sequence level, and the A and B letters at the end of each gene corresponds to paralogs derived from the A and B subgenomes of *C. pepo*, respectively. The relative level of each transcript was assessed by qRT–PCR in three independent replicates and normalised by the ΔΔCT method. Different letters indicate statistically significant differences ($P < 0.05$) between samples

ethylene signal transduction pathway, but appears to be mediated by ABA signalling[36,39], it is also likely that the mechanisms underlying the function of squash ETRs under salt stress may also occur through ABA rather than the ethylene signalling pathway. The fact that the three *etrs* exhibit similar salt stress tolerance, but differ in the magnitude of their ethylene response (*etr1b* showed the most residual responsiveness and *etr2b* the least[43]), suggests that the function of *C. pepo* ETRs on germination under salt stress could take place independently of ethylene. The reduced germination rate of ethylene-insensitive *etr* mutants in water may also be the consequence of an increased biosynthesis or sensitivity to ABA, as found in Arabidopsis ethylene-insensitive mutants *etr1* and *ein2*[51]. Furthermore, the higher induction of the ABA biosynthesis genes *CpNCED3A* and *CpNCED3B* in *etr2b* plants under salt stress also supports the involvement of ABA in the salt tolerance of this mutant. The assessment of ABA sensitivity and ABA biosynthesis of *C. pepo etr* mutants in the presence and the absence of NaCl will provide insight into the interactions between ABA and ethylene signalling cascades during seed germination.

We also observed that the three *C. pepo etr* mutations promote seedling and plant growth, resulting in higher plant height, and higher root and leaf biomass when grown under control standard conditions. This higher vegetative vigour of *etr* mutants was also identified in adult plants[42,43], indicating that ethylene is a negative regulator throughout the vegetative development cycle of the plant. The stimulating effect of ethylene insensitivity on vegetative growth was also found in Arabidopsis ethylene-insensitive gain-of-function mutants[49,52,53], although other studies found no differences in total leaf area between WT and the *etr1-1* mutant at earlier stages of vegetative development[54]. The higher constitutive growth and vigour of squash ethylene-insensitive mutants was correlated with their higher salt tolerance during seedling and vegetative plant development. These data contrast with those found in Arabidopsis, in which the higher vegetative growth of the ethylene-insensitive gain-of-function *etr1-1* mutant and the transgenic Arabidopsis plants overexpressing the tobacco ethylene receptor NTHK1 were associated with a higher salt sensitivity, while the reduced seedling growth of the *etr1-7* loss-of-function mutant was associated with greater salt tolerance[49,55]. The reduced ABA sensitivity of *etr1-7* and the enhanced ABA sensitivity of *etr1-1* may account for differences in plant growth and salt-tolerance, as explained for germination[49,51].

The enhanced salt tolerance of *C. pepo etrs* during seedling and plant vegetative growth could result from the inhibitory role of ethylene receptors in the ethylene signalling pathway[42,43]. However, it is also likely that the vegetative growth regulation of ethylene receptors occurs through the abscisic acid signalling pathway, as has been observed for ETRs and EIN2 in Arabidopsis[49,51,56]. Genes involved in both ABA biosynthesis and intracellular Ca^{2+} signalling pathway were more induced in the mutant than in WT, which indicates that these two signalling pathways can coordinate the tolerance response of *etr2b* to salt stress. ABA is known to control the expression of ion transport genes and the influx of Ca^{2+} in the guard cells that leads to stomata closure limiting water loss in leaves[57,58], but also a number of ABA responsive genes that are involved in ion homoeostasis and osmotic adjustment[59].

Mechanisms of salt tolerance in *C. pepo etr* mutants

A number of physiological and molecular responses, including Na^+ detoxification, ion homoeostasis, osmotic adjustment and ROS scavenging, have been developed in plants to combat salt stress[7]. The exclusion of Na^+ in photosynthetic organs is a mechanism that is widely used by salt-tolerant genotypes to maintain vegetative growth while dealing with the high toxicity of these elements in leaves[3]. In our experiments, the leaves of the salt-stressed WT plant accumulated seven times more Na than non-stressed plants, but the leaves of the salt-tolerant *etr2b* only accumulated 5.3 more Na. Given that WT and *etr2b* roots have similar Na content, these data demonstrate a high ability of the salt-tolerant mutant to restrict the transport of Na^+ from roots to leaves.

The exclusion of Na^+ and the higher growth rates of *etr2b* plants are likely to be regulated by the induced Na^+ and K^+ transporter genes in the leaf. As occurs with Arabidopsis AtNHX1 and AtNHX2 Na^+/H^+ antiporters in the tonoplast, the induced *CpNHX1-3B* may be involved in sequestering Na^+ into the vacuole, thus reducing the content of Na^+ in the cytoplasm and alleviating osmotic stress[60,61]. They also function as K^+/H^+ antiporters to maintain K^+ homoeostasis[13]. The CpHTK1A transporter is particularly interesting because it was upregulated 300 times more in *etr2b* than in WT. HTKs are high-affinity transporters for both Na^+ and K^+, mediating root Na^+ uptake, Na^+ unloading from xylem sap, and leaf Na^+ refluxing to the phloem, which are mechanisms that increase leaf Na^+ exclusion[62–65].

Gene expression data also suggest a positive role of the K^+ transporters KEAs and KUPs in combating salt stress. The Arabidopsis KEAs are K^+/H^+ antiporters that mediate pH and K^+ homoeostasis in the inner and thylakoid membranes of chloroplast (KEA1, KEA2, and KEA3) or in endomembrane compartments (KEA4, KEA5, and KEA6)[66,67]. The *C. pepo KEAs* genes that were highly induced in *etr2b* under salt stress are highly homologous to the second clade. KUP/HAK/KT, on the other hand, is a large family of high-affinity K^+ transporters that function in potassium acquisition and translocation from roots to shoots[68,69], facilitate K^+ efflux from the vacuole to regulate osmotic adjustment, and some of them are involved in plant growth and development[58,68,70]. The *C. pepo* KUPs that were upregulated in salt-stressed *etr2b* leaf have a higher homology with Arabidopsis KUP6, an ABA responsive K^+ subfamily transporter that has a key role in osmotic adjustment and K^+ homoeostasis of guard cells[58].

C. pepo etr2b plants induced the accumulation of metabolites, such as proline, total sugars (glucose, fructose, sucrose, and trehalose) and anthocyanins at both the roots and shoots under salt stress, which demonstrates that ethylene receptors and the subsequent ethylene or ABA signal transduction pathways are mediating the production of these osmolytes and therefore the osmotic adjustment of cells under salt stress[71]. These osmolytes can lower osmotic potential[72], but can also act as stabilisers of proteins and cell components against ion toxicity and NaCl-induced oxidative damage[71,73]. Proline is perhaps the main salinity-related osmolyte, and is considered a biochemical marker of salt stress[74]. Exogenous proline treatments and transgenics plants with enhanced production of proline are more tolerant to salt, while mutants that are deficient in proline exhibited a limited growth and development under salt stress[75,76]. The biosynthesis of proline and other osmolytes is induced by ABA in different systems[77], suggesting again that the enhanced response of mutant ethylene receptors of *C. pepo* to salt stress is likely mediated by ABA.

Materials and methods

Plant material

The ethylene receptor mutants analysed in this study, *etr1b*, *etr1a* and *etr2b*, were selected from a high-throughput screening of a *Cucurbita pepo* mutant collection by using the triple response of etiolated seedlings to ethylene[41]. In addition to their reduced triple response to ethylene, the three mutations convert female into hermaphrodite or male flowers, reducing or preventing self-fertilisation[42,43]. The mutants were therefore maintained in BC_2S_1 segregating generations, obtained by crossing each mutant twice or more times with the background genotype MUC16, and then selfed. The mutations affect *CpETR1B*, *CpETR1A*, and *CpETR2B* genes; thus, the WT and mutant plants in segregating populations were selected by detecting the WT and *etr1b, etr1a*, and *etr2b* alleles using real-time PCR with TaqMan probes[42,43]. DNA was isolated from the cotyledon of seedlings after the development of the first true leaf (5 or

7 days after sowing, DAS) by using the CTAB protocol. The multiplex PCRs were done using the Bioline Sensi-FAST™ Probe No-ROX Kit, a set of forward and reverse primers amplifying the polymorphic sequence, and two allele-specific probes descriptive of the SNP of interest. The WT probe was labelled with FAM dye, while the mutant probe was labelled with HEX reporter dye. BHQ1 quencher molecule was used in both probes (Supplementary Table S1).

Seed germination under salinity stress

Seed germination of WT and *etr1b*, *etr1a*, and *etr2b* was tested under salinity stress. Seeds were sterilised with a 5% sodium hypochlorite solution for 10 min and rinsed in distilled water three times, before being incubated in 50 ml Falcon tubes containing 25 ml of distilled water (control) or 100 mM NaCl for 12 h at 25 °C in darkness under continuous shaking. After the imbibition, the seeds were transferred to a dispositive designed to study seed germination (Supplementary Fig. S1). Seeds were placed in a foam strip between two pieces of filter paper and two panes of glass of 12 × 20 cm. This "sandwich glass" was secured with two clips and situated vertically in a recipient with water (control) or 100 mM NaCl solution for seeds to germinate and grow vertically. The sandwich glass with seeds was then incubated in a growth chamber in darkness at 24 °C and 80% RH for 55 h. Three-hundred BC_2S_1 seeds, segregating for each *etr* mutant, were germinated and grown using both water and salt in four independent experiments.

The germinated seeds were recorded every 2 h for 55 h through digital images that were processed using ImageJ®. Seeds were considered germinated when the seed coat was broken and primary root protrusion was visible (>1 mm). Germination initiation, time of germination at 50% of seeds, and average germination time were determined according to procedures described by Ranal and De Santana[78]. Root elongation from both WT and *ert* mutants was assessed from seedling images at 48 h of initiating germination.

Seedling and plantlets growth under salinity stress

After germination, seeds were transplanted into 54 seedling trays filled with a mixture of perlite and coconut fibre (20–80%), a substrate with low-cation exchange capacity. 150 seeds of each genotype (WT/WT and *etr*/*etr*), 75 germinated under salt stress and 75 germinated in water, were distributed in three independent experiments. Trays were incubated in a growth chamber in darkness at 24 °C and 80% RH for 72 h, and hypocotyl elongation was assessed in all plants. Control seedlings were irrigated with a nutritive Hoogland solution with a conductivity of 2 dS/m; whereas, for those subjected to salt stress, the nutritive solution was supplemented with 35 mM of NaCl, which increased its conductivity to 5 dS/m.

Seedlings of each segregating population were then genotyped with Taqman probes, and 72 WT/WT and 72 *etr*/*etr* plants from each mutant family were transplanted into 1 l pots containing the same substrate as previously, and grown for 20 additional days at 24 °C under long-day photoperiod (16 h light/8 h dark) and 70% RH in three independent experiments. Half of the plants (36) continued to be irrigated with the standard nutritive solution as previously, while the other half (36) were supplemented with 35 mM of NaCl. Leaf and root biomass were compared between each WT and *ert* mutant grown under both control and salinity conditions.

Vegetative growth of WT and *etr2b* under salinity stress

Although *etr* mutations affect female fertility and prevent selfing[42,43], we were able to pollinate the mutant flowers several days prior to anthesis, thus forcing self-fertilisation of the mutant plants and obtaining 100% mutant offspring. This was only achieved in the *etr2b* mutant, which allowed the evaluation of a higher number of plants implementing the analysis of growth parameters in additional plant developmental stages, as well as biochemical and gene expression studies in this mutant. In this mutant family, separated WT and *ert2b* plants were cultivated for up to 45 days under either control or salt conditions following the protocol described in the previous section. The development of different growth parameters, including root length, plant height, and root and leaf fresh and dry weight, were compared between WT and *ert2b* at 5, 10, 20, 30, and 45 DAS. Three independent replicates of ten plants each were analysed for each genotype and irrigation conditions at each developmental stage. At 45 DAS, plants were also used to analyse the effect of *etr2b* mutation on the content in micro- and macro-elements, the accumulation of stress metabolites, and the relative expression of stress-related genes.

Evaluation of stress-associated metabolites in WT and *etr2b* plants

The concentration of different stress metabolites, including proline, total carbohydrates and anthocyanins, was assessed in dry leaves and dry roots of WT and *etr2b* plants at 45 DAS under control and salinity stress conditions. All determinations were carried out in triplicate, each containing plant material from four plants.

Proline was determined through the ninhydrin method[79] with minor modifications. 100 mg of dry sample was incubated in a 2 ml of ethanol 60% at 4 °C for 12 h. 0.5 ml of this solution was then mixed with 1 ml of ninhydrin 1%, dissolved in 60% acetic acid, and incubated at 95 °C for 20 min at room temperature. Proline concentration was finally determined by spectrophotometry at 520 nm, and expressed as μmol/g DW. Total carbohydrates concentration was assessed by the phenol-

sulphuric method[80] with minor modifications. 100 mg of dry sample was incubated in 5 ml of ethanol 80% at 80 °C for 1 h, and 1 ml of this solution was then mixed with 1 ml of a solution of phenol 5% and 5 ml of sulphuric acid 95–97%. Total carbohydrates were determined at 490 nm, and expressed as mg/g DW. Anthocyanin content was measured according to Mancinelli[81]. 100 mg of dry sample was incubated at 4 °C for 12 h in 3 ml of a solution of ethanol acidified with 1% of HCl 37%. The spectrophotometry measurements were done at 530 and 657 nm, and the concentrations expressed as μg/g DW. All spectrophotometric readings were performed on 96-well microplates using the BioTek® UV-Visible Epoch™ spectrophotometer.

Comparison of micro- and macro-elements in WT and *etr2b* plants

Micro- and macro-elements were measured in 5 g of dry leaves and roots coming from the same three samples for each genotype and salinity condition used in the determination of stress metabolites. The elemental measurements were carried out according to the standard protocols dictated by the International Organisation for Standardisation (ISO) (https://www.iso.org/home.html). Total nitrogen was measured through elemental analysis (ISO-13878), chloride was determined by fragmented flow analysis (ISO-15682), and the rest of macro- and micronutrients studied (phosphorus, potassium, calcium, magnesium, sulphur, iron, manganese, copper, zinc, boron, molybdenum, and sodium) were assessed by ICP-OES Spectrophotometry (ISO-11885).

Assessment of gene expression by qRT–PCR in WT and *etr2b* plant

The relative expression of different salt-stress-associated genes was assessed by quantitative reverse transcription (qRT)–PCR in WT and *etr2b* plants grown under control and salt conditions for 45 DAS. The analysis was performed in three biological replicates for each genotype and growing condition, each one derived from a pool of leaves from four plants. Total RNA was isolated from 1 g of leaves according to the protocol of the GeneJET Plant RNA Purification Kit (Thermo Fisher). RNA was reverted to cDNA with the ADNc RevertAid™ Kit (Thermo Fisher). The qRT–PCR was performed in 10 μl total volume with 1×Top Green qPCR Super Mix (BioRad) in the CFX96 Touch Real-Time PCR Detection System Thermocycler (BioRad). The gene expression values were calculated using the $2^{-\Delta\Delta CT}$ method[82]. EF1α was used as the internal reference gene. Supplementary Table S2 shows the primers used for qRT–PCR reactions in each analysed gene.

Phylogenetic analysis

MEGA 10 software[83] was used to establish the phylogenetic relationships between *C. pepo* and *Arabidopsis thaliana* genes encoding for Na^+ and K^+ membrane transporters (KUPs, KEAs, NHXs, and HKTs), abscisic acid biosynthesis enzymes (NCEDs), and Calmodulin-binding receptor-like cytoplasmic kinases (CRCKs). Phylogenetic trees were performed using the Maximum Likelihood method based on the Poisson correction model, with 2000 bootstrap replicates. The protein sequences and information were obtained from the Arabidopsis Information Resource (https://www.arabidopsis.org/) and the Cucurbit Genomic Database (http://cucurbitgenomics.org/).

Statistical analysis

Data were analysed for multiple comparisons by analysis of variance (ANOVA) using the statistical software Statgraphic Centurion XVIII. Differences between genotypes and treatments were separated by the least significant difference (LSD) at a significance level of $P \leq 0.05$.

Acknowledgements

This work has been supported by grant AGL2017-82885-C2-1-R, partly funded by the ERDF (European Regional Development Fund) and by the Spanish Ministry of Science and Innovation, and grant P12-AGR-1423, funded by Junta de Andalucía, Spain. G.C. and J.I. acknowledge FPU and FPI scholarship programmers from MEC, and C.M. is awarded a Hipatia post-doctoral grant.

Conflict of interest

The authors declare no competing interests.

Supplementary Information The online version contains supplementary material available at https://doi.org/10.1038/s41438-021-00508-z.

Received: 13 November 2020 Revised: 19 January 2021 Accepted: 24 January 2021
Published online: 01 April 2021

References

1. Zhang, P., Zhang, J. & Chen, M. Economic impacts of climate change on agriculture: the importance of additional climatic variables other than temperature and precipitation. *J. Environ. Econ. Manag.* **83**, 8–31 (2016).
2. Montanarella, L. et al (eds). *Status of the World's Soil Resources (Swsr)-main Report*. (FAO, 2015).
3. Isayenkov, S. V. & Maathuis, F. J. M. Plant salinity stress: many unanswered questions remain. *Front. Plant Sci.* **10**, 80 (2019).
4. Gull, A., Ahmad Lone, A. & Ul Islam Wani, N. in *Abiotic and Biotic Stress in Plants* (ed. De Oliveira, A.) 3–9 (IntechOpen, 2019).
5. Demidchik, V. & Maathuis, F. J. M. Physiological roles of nonselective cation channels in plants: from salt stress to signalling and development. *N. Phytol.* **175**, 387–404 (2007).
6. Jiang, Z. et al. Plant cell-surface GIPC sphingolipids sense salt to trigger Ca2+ influx. *Nature* **572**, 341–346 (2019).
7. Van Zelm, E., Zhang, Y. & Testerink, C. Salt tolerance mechanisms of plants. *Annu. Rev. Plant Biol.* **71**, 403–433 (2020).
8. Choi, W. G., Toyota, M., Kim, S. H., Hilleary, R. & Gilroy, S. Salt stress-induced Ca2 + waves are associated with rapid, long-distance root-to-shoot signaling in plants. *Proc. Natl Acad. Sci. USA* **111**, 6497–6502 (2014).

9. Manishankar, P., Wang, N., Köster, P., Alatar, A. A. & Kudla, J. Calcium signaling during salt stress and in the regulation of ion homeostasis. *J. Exp. Bot.* **69**, 4215–4226 (2018).
10. Sunarpi et al. Enhanced salt tolerance mediated by AtHKT1 transporter-induced Na+ unloading from xylem vessels to xylem parenchyma cells. *Plant J.* **44**, 928–938 (2005).
11. Pardo, J. M. Biotechnology of water and salinity stress tolerance. *Curr. Opin. Biotechnol.* **21**, 185–196 (2010).
12. Rodríguez-Rosales, M. P. et al. Plant NHX cation/proton antiporters. *Plant Signal. Behav.* **4**, 265–276 (2009).
13. Bassil, E. et al. The Arabidopsis Na+/H+ antiporters NHX1 and NHX2 control vacuolar pH and K+ homeostasis to regulate growth, flower development, and reproduction. *Plant Cell* **23**, 3482–3497 (2011).
14. Reguera, M. et al. pH regulation by NHX-type antiporters is required for receptor-mediated protein trafficking to the vacuole in Arabidopsis. *Plant Cell* **27**, 1200–1217 (2015).
15. Apse, M. P., Aharon, G. S., Snedden, W. A. & Blumwald, E. Salt tolerance conferred by overexpression of a vacuolar Na+/H+ antiport in Arabidopsis. *Science (80-.)* **285**, 1256–1258 (1999).
16. Zhang, H. X. & Blumwald, E. Transgenic salt-tolerant tomato plants accumulate salt in foliage but not in fruit. *Nat. Biotechnol.* **19**, 765–768 (2001).
17. Mian, A. et al. Over-expression of an Na+- and K+- permeable HKT transporter in barley improves salt tolerance. *Plant J.* **68**, 468–479 (2011).
18. Slama, I., Abdelly, C., Bouchereau, A., Flowers, T. & Savouré, A. Diversity, distribution and roles of osmoprotective compounds accumulated in halophytes under abiotic stress. *Ann. Bot.* **115**, 433–447 (2015).
19. Munns, R. & Gilliham, M. Salinity tolerance of crops-what is the cost? *N. Phytol.* **208**, 668–673 (2015).
20. Niu, M. et al. Root respiratory burst oxidase homologue-dependent H2O2 production confers salt tolerance on a grafted cucumber by controlling Na+ exclusion and stomatal closure. *J. Exp. Bot.* **69**, 3465–3476 (2018).
21. Keunen, E., Peshev, D., Vangronsveld, J., Van Den Ende, W. & Cuypers, A. Plant sugars are crucial players in the oxidative challenge during abiotic stress: extending the traditional concept. *Plant. Cell Environ.* **36**, 1242–1255 (2013).
22. Lockhart, J. Salt of the earth: ethylene promotes salt tolerance by enhancing Na/K homeostasis. *Plant Cell* **25**, 3150 (2013).
23. Verma, R. K. et al. Overexpression of ABA receptor PYL10 gene confers drought and cold tolerance to indica rice. *Front. Plant Sci.* **10**, 1488 (2019).values were calculated
24. Tao, J. J. et al. The role of ethylene in plants under salinity stress. *Front. Plant Sci.* **6**, 1–12 (2015).
25. Arraes, F. B. et al. Implications of ethylene biosynthesis and signaling in soybean drought stress tolerance. *BMC Plant Biol.* **15**, 1–20 (2015).
26. Albacete, A. et al. Rootstock-mediated changes in xylem ionic and hormonal status are correlated with delayed leaf senescence, and increased leaf area and crop productivity in salinized tomato. *Plant Cell Environ.* **32**, 928–938 (2009).
27. Riyazuddin, R. et al. Ethylene: a master regulator of salinity stress tolerance in plants. *Biomolecules* **10**, 959 (2020).
28. Peng, J. et al. Salt-induced stabilization of EIN3/EIL1 confers salinity tolerance by deterring ROS accumulation in Arabidopsis. *PLoS Genet.* **10**, e1004664 (2014).
29. Dong, H. et al. Loss of ACS7 confers abiotic stress tolerance by modulating ABA sensitivity and accumulation in Arabidopsis. *J. Exp. Bot.* **62**, 4875–4887 (2011).
30. Chen, D. et al. A wheat aminocyclopropane-1-carboxylate oxidase gene, TaACO1, negatively regulates salinity stress in Arabidopsis thaliana. *Plant Cell Rep.* **33**, 1815–1827 (2014).
31. Li, C. H. et al. The receptor-like kinase SIT1 mediates salt sensitivity by activating MAPK3/6 and regulating ethylene homeostasis in rice. *Plant Cell* **26**, 2538–2553 (2014).
32. Yang, C., Lu, X., Ma, B., Chen, S. Y. & Zhang, J. S. Ethylene signaling in rice and Arabidopsis: conserved and diverged aspects. *Mol. Plant* **8**, 495–505 (2015).
33. Ju, C. & Chang, C. Mechanistic insights in ethylene perception and signal transduction. *Plant Physiol.* **169**, 85–95 (2015).
34. Binder, B. M., Chang, C. & Schaller, G. E. in *Annual Plant Reviews*. Vol. 44 (ed. McManus, M. T.) 117–145 (Wiley-Blackwell, 2012).
35. Hua, J. & Meyerowitz, E. M. Ethylene responses are negatively regulated by a receptor gene family in Arabidopsis thaliana. *Cell* **94**, 261–271 (1998).
36. Wilson, R. L., Kim, H., Bakshi, A. & Binder, B. M. The ethylene receptors ETHYLENE RESPONSE1 and ETHYLENE RESPONSE2 have contrasting roles in seed germination of Arabidopsis during salt stress. *Plant Physiol.* **165**, 1353–1366 (2014).
37. Wilson, R. L., Bakshi, A. & Binder, B. M. Loss of the ETR1 ethylene receptor reduces the inhibitory effect of far-red light and darkness on seed germination of Arabidopsis thaliana. *Front. Plant Sci.* **5**, 433 (2014).
38. Bakshi, A. et al. Identification of regions in the receiver domain of the ETHYLENE RESPONSE1 ethylene receptor of Arabidopsis important for functional divergence. *Plant Physiol.* **169**, 219–232 (2015).
39. Bakshi, A. et al. Ethylene receptors signal via a noncanonical pathway to regulate abscisic acid responses. *Plant Physiol.* **176**, 910–929 (2018).
40. Wang, Y. et al. Ethylene enhances seed germination and seedling growth under salinity by reducing oxidative stress and promoting chlorophyll content via ETR2 pathway. *Front. Plant Sci.* **11**, 1066 (2020).
41. García, A. et al. Phenomic and genomic characterization of a mutant platform in Cucurbita pepo. *Front. Plant Sci.* **9**, 1049 (2018).
42. García, A. et al. The ethylene receptors CpETR1A and CpETR2B cooperate in the control of sex determination in Cucurbita pepo. *J. Exp. Bot.* **71**, 154–167 (2020).
43. García, A., Aguado, E., Garrido, D., Martínez, C. & Jamilena, M. Two androecious mutations reveal the crucial role of ethylene receptors in the initiation of female flower development in Cucurbita pepo. *Plant J.* **103**, 1548–1560 (2020).
44. Montero-Pau, J. et al. De novo assembly of the zucchini genome reveals a whole-genome duplication associated with the origin of the Cucurbita genus. *Plant Biotechnol. J.* **16**, 1161–1171 (2018).
45. Zhao, X. C. & Schaller, G. E. Effect of salt and osmotic stress upon expression of the ethylene receptor ETR1 in Arabidopsis thaliana. *FEBS Lett.* **562**, 189–192 (2004).
46. Yang, L., Zu, Y. G. & Tang, Z. H. Ethylene improves Arabidopsis salt tolerance mainly via retaining K+ in shoots and roots rather than decreasing tissue Na+ content. *Environ. Exp. Bot.* **86**, 60–69 (2013).
47. Gharbi, E. et al. Inhibition of ethylene synthesis reduces salt-tolerance in tomato wild relative species Solanum chilense. *J. Plant Physiol.* **210**, 24–37 (2017).
48. Chiwocha, S. D. et al. The etr1-2 mutation in Arabidopsis thaliana affects the abscisic acid, auxin, cytokinin and gibberellin metabolic pathways during maintenance of seed dormancy, moist-chilling and germination. *Plant J.* **42**, 35–48 (2005).
49. Wang, Y., Wang, T., Li, K. & Li, X. Genetic analysis of involvement of ETR1 in plant response to salt and osmotic stress. *Plant Growth Regul.* **54**, 261–269 (2008).
50. Li, Z., Peng, J., Wen, X. & Guo, H. ETHYLENE-INSENSITIVE3 is a senescence-associated gene that accelerates age-dependent leaf senescence by directly repressing miR164 transcription in Arabidopsis. *Plant Cell* **25**, 3311–3328 (2013).
51. Beaudoin, N., Serizet, C., Gosti, F. & Giraudat, J. Interactions between abscisic acid and ethylene signaling cascades. *Plant Cell* **12**, 1103–1115 (2000).
52. Bleecker, A. B., Estelle, M. A., Somerville, C. & Kende, H. Insensitivity to ethylene conferred by a dominant mutation in Arabidopsis thaliana. *Science. (80-.)* **241**, 1086–1089 (1988).
53. Grbic, V. & Bleecker, A. B. Ethylene regulates the timing of leaf senescence in Arabidopsis. *Plant J.* **8**, 595–602 (1995).
54. Tholen, D., Voesenek, L. A. C. J. & Poorter, H. Ethylene insensitivity does not increase leaf area or relative growth rate in Arabidopsis, Nicotiana tabacum, and Petunia x hybrida. *Plant Physiol.* **134**, 1803–1812 (2004).
55. Cao, W. H. et al. in *Advances in Plant Ethylene Research* (eds Klee, H. et al) 333–339 (Springer, 2007).
56. Kazan, K. Diverse roles of jasmonates and ethylene in abiotic stress tolerance. *Trends Plant Sci.* **20**, 219–229 (2015).
57. DeFalco, T. A., Bender, K. W. & Snedden, W. A. Breaking the code: Ca2+ sensors in plant signalling. *Biochem. J.* **425**, 27–40 (2010).
58. Osakabe, Y. et al. Osmotic stress responses and plant growth controlled by potassium transporters in Arabidopsis. *Plant Cell* **25**, 609–624 (2013).
59. Verslues, P. E. & Bray, E. A. Role of abscisic acid (ABA) and Arabidopsis thaliana ABA-insensitive loci in low water potential-induced ABA and proline accumulation. *J. Exp. Bot.* **57**, 201–212 (2006).
60. Leidi, E. O. et al. The AtNHX1 exchanger mediates potassium compartmentation in vacuoles of transgenic tomato. *Plant J.* **61**, 495–506 (2010).
61. Fukuda, A., Nakamura, A., Hara, N., Toki, S. & Tanaka, Y. Molecular and functional analyses of rice NHX-type Na+/H+ antiporter genes. *Planta* **233**, 175–188 (2011).

62. Berthomieu, P. et al. Functional analysis of AtHKT1 in Arabidopsis shows that Na+ recirculation by the phloem is crucial for salt tolerance. *EMBO J.* **22**, 2004–2014 (2003).
63. Garciadeblás, B., Senn, M. E., Bañuelos, M. A. & Rodríguez-Navarro, A. Sodium transport and HKT transporters: the rice model. *Plant J.* **34**, 788–801 (2003).
64. Horie, T., Hauser, F. & Schroeder, J. I. HKT transporter-mediated salinity resistance mechanisms in Arabidopsis and monocot crop plants. *Trends Plant Sci.* **14**, 660–668 (2009).
65. Kobayashi, N. I. et al. OsHKT1;5 mediates Na+ exclusion in the vasculature to protect leaf blades and reproductive tissues from salt toxicity in rice. *Plant J.* **91**, 657–670 (2017).
66. Kunz, H. H. et al. Plastidial transporters KEA1, -2, and -3 are essential for chloroplast osmoregulation, integrity, and pH regulation in Arabidopsis. *Proc. Natl Acad. Sci. USA* **111**, 7480–7485 (2014).
67. Zhu, X. et al. K+ efflux antiporters 4, 5, and 6 mediate pH and K+ homeostasis in endomembrane compartments. *Plant Physiol.* **178**, 1657–1678 (2018).
68. Yang, T. et al. The role of a potassium transporter OsHAK5 in potassium acquisition and transport from roots to shoots in rice at low potassium supply levels. *Plant Physiol.* **166**, 945–959 (2014).
69. Han, M., Wu, W., Wu, W. H. & Wang, Y. Potassium transporter KUP7 is involved in K+ acquisition and translocation in Arabidopsis root under K+-limited conditions. *Mol. Plant.* **9**, 437–446 (2016).
70. Grabov, A. Plant KT/KUP/HAK potassium transporters: single family-multiple functions. *Ann. Bot.* **99**, 1035–1041 (2007).
71. Nahar, K., Hasanuzzaman, M. & Fujita, M. in *Osmolytes and Plants Acclimation to Changing Environment: Emerging Omics Technologies* (eds Iqbal, N., Nazar, R. & Khan, N. A.) 37–68 (Springer, 2015).
72. Argiolas, A., Puleo, G. L., Sinibaldi, E. & Mazzolai, B. Osmolyte cooperation affects turgor dynamics in plants. *Sci. Rep.* **6**, 1–8 (2016).
73. Gharsallah, C., Fakhfakh, H., Grubb, D. & Gorsane, F. Effect of salt stress on ion concentration, proline content, antioxidant enzyme activities and gene expression in tomato cultivars. *AoB Plants* **8**, plw055 (2016).
74. Hayat, S. et al. Role of proline under changing environments: a review. *Plant Signal. Behav.* **7**, 1456–1466 (2012).
75. Khedr, A. H. A., Abbas, M. A., Wahid, A. A. A., Quick, W. P. & Abogadallah, G. M. Proline induces the expression of salt-stress-responsive proteins and may improve the adaptation of Pancratium maritimum L. to salt-stress. *J. Exp. Bot.* **54**, 2553–2562 (2003).
76. Simon-Sarkadi, L., Kocsy, G., Várhegyi, Á., Galiba, G. & De Ronde, J. A. Stress-induced changes in the free amino acid composition in transgenic soybean plants having increased proline content. *Biol. Plant.* **50**, 793–796 (2006).
77. Yu, Z. et al. How plant hormones mediate salt stress responses. *Trends Plant Sci.* **25**, 1117–1130 (2020).
78. Ranal, M. A. & De Santana, D. G. How and why to measure the germination process? *Rev. Bras. Bot.* **29**, 1–11 (2006).
79. Abrahám, E., Hourton-Cabassa, C., Erdei, L. & Szabados, L. Methods for determination of proline in plants. *Methods Mol. Biol.* **639**, 317–331 (2010).
80. Chow, P. S. & Landhäusser, S. M. A method for routine measurements of total sugar and starch content in woody plant tissues. *Tree Physiol.* **24**, 1129–1136 (2004).
81. Mancinelli, A. L. Interaction between light quality and light quantity in the photoregulation of anthocyanin production. *Plant Physiol.* **92**, 1191–1195 (1990).
82. Livak, K. J. & Schmittgen, T. D. Analysis of relative gene expression data using real-time quantitative PCR and the $2^{-\Delta\Delta CT}$ method. *Methods* **25**, 402–408 (2001).
83. Kumar, S., Stecher, G., Li, M., Knyaz, C. & Tamura, K. MEGA X: molecular evolutionary genetics analysis across computing platforms. *Mol. Biol. Evol.* **35**, 1547–1549 (2018).

frontiers in Plant Science

ORIGINAL RESEARCH
published: 24 January 2022
doi: 10.3389/fpls.2021.817922

The Ethylene Biosynthesis Gene *CpACO1A*: A New Player in the Regulation of Sex Determination and Female Flower Development in *Cucurbita pepo*

Gustavo Cebrián[1†], Jessica Iglesias-Moya[1†], Jonathan Romero[1†], Cecilia Martínez[1†], Dolores Garrido[2†] and Manuel Jamilena[1*†]

[1] Department of Biology and Geology, Agrifood Campus of International Excellence and Research Centre CIAMBITAL, University of Almería, Almería, Spain, [2] Department of Plant Physiology, University of Granada, Granada, Spain

A methanesulfonate-generated mutant has been identified in *Cucurbita pepo* that alters sex determination. The mutation converts female into hermaphrodite flowers and disrupts the growth rate and maturation of petals and carpels, delaying female flower opening, and promoting the growth rate of ovaries and the parthenocarpic development of the fruit. Whole-genome resequencing allowed identification of the causal mutation of the phenotypes as a missense mutation in the coding region of *CpACO1A*, which encodes for a type I ACO enzyme that shares a high identity with *Cucumis sativus* CsACO3 and *Cucumis melo* CmACO1. The so-called *aco1a* reduced ACO1 activity and ethylene production in the different organs where the gene is expressed, and reduced ethylene sensitivity in flowers. Other sex-determining genes, such as *CpACO2B*, *CpACS11A,* and *CpACS27A*, were differentially expressed in the mutant, indicating that ethylene provided by CpACO1A but also the transcriptional regulation of *CpACO1A*, *CpACO2B*, *CpACS11A*, and *CpACS27A* are responsible for determining the fate of the floral meristem toward a female flower, promoting the development of carpels and arresting the development of stamens. The positive regulation of ethylene on petal maturation and flower opening can be mediated by inducing the biosynthesis of JA, while its negative control on ovary growth and fruit set could be mediated by its repressive effect on IAA biosynthesis.

Keywords: *ACO* gene regulation, andromonoecy, monoecy, ethylene, flower maturation, parthenocarpy

HIGHLIGHTS

- CpACO1A is a type I ACO enzyme involved in ethylene production in different *Cucurbita pepo* organs.
- A mutation in *CpACO1A* disrupts ethylene production and converts female into hermaphrodite flowers.
- Transcription of the ethylene biosynthesis genes is feedback-regulated in the female flower.
- The mutation *aco1a* alters the homeostasis of IAA, ABA, JA, and SA in the female flower.

OPEN ACCESS

Edited by:
Silvia Vieira Coimbra, University of Porto, Portugal

Reviewed by:
Ana Maria Rocha De Almeida, California State University, East Bay, United States
Tangren Cheng, Beijing Forestry University, China
Haifeng Li, Northwest A&F University, China
Simona Masiero, University of Milan, Italy

***Correspondence:**
Manuel Jamilena
mjamille@ual.es

†ORCID:
Gustavo Cebrián
orcid.org/0000-0001-8969-1976
Jessica Iglesias-Moya
orcid.org/0000-0002-4632-8162
Jonathan Romero
orcid.org/0000-0003-0812-0309
Cecilia Martínez
orcid.org/0000-0003-0464-1828
Dolores Garrido
orcid.org/0000-0002-0426-7146
Manuel Jamilena
orcid.org/0000-0001-7072-0458

Specialty section:
This article was submitted to Plant Breeding, a section of the journal Frontiers in Plant Science

Received: *18 November 2021*
Accepted: *27 December 2021*
Published: *24 January 2022*

Citation:
Cebrián G, Iglesias-Moya J, Romero J, Martínez C, Garrido D and Jamilena M (2022) The Ethylene Biosynthesis Gene CpACO1A: A New Player in the Regulation of Sex Determination and Female Flower Development in Cucurbita pepo. Front. Plant Sci. 12:817922. doi: 10.3389/fpls.2021.817922

INTRODUCTION

The cultivated species of the Cucurbitaceae family are a group of monoecious plants that have been utilized as a model for the study of the genetic control of sex determination in plants (Martínez and Jamilena, 2021). Many varieties in cultivated species are monoecious, developing male and female flower in the same plant, but some of the varieties are andromonoecious (male and hermaphroditic flowers), trimonoecious (male, female, and hermaphroditic flowers), gynoecious (only female flowers), and androecious (only male flowers). This natural variability makes this an ideal family to investigate the genetics of sex determination. The first sex-determining genes were discovered in *Cucumis sativus* (cucumber) and *Cucumis melo* (melon) (Boualem et al., 2008, 2009, 2015; Martin et al., 2009; Chen et al., 2016), but recent years have witnessed important discoveries in *Cucurbita pepo* (pumpkin and squash) (Martínez et al., 2014; García et al., 2020a,b) and *Citrullus lanatus* (watermelon) (Boualem et al., 2016; Ji et al., 2016; Manzano et al., 2016; Aguado et al., 2020; Zhang et al., 2020). Although many of the findings are similar in all species, the genetic control of sexual determination in some species differs slightly from the rest of the species (Aguado et al., 2020).

Ethylene is the key regulator of sex determination in cucurbits. External treatments with ethylene-releasing or -inhibiting agents have been used to determine the role of this hormone in the control of sex expression, i.e., female flowering transition and the number of female and male flowers per plant, as well as sex determination, which are the mechanisms that lead to a female or a male flower from a potentially hermaphrodite floral bud (Manzano et al., 2013, 2014). The latter was achieved by arresting the growth of the stamens or carpels, respectively (Bai et al., 2004). Ethylene increases the ratio of female to male flowers in *Cucumis* and *Cucurbita* (Rudich et al., 1969; Byers et al., 1972; Manzano et al., 2011, 2013), but reduces this ratio in *Citrullus* plants. Inhibition of ethylene biosynthesis or perception, on the other hand, reduces the number of female flowers per plant in *Cucumis* and *Cucurbita*, and transforms the female flowers into bisexual or hermaphrodite ones. In *Citrullus*, this last treatment increases the number of female flowers per plant, but also transforms female flowers into hermaphroditic flowers, indicating that ethylene is required to arrest the development of stamens in female flowers of all cucurbits (Manzano et al., 2014). Although gibberellins, auxins, and brassinosteroids have also been associated with sex control in cucurbits, some of their functions seem to be mediated by ethylene (Papadopoulou et al., 2005; Manzano et al., 2011; Zhang et al., 2014, 2017).

So far, all of the discovered sex-determining genes are either in the ethylene biosynthesis and signaling pathway, or are transcriptional factors that regulate the former. The gene that regulates abortion of stamens during the formation of a female flower in all studied cucurbits encodes for an ethylene biosynthesis enzyme: cucumber *ACS2* and its orthologs (Boualem et al., 2008, 2009, 2016; Martínez et al., 2014; Ji et al., 2016; Manzano et al., 2016). This female-forming gene is negatively regulated by the transcription factor *WIP1*, which is responsible for the arrest of carpels in the formation of male flowers (Martin et al., 2009; Hu et al., 2017; Zhang et al., 2020). The male-forming *WIP1* gene is negatively regulated by *ACS11* and *ACO2/ACO3* in cucumber and melon, which are expressed very early in the floral meristem and determine the formation of a female flower. The disruption of either of these genes promotes the conversion of monoecy into androecy (Boualem et al., 2015; Chen et al., 2016). EMS mutation in ethylene receptor genes of *C. pepo* has demonstrated that ethylene perception at early and late stages of flower development is crucial for female flower determination. The *etr1a*, *etr1a-1*, *etr1b*, and *etr2b* gain of function mutations, in fact, lead to andromonoecy and androecy concomitantly with a reduced ethylene sensitivity (García et al., 2018, 2020a,b).

The role of other ethylene biosynthesis genes in sex determination is unknown. In this paper, we demonstrate that the ethylene biosynthesis gene *CpACO1A* is involved in sex determination and flower development in *C. pepo*. Although the gene is not flower-specific, its role in ethylene biosynthesis is required for arresting stamen development, and the proper maturation and development of corolla and ovary of the female flower. *CpACO1A* and other sex-determining *ACO* and *ACS* ethylene biosynthesis genes were regulated by *CpACO1A*-producing ethylene in the female flower. The ethylene provided by CpACO1A also regulates hormonal balance in the female flowers. The increased indole-3-acetic acid (IAA) and the reduced abscisic acid (ABA) and jasmonic acid (JA) contents in the *aco1a* mutant may be responsible for the parthenocarpic fruit development and the delayed flower opening of the mutant female flower.

MATERIALS AND METHODS

Plant Material and Isolation of Mutants

The *aco1a* mutant analyzed in this study was isolated from a high-throughput screening of *C. pepo* EMS collection (García et al., 2018). M2 plants from 600 lines were grown to maturity under standard greenhouse conditions, and alterations in reproductive developmental traits were evaluated. A mutant family was detected that produced hermaphrodite flowers, instead of female flowers. This mutant was selected for further characterization, and named *aco1a*. The monitoring of the development of the growth of the female floral organs, corolla, and ovary, as well as the degree of their stamen development detected in the flowers, showed similarity with the phenotype found for other families of mutants previously described and characterized by García et al. (2020a,b) in *C. pepo*, which led us to deduce the possible relationship of ethylene with this new mutation. Prior to phenotyping, *aco1a* mutant plants were crossed twice with the background genotype MUC16, and the resulting BC_2 generation was selfed to obtain the BC_2S_1 generation.

Phenotyping for Monoecy Stability, Sex Expression, and Floral Traits

The total of 300 BC_2S_1 plants from wt/wt, wt/*aco1a*, and *aco1a*/*aco1a* were transplanted to a greenhouse and grown to

maturity under local greenhouse conditions without climate control, and under standard crop management of the region, in Almería, Spain. The sex phenotype of each plant was determined according to the sex of the flowers in the first 40 nodes of each plant. A minimum of 30 wt/wt, 30 wt/*aco1a*, and 30 *aco1a*/*aco1a* plants were phenotyped. Phenotypic evaluations were performed in the spring-summer seasons 2019 and 2020.

The sex expression of each genotype was assessed by determining the node at which plants transitioned to pistillate flowering, and the number of male or pistillate/hermaphrodite flower nodes. The sex phenotype of each individual pistillate/hermaphrodite flower was assessed by the so-called andromonoecy index (AI) (Martínez et al., 2014; Manzano et al., 2016). Pistillate flowers were separated into three phenotypic classes that were given a score from 0 to 3 according to the degree of their stamen development: female (AI = 0), showing no stamen development; bisexual or pistillate (AI = 1; AI = 2), showing partial development of stamens and no pollen; and hermaphrodite (AI = 3), showing complete development of stamens and pollen. The average AI of each plant and each genotype was then assessed from the resulting AI score of at least 10 individual female flowers from each plant, using a minimum of 30 plants for each genotype. To assess floral organ development, the growth rates of ovaries and petals in both female and male flowers of WT and *aco1a* mutant plants were determined by measuring the length and diameter of these floral organs every 2 day for 28 day in 20 flowers of each genotype, starting with flower buds ∼2 mm in length. The anthesis time was estimated as the number of days taken for a 2 mm pistillate or male floral bud to reach anthesis.

Identification of *aco1a* Mutation by Whole-Genome Sequencing Analysis

To identify the causal mutations of the *aco1a* phenotype, WT, and mutant plants derived from BC_1S_1-segregating populations were subjected to whole-genome sequencing (WGS). In total, 120 BC_1S_1 seedlings were transplanted to a greenhouse and grown to maturity. The phenotype of those seedlings was verified in the adult plants, as wt/wt and wt/*aco1a* plants were monoecious while *aco1a*/*aco1a* plants were andromonoecious or partially andromonoecious.

The genomic DNA from 30 WT and 30 *aco1a* plants was isolated by using the Gene JET Genomic DNA Purification Kit (Thermo Fisher Scientific®), and pooled into two different bulks: WT bulk and *aco1a* mutant bulk. DNA from each bulk was randomly sheared into short fragments of approximately 350 bp for library construction using the NEBNext® DNA Library Prep Kit[1], and fragments were briefly PCR enriched with indexed oligos. Pair-end sequencing was performed using the Illumina® sequencing platform, with a read length of PE150 bp at each end. The effective sequencing data were aligned with the reference *C. pepo* genome v.4.1 through BWA software (Li and Durbin, 2009). Single nucleotide polymorphisms (SNPs) were detected using the GATK HAPLOTYPECALLER (Depristo et al., 2011). ANNOVAR was used to annotate the detected SNPs (Wang et al., 2010). Common variants between these mutant families (and other sequenced mutant families in the laboratory) were discarded, as they are likely common genomic differences with the reference genome. The genotype of the WT bulk (wt/wt and wt/*aco1a* plants) was expected to be 0/1 with an alternative allelic frequency (AF) of 0.3, while the genotype of the mutant bulk (*aco1a*/*aco1a* plants) was expected to be 1/1 with an AF = 1. Therefore, the sequencing data were filtered according to the following parameters: genotype quality $\geq$ 90, read depth $\geq$ 10, AF = 1 in the mutant bulks, and AF $\leq$ 0.3 in the WT bulks. Once we had a set of positions that were differentially enriched in each bulk, we filtered out SNPs that were not canonical EMS changes (G > A or C > T transitions) (Till et al., 2004). All filters were performed with RStudio® software. The impact of this final set EMS SNPs on gene function was finally determined by using Integrative Genomics Viewer (IGV) software and the Cucurbit Genomics Database (CuGenDB)[2].

Validation of the Identified Mutations by High-Throughput Genotyping of Individual Segregating Plants

Segregation analysis was performed to confirm that the identified mutations were causal mutations of the *aco1a* phenotype. Approximately 300 BC_2S_1 plants segregating for the mutation were genotyped using Kompetitive allele-specific PCR (KASP) technology. Primers were synthesized by LGC Genomics®[3], and the KASP assay was performed in the FX96 Touch Real−Time PCR Detection System (Bio-Rad®) using the LGC protocol[4]. The multiplex PCRs were run with 10 μL final reaction volume containing 5 μL KASP V4.0 2× Master mix standard ROX (LCG Genomics®), 0.14 μL KASP-by-Design primer mix (LCG Genomics®), 2 μL of 10–20 ng/μL genomic DNA, and 2.86 μL of water. The PCR thermocycling conditions were 15 min at 94°C (hot-start activation) followed by 10 cycles of 94°C for 20 s and 61°C for 1 min (dropping −0.6°C per cycle to achieve a 55°C annealing temperature) followed by 26 cycles of 94°C for 20 s and 55°C for 1 min. Data were then analyzed using CFX Maestro™ Software (Bio-Rad®) to identify SNP genotypes.

1-Aminocyclopropane-1-Carboxylic Acid Oxidase Enzyme Activity

1-Aminocyclopropane-1-carboxylic acid oxidase (ACO) activity was assessed following the protocol described in Bulens et al. (2011). The enzyme activity was quantified in leaves, stems, roots, cotyledon, and flowers in triplicate. About 0.5 g of each material was pulverized in liquid nitrogen, and 1 mL of extraction buffer MOPS (pH 7.2) and 50 mg of polyvinylpolypyrrolidone (PVPP) were added to each sample. The samples were subsequently incubated for 10 min at 4°C and finally centrifuged for 30 min at 22,000 × *g* at 4°C. About 400 μL of the resulting supernatant

[1]https://international.neb.com

[2]http://cucurbitgenomics.org

[3]http://www.lgcgroup.com

[4]https://afly.co/xyn2

was mixed with 3.6 mL of MOPS reaction buffer (pH 7.2) in a 20 mL glass vial. After homogenizing the mixture for 5 s, samples were incubated in a water bath for 1 h at 30°C while gently shaking. The amount of ethylene formed was determined by analyzing 1 mL of gas from the headspace of the reaction tube on a Varian® 3900 gas chromatograph (GC) fitted with a flame ionisation detector (FID). A blank sample (3.6 mL reaction buffer + 400 μL DW) was used as a control for the whole process. Enzyme reactions and ethylene readings were done in triplicate. The activity of ACO was expressed as nmol $\times$ $gFW^{-1} \times h^{-1}$.

Ethylene Production Measurements

The production of ethylene in WT and *aco1a* flowers was assessed throughout the different stages of development. Female and male floral buds of 8–55 mm in length (FFB/MFB) and the apical shoots of plants growing under climatic controlled conditions were collected and incubated at room temperature for 6 h in hermetic glass containers of 50–450 mL. Ethylene production was determined by analyzing 1 mL of gas from the headspace in a Varian® 3900 gas chromatograph (GC) fitted with a FID. The instrument was calibrated with standard ethylene gas. Four biological replicates were made for each one of the flower developmental stages analyzed and three measurements per sample. Ethylene production was expressed as $nL \times gFW^{-1} \times 6\,h^{-1}$.

Assessing Ethylene Sensitivity

To evaluate the level of sensitivity to ethylene, flower abscission was assessed for male flowers in response to an external treatment with ethylene. Male flowers from WT and *aco1a* plants were collected at two stages of development: A (anthesis) and A-2 (2 day before anthesis). For each stage, 30 WT and *aco1a* flowers were placed in glass vases with water, and incubated in two culture chambers with equal humidity and temperature, 50% RH and 20°C. One of the chambers was used as a control (Ct), and the other was filled with 50 ppm of ethylene (ET). The tests were performed in triplicate. Both chambers remained closed for 72 h, and the percentage of abscission produced was evaluated after 24, 36, 48, and 72 h for each stage of development.

Hormone Concentration Measurements

Female flower buds of 5–8 mm from WT and *aco1a* plants were collected for hormone concentration measurements. Representative samples consisted of three bulks of approximately 30 female flowers each. To preserve the samples, WT and *aco1a* bulks were quickly stored on dry ice. Then, the samples were placed in a freeze dryer CRYODOS V3.1-50 (Telstar®), where they were lyophilized for 1 week and subsequently pulverized in a mixer mill MM200 (Retsch™). The concentration of salicylic acid (SA), indol-3-butyric acid (IBA), IAA, gibberellic acid (GA3), 6-benzyladenine (BA), ABA, and JA were determined in each triplicated sample through ultra-performance liquid chromatography coupled with a hybrid quadrupole orthogonal time-of-flight mass spectrometer (UPLC-Q-TOF/MS/MS) according to the hormone determination method of Müller and Munné-Bosch (2011).

Bioinformatics and Phylogenetic Analysis

Alignments and protein sequences analysis were performed using the BLAST alignment tools at NCBI[5]. Protein structure information and homology-modeling were analyzed using the Protein Data Bank RCSB PDB[6] and SWISS-MODEL[7]. The phylogenetic relationships between *C. pepo*, *Arabidopsis thaliana*, *Solanum lycopersicum*, *Oryza sativa*, *C. sativus*, and *C. melo* of *ACO* genes were studied using MEGA X software (Kumar et al., 2018), which allowed the alignment of proteins and the construction of phylogenetic trees using MUSCLE (Edgar, 2004) and the maximum likelihood method based on the Poisson correction model (Zuckerkandl and Pauling, 1965), with 2,000 bootstrap replicates. The protein sequences (**Supplementary Table 1**) were obtained using the Arabidopsis Information Resource[8], the Cucurbit Genomics Database (CuGenDB)[9], the Rice Database Oryzabase-SHIGEN[10], and the Sol Genomics Network[11]. Cucurbits *ACO* genes structure visualization, such as the composition and position of exons and introns, were performed with the Gene Structure Display Server (GSDS)[12]. Finally, Delta Delta G ($\Delta\Delta G$), a metric for predicting how a single point mutation will affect protein stability, was assessed with the tools SNAP2[13] and I-Mutant3.0.[14] MUpro[15] and CUPSAT[16] tools were also used to predict the stability of the CpACO1A protein.

Assessment of Relative Gene Expression by Quantitative RT-PCR

Gene expression analysis was carried out in samples of WT and *aco1a* plants growing in a greenhouse during the spring-summer season. The expression level was studied in male and female flowers' organs (corolla and ovaries) at different flower developmental stages, as well as in plant apical shoots, leaves, shoots, cotyledons, and roots. The analysis was performed in three biological replicates for each genotype, each of which was derived from a pool of four plants. Total RNA was isolated according to the protocol of the GeneJET Plant RNA Purification Kit (Thermo Fisher Scientific®). RNA was converted into cDNA with the ADNc RevertAid™ kit (Thermo Fisher Scientific®). The qRT-PCR was performed in 10 μL total volume with 1× Top Green qPCR Super Mix (Bio-Rad®) in the CFX96 Touch Real-Time PCR Detection System thermocycler (Bio-Rad®). The gene expression values were calculated using the $2^{-\Delta\Delta CT}$ method (Livak and Schmittgen, 2001). The constitutive *EF1α* gene was

[5]https://blast.ncbi.nlm.nih.gov/Blast.cgi
[6]https://www.rcsb.org
[7]https://swissmodel.expasy.org
[8]https://www.arabidopsis.org
[9]http://cucurbitgenomics.org
[10]https://shigen.nig.ac.jp/rice/oryzabase
[11]https://solgenomics.net
[12]http://gsds.gao-lab.org/Gsds_about.php
[13]https://rostlab.org/services/snap2web
[14]https://folding.biofold.org/i-mutant/i-mutant2.0.html
[15]http://mupro.proteomics.ics.uci.edu
[16]http://cupsat.tu-bs.de

used as the internal reference. **Supplementary Table 2** shows the primers used for each qRT-PCR reaction.

Statistical Analyses

Data were analyzed for multiple comparisons by analysis of variance (ANOVA) using the statistical software Statgraphic Centurion XVIII. Differences between genotypes and treatments were separated by least significant difference (LSD) at a significance level of $p \leq 0.05$.

RESULTS

aco1a Impairs Sex Determination and Petals and Ovary Development

The mutant *aco1a* was found in a high-throughput screening of a *C. pepo* mutant collection for alterations in flower and fruit development. To ensure accurate phenotyping, mutant plants were backcrossed with the background genotype MUC16 for two generations, and then selfed. The resulting BC_2S_1 generations segregated 3:1 for WT and *aco1a* phenotypes, indicating that the mutation is recessive (**Supplementary Table 3**).

The sex phenotype of *aco1a* was assessed in BC_2S_1 plants growing under spring-summer conditions (**Figure 1**). Male flowers were not affected, but most female flowers were converted into bisexual flowers with partially or totally developed stamens (**Figure 1A**). This partial conversion of monoecy into andromonoecy, also termed unstable monoecy, partial andromonoecy, or trimonoecy, indicates that *aco1a* impairs the sex determination mechanism which is responsible for arresting stamen development in the female flower. Pistillate flowers in the first 40 nodes were classified according to the andromonoecious index (AI) in either homozygous WT (wt/wt), heterozygous (wt/*aco1a*), or homozygous mutant (*aco1a*/*aco1a*) plants (**Figure 1B**). The wt/wt and wt/*aco1a* plants produced only female flowers (AI = 0), indicating a complete arrest of stamen development in the pistillate flowers of these plants (**Figure 1C**). The *aco1a*/*aco1a* pistillate flowers, however, exhibited different degrees of stamen development (AI ranging from 0 to 3), and plants had an average AI of 2.1 (**Figures 1B,C**).

Figure 2 shows the effects of the *aco1a* mutation on petal and ovary/fruit development. In the bisexual and hermaphrodite flowers of *aco1a* (AI = 2–3), the petal growth rate was reduced and resembled petal development in male flowers. Petal maturity and subsequent anthesis of the flower were delayed in the mutant with respect to WT (**Figures 2A,B**). Anthesis time, the period of time taken for a 2 mm floral bud to reach anthesis and to open, was longer in male WT flowers (average 21 days) than in female WT flowers (average 12 days) (**Figure 2B**). Bisexual and hermaphrodite *aco1a* flowers also took an average of 21 days to reach anthesis (range 20–25 days). No alterations in petal development or anthesis time were observed in WT and *aco1a* male flowers (**Figure 2B**).

Pollination was attempted in *aco1a* hermaphrodite flowers (AI = 2–3), but none of the fruits were able to set seeds. Since the pollen is fertile in other plants, this female sterility could be associated with the over-maturation of stigma and style because

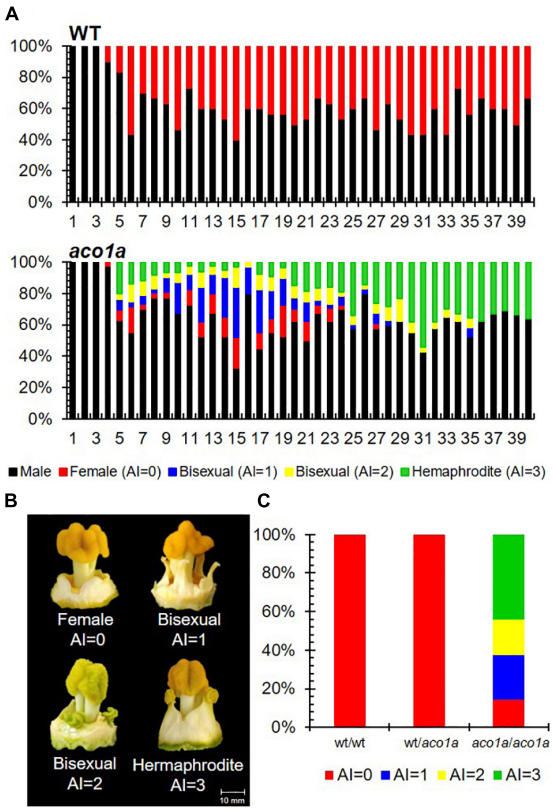

FIGURE 1 | Sex phenotype of WT and *aco1a* plants. **(A)** Distribution of male and pistillate flowers in the first 40 nodes of the main shoot. In each node, color bars indicate the percentages of male (black), female (red), and bisexual and hermaphrodite flowers (blue, yellow, and green) in the total number of plants analyzed ($n = 30$ for each genotype). **(B)** Phenotype of pistillate flowers with different stamen development and AI index. Female flowers (AI = 0) develop no stamen, bisexual flowers (AI = 1–2) develop intermediate stamens, and hermaphrodite flowers (AI = 3) develop entire stamens with pollen. **(C)** Percentage of each pistillate flower in each genotype.

of the delayed corolla aperture. However, we were able to self *aco1a*/*aco1a* plants by using the few female flowers with no stamen (AI = 0). Significant differences were detected in ovary size between WT and *aco1a* pistillate flowers (**Figures 2A,C**). At anthesis, the WT ovary reached approximately 12 cm in length and then aborted. The *aco1a* ovary, in contrast, continued to grow until it reached 18–30 cm at anthesis (**Figures 2A,C**). The growth rate of WT and *aco1a* ovary/fruit was similar during the first 16 days. After that time, WT ovaries aborted, and those of *aco1a* maintained growth up to anthesis (**Figure 2C**). The *aco1a* fruits can be considered parthenocarpic since they grew in the absence of pollination, as the corolla was closed.

aco1a Is a Missense Mutation Causing P5L Substitution in the Ethylene Biosynthesis Enzyme CpACO1A

To elucidate the causal mutation of *aco1a* phenotype, we performed WGS of two bulked DNA samples from a BC_2S_1 segregating population: the WT bulk, having DNA from 30 WT

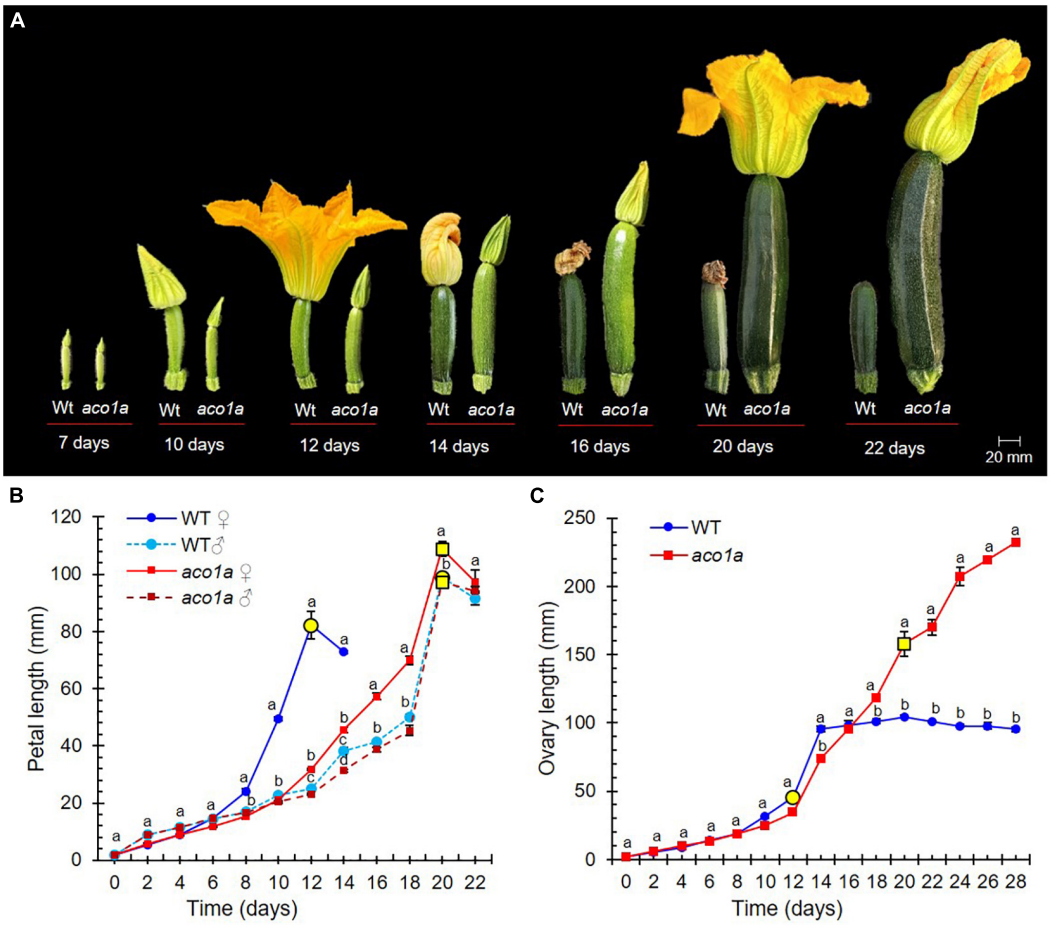

FIGURE 2 | Comparison of WT and *aco1a* flower development. **(A)** Effect of *aco1a* mutation on the development of ovary and corolla of the pistillate flower. Note that the mutant pistillate flower reaches anthesis later than the WT, and that the ovary continues its growth until producing a parthenocarpic fruit. **(B)** Comparison of the growth rate of WT and mutant corolla. Flowers were labeled when their ovaries were 2 mm long, and then measured every 2 days for 22 days. Yellow circles indicate the time at which more than 80% of the flowers reached anthesis. **(C)** Comparison of the growth rate of WT and mutant ovaries/fruits over a period of 22 days. Error bars represent SE. Different letters indicate significant differences in flowers of the different genotypes at each developmental time ($p \leq 0.05$).

plants (monoecious); and the *aco1a* bulk, having DNA from 30 mutant plants (partially andromonoecious). In the mutant bulk, only the plants that showed the most extreme andromonoecious phenotype were selected.

More than 98% of the sequencing reads (more than 80 million in each bulk) were mapped against the *C. pepo* reference genome version 4.1, which represented an average depth of 47.41 (**Table 1**). The identified SNPs (more than 370,000 in each of the bulks) were filtered for their mutant allele frequency (AF) in the WT and the mutant DNA bulks. For the causal mutation of the phenotype, it is expected that the genotype was 0/1 for WT bulk (alternative allele frequency AF = 0.25) and 1/1 for the mutant bulk (AF = 1). For the non-causal SNPs, however, we expected an AF of 0.5 in both bulks. A putative causal region in chromosome 4 was found that has the expected AF in WT and mutant bulk (**Figure 3A**). In fact, after filtering for AF = 1 in the mutant bulk and AF < 0.3 in the WT bulk, 412 SNPs were selected (**Table 1**). Among them, 145 corresponded to canonical EMS mutations (C > T and G > A), and only one on chromosome 4 was positioned on the exome and had a high impact on the protein (**Table 1** and **Figure 3**).

The sequence surrounding the candidate *aco1a* mutation (±500 bp) was then used in BLAST searches against the DNA and protein databases at NCBI. It was found that the C > T transition was a missense mutation changing proline by leucine at residue 5 (P5L) of the ethylene biosynthesis enzyme 1-aminocyclopropane-1-1carboxylate oxidase 1A (CpACO1A) (**Figure 3A**). To prove that the selected EMS mutation was the one responsible for *aco1a* phenotype, we genotyped the SNP alleles in 300 plants from a BC_2S_1 population. The results demonstrated a 100% co-segregation between the *aco1a* phenotype and the C > T mutation in *CpACO1A* (**Supplementary Table 4**). Other three EMS-induced mutations in chromosome 4 were also tested (**Supplementary Table 5**), but none of them co-segregated with the mutant phenotype in the 300 BC_2S_1 plants analyzed.

The identified mutation has a deleterious effect on CpACO1A enzyme (**Figure 3B**). Bioinformatics analysis with the SNAP[2] tool predicted a negative effect of P5L substitution on protein function

TABLE 1 | Summary sequencing data for WT and *aco1a*.

Sequencing				WT	*aco1a*
No. reads				106,448,438	84,600,742
Mapped reads (%)				98.10	98.06
Average depth				47.41	40.41
Coverage at least 4× (%)				95.81	95.41
SNPs filtering					
Total No. SNPs				381,666	374,917
AF (WT) < 0.3; AF (*aco1a*) = 1				412	412
EMS SNPs G > A or C > T				145	145
EMS SNPs (GQ > 90; DP > 10)				4	4
High impact SNPs				0	1
Candidate SNP					
Chr	**Position**	**Ref**	**Alt**	**Gene ID**	**Effect**	**Functional annotation**
4	7,715,975	C	T	Cp4.1LG04g02610	P5L	1-Aminocyclopropane-1-carboxylate oxidase 1

AF, allelic frequency; GQ, genotype quality; DP, read depth.

(**Figure 3B**). Other bioinformatics tools, such as PredictSNP, MAPP and iStable, among others, showed the same evidence (**Figure 3B**). Moreover, predicted Gibbs free energy changes ($\Delta\Delta G$), a metric for predicting how a single point mutation could affect protein stability, was assessed for P5L mutation by using I-mutant3.0 predictor, CUPSAT, and MUpro. The comparison of *aco1a* and WT CpACO1A resulted in negative $\Delta\Delta G$ values, which indicated a decreased stability of the mutated protein (**Figure 3B**).

Gene Structure and Phylogenetic Relationships of *CpACO1A*

Given that the genomes of *C. pepo* are duplicated (Sun et al., 2017; Montero-Pau et al., 2018), the gene *CpACO1A* on chromosome 4 (Cp4.1LG04g02610) has a paralog (*CpACO1B*) with more than 80% of homology on an syntenic block of chromosome 5 (Cp4.1LG05g15190). The duplicates did not maintain the same molecular structure: four exons for *CpACO1A* and three exons for *CpACO1B* (**Figure 4A**). *ACO1*, like genes in other plants, including those of *Cucurbita maxima*, *Cucurbita moschata*, *C. melo*, *C. lanatus,* and *C. sativus*, conserve the four exonic structure of *CpACO1A* (**Figure 4A**). All ACO proteins in the NCBI database were found to conserve the proline residue on position five, indicating that this is an essential residue for ACO activity (**Figure 4B**).

Based on residues conserved at specific positions toward the carboxylic end of the proteins, three types of ACO enzymes have been established in plants (**Figure 4B**), which also defines its specific functionality and biological activity. A phylogenetic tree was inferred by using ACO protein sequences from different cucurbit species, including different *Cucurbita* sp., *C. melo* and *C. sativus*, together with those of the most studied model species, *A. thaliana*, *S. lycopersicum*, and *O. sativa* (**Figures 4B,C**). The *C. pepo* CpACO1A is a type I ACO that clustered together with melon CmACO1 and cucumber CsACO3 (also called CsACO1-like). Furthermore, the genes coding for the type I ACO1 enzymes of these three cucurbits were found to be positioned in a syntenic block of *C. pepo*, *C. melo*, and *C. sativus* genomes. The paralogous CpACO1B is also a type I ACO, but clustered separately from CpACO1A, CsACO3, and CmACO1 (**Figure 4C**).

The *aco1a* Mutation Impairs *CpACO1A* Expression, ACO Activity, and Ethylene Production and Sensitivity

The expression of *CpACO1A* and *CpACO1B* in different WT and *aco1a* tissues is shown in **Figure 5A**. *CpACO1B* was not expressed in any of the analyzed tissues, indicating that this is a non-functional paralogous gene. *CpACO1A* was found to be expressed in all tissues, except in cotyledons. Its transcript was, however, much more accumulated in roots and flowers (**Figure 5A**). *CpACO1A* was similarly expressed in the different WT and mutant tissues, except in the female flower buds, where the gene showed a higher expression in the mutant. To understand the function of *CpACO1A* in flower development, its expression was compared in WT and *aco1a* apical shoots and female and male flowers buds (FFB/MFB) at different stages of development (**Figure 5B**). In the apical shoot, *CpACO1A* expression was similar in WT and *aco1a* plants. In the mutant female and male flowers, *CpACO1A* transcripts are similarly more highly accumulated in the mutants, suggesting that the andromonoecious *aco1a* phenotype is not caused by a reduction of gene expression.

Although there are other ACO isoenzymes in the *C. pepo* genome, we have assessed the total ACO activity and ethylene production in different WT and *aco1*a plant tissues (**Figure 5C**). The *aco1a* mutation was found to cause a reduction of ACO activity in all studied tissues, except in cotyledons, where the gene was not found to be expressed (**Figure 5C**). These data suggest that the mutation *aco1a* likely impairs CpACO1A activity.

The *aco1a* mutation significantly reduced the production of ethylene in the apical shoots of the plants, where a number of small floral buds are developing, and in pistillate flowers (**Figure 5D**). As previously reported, ethylene increased throughout the development of male, female (WT) and bisexual/hermaphrodite (*aco1a*) flowers, and pistillate flowers produced significantly more ethylene than male flowers at the same developmental stage (**Figure 5D**). The bisexual flowers of *aco1a* showed a significant reduction of ethylene production during their development, especially those flowers with more than 35 mm in length (**Figure 5D**). A slight reduction in ethylene production was also found in *aco1a* male flowers of 50–55 mm in length (**Figure 5D**).

Ethylene sensitivity in WT and *aco1a* plants was also assessed by measuring the abscission time of male flowers in response to external treatments with ethylene (**Figure 6**). The male floral buds were collected at two developmental stages: anthesis (A) and 2 day before anthesis (A-2). The flowers were put in a container with water and treated in an atmosphere with air (control) or ethylene (ET) up to 72 h, and floral abscission was evaluated

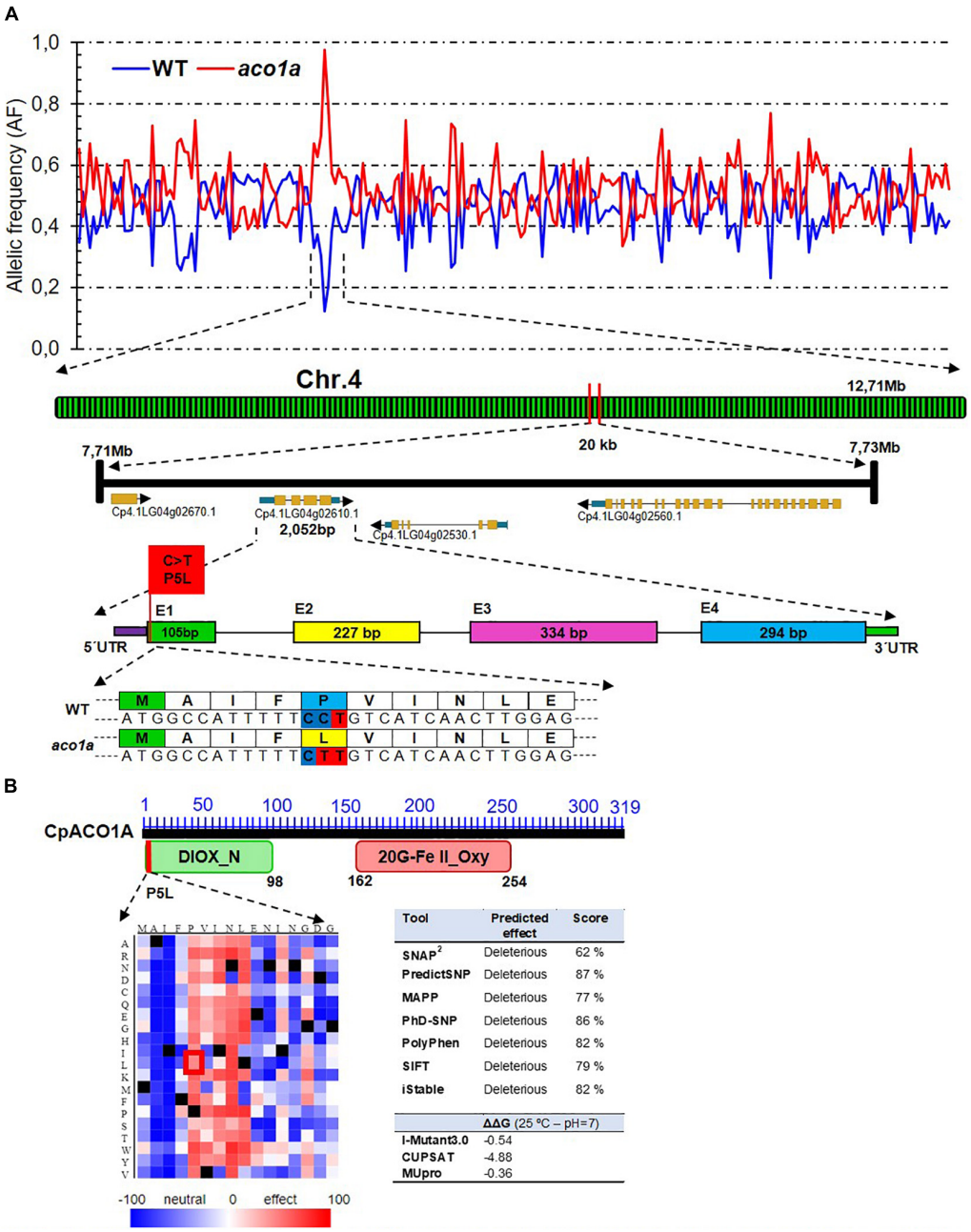

FIGURE 3 | Identification of *aco1a* causal mutation by BSA-sequencing. **(A)** Frequency of the alternate allele in the WT and *aco1a* bulks along the physical map of squash genome. The analysis indicates that a region of chromosome 4 is responsible for the mutant phenotype. A missense mutation on the gene *Cp4.1LG04g02610.1* (*CpACO1A*) produces a change of proline by leucine at residue 5 (P5L) of the ethylene biosynthesis enzyme CpACO1A. **(B)** Impact of P5L mutation in the N-terminal conservative non-heme dioxygenase DIOX_N region of ACO enzymes. The SNAP^2-generated heatmap of CpACO1A N-domain indicates that changes in residue 5–9 have a high impact on protein function. The red box indicates the impact of the *aco1a* mutation. The table on the right shows the predicted effect of the mutation on protein function and stability by using different bioinformatics tools.

every 12 h (**Figure 6A**). Both WT and *aco1a* flowers responded to ethylene by accelerating their senescence and abscission (**Figure 6B**). However, the increase in the percentage of flower abscission in response to ethylene was lower in *aco1a* than in WT flowers (**Figure 6B**), indicating a partially ethylene-insensitive phenotype of the mutant *aco1a* male flowers.

Expression of Different Sex-Determining Genes in WT and *aco1a* Flowers

The possible regulation of *CpACO1A* over other sex-determining genes was investigated by assessing the expression of those genes in WT and *aco1a* pistillate and male flowers (**Figure 7**). The ethylene biosynthesis genes *CpACO2B*, *CpACS11A*, and

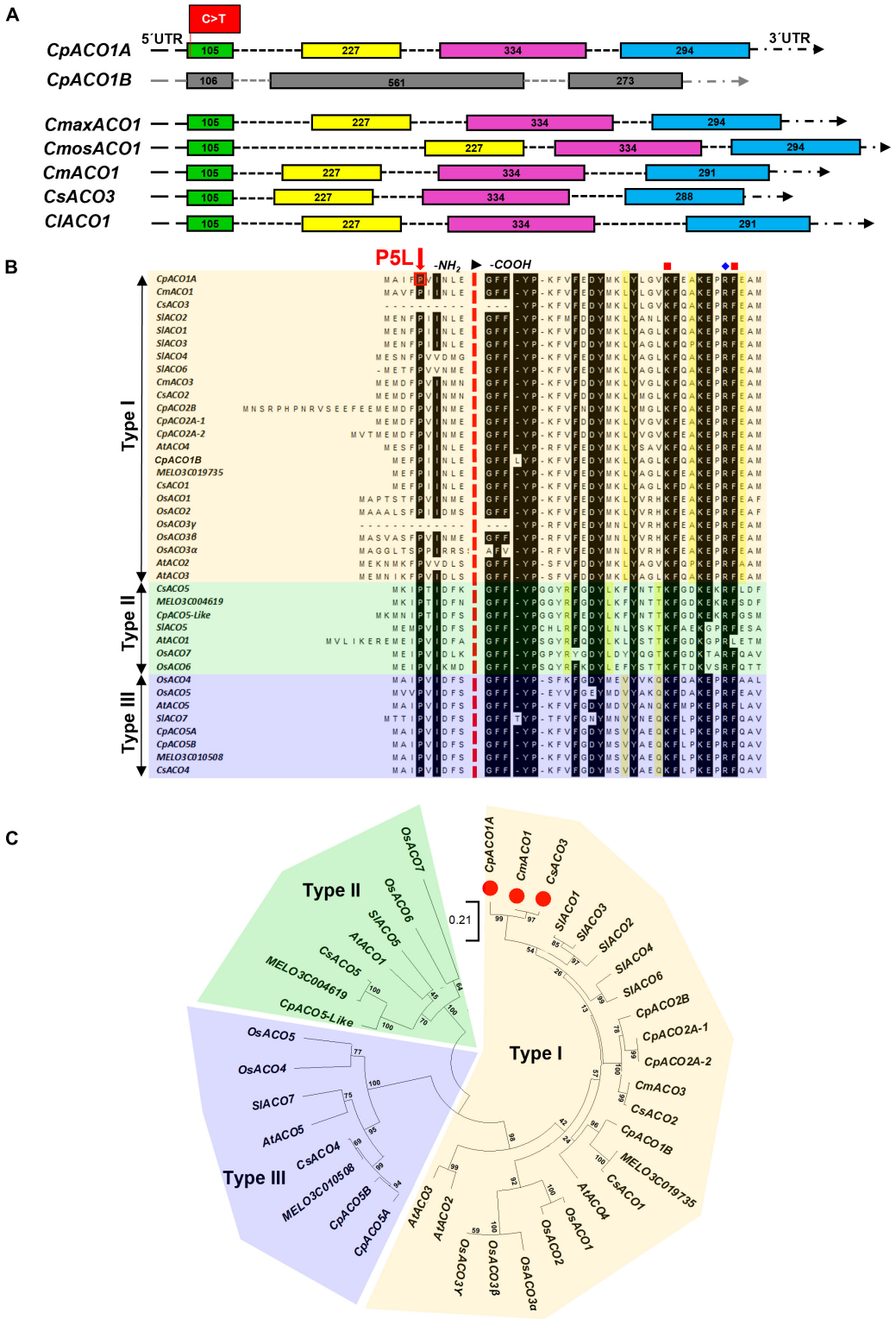

FIGURE 4 | Genetic relationships among ACO enzymes in different plant species. **(A)** Comparison of the gene structure of *CpACO1A* and *CpACO1B* of *C. pepo* with other homologs in cucurbit species: *Cucurbita maxima* (*CmaxACO1*), *Cucurbita moschata* (*CmosACO1*), *Cucumis melo* (*CmACO1*), *Cucumis sativus* (*CsACO3*), and *Citrullus lanatus* (*ClACO1*). **(B)** Consensus proline residue in position 5 and ACO classification according to conserved residues in a specific position toward the -COOH end of the proteins. **(C)** Phylogenetic ACO tree from different cucurbit species: *C. melo*, *C. sativus*, and *C. pepo* together with those of the most studied model species, *Arabidopsis thaliana*, *Solanum lycopersicum*, and *Oryza sativa*. Bootstrap values for the main branches are depicted on the tree.

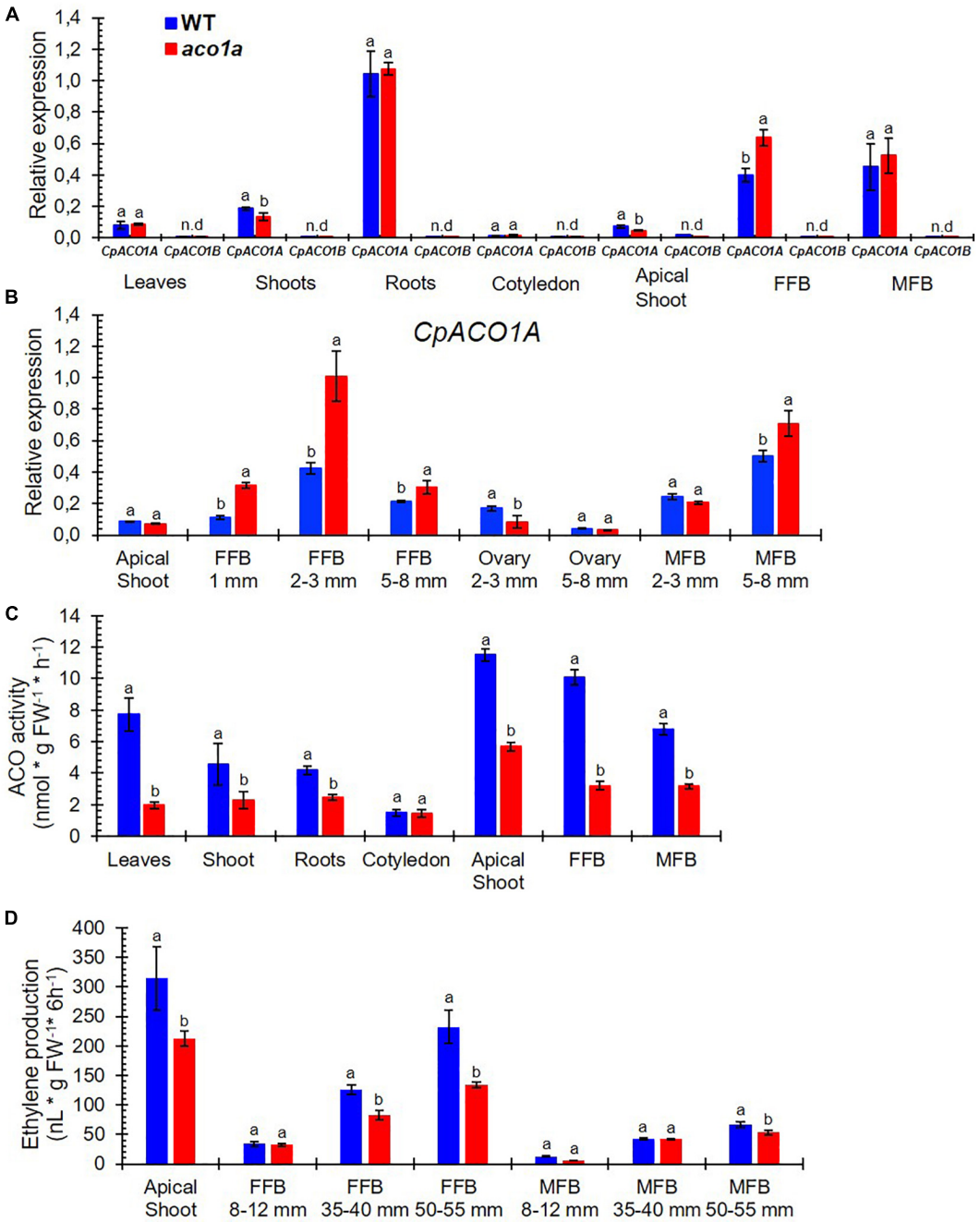

FIGURE 5 | Comparison of *CpACO1A* gene expression, ACO activity, and ethylene production in WT and *aco1a* plants. **(A)** Relative gene expression of *CpACO1A* and *CpACO1B* in different WT and *aco1a* plant organs. **(B)** Relative expression of *CpACO1A* in the apical shoots and in female and male floral buds at different stages of development. **(C)** ACO1 activity in different WT and *aco1a plant* organs. **(D)** Ethylene production in the apical shoot and in female and male floral buds of WT and *aco1a* plants. FFB, female floral bud excluding the ovary; MFB, male floral bud. The assessments were performed in three independent replicates for each tissue. Error bars represent SE. Different letters indicate significant differences between WT and mutant organs at the same stage of development ($p \leq 0.05$).

CpACS27A, which are expressed at early stages of female flower development and make the floral meristem to be determined as a female flower (Martínez and Jamilena, 2021), were differentially expressed in WT and *aco1a* pistillate flowers, but not in the apical shoots or in male flowers (**Figure 7**). In very small floral buds (1 mm), the *aco1a* mutation repressed the expression of the three genes. In 2–3 mm floral buds, the expression of the *CpACS11A* and *CpACS27A* was repressed in the ovary, and the expression of *CpACO2B* and *CpACS11A* was induced in the rest of the floral organs (petals, style, and stigma). In 5–8 mm female floral buds,

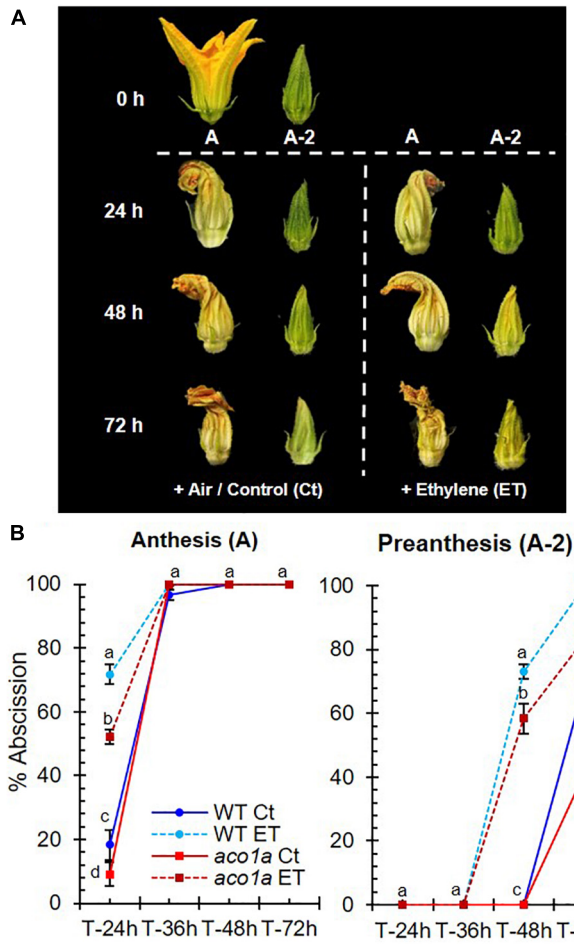

FIGURE 6 | Ethylene sensitivity of WT and *aco1a* plants. The sensitivity to ethylene was determined by assessing the percentage of flower abscission in response to ethylene in male flowers at two stages of development. **(A)** Phenotype of male flowers at two stages of development: anthesis **(A)** and 2 days before anthesis (A-2). Photographs were taken at harvest (0 h of treatment) and 24, 48, and 72 h after the treatment with air or ethylene (ET). **(B)** Percentage of abscission in male flowers harvested at anthesis **(A)** or 2 days before anthesis (A-2). Error bars represent SE. Different letters indicate significant differences between flower abscission of each treatment and genotype at the same time after the treatment ($p \leq 0.05$).

the expressions of these three ethylene biosynthesis genes were not altered by *aco1a* (**Figure 7**).

The mutation *aco1a* also diminished the expression of the ethylene receptor *CpETR1A* and the ethylene signaling gene *CpEIN3A* (**Figure 7**) at early stages of female flower development (female floral buds of 1 mm and 2–3 mm in length) and in ovaries of flowers 2–3 mm in length. In the rest of the analyzed tissues, including the apical shoot, female flowers at later stages of development and male flowers, no difference was found in the expression of these two ethylene signaling genes between WT and *aco1a* tissues (**Figure 7**). The expression *CpWIP1B*, a homolog of melon *WIP1* involved in the arrest of stamen during the development of male flowers, was unaltered by the mutation in most of the studied tissues, but in the apical shoot and in male floral buds of 5–8 mm in length, the gene was induced in the mutant.

Hormone Imbalance in Early Female Development of *aco1a* Flowers

To examine whether the mutation *aco1a* can change the hormonal balance of pistillate flower, we proceeded to compare phytohormone contents of WT female flower and *aco1a* hermaphrodite flowers. **Table 2** shows phytohormone concentrations of pistillate flower buds of 5–8 mm from WT and *aco1a* plants. No difference was detected for IBA, GA3, and BA contents. However, the *aco1a* flowers showed a considerable reduction in the content of ABA and JA, as well as SA (**Table 2**). In contrast, the auxin (IAA) content in the *aco1a* hermaphrodite flowers was much higher than that in female WT flowers (**Table 2**).

DISCUSSION

It has been assumed that not ACO, but ACS, is the rate-limiting enzyme in ethylene biosynthesis. However, there is an increasing amount of evidence demonstrating the importance of ACO in controlling ethylene production in plants (Houben and Van de Poel, 2019). In cucurbits, mutations in *CmACO1* are known to inhibit fruit ripening and extend fruit shelf life (Dahmani-Mardas et al., 2010). An essential role of *CsACO2* and *CmACO3* orthologs in carpel development has been recently reported in cucumber and melon (Chen et al., 2016). In this paper, we establish that *CpACO1A* is a key regulator in sex determination and female flower development of *C. pepo*.

aco1a Disrupts Ethylene Biosynthesis and Hormonal Balance During Female Flower Development

The ACO protein family can be divided in three phylogenetic groups based on amino-acid sequence similarity (Houben and Van de Poel, 2019). At a functional level, the ACO protein has two highly conserved and well-distinguished domains, one N-terminal, highly conservative non-heme dioxygenase DIOX_N region and a C-terminally located 2OG-FeII_Oxy region, both of which are critical for ACO activity (Ruduś et al., 2013). The sequence alignment and the phylogenetic tree constructed by using ACO proteins from diverse plant species have proven that CpACO1A is a type I ACO enzyme, and that the *aco1a* P5L mutation affects the first amino acid of the CpACO1A DIOX_N domain, which is a conserved proline residue in all analyzed plant ACOs. The reduced ACO activity and ethylene production in *aco1a* plant organs confirmed the disfunction of P5L isoform of CpACO1A and the importance of 5P residue for its activity.

CpACO1A transcript differentially accumulated in different tissues and stages of development. Comparison of ethylene production and gene expression in WT and *aco1a* organs indicated that *CpACO1A* may be regulated by ethylene in a tissue- and temporal-specific manner. This feedback regulation

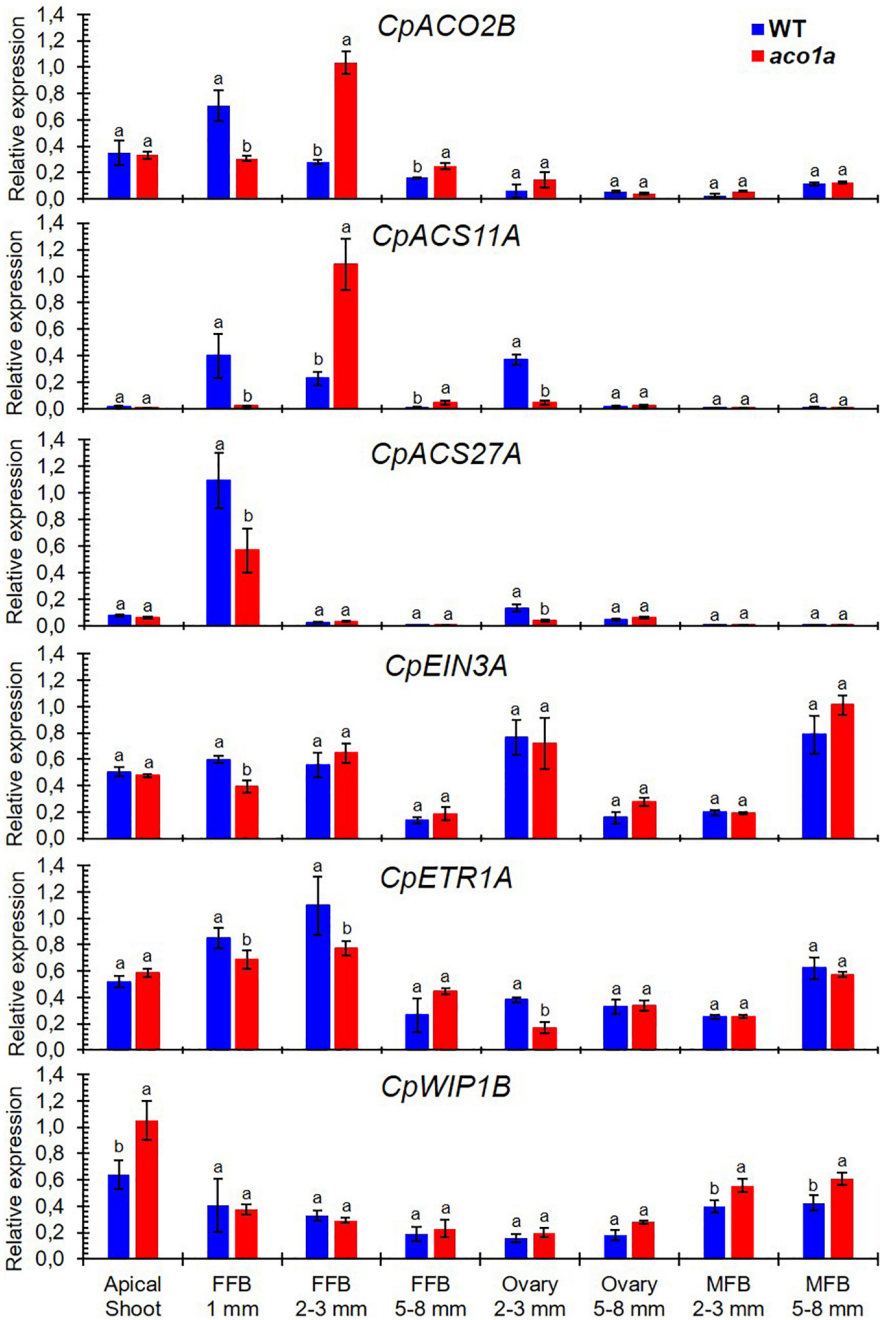

FIGURE 7 | Relative expression of different sex-determining genes in the apical shoots and flowers of WT and *aco1a* plants. The expression was assessed for genes involved in ethylene biosynthesis (*CpACO2B*, *CpACS11A*, and *CpACS27A*), ethylene perception and signaling (*CpETR1A* and *CpEIN3A*), and coding for the transcription factors (*CpWIP1B*) that are known to be involved in sex determination in cucurbit species. The relative level of each transcript was quantified by quantitative PCR in three independent replicates of each tissue. FFB, female floral bud excluding the ovary; MFB, male floral bud. Error bars represent SE. Different letters indicate significant differences between WT and mutant apical shoots and flowers at the same stage of development ($p \leq 0.05$).

could also affect other ethylene biosynthesis genes involved in flower development and sex determination, including *CpACO2B*, *CpACS11A*, and *CpACS27A*. Both positive and negative feedback ethylene-mediated regulation of *ACS* and *ACO* transcription have been reported in other systems in a tissue- and temporal-specific manner during flower and fruit development (Barry et al., 1996; Nakatsuka et al., 1998; Inaba et al., 2007; Trivellini et al., 2011; Houben and Van de Poel, 2019; Pattyn et al., 2020). However, we do not exclude the possibility that the regulation of *ACS* and *ACO* genes in the female flower is mediated by other hormones, such as IAA, which was found to be highly accumulated in the ethylene-deficient *aco1a* pistillate flowers.

TABLE 2 | Hormone concentrations ng/mL (ppb).

Hormones	WT	*aco1a*
Salicylic acid (SA)	4661.94 ± 41.00 **a**	3196.83 ± 46.34 **b**
Indole-3-butyric acid (IBA)	n.d	n.d
Indole-3-acetic acid (IAA)	<LOQ **b**	23.25 ± 2.47 **a**
Gibberellic acid (GA3)	n.d	n.d
6-Benzyladenine (BA)	n.d	n.d
Abscisic acid (ABA)	124.81 ± 4.06 **a**	36.02 ± 2.35 **b**
Jasmonic acid (JA)	656.65 ± 19.11 **a**	248.56 ± 5.41 **b**

Different letters within the same row indicate significant differences between WT and aco1a hormone content ($p < 0.05$); n = 3. LOQ, results below the limit of quantification (5 ppb). n.d, not detected.

The hormonal imbalance detected in *aco1a* female flowers reveals the existence of crosstalk between ethylene and other hormones, such as IAA, SA, ABA, and JA, during female flower development. The coaction of ethylene and auxin has been reported in various growth and developmental processes, including root elongation, lateral root formation, hypocotyl growth, and fruit development and ripening, where both hormones may act synergistically or antagonistically (Stepanova et al., 2007; Muday et al., 2012; Li et al., 2016; Yue et al., 2020). The reciprocal positive regulation between auxin and ethylene is well established; elevated levels of auxin trigger transcriptional activation of subsets of *ACS* and *ACO* genes, leading to increased ethylene production; and ethylene positively controls IAA biosynthesis by the up-regulation of *Weak ET Insensitive 2* (*WEI2*) and *WEI7* (Růžička et al., 2007; Stepanova et al., 2007; Swarup et al., 2007; Zemlyanskaya et al., 2018). However, ethylene has also been reported to negatively regulate auxin biosynthesis (Harkey et al., 2018; Li et al., 2018). We found that ethylene and auxin are mutually repressed, likely having an antagonistic action in squash female flower development. Auxin down-regulates the expression of ethylene biosynthesis and signaling genes in the female flower upon fruit set (Martínez et al., 2013), and here we demonstrated that ethylene has a negative regulation on auxin in female flowers, accumulating much higher content of IAA in ethylene-deficient *aco1a* than in WT. On the other hand, the reduced levels of ABA, JA, and SA in the ethylene-deficient mutant *aco1a* indicates that ethylene positively regulates the homeostasis of these three phytohormones in the female flower. As discussed below, all of these hormones have key functions in flower development (Chandler, 2011), and can cooperate with ethylene in the regulation of squash female flower development.

CpACO1A Prevents Stamen Development in Squash Female Flowers

Different sex-determining mechanisms prevent the development of either the stamens or the carpel in a primarily hermaphrodite floral meristem (Martínez and Jamilena, 2021). In Cucurbitaceae, ethylene arrests the development of stamens and promotes the development of carpels during the determination of female flowers. Early ethylene biosynthesis genes, such as *ACS11* and *ACO2*, in cucumber and melon are able to promote carpel development and determine the fate of floral meristem toward a female flower. The LOF mutation in these two ethylene biosynthesis genes leads to androecy in both cucumber and melon (Boualem et al., 2015; Chen et al., 2016), as occurs with mutation in some ethylene receptor genes (García et al., 2020a,b). Our results demonstrate that *aco1a* mutation led to a reduction in ACO activity and ethylene production, but induced the expression of *CpACO1A*. This upregulation also occurs for *CpACO2B* and *CpACS11A* in *aco1a*, but the induction of these two genes occurs in flowers where sex determination has already taken place (flowers above 2–3 mm in length). At earlier stages of female flower development (female floral buds less than 1 mm), the genes *CpACO2B* and *CpACS11A* were down-regulated in the mutant, and could not compensate for the reduced ethylene caused by *CpACO1A* disfunction.

The later-acting ethylene biosynthesis gene *ACS2* is specifically expressed in female flowers at early stages of development to control the arrest of stamen development. LOF mutations for *ACS2* orthologs (*CsACS2* in cucumber, *CmACS7* in melon, *CpACS27A* in *C. pepo*, and *CitACS4* in watermelon) promote the conversion of female into hermaphrodite flowers and monoecy into andromonoecy (Boualem et al., 2008, 2009, 2016; Martínez et al., 2014; Ji et al., 2016; Manzano et al., 2016). The phenotype of *aco1a* mutant described in this paper resembles those of *acs2-like* mutants, indicating that *CpACO1A* is, together with *CpACS27A*, the key enzymes that produce the requisite ethylene to prevent the development of stamens in squash female flowers. The reduced expression of *CpACS27A* in *aco1a* pistillate flowers at early stages of development suggests that the regulation of

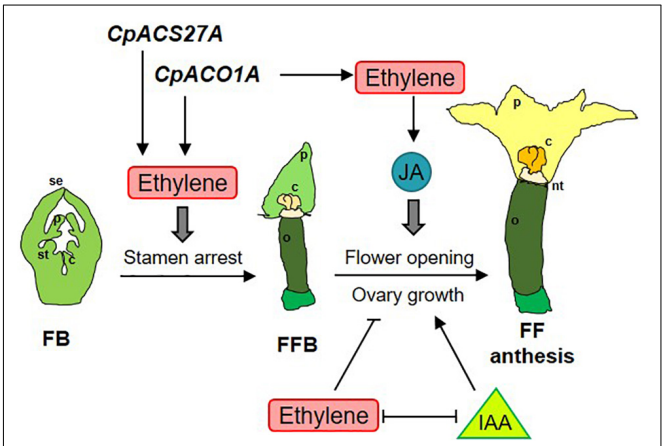

FIGURE 8 | Model integrating ethylene, jasmonate (JA) and auxin (IAA) in the regulation of sex determination (stamen arrest), female flower opening and ovary growth and fruit set and development in *Cucurbita pepo*. The genes *CpACO1A* and *CpACS27A* participate in the biosynthesis of the ethylene required for carpel promotion and stamen arrest at earlier stages of female floral bud (FFB) development. *CpACO1A* also participates in the ethylene produced at later stages of FFB for controlling flower opening and ovary growth and fruit set. Petal maturation and female flower opening is mediated by jasmonic acid (JA), while ovary growth and fruit set is coordinated by the antagonist action of ethylene and IAA, which are mutually repressed during the development of the female flower. se, sepal; p, petal; st, stamen; c, carpel; o, ovary; nt, nectary; FB, floral bud, FFB, female floral bud, FF, female flower.

these two key enzymes is coordinated, producing the required ethylene for the proper development of the female flower. This coordinated regulation may be mediated by ethylene, as occurs in other systems (Barry et al., 2000; Inaba et al., 2007).

CpACO1A Controls Flower Opening and Ovary Development in the Absence of Pollination

The phenotype of *aco1a* flowers also indicates that ethylene regulates the growth and development of other floral organs in the pistillate flowers of squash, including the corolla and the ovary/fruit. The delayed anthesis time of the *aco1a* pistillate flower demonstrates that ethylene is a positive regulator of petal growth and maturation in squash. This was also found in squash ethylene-insensitive mutants (García et al., 2020a,b), and seems to be associated with pistillate flower masculinization. Ethylene, which is the hormone that activates the developmental program of a female flower, is also used to promote the growing rate and maturation of female corolla. In the male flower, where ethylene production is very low, petals develop slower and anthesis is markedly more delayed. Given that male flowers are produced in the first nodes of the plant, this ethylene-mediated mechanism ensures that male and female flowers reach anthesis at the same time to achieve successful pollination. JA is known to be involved in anther and pollen maturation (Stintzi and Browse, 2000; Wang et al., 2005; Browse and Wallis, 2019), but also participates in petal maturation and flower opening (Reeves et al., 2012; Oh et al., 2013; Niwa et al., 2018; Schubert et al., 2019). The delayed flower opening and reduced JA in the ethylene-deficient hermaphrodite flowers of *aco1a* indicate that ethylene can regulate the maturation and opening of the female flower by inducing the biosynthesis of JA (**Figure 8**).

We have previously reported that external treatments with ethylene inhibitors were able induce fruit set and early fruit development in the absence of pollination (parthenocarpic fruit), and that fruit set is concomitant with a reduction in ethylene production, ethylene biosynthesis, and signaling gene expression in the days immediately after anthesis (Martínez et al., 2013). Mutations in ethylene receptor genes of squash confer partial ethylene insensitivity, and also result in parthenocarpic fruits (García et al., 2020a,b). The negative role of ethylene in fruit set has been also found in tomato, where ethylene and signaling genes are down-regulated in early-developing fruit (Vriezen et al., 2008; Wang et al., 2009), and the blocking of ethylene perception, using the ethylene-insensitive mutation *Sletr1-1* or treatments with 1MCP, leads to parthenocarpic fruits through the induction of auxin and gibberellin (Wang et al., 2009; Shinozaki et al., 2015, 2018; An et al., 2020). The up-regulation of IAA in *aco1a* may be responsible for the continued growth of *aco1a* ovaries in the absence of pollination. Auxins are the key hormones regulating fruit set in the Cucurbitaceae family (Trebitsh et al., 1987; Kim et al., 1992; Martínez et al., 2013), and were found to be highly induced in the *aco1a* flowers. This means that auxins not only repress the production, perception and signaling of ethylene in the squash developing fruit, as reported by Martínez et al. (2013), but can be negatively regulated by ethylene in the developing ovary (**Figure 8**). It is feasible that the two hormones are specifically accumulated in different floral organs, i.e., ethylene in the upper flower organs for promoting the development of carpels and petals and arresting the development of stamens, and auxin in the inferior ovary for inducing fruit set and development (**Figure 8**).

DATA AVAILABILITY STATEMENT

The datasets presented in this study can be found in online repositories. The names of the repository/repositories and accession number(s) can be found in the article/**Supplementary Material**.

AUTHOR CONTRIBUTIONS

MJ designed and coordinated the research. GC conducted most of the experiments and data analysis. JI-M and JR collaborated in phenotyping. CM and DG collaborated in data analysis. MJ and GC wrote the first version of the manuscript, and the other authors contributed later to improve it and approved the final version for submission. All authors contributed to the article and approved the submitted version.

FUNDING

This work was supported by grants AGL2017-82885-C2-1-R and PID2020-118080RB-C21, funded by the Spanish Ministry of Science and Innovation, and grant P12-AGR-1423, funded by Junta de Andalucía, Spain.

ACKNOWLEDGMENTS

GC and JI-M gratefully acknowledge the FPU and FPI scholarship program from MEC.

SUPPLEMENTARY MATERIAL

The Supplementary Material for this article can be found online at: https://www.frontiersin.org/articles/10.3389/fpls.2021.817922/full#supplementary-material

REFERENCES

Aguado, E., García, A., Iglesias-Moya, J., Romero, J., Wehner, T. C., Gómez-Guillamón, M. L., et al. (2020). Mapping a partial andromonoecy locus in *Citrullus lanatus* using BSA-Seq and GWAS approaches. *Front. Plant Sci.* 11:1243. doi: 10.3389/fpls.2020.01243

An, J., Althiab Almasaud, R., Bouzayen, M., Zouine, M., and Chervin, C. (2020). Auxin and ethylene regulation of fruit set. *Plant Sci.* 292:110381. doi: 10.1016/j.plantsci.2019.110381

Bai, S. L., Peng, Y.-B., Cui, J. X., Gu, H. T., Xu, L. Y., Li, Y. Q., et al. (2004). Developmental analyses reveal early arrests of the spore-bearing parts of reproductive organs in unisexual flowers of cucumber (*Cucumis sativus* L.). *Planta* 220, 230–240. doi: 10.1007/s00425-004-1342-2

Barry, C. S., Blume, B., Bouzayen, M., Cooper, W., Hamilton, A. J., and Grierson, D. (1996). Differential expression of the 1-aminocyclopropane-1-carboxylate oxidase gene family of tomato. *Plant J.* 9, 525–535. doi: 10.1046/j.1365-313X.1996.09040525.x

Barry, C. S., Llop-Tous, M. I., and Grierson, D. (2000). The regulation of 1-aminocyclopropane-1-carboxylic acid synthase gene expression during the transition from system-1 to system-2 ethylene synthesis in tomato. *Plant Physiol.* 123, 979–986. doi: 10.1104/pp.123.3.979

Boualem, A., Fergany, M., Fernandez, R., Troadec, C., Martin, A., Morin, H., et al. (2008). A conserved mutation in an ethylene biosynthesis enzyme leads to andromonoecy in melons. *Science* 321, 836–838. doi: 10.1126/science.1159023

Boualem, A., Lemhemdi, A., Sari, M. A., Pignoly, S., Troadec, C., Choucha, F. A., et al. (2016). The andromonoecious sex determination gene predates the separation of *Cucumis* and *Citrullus genera*. *PLoS One* 11:e0155444. doi: 10.1371/journal.pone.0155444

Boualem, A., Troadec, C., Camps, C., Lemhemdi, A., Morin, H., Sari, M.-A., et al. (2015). A cucurbit androecy gene reveals how unisexual flowers develop and dioecy emerges. *Science* 350, 688–691. doi: 10.1126/SCIENCE.AAC8370

Boualem, A., Troadec, C., Kovalski, I., Sari, M. A., Perl-Treves, R., and Bendahmane, A. (2009). A conserved ethylene biosynthesis enzyme leads to andromonoecy in two *Cucumis* species. *PLoS One* 4:e6144. doi: 10.1371/journal.pone.0006144

Browse, J., and Wallis, J. G. (2019). *Arabidopsis* flowers unlocked the mechanism of jasmonate signaling. *Plants* 8:285. doi: 10.3390/plants8080285

Bulens, I., Van de Poel, B., Hertog, M. L., De Proft, M. P., Geeraerd, A. H., and Nicolaï, B. M. (2011). Protocol: an updated integrated methodology for analysis of metabolites and enzyme activities of ethylene biosynthesis. *Plant Methods* 7:17. doi: 10.1186/1746-4811-7-17

Byers, R. E., Baker, L. R., Sell, H. M., Herner, R. C., and Dilley, D. R. (1972). Ethylene: a natural regulator of sex expression of *Cucumis melo* L. *Proc. Natl. Acad. Sci. U.S.A.* 69, 717–720. doi: 10.1073/pnas.69.3.717

Chandler, J. W. (2011). The hormonal regulation of flower development. *J. Plant Growth Regul.* 30, 242–254. doi: 10.1007/s00344-010-9180-x

Chen, H., Sun, J., Li, S., Cui, Q., Zhang, H., Xin, F., et al. (2016). An ACC oxidase gene essential for cucumber carpel development. *Mol. Plant* 9, 1315–1327. doi: 10.1016/J.MOLP.2016.06.018

Dahmani-Mardas, F., Troadec, C., Boualem, A., Lévêque, S., Alsadon, A. A., Aldoss, A. A., et al. (2010). Engineering melon plants with improved fruit shelf life using the TILLING approach. *PLoS One* 5:e15776. doi: 10.1371/journal.pone.0015776

Depristo, M. A., Banks, E., Poplin, R., Garimella, K. V., Maguire, J. R., Hartl, C., et al. (2011). A framework for variation discovery and genotyping using next-generation DNA sequencing data. *Nat. Genet.* 43, 491–501. doi: 10.1038/ng.806

Edgar, R. C. (2004). MUSCLE: multiple sequence alignment with high accuracy and high throughput. *Nucleic Acids Res.* 32, 1792–1797. doi: 10.1093/nar/gkh340

García, A., Aguado, E., Garrido, D., Martínez, C., and Jamilena, M. (2020a). Two androecious mutations reveal the crucial role of ethylene receptors in the initiation of female flower development in *Cucurbita pepo*. *Plant J.* 103, 1548–1560. doi: 10.1111/TPJ.14846

García, A., Aguado, E., Martínez, C., Loska, D., Beltrán, S., Valenzuela, J. L., et al. (2020b). The ethylene receptors CpETR1A and CpETR2B cooperate in the control of sex determination in *Cucurbita pepo*. *J. Exp. Bot.* 71, 154–167. doi: 10.1093/jxb/erz417

García, A., Aguado, E., Parra, G., Manzano, S., Martínez, C., Megías, Z., et al. (2018). Phenomic and genomic characterization of a mutant platform in *Cucurbita pepo*. *Front. Plant Sci.* 9:1049. doi: 10.3389/fpls.2018.01049

Harkey, A. F., Watkins, J. M., Olex, A. L., DiNapoli, K. T., Lewis, D. R., Fetrow, J. S., et al. (2018). Identification of transcriptional and receptor networks that control root responses to ethylene. *Plant Physiol.* 176, 2095–2118. doi: 10.1104/pp.17.00907

Houben, M., and Van de Poel, B. (2019). 1-aminocyclopropane-1-carboxylic acid oxidase (ACO): the enzyme that makes the plant hormone ethylene. *Front. Plant Sci.* 10:695. doi: 10.3389/fpls.2019.00695

Hu, B., Li, D., Liu, X., Qi, J., Gao, D., Zhao, S., et al. (2017). Engineering non-transgenic gynoecious cucumber using an improved transformation protocol and optimized CRISPR/Cas9 system. *Mol. Plant* 10, 1575–1578. doi: 10.1016/j.molp.2017.09.005

Inaba, A., Liu, X., Yokotani, N., Yamane, M., Lu, W. J., Nakano, R., et al. (2007). Differential feedback regulation of ethylene biosynthesis in pulp and peel tissues of banana fruit. *J. Exp. Bot.* 58, 1047–1057. doi: 10.1093/jxb/erl265

Ji, G., Zhang, J., Zhang, H., Sun, H., Gong, G., Shi, J., et al. (2016). Mutation in the gene encoding 1-aminocyclopropane-1-carboxylate synthase 4 (CitACS4) led to andromonoecy in watermelon. *J. Integr. Plant Biol.* 58, 762–765. doi: 10.1111/jipb.12466

Kim, I. S., Okubo, H., and Fujieda, K. (1992). Endogenous levels of IAA in relation to parthenocarpy in cucumber (*Cucumis sativus* L.). *Sci. Hortic.* 52, 1–8. doi: 10.1016/0304-4238(92)90002-T

Kumar, S., Stecher, G., Li, M., Knyaz, C., and Tamura, K. (2018). MEGA X: molecular evolutionary genetics analysis across computing platforms. *Mol. Biol. Evol.* 35, 1547–1549. doi: 10.1093/molbev/msy096

Li, H., and Durbin, R. (2009). Fast and accurate short read alignment with Burrows-Wheeler transform. *Bioinformatics* 25, 1754–1760. doi: 10.1093/bioinformatics/btp324

Li, S., Xu, H., Ju, Z., Cao, D., Zhu, H., Fu, D., et al. (2018). The RIN-MC fusion of MADs-box transcription factors has transcriptional activity and modulates expression of many ripening genes. *Plant Physiol.* 176, 891–909. doi: 10.1104/pp.17.01449

Li, S. B., Xie, Z. Z., Hu, C. G., and Zhang, J. Z. (2016). A review of auxin response factors (ARFs) in plants. *Front. Plant Sci.* 7:47. doi: 10.3389/fpls.2016.00047

Livak, K. J., and Schmittgen, T. D. (2001). Analysis of relative gene expression data using real-time quantitative PCR and the 2-ΔΔCT method. *Methods* 25, 402–408. doi: 10.1006/meth.2001.1262

Manzano, S., Aguado, E., Martínez, C., Megías, Z., García, A., and Jamilena, M. (2016). The ethylene biosynthesis gene CitACS4 regulates monoecy/andromonoecy in watermelon (*Citrullus lanatus*). *PLoS One* 11:e0154362. doi: 10.1371/journal.pone.0154362

Manzano, S., Martínez, C., García, J. M., Megías, Z., and Jamilena, M. (2014). Involvement of ethylene in sex expression and female flower development in watermelon (*Citrullus lanatus*). *Plant Physiol. Biochem.* 85, 96–104. doi: 10.1016/j.plaphy.2014.11.004

Manzano, S., Martínez, C., Megías, Z., Garrido, D., and Jamilena, M. (2013). Involvement of ethylene biosynthesis and signalling in the transition from male to female flowering in the monoecious *Cucurbita pepo*. *J. Plant Growth Regul.* 32, 789–798. doi: 10.1007/s00344-013-9344-6

Manzano, S., Martínez, C., Megías, Z., Gómez, P., Garrido, D., and Jamilena, M. (2011). The role of ethylene and brassinosteroids in the control of sex expression and flower development in *Cucurbita pepo*. *Plant Growth Regul.* 65, 213–221. doi: 10.1007/s10725-011-9589-7

Martin, A., Troadec, C., Boualem, A., Rajab, M., Fernandez, R., Morin, H., et al. (2009). A transposon-induced epigenetic change leads to sex determination in melon. *Nature* 461, 1135–1138. doi: 10.1038/nature08498

Martínez, C., and Jamilena, M. (2021). To be a male or a female flower, a question of ethylene in cucurbits. *Curr. Opin. Plant Biol.* 59:101981. doi: 10.1016/J.PBI.2020.101981

Martínez, C., Manzano, S., Megías, Z., Barrera, A., Boualem, A., Garrido, D., et al. (2014). Molecular and functional characterization of CpACS27A gene reveals its involvement in monoecy instability and other associated traits in squash (*Cucurbita pepo* L.). *Planta* 239, 1201–1215. doi: 10.1007/s00425-014-2043-0

Martínez, C., Manzano, S., Megías, Z., Garrido, D., Picó, B., and Jamilena, M. (2013). Involvement of ethylene biosynthesis and signalling in fruit set and early fruit development in zucchini squash (*Cucurbita pepo* L.). *BMC Plant Biol.* 13:139. doi: 10.1186/1471-2229-13-139

Montero-Pau, J., Blanca, J., Bombarely, A., Ziarsolo, P., Esteras, C., Martí-Gómez, C., et al. (2018). De novo assembly of the zucchini genome reveals a whole-genome duplication associated with the origin of the *Cucurbita* genus. *Plant Biotechnol. J.* 16, 1161–1171. doi: 10.1111/pbi.12860

Muday, G. K., Rahman, A., and Binder, B. M. (2012). Auxin and ethylene: collaborators or competitors? *Trends Plant Sci.* 17, 181–195. doi: 10.1016/j.tplants.2012.02.001

Müller, M., and Munné-Bosch, S. (2011). Rapid and sensitive hormonal profiling of complex plant samples by liquid chromatography coupled to electrospray ionization tandem mass spectrometry. *Plant Methods* 7:37. doi: 10.1186/1746-4811-7-37

Nakatsuka, A., Murachi, S., Okunishi, H., Shiomi, S., Nakano, R., Kubo, Y., et al. (1998). Differential expression and internal feedback regulation of 1-aminocyclopropane-1-carboxylate synthase, l-aminocyclopropane-1-carboxylate oxidase, and ethylene receptor genes in tomato fruit during development and ripening. *Plant Physiol.* 118, 1295–1305. doi: 10.1104/pp.118.4.1295

Niwa, T., Suzuki, T., Takebayashi, Y., Ishiguro, R., Higashiyama, T., Sakakibaraa, H., et al. (2018). Jasmonic acid facilitates flower opening and floral organ development through the upregulated expression of SlMYB21 transcription factor in tomato. *Biosci. Biotechnol. Biochem.* 82, 292–303. doi: 10.1080/09168451.2017.1422107

Oh, Y., Baldwin, I. T., and Galis, I. (2013). A jasmonate ZIM-domain protein NaJAZd regulates floral jasmonic acid levels and counteracts flower abscission in *Nicotiana attenuata* plants. *PLoS One* 8:e57868. doi: 10.1371/journal.pone.0057868

Papadopoulou, E., Little, H. A., Hammar, S. A., and Grumet, R. (2005). Effect of modified endogenous ethylene production on sex expression, bisexual flower development and fruit production in melon (*Cucumis melo* L.). *Sex. Plant Reprod.* 18, 131–142. doi: 10.1007/s00497-005-0006-0

Pattyn, J., Vaughan-Hirsch, J., and Van de Poel, B. (2020). The regulation of ethylene biosynthesis: a complex multilevel control circuitry. *New Phytol.* 229, 770–782. doi: 10.1111/nph.16873

Reeves, P. H., Ellis, C. M., Ploense, S. E., Wu, M. F., Yadav, V., Tholl, D., et al. (2012). A regulatory network for coordinated flower maturation. *PLoS Genet.* 8:e1002506. doi: 10.1371/journal.pgen.1002506

Rudich, J., Halevy, A. H., and Kedar, N. (1969). Increase in femaleness of three cucurbits by treatment with Ethrel, an ethylene releasing compound. *Planta* 86, 69–76. doi: 10.1007/BF00385305

Ruduś, I., Sasiak, M., and Kępczyński, J. (2013). Regulation of ethylene biosynthesis at the level of 1-aminocyclopropane-1-carboxylate oxidase (ACO) gene. *Acta Physiol. Plant.* 35, 295–307. doi: 10.1007/s11738-012-1096-6

Růžička, K., Ljung, K., Vanneste, S., Podhorská, R., Beeckman, T., Friml, J., et al. (2007). Ethylene regulates root growth through effects on auxin biosynthesis and transport-dependent auxin distribution. *Plant Cell* 19, 2197–2212. doi: 10.1105/tpc.107.052126

Schubert, R., Dobritzsch, S., Gruber, C., Hause, G., Athmer, B., Schreiber, T., et al. (2019). Tomato MYB21 acts in ovules to mediate jasmonate-regulated fertility. *Plant Cell* 31, 1043–1062. doi: 10.1105/tpc.18.00978

Shinozaki, Y., Hao, S., Kojima, M., Sakakibara, H., Ozeki-Iida, Y., Zheng, Y., et al. (2015). Ethylene suppresses tomato (*Solanum lycopersicum*) fruit set through modification of gibberellin metabolism. *Plant J.* 83, 237–251. doi: 10.1111/tpj.12882

Shinozaki, Y., Nicolas, P., Fernandez-Pozo, N., Ma, Q., Evanich, D. J., Shi, Y., et al. (2018). High-resolution spatiotemporal transcriptome mapping of tomato fruit development and ripening. *Nat. Commun.* 9:364. doi: 10.1038/s41467-017-02782-9

Stepanova, A. N., Yun, J., Likhacheva, A. V., and Alonso, J. M. (2007). Multilevel interactions between ethylene and auxin in *Arabidopsis* roots. *Plant Cell* 19, 2169–2185. doi: 10.1105/tpc.107.052068

Stintzi, A., and Browse, J. (2000). The *Arabidopsis* male-sterile mutant, opr3, lacks the 12-oxophytodienoic acid reductase required for jasmonate synthesis. *Proc. Natl. Acad. Sci. U.S.A.* 97, 10625–10630. doi: 10.1073/pnas.190264497

Sun, H., Wu, S., Zhang, G., Jiao, C., Guo, S., Ren, Y., et al. (2017). Karyotype stability and unbiased fractionation in the paleo-allotetraploid *Cucurbita* genomes. *Mol. Plant* 10, 1293–1306. doi: 10.1016/j.molp.2017.09.003

Swarup, R., Perry, P., Hagenbeek, D., Van Der Straeten, D., Beemster, G. T. S., Sandberg, G., et al. (2007). Ethylene upregulates auxin biosynthesis in *Arabidopsis* seedlings to enhance inhibition of root cell elongation. *Plant Cell* 19, 2186–2196. doi: 10.1105/tpc.107.052100

Till, B. J., Reynolds, S. H., Weil, C., Springer, N., Burtner, C., Young, K., et al. (2004). Discovery of induced point mutations in maize genes by TILLING. *BMC Plant Biol.* 4:12. doi: 10.1186/1471-2229-4-12

Trebitsh, T., Rudich, J., and Riov, J. (1987). Auxin, biosynthesis of ethylene and sex expression in cucumber (*Cucumis sativus*). *Plant Growth Regul.* 5, 105–113. doi: 10.1007/BF00024738

Trivellini, A., Ferrante, A., Vernieri, P., and Serra, G. (2011). Effects of abscisic acid on ethylene biosynthesis and perception in *Hibiscus rosa-sinensis* L. flower development. *J. Exp. Bot.* 62, 5437–5452. doi: 10.1093/jxb/err218

Vriezen, W. H., Feron, R., Maretto, F., Keijman, J., and Mariani, C. (2008). Changes in tomato ovary transcriptome demonstrate complex hormonal regulation of fruit set. *New Phytol.* 177, 60–76. doi: 10.1111/j.1469-8137.2007.02254.x

Wang, H., Schauer, N., Usadel, B., Frasse, P., Zouine, M., Hernould, M., et al. (2009). Regulatory features underlying pollination-dependent and-independent tomato fruit set revealed by transcript and primary metabolite profiling. *Plant Cell* 21, 1428–1452. doi: 10.1105/tpc.108.060830

Wang, K., Li, M., and Hakonarson, H. (2010). ANNOVAR: functional annotation of genetic variants from high-throughput sequencing data. *Nucleic Acids Res.* 38, e164. doi: 10.1093/nar/gkq603

Wang, Z., Dai, L., Jiang, Z., Peng, W., Zhang, L., Wang, G., et al. (2005). GmCOI1, a soybean F-box protein gene, shows ability to mediate jasmonate-regulated plant defense and fertility in *Arabidopsis*. *Mol. Plant Microbe Interact.* 18, 1285–1295. doi: 10.1094/MPMI-18-1285

Yue, P., Lu, Q., Liu, Z., Lv, T., Li, X., Bu, H., et al. (2020). Auxin-activated MdARF5 induces the expression of ethylene biosynthetic genes to initiate apple fruit ripening. *New Phytol.* 226, 1781–1795. doi: 10.1111/nph.16500

Zemlyanskaya, E. V., Omelyanchuk, N. A., Ubogoeva, E. V., and Mironova, V. V. (2018). Deciphering auxin-ethylene crosstalk at a systems level. *Int. J. Mol. Sci.* 19:4060. doi: 10.3390/ijms19124060

Zhang, J., Guo, S., Ji, G., Zhao, H., Sun, H., Ren, Y., et al. (2020). A unique chromosome translocation disrupting ClWIP1 leads to gynoecy in watermelon. *Plant J.* 101, 265–277. doi: 10.1111/tpj.14537

Zhang, J., Shi, J., Ji, G., Zhang, H., Gong, G., Guo, S., et al. (2017). Modulation of sex expression in four forms of watermelon by gibberellin, ethephone and silver nitrate. *Hortic. Plant J.* 3, 91–100. doi: 10.1016/j.hpj.2017.07.010

Zhang, Y., Zhang, X., Liu, B., Wang, W., Liu, X., Chen, C., et al. (2014). A GAMYB homologue CsGAMYB1 regulates sex expression of cucumber via an ethylene-independent pathway. *J. Exp. Bot.* 65, 3201–3213. doi: 10.1093/jxb/eru176

Zuckerkandl, E., and Pauling, L. (1965). Molecules as documents of evolutionary history. *J. Theor. Biol.* 8, 357–366. doi: 10.1016/0022-5193(65)90083-4

Conflict of Interest: The authors declare that the research was conducted in the absence of any commercial or financial relationships that could be construed as a potential conflict of interest.

Publisher's Note: All claims expressed in this article are solely those of the authors and do not necessarily represent those of their affiliated organizations, or those of the publisher, the editors and the reviewers. Any product that may be evaluated in this article, or claim that may be made by its manufacturer, is not guaranteed or endorsed by the publisher.